

AN EXPERIMENTAL INVESTIGATION OF
SANDWICH FLAT PANELS UNDER LOW
VELOCITY IMPACT

THESIS

Timberlyn Michelle Harrington
Captain, USAF

AFIT/GAE/ENY/94D-22

19950103 059

DISTRIBUTION STATEMENT 1
Approved for public release
Distribution Unlimited

DEPARTMENT OF THE AIR FORCE
AIR UNIVERSITY

AIR FORCE INSTITUTE OF TECHNOLOGY

Wright-Patterson Air Force Base, Ohio

AFIT/GAE/ENY/94D-22

AN EXPERIMENTAL INVESTIGATION OF
SANDWICH FLAT PANELS UNDER LOW
VELOCITY IMPACT

THESIS

Timberlyn Michelle Harrington
Captain, USAF

AFIT/GAE/ENY/94D-22

Approved for public release; distribution unlimited

THIS QUALITY INSPECTED 8

AN EXPERIMENTAL INVESTIGATION OF
SANDWICH FLAT PANELS UNDER LOW
VELOCITY IMPACT

THESIS

Presented to the Faculty of the Graduate School of Engineering
of the Air Force Institute of Technology
Air University
In Partial Fulfillment of the
Requirements for the Degree of
Master of Science in Aeronautical Engineering

Timberlyn Michelle Harrington
Captain, USAF

December 1994

Accession For	
NTIS GRA&I	<input checked="" type="checkbox"/>
DTIC TAB	<input type="checkbox"/>
Unannounced	<input type="checkbox"/>
Justification	
By	
Distribution/	
Availability Codes	
Dist	Avail and/or Special
A-1	

Approved for public release; distribution unlimited

The views expressed in this thesis are those of the author
and do not reflect the official policy or position of the
Department of Defense or the U. S. Government

Acknowledgments

I would like to express my sincere gratitude to Dr. Anthony Palazotto, my thesis advisor, for his patience, guidance, and positive attitude throughout the course of this work. When I felt as if my rope of hope was almost broke, he always encouraged me to reach beyond the break.

I would like to thank Mr. William Baron and the people of the Air Force Flight Dynamics Directorate for sponsoring my thesis. It was a pleasure to work with Dr. Greg Schoeppner, my advisor in the Directorate. His insight into low velocity impact was extremely helpful. I would also like to thank Larry Mack and the personnel of Select Tech for fabricating my sandwich specimens, and the personnel of University of Dayton Research Institute for the C-scans and micrographs. I am also appreciative to John Brooks for letting me take over part of his office space and Forest Sandow for not letting me take over his.

As always, I would like to give thanks to God for my family for their prayers and encouragement. A special thank you to my husband, Michael for his love, support and understanding as well as the candle-lit home cooked meals. This thesis is dedicated to the memory of Mrs. Sally Mae Earl, a special friend.

TABLE OF CONTENTS

	<u>Page</u>
Acknowledgments	ii
List of Figures	iv
List of Tables	xii
Abstract	xvii
I. Introduction	1-1
1.1. Background	1-1
1.2. Purpose	1-5
1.3. Scope	1-6
II. Experimental Procedures	2-1
2.1. Test Specimens	2-1
2.2. Impact Facilities and Equipment	2-9
2.3. Data Collection and Processing	2-15
2.4. Post-Impact	2-17
III. Experimental Results	3-1
3.1. Load and Energy Curves from Dynatup	3-1
3.2. Failure Characteristics	3-5
3.3. Sandwich Panels with 4-Ply Face Sheets	3-7
(1) Impact Energy = 1.27J	3-7
(2) Impact Energy = 1.68 J	3-9
(3) Impact Energy = 2.06 J	3-23
(4) Impact Energy = 2.62 J	3-33
(5) C-scans	3-43
(6) Additional Analysis	3-44
3.4. Sandwich Panels with 8-Ply Face Sheets	3-49
(1) Impact Energy = 2.60 J and 2.56 J	3-49
(2) Impact Energy = 3.05 J	3-64
(3) Impact Energy = 3.35 J	3-64
(4) C-scans	3-83
(5) Additional Analysis	3-84
3.5. Sandwich Panels with 16-Ply Face Sheets	3-88
(1) Impact Energy = 3.95J and 3.97J	3-88
(2) Impact Energy = 4.26 J	3-104
(3) Impact Energy = 4.85 J	3-104
(4) Impact Energy = 5.21 J	3-104
(5) Impact Energy = 5.74 J	3-108
(6) C-scans	3-119
(7) Additional Analysis	3-120
3.6. Sandwich Panels with 32-Ply Face Sheets	3-124

(1) Impact Energy = 4.27J	3-124
(2) Impact Energy = 4.70 J	3-126
(3) Impact Energy = 5.18 and 5.17 J	3-133
(4) Impact Energy = 5.67 J	3-153
(4) C-scans	3-153
(5) Additional Analysis	3-153
3.7. Sandwich Panels with 48-Ply Face Sheets	3-161
(1) Impact Energy = 6.89 J	3-161
(2) Impact Energy = 7.78 J	3-161
(3) Impact Energy = 8.84 J	3-163
(4) Impact Energy = 9.67 J	3-163
(5) C-scans	3-170
(6) Additional Analysis	3-170
3.8. Comparison of Sandwich Panels with Different Face Sheet Thicknesses	3-180
3.9. Summary	3-195
V. Conclusions	4-1
Appendix A: Test Plans	A-1
Appendix B: Face Sheet Material Property Curves	B-1
Appendix C: Impact Testing Procedure	C-1
Appendix D: Dynatup Data Processing Technique	D-1
Bibliography	BIB-1
Vita	V-1

List of Figures

Figure		Page
1-1.	Sandwich Construction	1-1
1-2.	Honeycomb Core	1-2
1-3.	I Beam	1-3
1-4.	Low Velocity Impact	1-4
2-1.	Comparison of 4-ply and 48 ply sandwich panels	2-1
2-2.	Honeycomb Core Two-Dimensional Measurements	2-2
2-3.	Honeycomb Core before Sandwich Panel Fabrication	2-3
2-4.	Room Temperature Stabilized Compression Stress-Strain Curve for Nomex HRH-10-1/8-9.0 Honeycomb Core	2-5
2-5.	Room Temperature "L-Direction" Stress-Strain Curve for Nomex HRH-10-1/8-9.0 Honeycomb Core	2-6
2-6.	Room Temperature Shear Stress-Strain Curve for FM 300-2 Film Adhesive	2-7
2-7.	48 Ply Sandwich Panel with Only One Face Sheet	2-9
2-8.	Dynatup Impact Machine	2-11
2-9.	Close-up of Impact Drop Weight Assembly	2-12
2-10.	Impact Tup in Contact with Sandwich Specimen	2-13
2-11.	Sandwich Panel Secured in Between Support Block and Hold-down Plate	2-14
2-12.	Example of Load and Energy Plot from Dynatup	2-16
2-13.	Cross-Sectioning	2-18
3-1.	Significant Points on Load and Energy Curves.	3-5
3-2.	Honeycomb Core Failure Modes	3-7
3-3.	Load and Energy from Dynatup for 4-ply at 3.81 cm (1.5 in) drop height	3-8
3-4.	Load and Energy from Dynatup for 4-ply at 5.08 cm (2.0 in) drop height	3-10

3-5.	Comparison of Load Curves for 4-ply at 3.81 cm (1.5 in) and 5.08 cm (2.0 in) drop heights	3-11
3-6.	0° Cross-Section 16694-3-2 (2.7X)	3-12
3-7.	90° Cross-Section 16694-3-2 (2.7X)	3-12
3-8.	Guide to Micrograph of 0 Degree Cross-Section (25X) - 16694-3-2	3-13
3-9.	0° Cross-Section 16694-3-2 (25X) Part A.	3-15
3-10.	0° Cross-Section 16694-3-2 (25X) Part B.	3-16
3-11.	0° Cross-Section 16694-3-2 (25X) Part C.	3-17
3-12.	90° Cross-Section 16694-3-2 (25X)	3-18
3-13.	0° Cross-Section Analysis 16694-3-2	3-19
3-14.	90° Cross-Section Analysis 16694-3-2	3-20
3-15.	Load and Energy from Dynatup for 4-ply at 6.35 cm (2.5 in) drop height	3-24
3-16.	0° Cross-Section 16694-3-5 (2.7X)	3-25
3-17.	90° Cross-Section 16694-3-5 (2.7X)	3-25
3-18.	Guide to Micrograph of 0 Degree Cross-Section (25X) - 16694-3-5.	3-26
3-19.	0° Cross-Section 16694-3-5 (25X) Part A.	3-27
3-20.	0° Cross-Section 16694-3-5 (25X) Part B.	3-28
3-21.	0° Cross-Section 16694-3-5 (25X) Part C.	3-29
3-22.	90° Cross-Section 16694-3-2 (25X)	3-30
3-23.	0° Cross-Section Analysis 16694-3-5	3-31
3-24.	90° Cross-Section Analysis 16694-3-5	3-32
3-25.	Load and Energy from Dynatup for 4-ply at 7.62 cm (3.0 in) drop height	3-34
3-26.	0° Cross-Section 16694-3-6 (2.7X)	3-35
3-27.	90° Cross-Section 16694-3-6 (2.7X)	3-35
3-28.	Guide to Micrograph of 0 Degree Cross-Section	

	(25X) - 16694-3-6.....	3-36
3-29.	0° Cross-Section 16694-3-6 (25X) Part A.....	3-37
3-30.	0° Cross-Section 16694-3-6 (25X) Part B.....	3-38
3-31.	0° Cross-Section 16694-3-6 (25X) Part C.....	3-39
3-32.	90° Cross-Section 16694-3-6 (25X)	3-40
3-33.	0° Cross-Section Analysis 16694-3-6	3-41
3-34.	90° Cross-Section Analysis 16694-3-6	3-42
3-35.	Pulse-Echo C-scans for Sandwich Panels with 4-ply Face Sheets	3-44
3-36.	Damage Area vs Impact and Total Energies - 4-ply	3-45
3-37.	Delamination Length vs Delamination Area - 4-ply	3-45
3-38.	Comparison of Energy Curves for Sandwich Panels with 4-ply Face Sheets	3-47
3-39.	Comparison of Absorbed Energy and Impact Energy vs Drop Height for Sandwich Panels with 4-ply Face Sheets	3-48
3-40.	Load and Energy from Dynatup for 8-ply Specimen ID 16894-2-1 at 7.62 cm (3.0 in) drop height	3-50
3-41.	Load and Energy from Dynatup for 8-ply Specimen ID 16894-2-2 at 7.62 cm (3.0 in) drop height	3-51
3-42.	0° Cross-Section 16894-2-1 (2.7X)	3-53
3-43.	0° Cross-Section 16894-2-2 (2.7X)	3-53
3-44.	90° Cross-Section 16894-2-1 (2.7X)	3-54
3-45.	90° Cross-Section 16894-2-2 (2.7X)	3-54
3-46.	Guide to Micrograph of 0 Degree Cross-Section (25X) - 16894-2-1.....	3-55
3-47.	0° Cross-Section 16894-2-1 (25X) Part A.....	3-56
3-48.	0° Cross-Section 16894-2-1 (25X) Part B.....	3-57
3-49.	Guide to Micrograph of 0 Degree Cross-Section (25X) - 16894-2-2.....	3-58
3-50.	0° Cross-Section 16894-2-2 (25X) Part A.....	3-59

3-51.	0° Cross-Section 16894-2-2 (25X) Part B	3-60
3-52.	90° Cross-Section 16894-2-1 (25X)	3-61
3-53.	90° Cross-Section 16894-2-2 (25X)	3-62
3-54.	Direction of Delamination Enlargement	3-63
3-55.	Load and Energy from Dynatup for 8-ply Specimen ID 16894-2-3 at 8.89 cm (3.5 in) drop height	3-65
3-56.	0° Cross-Section 16894-2-3 (2.7X).	3-66
3-57.	90° Cross-Section 16894-2-3 (2.7X)	3-66
3-58.	Guide to Micrograph of 0 Degree Cross-Section (25X) - 16894-2-3	3-67
3-59.	0° Cross-Section 16894-2-3 (25X) - Part A	3-68
3-60.	0° Cross-Section 16894-2-3 (25X) - Part B	3-69
3-61.	Guide to Micrograph of 90 Degree Cross-Section (25X) - 16894-2-2	3-70
3-62.	90° Cross-Section 16894-2-3 (25X) - Part A	3-71
3-63.	90° Cross-Section 16894-2-3 (25X) - Part B	3-72
3-64.	Load and Energy from Dynatup for 8-ply at 10.16 cm (4.0 in) drop height	3-74
3-65.	0° Cross-Section 16894-2-6 (2.7X).	3-75
3-66.	90° Cross-Section 16894-2-6 (2.7X)	3-76
3-67.	Guide to Micrograph of 0 Degree Cross-Section (25X) - 16894-2-6	3-77
3-68.	0° Cross-Section 16894-2-6 (25X) - Part A	3-78
3-69.	0° Cross-Section 16894-2-6 (25X) - Part B	3-79
3-70.	0° Cross-Section 16894-2-6 (25X) - Part C	3-80
3-71.	Guide to Micrograph of 90 Degree Cross-Section (25X) - 16894-2-6	3-80
3-72.	90° Cross-Section 16894-2-3 (25X) - Part A	3-81
3-73.	90° Cross-Section 16894-2-3 (25X) - Part B	3-82
3-74.	Pulse-Echo C-scan for Sandwich Panels with 8-ply Face Sheets.	3-83
3-75.	Damage Area vs Impact and Absorbed Energies - 8-ply	3-84

3-76	Comparison of Energy Curves for Sandwich Panels with 8-ply Face Sheets	3-85
3-77.	Comparison of Load Curves for Various Impact Energies for Sandwich Panels with 8-ply Face Sheets.	3-86
3-78.	Comparison of Absorbed Energy and Impact Energy vs Drop Height for Sandwich Panels with 8-ply Face Sheets	3-87
3-79.	Comparison of Elastic Energy for 4-ply and 8-ply Test Series	3-87
3-80.	Load and Energy from Dynatup for 16-ply Specimen ID 17895-1-1 at 11.43 cm (4.5 in) drop height	3-89
3-81.	Load and Energy from Dynatup for 16-ply Specimen ID 17895-1-2 at 11.43 cm (4.5 in) drop height	3-90
3-82.	0° Cross-Section 17294-1-1 (2.7X).....	3-92
3-83.	0° Cross-Section 17294-1-2 (2.7X).....	3-92
3-84.	90° Cross-Section 17294-1-1 (25X)	3-93
3-85.	90° Cross-Section 17294-1-2 (25X)	3-93
3-86.	Guide to Micrograph of 0 Degree Cross-Section (25X) - 17294-1-1	3-94
3-87.	0° Cross-Section 17294-1-1 (25X) - Part A	3-95
3-88.	0° Cross-Section 17294-1-1 (25X) - Part B	3-96
3-89.	Guide to Micrograph of 0 Degree Cross-Section (25X) - 17294-1-2	3-97
3-90.	0° Cross-Section 17294-1-2 (25X) - Part A	3-98
3-91.	0° Cross-Section 17294-1-2 (25X) - Part B	3-99
3-92.	Guide to Micrograph of 90 Degree Cross-Section (25X) - 17294-1-1	3-100
3-93.	90° Cross-Section 17294-1-1 (25X) - Part A	3-101
3-94.	90° Cross-Section 17294-1-1 (25X) - Part B	3-102
3-95.	90° Cross-Section 17294-1-2 (25X).....	3-103
3-96.	Load and Energy from Dynatup for 16-ply at 12.70 cm (5.0 in) drop height	3-105
3-97.	Load and Energy from Dynatup for 16-ply at 13.97 cm (5.5 in) drop height	3-106
3-98.	Load and Energy from Dynatup for 16-ply	

	at 15.24 cm (6.0 in) drop height	3-107
3-99.	Load and Energy from Dynatup for 16-ply at 16.51 cm (6.5 in) drop height	3-109
3-100.	0° Cross-Section 17294-1-6 (2.7X)	3-110
3-101.	90° Cross-Section 17294-1-6 (2.7X).....	3-111
3-102.	Guide to Micrograph of 0 Degree Cross-Section (25X) - 17294-1-6 ...	3-111
3-103.	0° Cross-Section 17294-1-6 (25X) - Part A	3-112
3-104.	0° Cross-Section 17294-1-6 (25X) - Part B	3-113
3-105.	0° Cross-Section 17294-1-6 (25X) - Part C	3-114
3-106.	Guide to Micrograph of 60 Degree Cross-Section (25X) - 17294-1-6 ...	3-115
3-107.	90° Cross-Section 17294-1-6 (25X) - Part A	3-116
3-108.	90° Cross-Section 17294-1-6 (25X) - Part B	3-117
3-109.	Pulse-Echo C-scan for Sandwich Panels with 16-ply Face Sheets.....	3-118
3-110.	Damage Area vs Impact and Absorbed Energies - 16-ply	3-120
3-111	Comparison of Energy Curves for Sandwich Panels with 16-ply Face Sheets	3-121
3-112.	Comparison of Load Curves for Sandwich Panels with 16-ply Face Sheets.....	3-122
3-113.	Comparison of Absorbed Energy and Impact Energy vs Drop Height for Sandwich Panels with 16-ply Face Sheets	3-123
3-114.	Load and Energy from Dynatup for 32-ply at 12.70 cm (5.0 in) drop height	3-125
3-115.	Load and Energy from Dynatup for 32-ply at 13.97 cm (5.5 in) drop height	3-127
3-116.	0° Cross-Section 17594-1-6b (2.7X)	3-128
3-117.	90° Cross-Section 17594-1-6b (2.7X).....	3-128
3-118.	Guide to Micrograph of 0 Degree Cross-Section (25X) - 17594-1-6b ...	3-129
3-119.	0° Cross-Section 17594-1-6b (25X) - Part A	3-130
3-120.	0° Cross-Section 17594-1-6b (25X) - Part A	3-131

3-121.	90° Cross-Section 17594-1-6 (25X)	3-132
3-122.	Load and Energy from Dynatup for 32-ply Specimen ID 17594-1-1 at 15.24 cm (6.0 in) drop height	3-134
3-123.	Load and Energy from Dynatup for 32-ply Specimen ID 17594-1-2 at 15.24 cm (6.0 in) drop height	3-135
3.124.	Comparison of Load Curves with Impact Energies = 5.18 J and 5.17 J for 32-ply	3-136
3-125.	0° Cross-Section 17594-1-1 (2.7X).	3-137
3-126.	0° Cross-Section 17594-1-2 (2.7X).	3-137
3-127.	90° Cross-Section 17594-1-1 (25X)	3-138
3-128.	90° Cross-Section 17594-1-2 (25X)	3-138
3-129.	Guide to Micrograph of 0 Degree Cross-Section (25X) - 17594-1-1	3-139
3-130.	0° Cross-Section 17594-1-1 (25X) - Part A	3-140
3-131.	0° Cross-Section 17594-1-1 (25X) - Part B	3-141
3-132.	0° Cross-Section 17594-1-1 (25X) - Part C	3-142
3-133.	Guide to Micrograph of 0 Degree Cross-Section (25X) - 17594-1-2	3-143
3-134.	0° Cross-Section 17494-1-2 (25X) - Part A	3-144
3-135.	0° Cross-Section 17294-1-2 (25X) - Part B	3-145
3-136.	0° Cross-Section 17594-1-2 (25X) - Part C	3-146
3-137.	Guide to Micrograph of 90 Degree Cross-Section (25X) - 17594-1-1 . . .	3-147
3-138.	90° Cross-Section 17594-1-1 (25X) - Part A	3-148
3-139.	90° Cross-Section 17594-1-1 (25X) - Part B	3-149
3-140.	Guide to Micrograph of 90 Degree Cross-Section (25X) - 17594-1-2 . . .	3-150
3-141.	90° Cross-Section 17294-1-2 (25X)- Part A	3-151
3-142.	90° Cross-Section 17294-1-2 (25X) - Part B	3-152
3-143.	Load and Energy from Dynatup for 32-ply at 16.51 cm (6.5 in) drop height	3-154
3-144.	Pulse-Echo C-scan for Sandwich Panels with 32-ply Face Sheets.	3-155

3-145.	Damage Area vs Impact and Absorbed Energies - 32-ply	3-156
3-146	Comparison of Energy Curves for Sandwich Panels with 32-ply Face Sheets	3-157
3-147.	Comparison of Load Curves for Sandwich Panels with 32-ply Face Sheets.	3-158
3-148.	Comparison of Absorbed Energy and Impact Energy vs Drop Height for Sandwich Panels with 32-ply Face Sheets	3-159
3-149.	Comparison of Absorbed Energy and Impact Energy and Energy at Maximum Load for Sandwich Panels with 32-ply Face Sheets	3-160
3-150	Load and Energy from Dynatup for 48-ply at 20.32 cm (8.0 in) drop height	3-162
3-151	Load and Energy from Dynatup for 48-ply at 22.86 cm (9.0 in) drop height	3-164
3-152.	0° Cross-Section 18294-2-2 (2.5X)	3-165
3-153.	90° Cross-Section 18294-2-2 (2.5X).	3-165
3-154.	0° Cross-Section 18294-2-2 (25X)	3-166
3-155.	90° Cross-Section 18294-2-2 (25X)	3-167
3-156	Load and Energy from Dynatup for 48-ply at 25.40 cm (10.0 in) drop height	3-168
3-157	Load and Energy from Dynatup for 48-ply at 27.94 cm (11.0 in) drop height	3-169
3-158.	0° Cross-Section 18294-2-4 (2.5X)	3-171
3-159.	90° Cross-Section 18294-2-4 (2.5X).	3-171
3-160.	Guide to Micrograph of 0 Degree Cross-Section (25X) - 18294-2-4	3-172
3-161.	0° Cross-Section 18294-2-4 (25X) - Part A	3-173
3-162.	0° Cross-Section 18294-2-4 (25X) - Part B	3-174
3-163.	90° Cross-Section 18294-2-4 (25X)	3-175
3-164.	Pulse-Echo C-scan for Sandwich Panels with 48-ply Face Sheets.	3-176
3-165.	Damage Area vs Impact and Absorbed Energies - 48-ply	3-176
3-166	Comparison of Energy Curves for Sandwich Panels with 48-ply Face Sheets	3-177

3-167.	Comparison of Load Curves for Sandwich Panels with 48-ply Face Sheets.	3-178
3-168.	Comparison of Absorbed Energy and Impact Energy for Sandwich Panels with 48-ply Face Sheets	3-179
3-169.	Comparison of Load Curves for Sandwich Panels with 4-ply and 8-ply Face Sheets at a Drop Height of 7.62 cm (3.0 in).	3-181
3-170.	Comparison of Load Curves (per ply) for Sandwich Panels with 4-ply and 8-ply Face Sheets at a Drop Height of 7.62 cm (3.0 in).	3-181
3-171.	Comparison of Energy Curves for Sandwich Panels with 4-ply and 8-ply Face Sheets at a Drop Height of 7.62 cm (3.0 in).	3-182
3-172.	Comparison of Energy Curves (per ply) for Sandwich Panels with 4-ply and 8-ply Face Sheets at a Drop Height of 7.62 cm (3.0 in).	3-182
3-173.	Time of Event vs Number of Plies of Face Sheets	3-183
3-174.	Comparioson of Load Curves for Face Sheet Thicknesses	3-184
3-175.	Comparison of Load Curves for Sandwich Panels with 16-ply and 32-ply Face Sheets at a Drop Height of 12.7 cm (5.0 in).	3-186
3-176.	Comparison of Load Curves (per ply) for Sandwich Panels with 16-ply and 32-ply Face Sheets at a Drop Height of 12.7 cm (5.0 in).	3-186
3-177.	Comparison of Energy Curves for Sandwich Panels with 16-ply and 32-ply Face Sheets at a Drop Height of 12.7 cm (5.0 in).	3-187
3-178.	Comparison of Energy Curves (per ply) for Sandwich Panels with 16-ply and 32-ply Face Sheets at a Drop Height of 12.7 cm (5.0 in).	3-187
3-179.	Comparison of Load Curves for Sandwich Panels with 16-ply and 32-ply Face Sheets at a Drop Height of 13.97 cm (5.5 in).	3-188
3-180.	Comparison of Load Curves (per ply) for Sandwich Panels with 16-ply and 32-ply Face Sheets at a Drop Height of 13.97cm (5.5 in).	3-188
3-181.	Comparison of Energy Curves for Sandwich Panels with 16-ply and 32-ply Face Sheets at a Drop Height of 13.97 cm (5.5 in).	3-189
3-182.	Comparison of Energy Curves (per ply) for Sandwich Panels with 16-ply and 32-ply Face Sheets at a Drop Height of 13.97 cm (5.5 in).	3-189
3-183.	Comparison of Load Curves for Sandwich Panels with 16-ply and 32-ply Face Sheets at a Drop Height of 15.24 cm (6.0 in).	3-190
3-184.	Comparison of Load Curves (per ply) for Sandwich Panels with 16-ply and 32-ply Face Sheets at a Drop Height of 15.24cm (6.0 in).	3-190

3-185.	Comparison of Energy Curves for Sandwich Panels with 16-ply and 32-ply Face Sheets at a Drop Height of 15.24 cm (6.0 in).	3-191
3-186.	Comparison of Energy Curves (per ply) for Sandwich Panels with 16-ply and 32-ply Face Sheets at a Drop Height of 15.24 cm (6.0 in).	3-191
3-187.	Comparison of Load Curves for Sandwich Panels with 16-ply and 32-ply Face Sheets at a Drop Height of 16.51 cm (6.5 in).	3-192
3-188.	Comparison of Load Curves (per ply) for Sandwich Panels with 16-ply and 32-ply Face Sheets at a Drop Height of 16.51cm (6.5 in).	3-192
3-189.	Comparison of Energy Curves for Sandwich Panels with 16-ply and 32-ply Face Sheets at a Drop Height of 16.51 cm (6.5 in).	3-193
3-190.	Comparison of Energy Curves (per ply) for Sandwich Panels with 16-ply and 32-ply Face Sheets at a Drop Height of 16.51 cm (6.5 in).	3-193
3-191.	Comparison of Absorbed Energy vs Drop Height of Sandwich Panels with 16-ply and 32-ply Face Sheets	3-194
3-192.	Comparison of Damage Area vs Absorbed Energy for Sandwich Panels with 16-ply and 32-ply Face Sheets	3-194
A-1.	Trim plan for sandwich panels	A-9
A-2.	Sandwich panel cut plan	A-10
A-3.	Thickness Measurement Locatios for Qualifications	A-11
A-4.	Trim plan for unidirectional specimens panel A	A-12
A-5.	Trim plan for shear specimens panel B.	A-12
A-6.	Panel 'A' cut plan	A-13
A-7.	Panel 'B' cut plan	A-14
A-8.	0T, 90T, and Shear Tension Test Specimens	A-15
A-9.	0C and 90C Test Specimens	A-16
B-1.	Axial Stress vs Axial Strain - 0° Tension	B-2
B-2.	Axial Stress vs Axial Strain - 0° Compression	B-3
B-3.	Transverse Stress vs Transverse Strain - 90° Tension	B-4
B-4.	Transverse Stress vs Transverse Strain - 90° Compression	B-5
B-5.	Shear Stress vs Shear Strain - ±45° Tension	B-6

B-6. Poisson's Ratio vs Axial Strain - 0° Tension B-7
B-7. Poisson's Ratio vs Axial Strain - 0° Compression B-8

List of Tables

Table		Page
2-1.	Face Sheet Stacking Sequences.	2-2
2-2.	Property Tests - Resulting Curves - Corresponding Basic Properties. . .	2-4
3-1.	Summary of Data Collected from Dynatup.	3-2
3-2.	Summary of Post Impact Data Collected	3-3
3-3.	Summary of Test Data	3-195
A-1	Low Velocity Impact Test Matrix	A-6
A-2	Impact Parameters (Nominal)	A-7

Abstract

This study evaluated the failure modes and mechanisms associated with increasing face sheet thickness of flat sandwich panels under low velocity impact. The sandwich panels were fabricated using 1.27 cm (0.5 in) thick, 145 kg/m^3 (9 lb/ft^3), 3.175 mm (1/8") cell size Nomex honeycomb core, FM 300-2 film adhesive and AS4/3501-6 graphite/epoxy face sheets. The thickness of the core remained 1.27 cm, and the thickness of the adhesive remained 0.25 mm. The thickness of the face sheet varied using the following stacking sequences: $[0/90]_S$, $[0/90]_{2S}$, $[0/90]_{4S}$, $[0/90]_{8S}$ and $[0/90]_{12S}$. The sandwich panels were subjected to various low velocity impacts using the Dynatup Impact Test Machine. Pulse Echo C-scans and optical microscopy of panel cross-sections were performed to characterize the damage. The cross-sections indicated that delamination and transverse cracking contribute to internal damage of the face sheets, while crushing, buckling, and crippling contribute to damage of the core. Cracks in the adhesive also contribute to damage in some cases.

AN EXPERIMENTAL INVESTIGATION OF SANDWICH PANELS
UNDER LOW VELOCITY IMPACT

I. Introduction

1.1 Background

The basic sandwich structure, a sandwich panel, consists of three or more layers of material bonded together so that they act in unison [1]. For example, a sandwich panel could consist of two graphite epoxy composite face sheets adhered to a honeycomb core as illustrated in Fig. 1.1. Fig. 1.2. shows a single honeycomb cell along with the terminology used to define the parts of the core [2]. The core to skin adhesive rigidly joins the sandwich components and allow them to act as one unit with a high torsional rigidity.

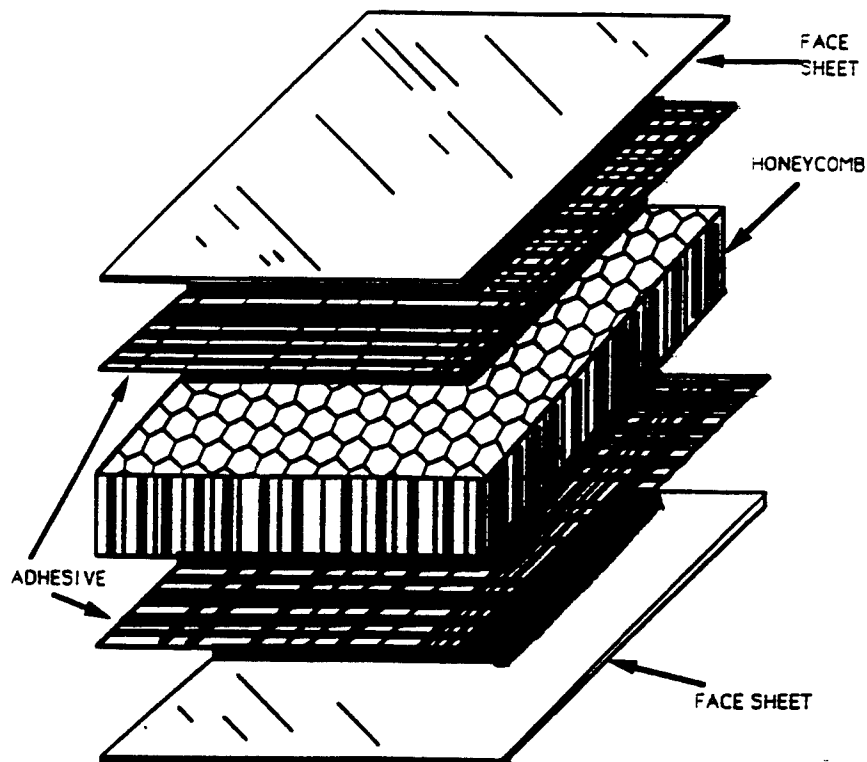


Figure 1.1. Sandwich Construction

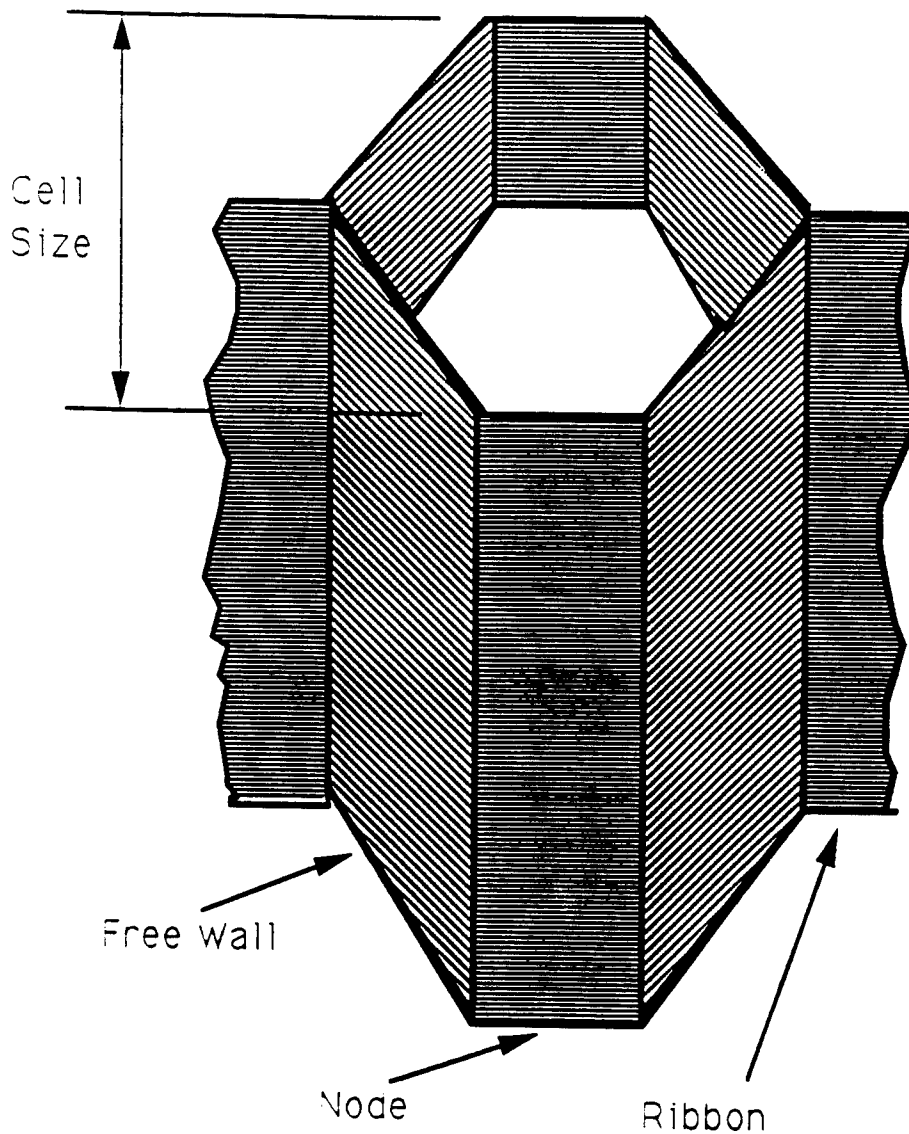


Figure 1.2. Honeycomb Core

In the early eighteenth century the concept of removing material doing the least work was developed and eventually led to the I beam design (See Fig. 1.3). The sandwich panel can be thought of as a type of I beam. The face sheets of the sandwich panel act similarly to the flanges by taking the bending loads. Expanding this comparison, the honeycomb core corresponds to the web of the I beam. The core resists the shear loads and increases the stiffness of the structure but unlike the I beam's web, gives continuous support to the face sheets [3].

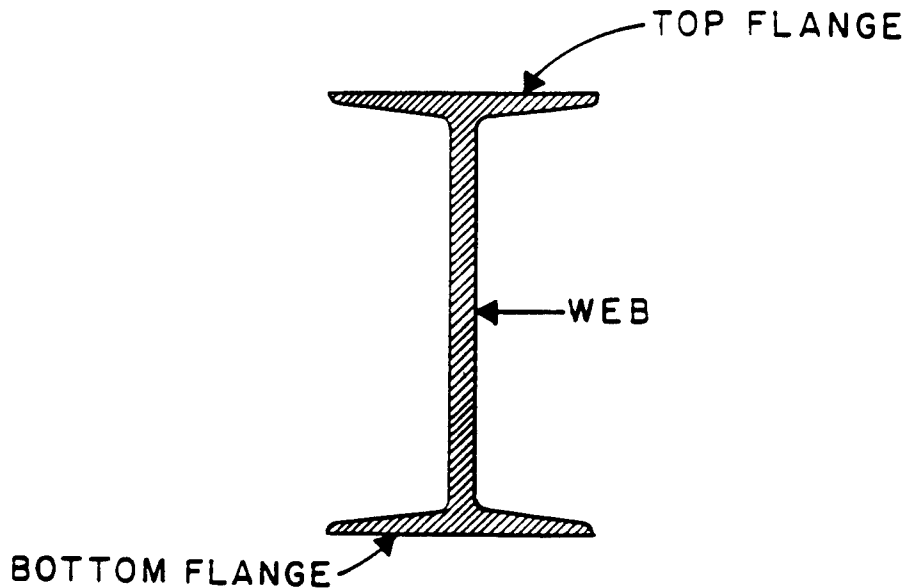


Figure 1.3. I Beam

The bending strength to weight ratio of composite sandwich structures, in general, is superior to that of solid configurations, the graphite epoxy composite material without the core. Also, composite sandwich construction lends itself to a practically unlimited variety of materials and panel configurations. The users may select from a wide range of core and composite face sheet materials combining the two to fit their individual needs.

Bonded honeycomb sandwich construction has been a basic structural concept in the aerospace industry for the last thirty years. Virtually every aircraft flying today depends upon the integrity and reliability offered by this structural approach [1]. The capability has been proven in secondary structures. Efforts continue toward the use of composite sandwich structure components in primary structures.

In order to integrate sandwich structure effectively into primary structure, the design of the sandwich structure must be optimized to reduce weight and costs through reduced complexity, reduced structural part count, and improved design efficiency. It has

been noted that unless very thick face sheets are used, the in-plane compressive strength is relatively poor because of possible face sheet wrinkling [4]. A thick face sheet design condition is a nonconventional configuration; therefore, the associated failure characteristics as well as the optimal face sheet thickness have not been addressed [5].

The failure characteristics of composite materials subjected to low velocity impact (Figure 1.4.) has been investigated by many researchers [6 - 9]; however relatively little has been done on sandwich structures. The effects of low velocity impact are important because aircraft structures can be susceptible to this type of damage on a daily basis. For example, tools may be dropped during maintenance or the aircraft may be subject to runway debris, hail, or other similar objects. Typically, low velocity impact damage does not result in the puncture of the structure but causes damage to the structure, and results in a loss of strength although the damage may not be visible to the naked eye [10]. In fact, it has been shown [11] that delamination induced by low energy, low velocity impact can reduce the tensile strength of composite laminates by as much as twenty-five percent and the static compressive strength by amounts in excess of sixty percent, with very little visible damage [12].

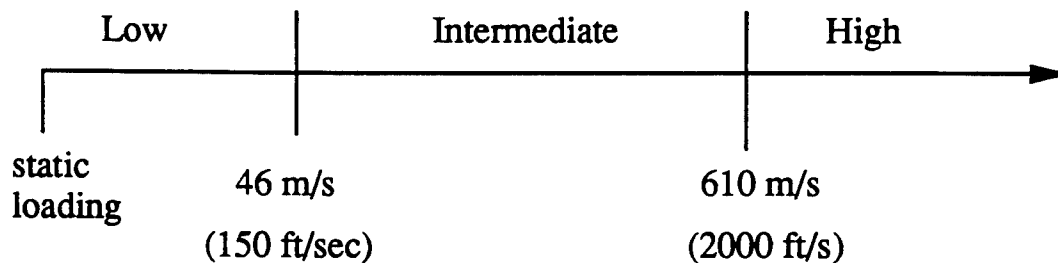


Figure 1.4. Low Velocity Impact

Damage of composite sandwich panels caused by low velocity impact has been studied both analytically [13, 14] and experimentally [15 - 17]. Impact damage tolerance testing of bonded composite sandwich panels were performed by Cadwell, Borris and Falabella [18]. Lee, Huang, Fan studied the dynamic responses of sandwich panels subjected to low velocity impact [19]. The effect of low energy impact damage on the edgewise compression strength of Graphite/Epoxy sandwich panels were determined experimentally by Palm [20]. Lagace, Tsang and Williamson studied the failure modes and mechanisms associated with impact damaged sandwich panels considering the separate contributions of face sheet damage and core damage [21, 22].

The failure mechanisms associated with low velocity impacted sandwich panels have not received much attention experimentally or analytically . Sandwich panels with thin face sheets are the only exception to this lack of documentation. Consequently, more research effort is needed to characterize the failure mechanism of face sheet panels of various thicknesses.

1.2 Purpose

The purpose of this thesis is to experimentally investigate the progression of failure of composite honeycomb sandwich panels with increasing face sheet thicknesses and constant core thickness. The panels consist of AS4/3501-6 Graphite Epoxy face sheets, HRH-10-1/8-9.0 Nomex honeycomb core and FM 300-2 film adhesive. The face sheets have the following stacking sequence: $[0/90]_s$, $[0/90]_{2s}$, $[0/90]_{4s}$, $[0/90]_{8s}$, and $[0/90]_{12s}$. The panels were subjected to various low velocity impacts at room temperature.

1.3 Scope

The experiments performed as part of this thesis incorporated both post-test inspection of the specimens and in-situ instrumentation to characterize the response of flat sandwich panels to low velocity impact. Post impact analysis was made possible using C-scans and optical cross-sectional microscopy.

II. Experimental Procedures

In this chapter, the materials and equipment used to complete the experiments are presented. Also, equipment performance parameters and data collection techniques are explained. The actual test results are given in Chapter III.

2.1 Test Specimens

The specimens used in this series of tests are flat sandwich panels made of AS4/3501-6 Graphite/Epoxy face sheets, HRH-10-1/8-9 Nomex (145 kg/m (9 lb/ft³), 0.3175 cm (1/8 in) cell size) honeycomb core and FM 300-2 film adhesive. The thickness of the sandwich panel face sheets, 0.0127 cm (0.005 in) per ply varied according to Table 2-1. The 4 ply lay-up is compared to the 48 ply lay-up in Figure 2.1.

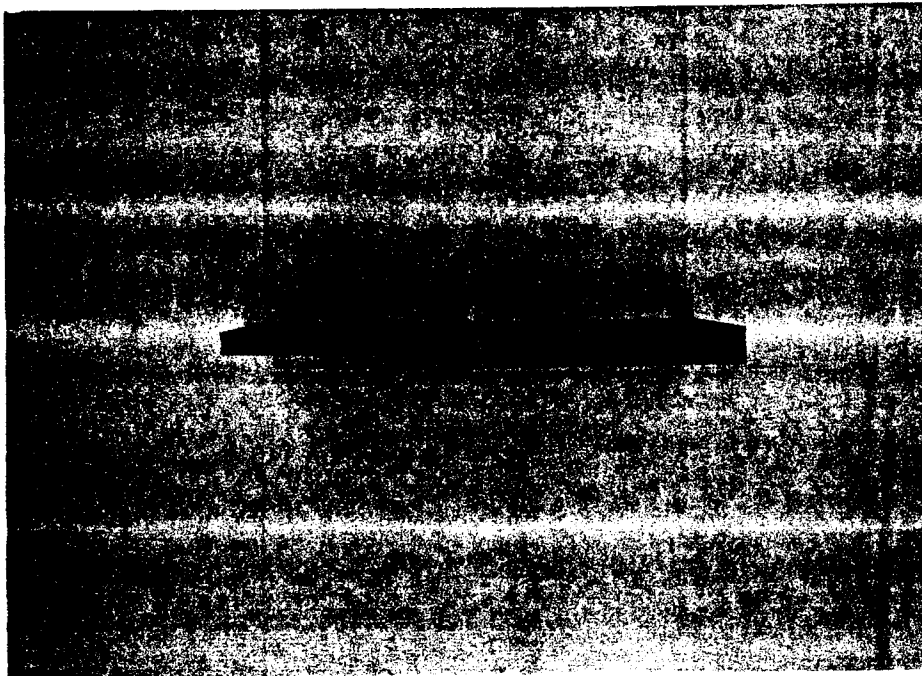


Figure 2.1. Comparison of 4-ply and 48-ply sandwich panels

The thickness of the core, 1.27 cm (0.5 in) and the thickness of the adhesive, 0.0254 cm (0.01 in) remained constant. The dimensional measurements of the core cells are shown in Figure 2.2. The honeycomb for the sandwich panels are shown in Figure 2.3. The overall thickness included in Table 2-1 includes the thickness of the top and bottom face sheets as well as the core and adhesive. Note that the thickness of the adhesive is equivalent to 2 plies of the face sheet material. Table 2-1 also indicates the various ply lay-ups tested.

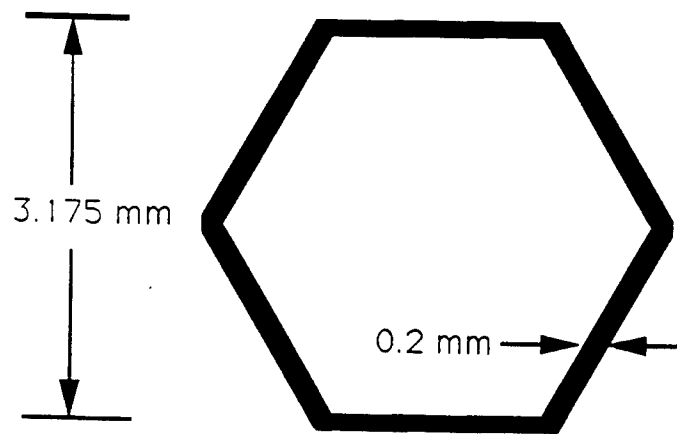


Figure 2.2 Honeycomb Core Two-Dimensional Measurements

TABLE 2-1
FACE SHEET STACKING SEQUENCES

<u>Lay-up</u>	<u>No. of Plies</u>	<u>Lay-up Thickness (cm)</u>	<u>Overall Thickness (cm)</u>
[0/90]s	4	0.0508	1.4224
[0/90]2s	8	0.1016	1.5240
[0/90]4s	16	0.2032	1.7272
[0/90]8s	32	0.4064	2.1336
[0/90]12s	48	0.6096	2.5400

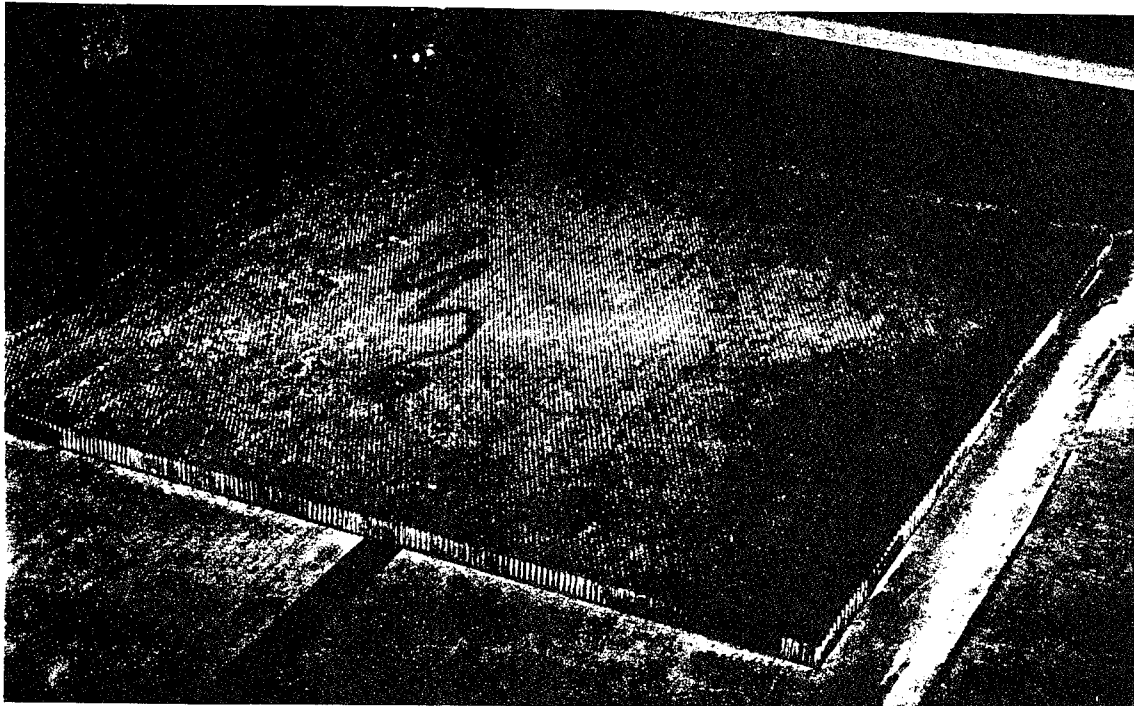


Figure 2.3. Honeycomb Core before Sandwich Panel Fabrication

To determine the basic property data for the face sheet material, 0° tension, 0° compression, 90° tension, 90° compression and $\pm 45^\circ$ shear specimens were fabricated and tested as outlined in Appendix A, the Test Plan submitted to Wright Laboratory. The Test Plan provides the specifications to construct the sandwich panels and basic property specimens for the AS4/3501-6 face sheet material. The results of the basic property tests are included in Appendix B. Table 2-2 outlines the property tests, resulting curves and corresponding basic properties. This information can be incorporated in a finite element program to determine ply failure [which was not carried out in this thesis].

The basic properties of the adhesive and core were determined from the manufacturer's specification. In the case of the core, the curves shown in Figure 2.4 and 2.5 were extrapolated from curves of a Nomex honeycomb core with a density of 64 kg/m^3 (4.0 lb/ft^3) rather than the 145 kg/m^3 (9.0 lb/ft^3) [23]. This was done because the manufacturer did not have the material property curves for the density of honeycomb core

used in this study. The shear properties of the adhesive (Figure 2.6) were obtained directly from the manufacturer [24].

TABLE 2-2
PROPERTY TESTS - RESULTING CURVES - CORRESPONDING BASIC
PROPERTIES [25]

<i>TEST</i>	<i>CURVE</i>	<i>PROPERTY OBTAINED</i>
0° Tension	σ_1 vs ϵ_1 \longrightarrow ν_{12} vs ϵ_1 \longrightarrow	E_1^T ν_{12}^T
0° Compression	σ_1 vs ϵ_1 \longrightarrow ν_{12} vs ϵ_1 \longrightarrow	E_1^C ν_{12}^C
90° Tension	σ_2 vs ϵ_2	E_2^T
90° Compression	σ_2 vs ϵ_2	E_2^C
$\pm 45^\circ$ Tension	τ_{12} vs γ_{12}	G_{12}

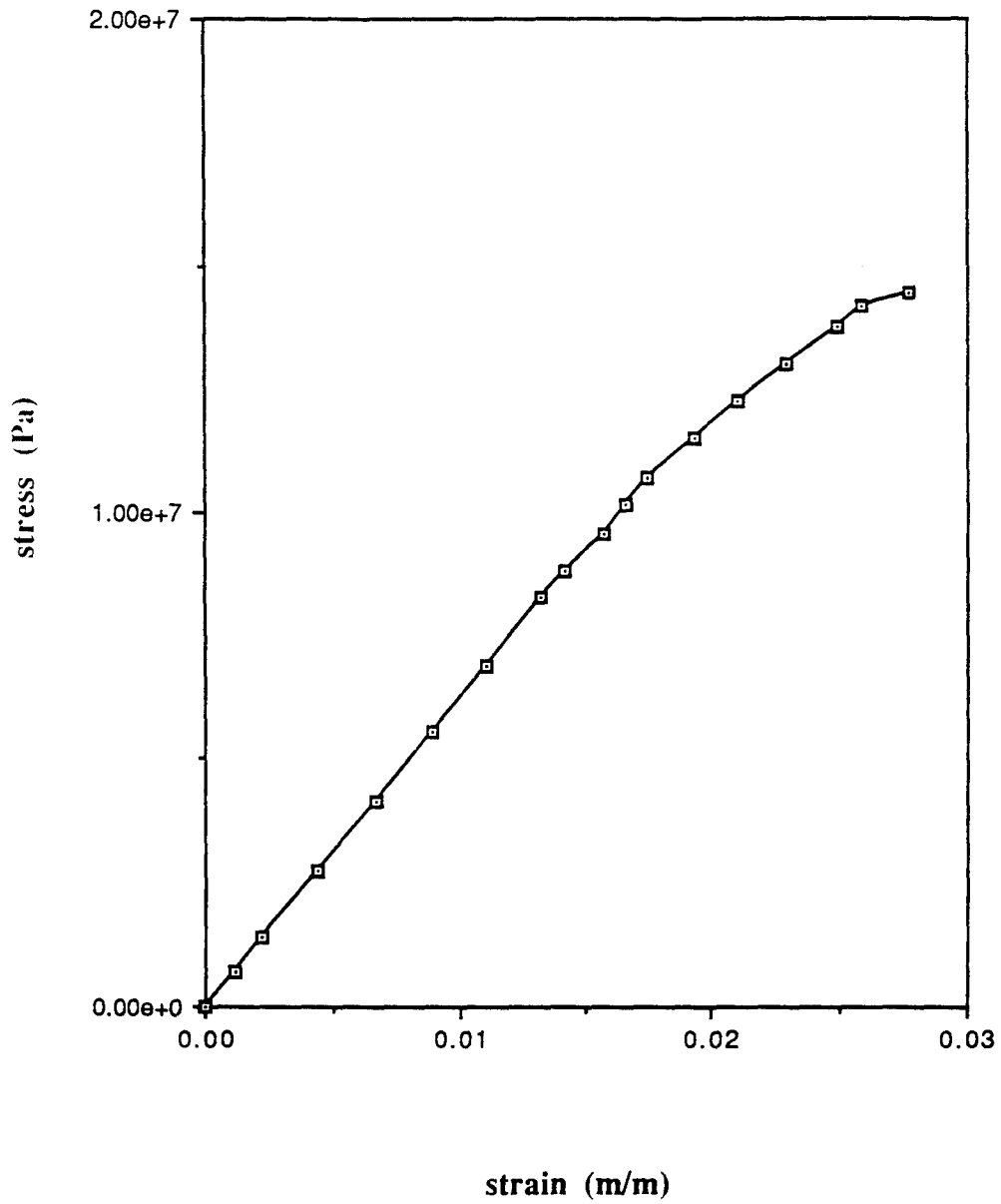


Figure 2.4. Room Temperature Stabilized Compression Stress-Strain Curve for Nomex HRH-10-1/8-9.0 Honeycomb Core (σ_2 vs ϵ_2)

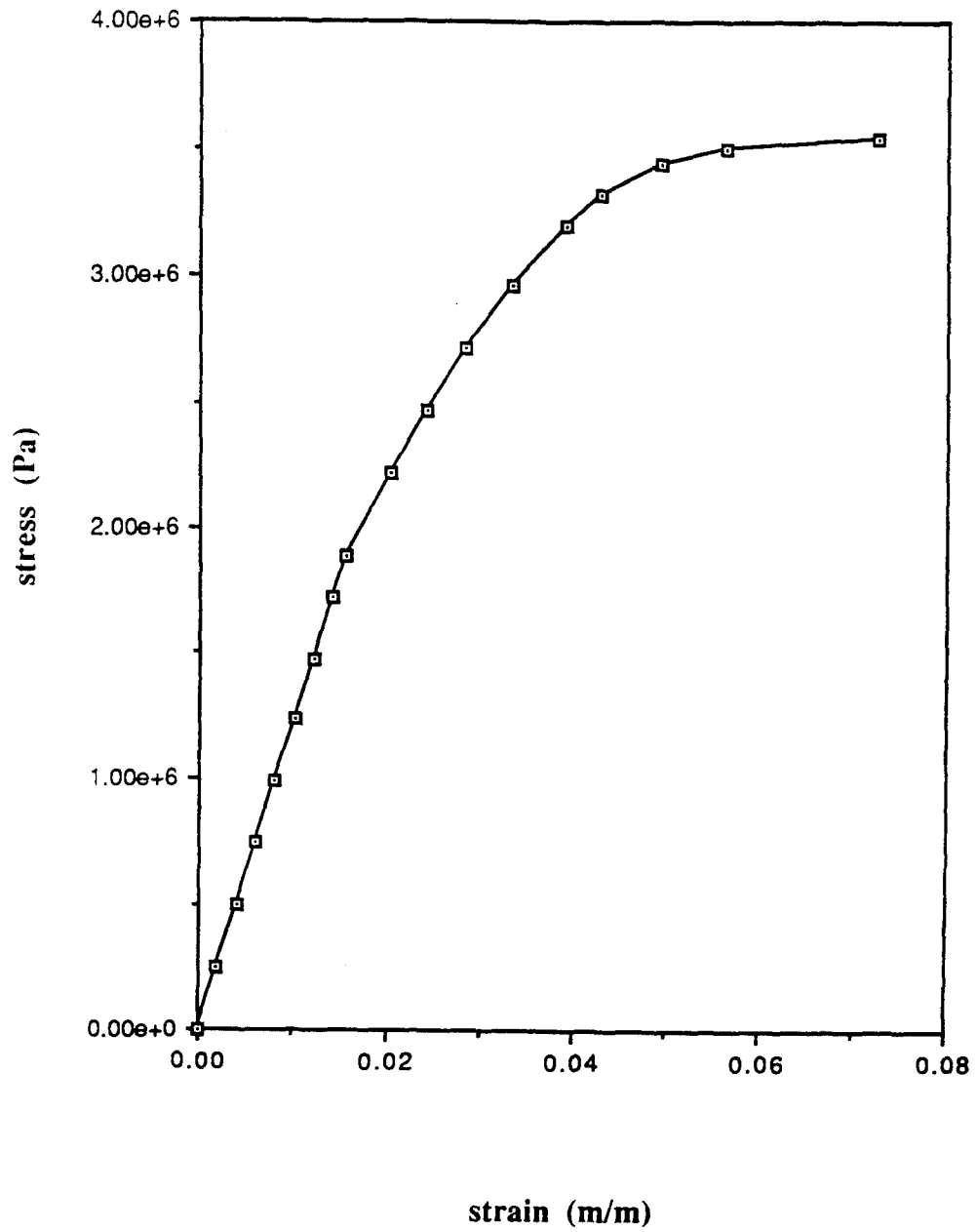


Figure 2.5. Room Temperature "L - Direction" Stress-Strain Curve for Nomex HRH-10-1/8-9.0 Honeycomb Core (τ_{12} vs γ_{12})

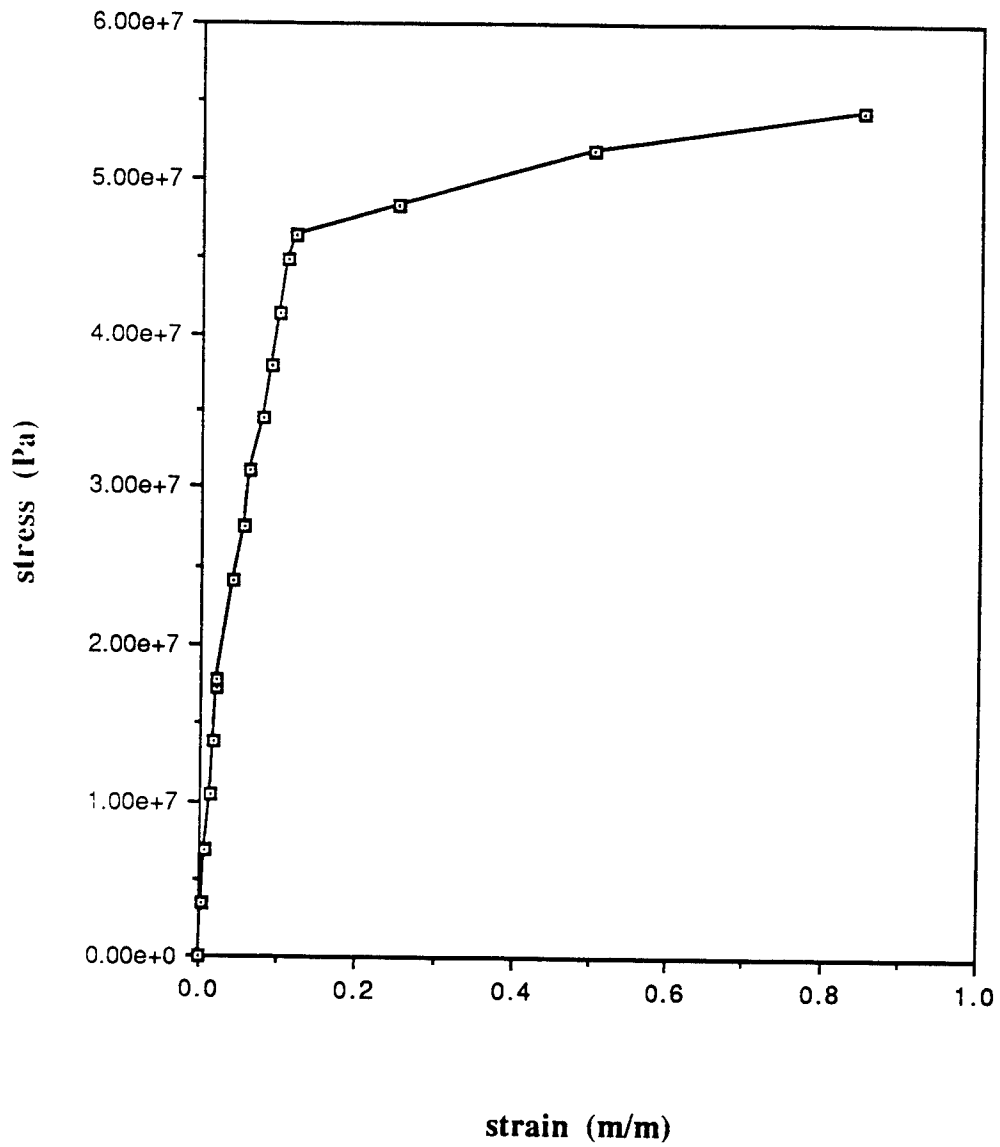


Figure 2.6. Room Temperature Shear Stress-Strain Curve for FM 300-2 Film Adhesive (τ_{12} vs γ_{12})

Before adhering the core, the thickness of the face sheets were carefully measured in several locations and recorded. To ensure uniformity in thickness, the variation of these measurements were not to be in excess of 0.001524 cm (0.0006 in) per ply. Next, the face sheets were subjected to thorough ultrasonic C-scan to detect voids or other flaws. The average void content was less than 1.1% for all panels. One significant flaw was found in the 16 ply lay-up, but this area of the panel was not used in the fabrication process. Resin content analyses were also conducted. Resin content varied from 24-30% by weight (Table 2-3). The fiber volume fraction V_f was determined from the resin content w_r and the fiber and resin densities, ρ_f and ρ_r , using the following relationship:

$$V_f = \frac{\rho_r(100-w_r)}{\rho_f w_r + \rho_r(100-w_r)} \quad (2.1)$$

with w_r in percent weight and ρ_f and ρ_r in gm/cm^3 [6]. For this study, $\rho_f = 1.7992$ and $\rho_r = 1.2660$, yielding fiber volume fractions from 63-69% (Table 2-3).

TABLE 2-3

FACE SHEETS RESIN VOLUME AND FIBER VOLUME FRACTION

Face Sheet Number of Plies	Resin Content (% by weight)	Fiber Volume Fraction (%)
4	27.0390	65.5017
8	24.3722	68.5874
16	29.6648	62.5236
32	24.1750	68.8181
48	27.5756	64.8883

Six 17.78 cm x 17.78 cm (7 in x 7 in) sandwich specimens for each face sheet thickness were fabricated. These specimens were cut from larger panels as outlined in Appendix A. When fabricating the sandwich panels, the honeycomb core was first adhered to one face sheet as shown in Figure 2.7. After this bond was secured, the other face sheet was adhered to make a complete sandwich panel. This was done to avoid the adhesive dripping down into the honeycomb cells during the bonding process.

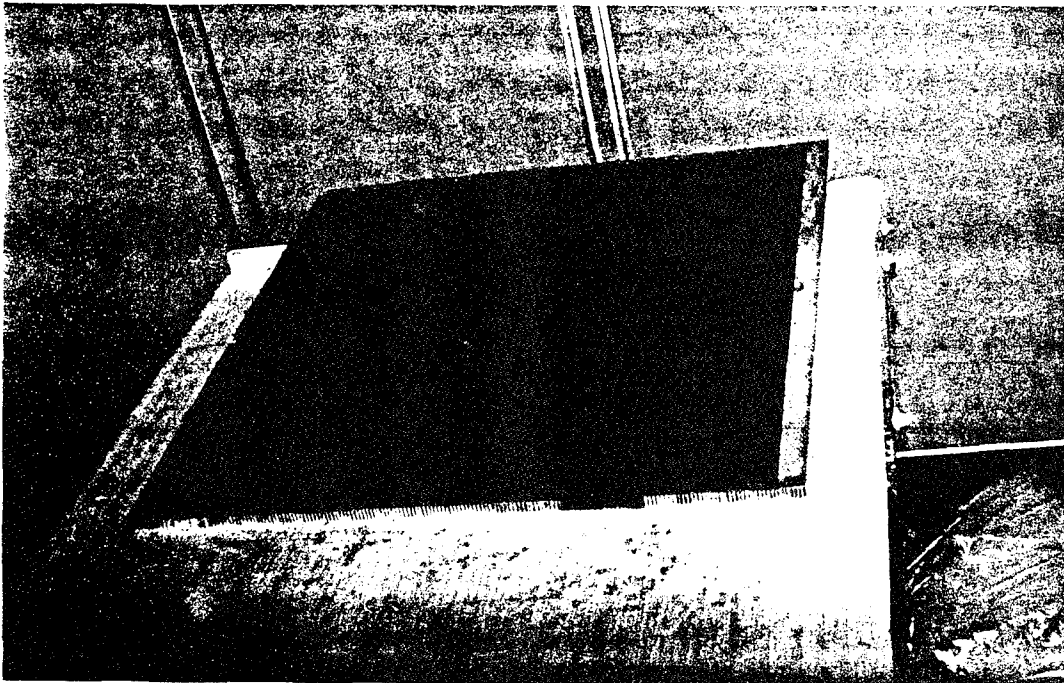


Figure 2.7. 48 Ply Sandwich Panel with Only One Face Sheet

2.2 Impact Facility and Equipment

The experiments were performed at the Low Velocity Impact Facility in the Wright Laboratory (WL) Structural Test Facility (building 65), Wright-Patterson Air Force Base, Ohio. The impact machine is a General Research Corporation GRC 8250 Dynatup drop impact machine as shown in Figure 2.8. The impactor drop weight is 3.63 kg (8 lb). This is the entire lower portion of the impactor assembly which is dropped,

including both the impact tup and the brackets which hold it centered on the impact site (Figure 2.9). The impact tup is the only part of the impactor assembly that come into contact with the specimen (Figure 2.10). The impactor assembly is adjusted to the correct drop height using a cable to raise and lower the impactor. The upper piece of the assembly has a clevis which is released to drop the lower part of the assembly onto the panel. The drop weight assembly slides down along a set of lubricated tubes to keep the impactor aligned on the center of the impact zone. A set of pneumatic brakes initiates to catch the impactor as it rebounds off the panel, preventing multiple bounces on the panel.

The panel is placed on an aluminum support block and secured in a plate (Figure 2.11). The complete assembly is then positioned beneath the impactor. The support block and hold-down plate each have a 12.7 by 12.7 cm (5.0 by 5.0 in) cutout area in the center. Since the panel is 17.8 by 17.8 cm (7.0 by 7.0 in), 5.08 cm (2.0 in) of the panel edges were secured on all four sides.

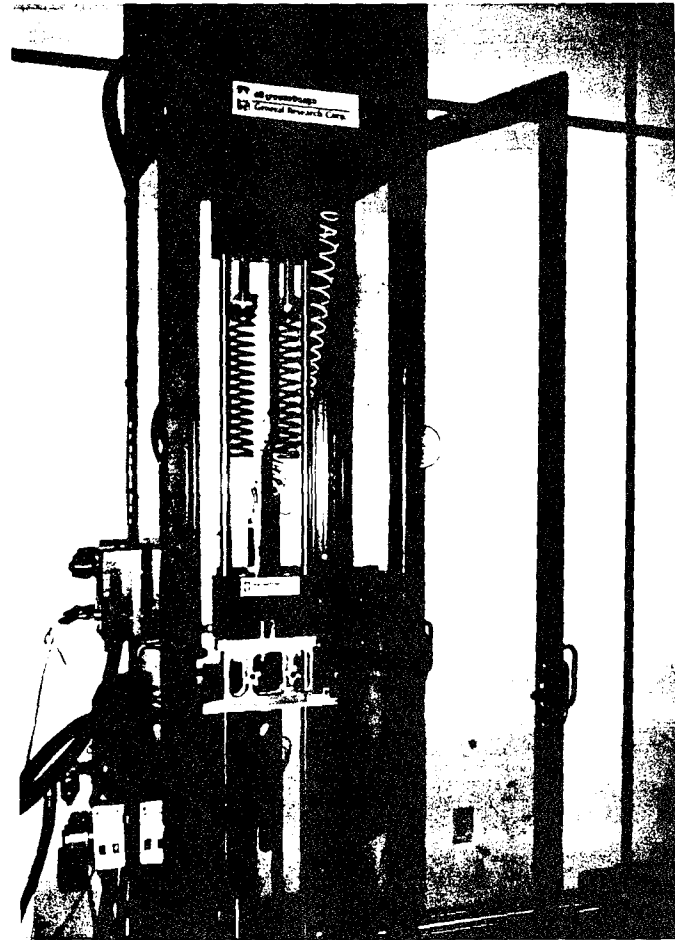


Figure 2.8. Dynatup Impact Machine

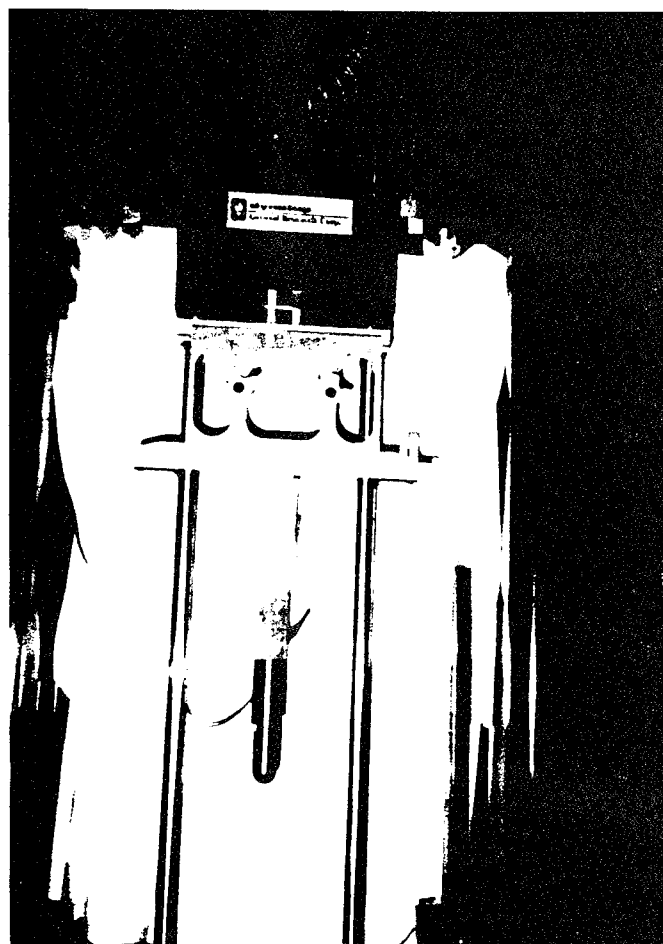


Figure 2.9. Close up of Impact Drop Weight Assembly

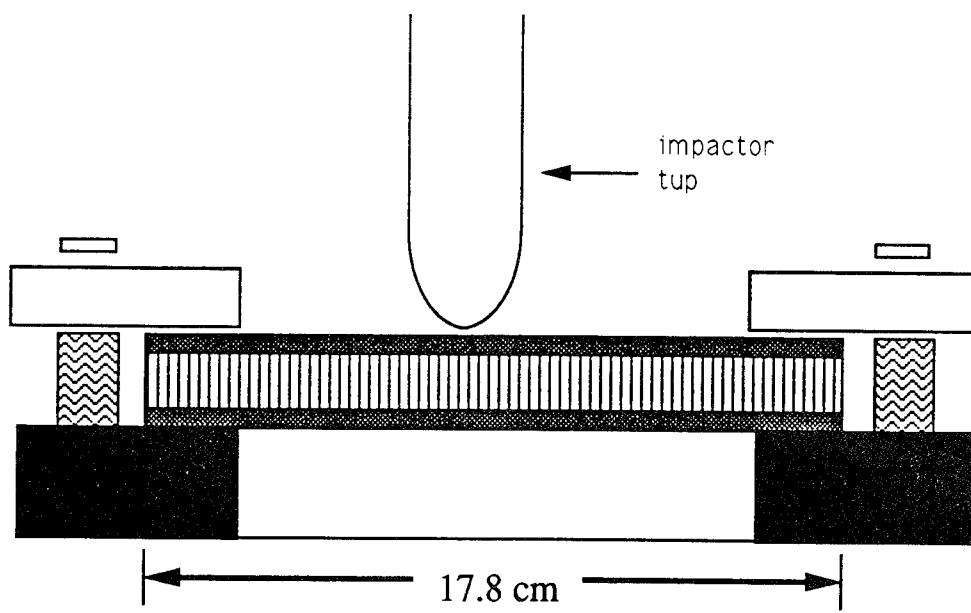


Figure 2.10. Impact Tup in Contact with Sandwich Specimen

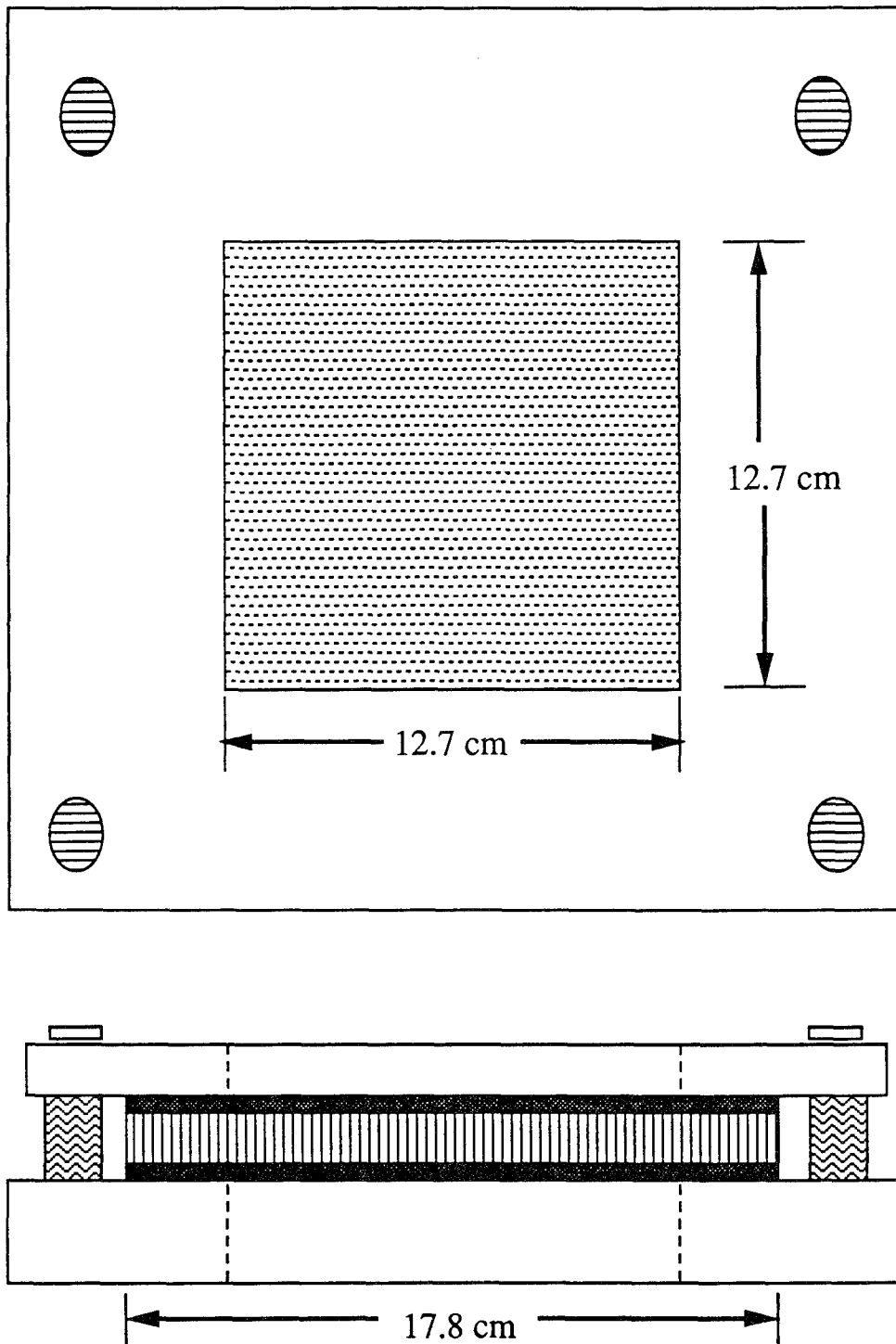


Figure 2.11. Sandwich Panel Secured in Between Support Block and Hold-down Plate

2.3 Data Collection and Processing

The data acquisition and analysis system used was devised by the manufacturer of the Dynatup for use in impact testing. Two instruments are used, a load cell and a velocity detector. The load cell is attached to the drop weight so that it measures the load applied by the impactor during the time it is in contact with the panel. The velocity is determined based on the time required for a strip of metal (a velocity flag) to pass a photo detector beam placed just above the panel being impacted. The velocity flag is attached to the drop weight assembly. When the velocity flag first occludes (blocks) the beam, the photo detector senses the drop in light intensity and toggles a voltage signal off. When the velocity flag passes the beam of light, the photo detector senses the increase in light intensity and toggles the voltage signal on again [26]. Energy calculations are carried out using the impact velocity. Thus the velocity flag is used both to initiate data acquisition and to determine the tup impact velocity.

The tup, which is the impactor/load cell combination, is a cylindrical stainless steel shaft of 2.54 cm (1.0 in) diameter with a hemispherical tip. This model is designed to incorporate various tup configurations. Only one tup configuration was used for all tests reported in this thesis.

The computations used by the system to determine the impact velocity, absorbed energy, and displacements are provided in Appendix D. This data can be displayed on the screen immediately after completion of the test using the General Research Corporation GRC 730-I Instrumented Impact Test Data System. This is an IBM PC-XT computer with a high speed data acquisition ability. The signals from both the load cell and velocity detector are collected, converted to engineering units and stored on disk. Figure 2.12 shows the output generated from a typical impact test. The graphs for the rest of the test performed are in Chapter 3.

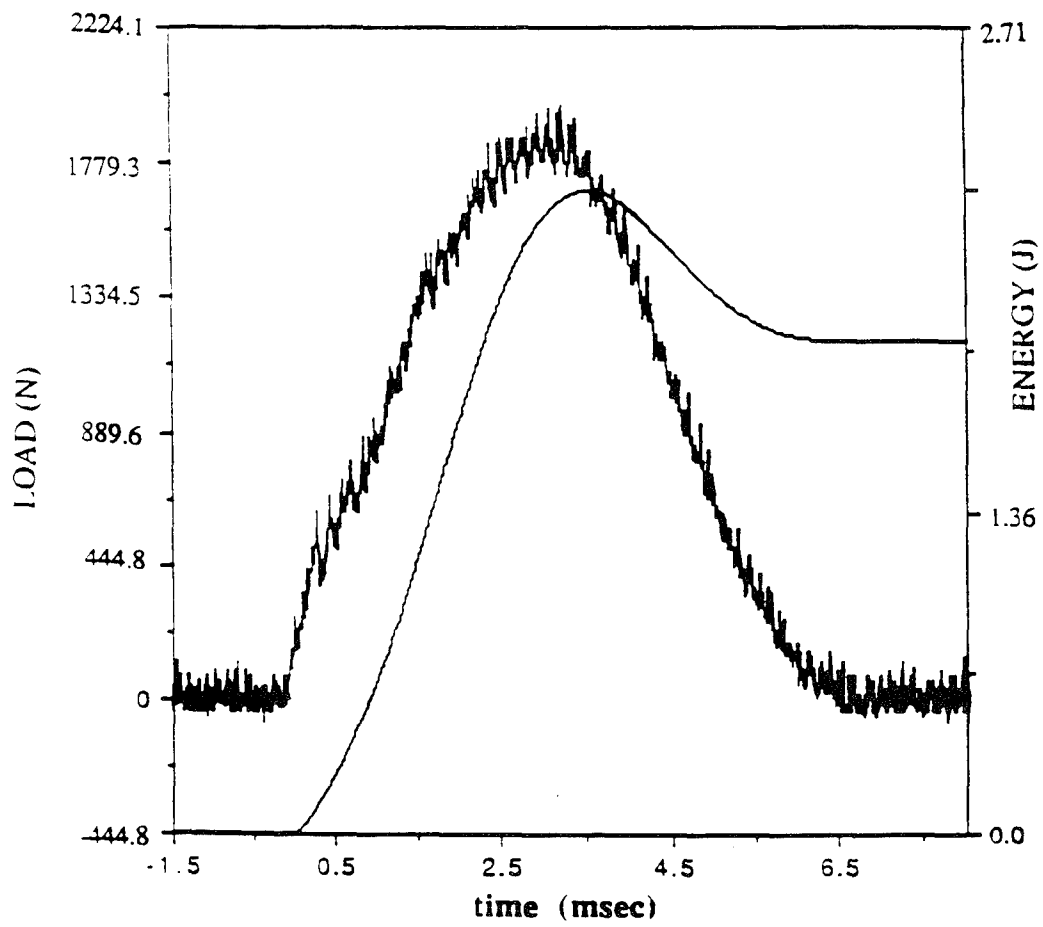


Figure 2.12 Example of Load and Energy Plot from Dynatup

2.4 Post Impact

Following impact, the depth of the dent of all sandwich panels with visible damage was measured using a dial gage indicator. The radius of the damage was measured across the widest point of the indented damage area using a measuring scale (± 0.08 cm/0.03 in). Next, the impacted specimens were subjected to pulse-echo C-scan to determine the extent of damage. Once the damage was ascertained from the C-scan, the area was cut along the longitudinal axis using a water-cooled diamond saw resulting in a 2.54 cm (1 in) x 1.27 cm (0.5 in) specimen. The small specimens were potted in an iridescent epoxy. The iridescence of the epoxy enhanced the visualization of damage. After curing, the specimens were polished, first with sandpaper and then with diamond paste of increasing fineness down to 1 micrometer diameter. Micrographs of the cross-sections were taken with an optical microscope. Next, the potted 2.54 cm x 1.27 cm specimens were cut along the transverse direction. Micrographs were also taken from this point of view. Figure 2.13 illustrates the cross-sectioning of the sandwich panel.

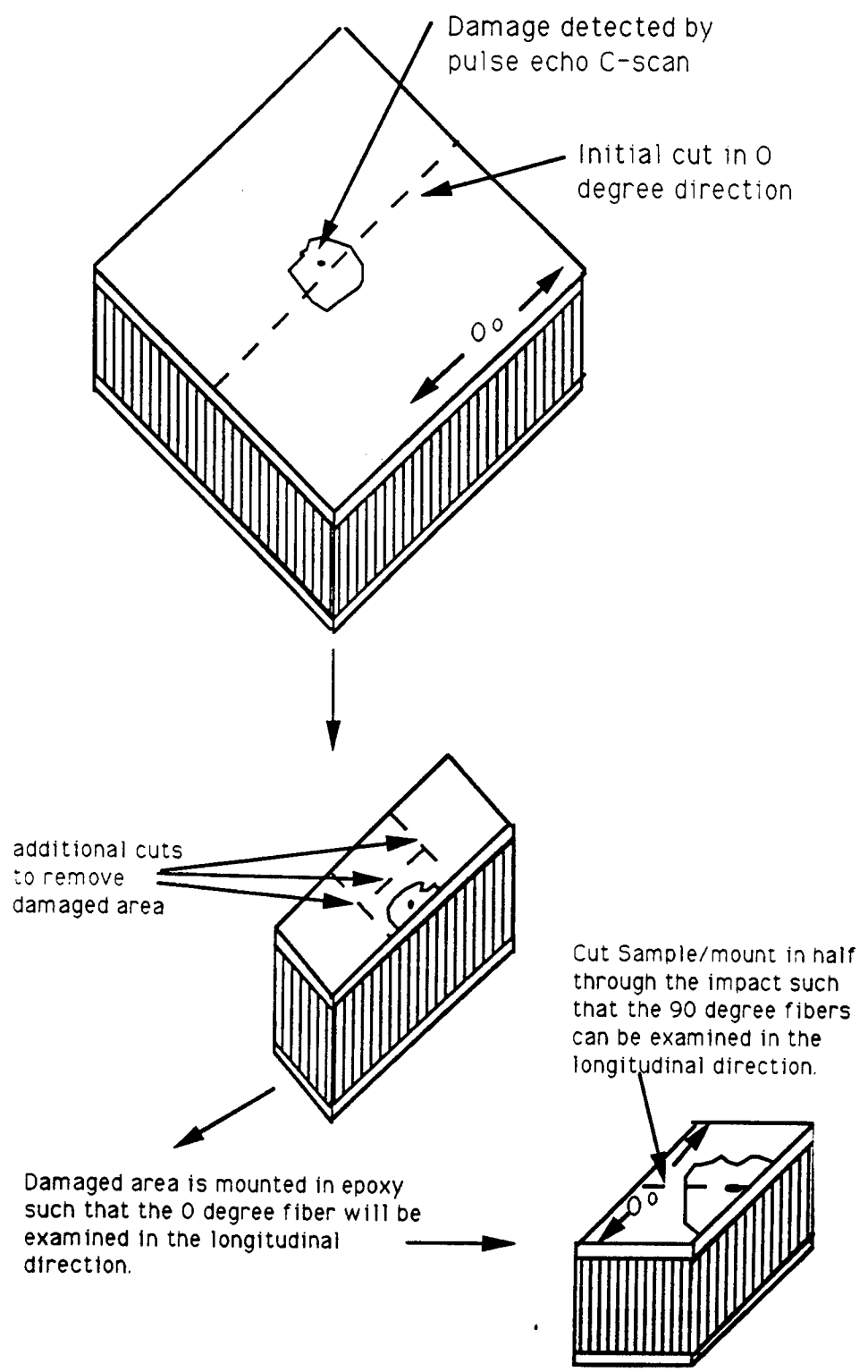


Figure 2.13 Cross-Sectioning [27]

III. Experimental Results

The experiments resulted in the measurement of the load, energy, velocity, and deflection of the tup as functions of time. The effect of these parameters is important in determining the sandwich panel response. Table 3.1 summarizes the key measurements obtained during the experiments. These results will be discussed in this chapter and the load and energy time curves will be presented.

After impact, the depths of the permanent indentation of all sandwich panels with visible damage were measured using a dial gage. The radius of the damage was measured across the widest point of the indentation using a ruler. The damage area obtained from the C-scans were measured using a planimeter. Table 3.2 summarizes these measurements. These results will be discussed.

The damage progression in the sandwich panels with 4-ply, 8-ply, 16-ply, 32-ply and 48-ply face sheets as the drop height increases will be examined individually. Next, a comparison of sandwich panels with different face sheet thicknesses impacted at the same drop height will be investigated.

3.1 Load and Energy Curves from Dynatup

After completion of each impact test, the General Research Corporation GRC 730-I Instrumented Impact Test Data System generated a load versus time and an energy versus time curve. Figure 3.1 displays the curves generated after impact of a sandwich panel with 16-ply face sheets. Significant points that describe the sandwich panel's response are indicated.

The first minor peaks of the load curve are repeatable in each test series of same face sheet thickness. These are believed to be elastic response due to the plate

TABLE 3-1. Summary of Data Collected from Dynatup

Panel Number	Stacking Sequence	Number of Plies	Drop Height (cm)	Max Load (N)	Energy at Max Load (J)	Absorbed Energy (J)	Impact Energy (J)	Impact Velocity (m/s)	Max Disp (cm)
16694-3-1	[0/90]s	4	3.81	1321.6	1.292	1.056	1.27	0.84	0.1862
16694-3-2	[0/90]s	4	5.08	1620.9	1.718	1.386	1.68	0.96	0.2003
16694-3-5	[0/90]s	4	6.35	1665.0	1.970	1.646	2.06	1.06	0.2417
16694-3-6	[0/90]s	4	7.62	1969.7	2.672	2.076	2.62	1.20	0.2640
16894-2-1	[0/90]2s	8	7.62	2106.7	2.653	2.129	2.60	1.20	0.2261
16894-2-2	[0/90]2s	8	7.62	2121.4	2.503	1.994	2.56	1.18	0.2197
16894-2-3	[0/90]2s	8	8.89	2391.8	2.954	2.451	3.05	1.30	0.2458
16894-2-6	[0/90]2s	8	10.16	2596.0	3.215	2.530	3.35	1.36	0.2483
17294-1-1	[0/90]4s	16	11.43	3304.6	3.628	3.109	3.97	1.48	0.2121
17294-1-2	[0/90]4s	16	11.43	3057.7	3.982	3.192	3.95	1.48	0.2103
17294-1-3	[0/90]4s	16	12.70	3473.2	4.225	3.364	4.26	1.53	0.2154
17294-1-4	[0/90]4s	16	13.97	3747.2	4.409	3.829	4.85	1.63	0.2310
17294-1-5	[0/90]4s	16	15.24	3669.8	4.852	4.126	5.21	1.69	0.2392
17294-1-6	[0/90]4s	16	16.51	3914.0	5.591	4.530	5.74	1.78	0.2584
17594-1-5	[0/90]8s	32	12.70	6377.0	3.537	2.644	4.27	1.53	0.1247
17594-1-6b	[0/90]8s	32	13.97	6377.0	3.944	4.137	4.70	1.61	0.1404
17594-1-1	[0/90]8s	32	15.24	6888.1	4.034	4.608	5.18	1.69	0.1460
17594-1-2	[0/90]8s	32	15.24	6320.0	3.962	4.455	5.17	1.69	0.1505
17594-1-3	[0/90]8s	32	16.51	6718.1	4.196	4.942	5.67	1.77	0.2154
18294-2-6	[0/90]12s	48	20.32	9978.7	6.428	4.678	6.89	1.95	0.1295
18294-2-2	[0/90]12s	48	22.86	10498.7	7.151	5.177	7.78	2.07	0.1366
18294-2-5	[0/90]12s	48	25.40	11210.9	8.256	6.587	8.84	2.21	0.1444
18294-2-4	[0/90]12s	48	27.94	11808.7	8.837	7.311	9.67	2.31	0.1522

TABLE 3-2. Summary of Post Impact Data Collected

Panel Number	Stacking Sequence	Number of Plies	Drop Height (cm)	Permanent Indentation Depth (cm)	Permanent Indentation Diameter (cm)	Damage Area (cm ²)
16694-3-1	[0/90]s	4	3.81	no data	no data	no data
16694-3-2	[0/90]s	4	5.08	0.008	1.02	1.7979
16694-3-5	[0/90]s	4	6.35	0.017	1.02	1.8835
16694-3-6	[0/90]s	4	7.62	0.025	1.52	2.2259
16894-2-1	[0/90]2s	8	7.62	0.015	1.02	1.6266
16894-2-2	[0/90]2s	8	7.62	0.015	1.02	1.6266
16894-2-3	[0/90]2s	8	8.89	0.017	1.02	1.7979
16894-2-6	[0/90]2s	8	10.16	0.030	1.27	2.1403
17294-1-1	[0/90]4s	16	11.43	0.013	0.77	2.0547
17294-1-2	[0/90]4s	16	11.43	0.015	0.77	2.0547
17294-1-3	[0/90]4s	16	12.70	0.017	0.77	1.9691
17294-1-4	[0/90]4s	16	13.97	0.017	1.02	2.1403
17294-1-5	[0/90]4s	16	15.24	0.020	1.02	2.6540
17294-1-6	[0/90]4s	16	16.51	0.023	1.27	2.7396
17594-1-5	[0/90]8s	32	12.70	no indentation	no indentation	no damage
17594-1-6b	[0/90]8s	32	13.97	0.005	0.77	3.3388
17594-1-1	[0/90]8s	32	15.24	0.013	1.02	4.6231
17594-1-2	[0/90]8s	32	15.24	0.010	0.77	4.6231
17594-1-3	[0/90]8s	32	16.51	0.013	0.77	5.1368
18294-2-6	[0/90]12s	48	20.32	no indentation	no indentation	no damage
18294-2-2	[0/90]12s	48	22.86	no indentation	no indentation	0.1712
18294-2-5	[0/90]12s	48	25.40	no indentation	no indentation	6.1574
18294-2-4	[0/90]12s	48	27.94	no indentation	no indentation	6.6778

vibration [28]. The maximum load value depends on the severity of the damage. The maximum load is the peak resistive force the plate produces to stop the impact of the tup. This is an indication of the sandwich panel's flexural stiffness [7]. If the impact causes major damage (such as core crushing and ply delamination), then the first drastic load decrease indicates a softening of the impacted sandwich panel due to damage. This damage may be due to delamination or core crushing. The internal load is then redistributed in the sandwich panel. This process continues until the maximum load is reached.

The calculation of the impact energy is shown in Appendix D. There is a finite level of impact energy where damage does not occur in the sandwich panel; however, a slight increase in the energy level of impact results in damage of the panel. This level of impact energy is referred to as the threshold energy. It is dependent upon the thickness of the sandwich panel, the specimen boundary conditions, stacking sequence, impactor shape etc. Another significant energy value is the absorbed energy. Absorbed energy is the amount of energy expended in the specimen during impact. Therefore, this is also the amount of energy the sandwich panel absorbs during the test that leads to damage.

The resolution of the load versus time curve is dependent upon the load cell sensitivity. For this test a 44,482 N (10,000 lb) load cell was used. The data acquisition system can distinguish 2,048 different discrete loads over the -44,482 N (-10,000 lb) load cell range. That is, 1,024 points can be distinguished in each of the positive and load ranges. Therefore, the resolution of the load is 43.4 N (9.76 lb) or ± 21.7 N (± 4.88 lb).

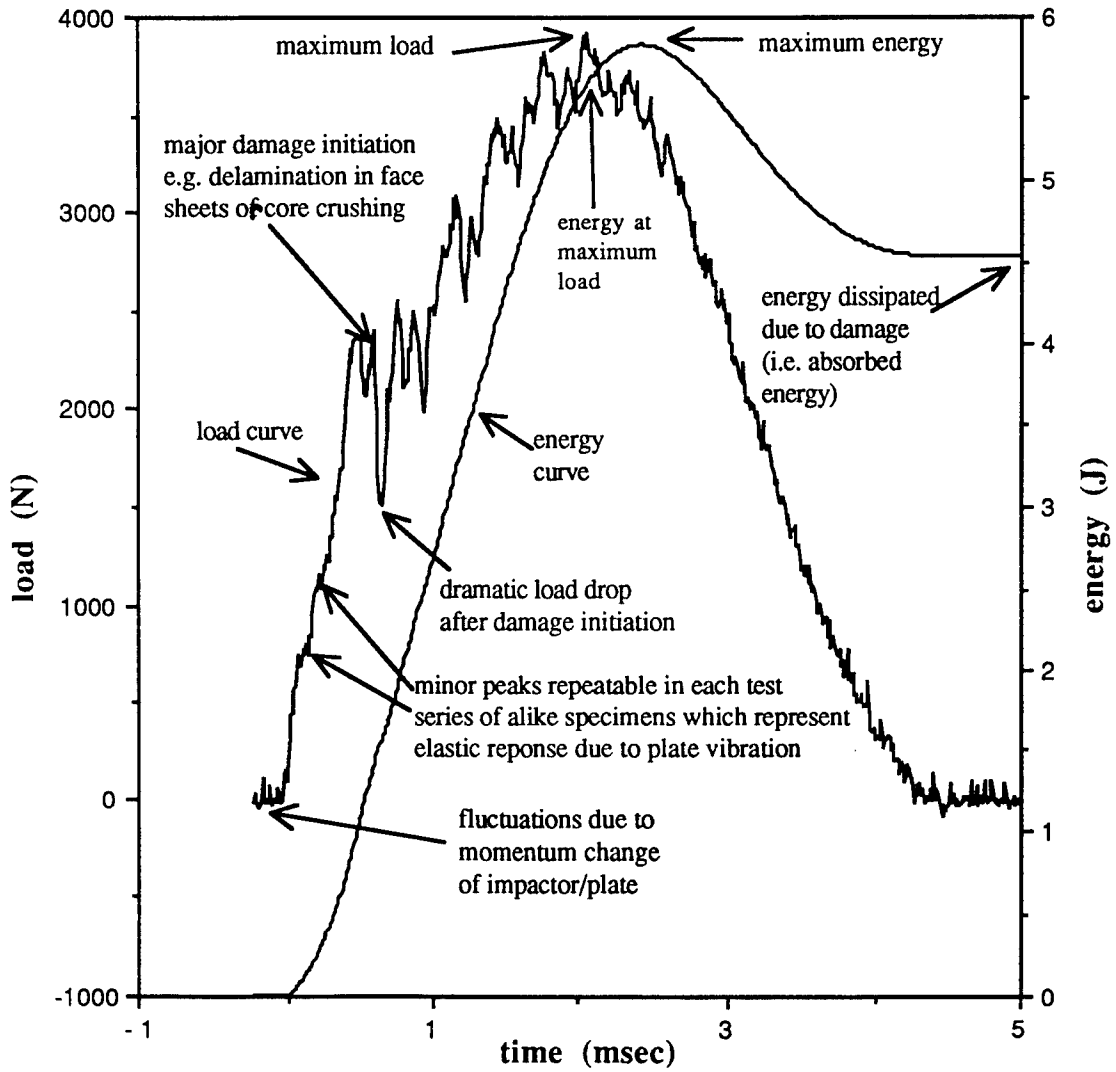


Figure 3.1. Significant Points on Load and Energy Curves

3.2 Failure Characteristics

Throughout this chapter, certain terms will be used to characterize the damage of the face sheet and core. Below are the terms used in this thesis [29. 30]. The terms used to describe core damage are further explained in Figures 3.2.

buckling (core) - failure mode characterized by deflection rather than breaking of honeycomb cell walls due to compressive loading

cripling (core) - failure mode characterized by breaking of honeycomb cell walls due to compressive loading

crushing (core) - failure mode characterized by ripples in honeycomb cell walls due to compressive loading

crazing (face sheet) - formation of fine cracks in the matrix material

delamination (face sheet) interply - separation between two plies

intraply - separation within a ply

matrix crack density (face sheet) - Number of distinctive cracks per unit length

successive ply failure (face sheet) - sequential failures of plies due to increasing impact energies

absorbed energy - the amount of energy dissipated due to damage

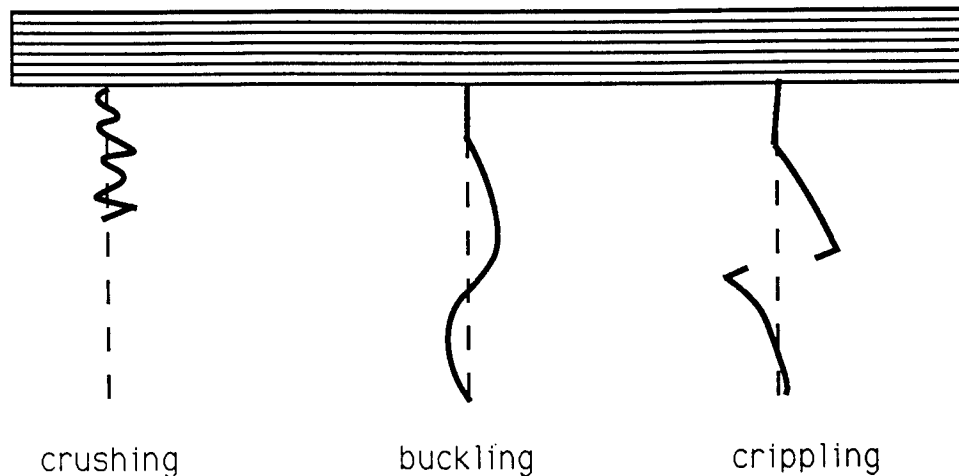


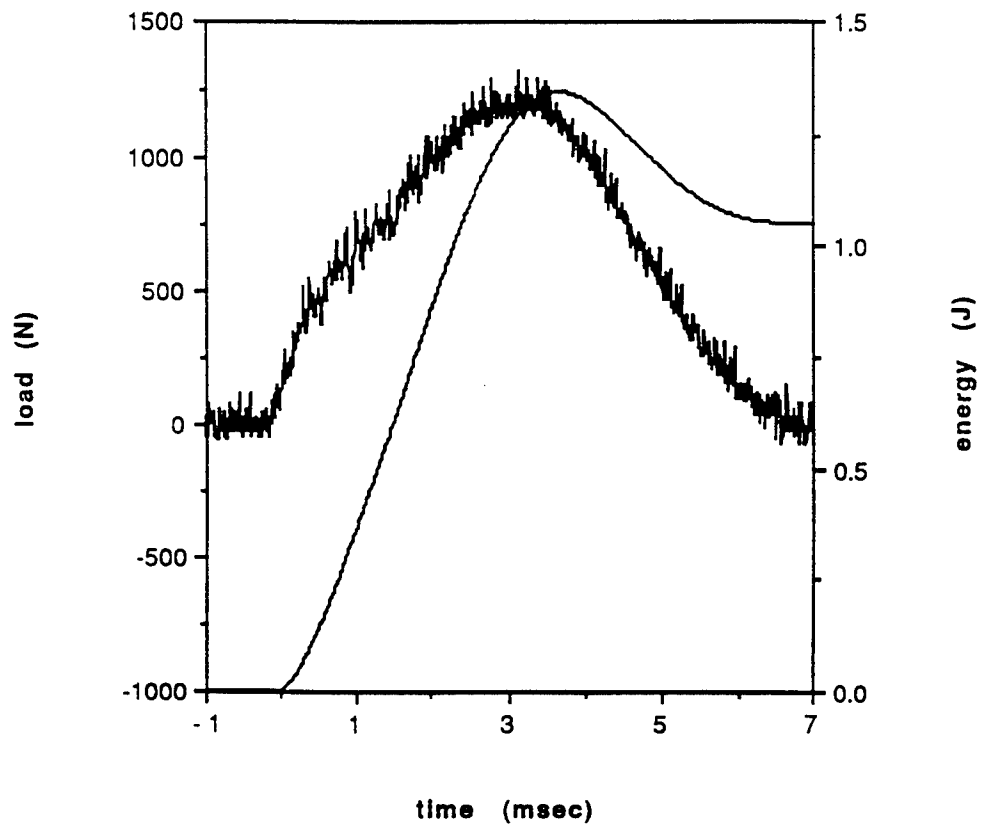
Figure 3.2. Honeycomb Core Failure Modes

3.3 Sandwich Panels with 4-ply Face Sheets

The sandwich panels with 4-ply face sheets were subjected to low energy (velocity) impacts with drop heights ranging from 3.81 cm (1.5 in) to 7.62 cm (3.0 in). Further details will be discussed for each test in this section.

- (1) Impact Energy = 1.27 J (0.94 ft-lb)

The load and energy curves for sandwich panels with 4-ply face sheets at a drop height of 3.81 cm (1.5 in) are shown in Figure 3.3. Because the load curve is not smooth, there are no apparent dramatic drops in the load curve, an indication of the initiation of major damage. The load curve is not smooth because the ratio of the instrumentation and background noise level (which statistically is constant for all tests) to total impact load is larger for the panels with thin face sheets than for the panels with thick face sheets.



Specimen ID -16694-3-1	Max load - 1321.6 N (297.1 lb)
Impact Velocity - 0.84 m/s (2.75 ft/s)	Energy at Max Load - 1.292 J (0.953 ft-lb)
Impact Energy - 1.27 J (0.94 ft-lb)	Time - at Max Load - 3.16 msec
Absorbed Energy - 1.056 J (0.779 ft-lb)	total - 6.29 msec
Max Disp. of Tup 0.186 cm (0.0733 in)	

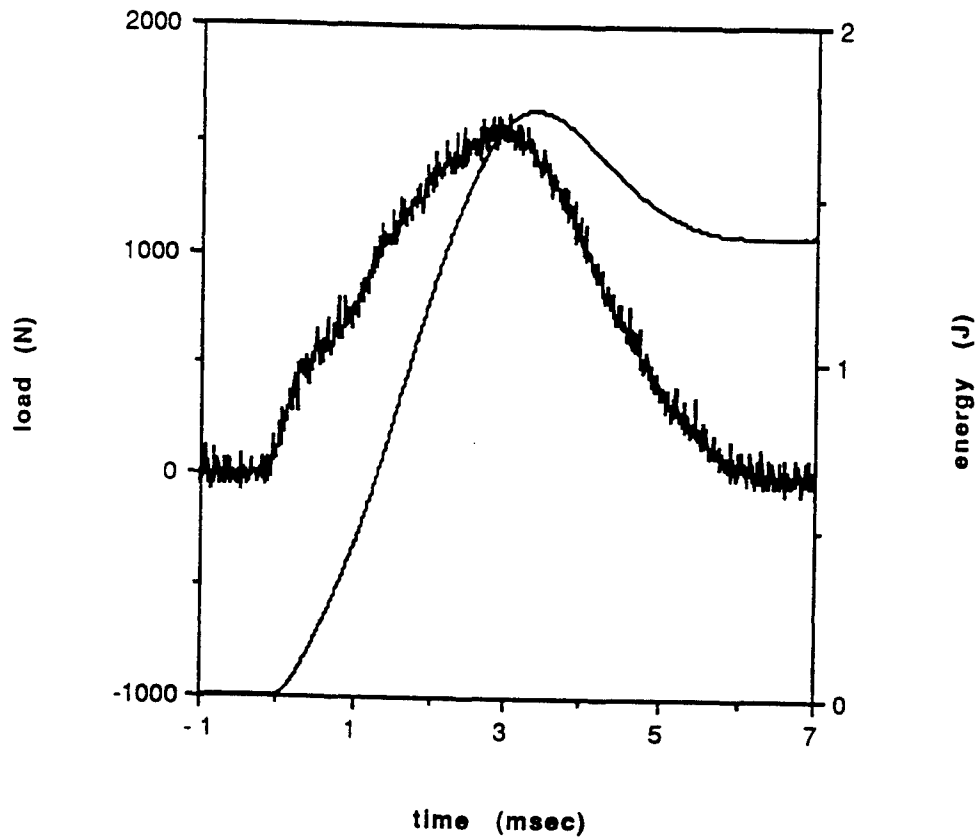
Figure 3.3. Load and Energy from Dynatup for 4-ply at 3.81 cm (1.5 in) drop height

An elastic impact is evident when the energy curve goes back to zero after impact. This did not occur. A total energy of 1.056 J (0.779 ft-lb) was expended in the sandwich panel during impact due to damage. Though the energy and load curves represent the specimen impacted once, the specimen was impacted twice. Because of this, micrographs were not taken for this test. Therefore, the extent of damage and failure modes cannot be examined.

(2) Impact Energy = 1.68 J (1.24 ft-lb)

The sandwich specimen was impacted at a drop height of 5.08 cm (2.0 in). The load curve for this test is presented in Figure 3.4. The load curve was compared with the previous test to see if any similarities exist between the curves (Figure 3.5). The first minor repeatable peaks are present until a load of approximately 500 N (112 lb) is reached. This implies that at this point, the sandwich panel no longer acts in an elastic manner. After this point the curves deviate from each other; however, a slight dip in load exists in each test at approximately 750 N (169 lb). This may be the initiation of major damage.

The maximum load for this test was 1620.9 N (364.4 lb) which is above the estimated start of major damage, 750 N (169 lb). As the load curve indicates, the specimen received major damage due to impact. The details of the damage can be seen in the micrographs. The 0° and 90° cross-sections (Figures 3.6 and 3.7 respectively) are further magnified to 25 times the original size. Because of the size of the 0° cross-section micrographs, the picture had to be separated onto different pages. Figure 3.8 is a guide to the picture organization. The vertical lines under the face sheets are the core walls. The letters on the guide refer to areas that will be discussed in detail. These letters are also on the micrographs. The 90° cross-section micrograph was small enough to fit



Specimen ID - 16694-3-2	Max load - 1620.9 N (364.4 lb)
Impact Velocity - 0.96 m/s (3.16 ft/s)	Energy at Max Load - 1.718 J (1.267 ft-lb)
Impact Energy - 1.68 J (1.24 ft-lb)	Time - at Max load - 3.05 msec
Absorbed Energy - 1.386 J (1.022 ft-lb)	total - 5.92 msec
Max Disp. of Tup 0.200 cm (0.0788 in)	Damage Area - 1.798 cm ² (0.279 in ²)
Damage Indent. - 0.008 cm (0.003 in)	Damage Radius - 1.01 cm (0.4 in)

Figure 3.4. Load and Energy from Dynatup for 4-ply at 5.08 cm (2.0 in) drop height

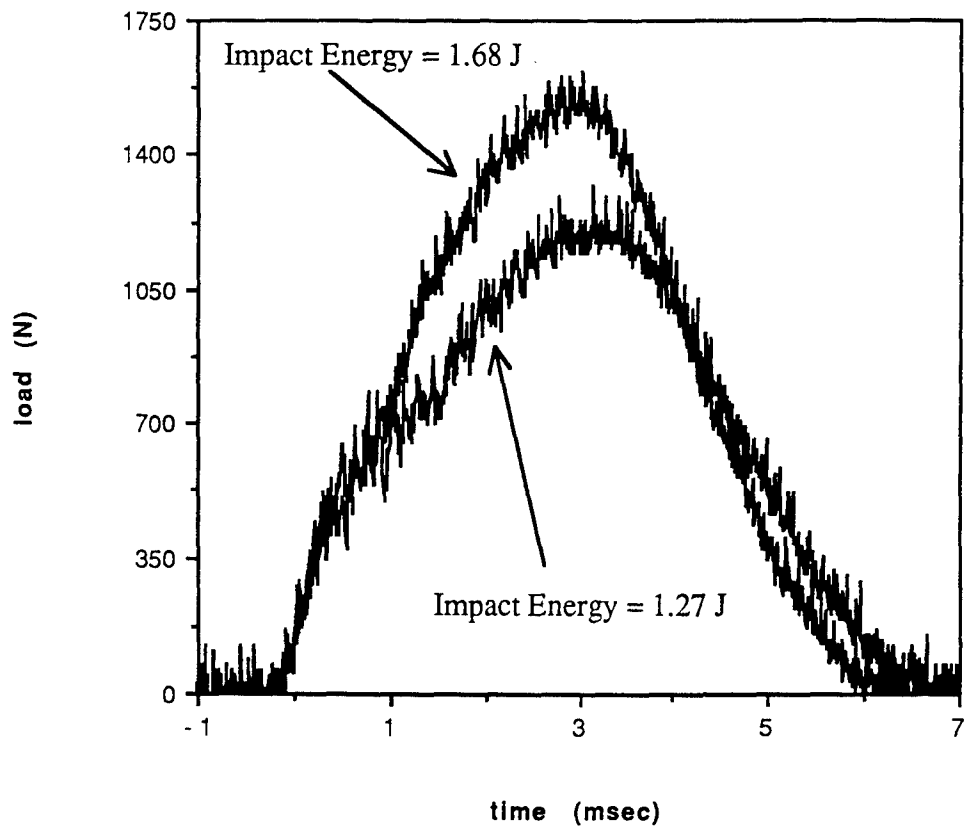


Figure 3.5. Comparison of Load Curves for 4-ply at 3.81 cm (1.5 in) and 5.08 cm (2.0 in) drop heights

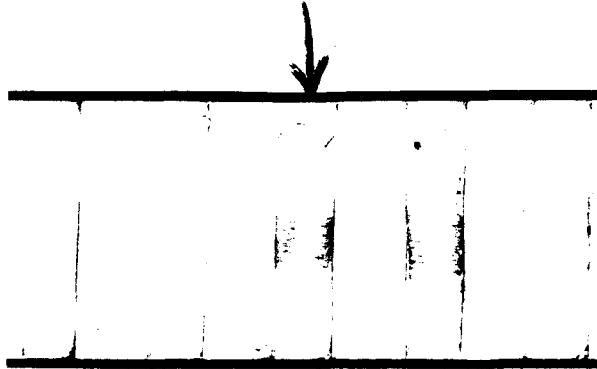


Figure 3.6. 0° Cross-Section 16694-3-2 (2.7 X)



Figure 3.7 90° Cross-Section 16694-3-2 (2.7 X)

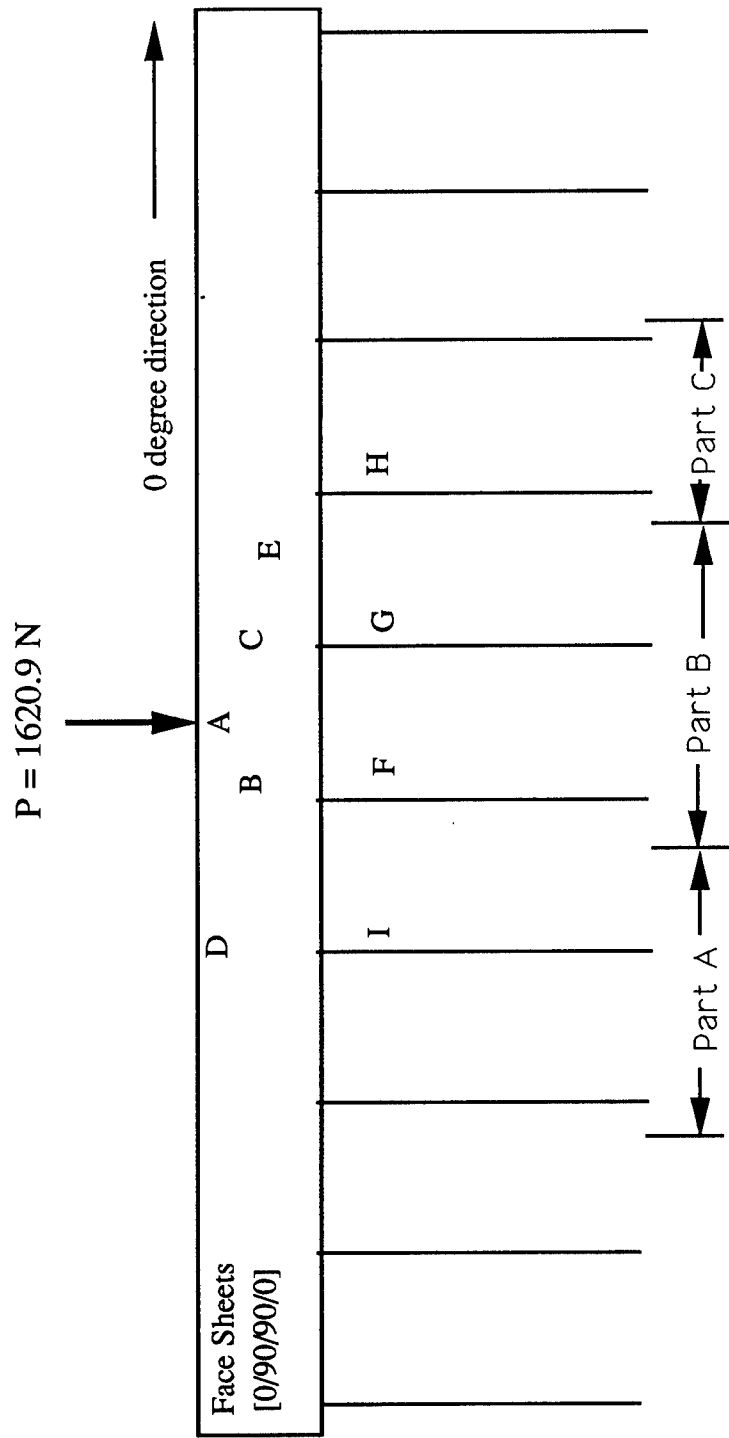


Figure 3.8. Guide to Micrograph of 0 Degree Cross-Section (25X) -16694-3-2

on one page. Note that this same approach to displaying large pictures will be adhered to throughout the chapter.

Figures 3.6 and 3.7 provide an overall view of the cross-sectioned damage area at 2.7 magnification. The damage congregates underneath the impact site with approximate dimensions of 1.7 cm (0.7 in) in the 0° cross-section and 0.5 cm in the 90° cross-section. The damage in the 90° cross-section is nearly all due to failure in the core. In fact, only a small (1 mm) delamination exists. This implies that major damage to the core, as seen in the 90° cross-section, occurs before damage to the face sheets because the damage in the core is severe (crippling) while the damage in the face sheet is comparatively minimal. On the other hand, the core walls, as shown in the 0° cross-section, crush and the top face sheet gives way to delamination that extends 15 times farther as that seen in the 90° cross-section. The bottom portion of the core and the bottom face sheet appear to be unaffected by the impact.

The 25X micrographs, Figures 3.9-3.12, show that major damage was initiated at this impact energy. This agrees with the conclusions drawn from the load versus time curve. Matrix cracking is seen in both the micrographs of the 0° and 90° cross-sections. Interply delamination exists between the bottom 0° and 90° plies. Damage also occurs in the core and cracks appear in the adhesive.

To characterize the damage, the crack and delamination development in the face sheets were recorded from the optical microscopy of the sandwich panels' cross-section beneath the impact point for both the 0° and 90° cross-sections (Figures 3.13 and 3.14). This data is presented in figures referred to as the cross-section analysis. Notice that the intensity of the cracks and delamination are distinguished by line thickness. The thin lines simulate fine cracks while the thicker lines depict cracks of greater openings. These figures also help describe the behavior of the core. The dashed lines under the face sheets



Figure 3.9. 0° Cross-Section 16694-3-2 (25X) Part A

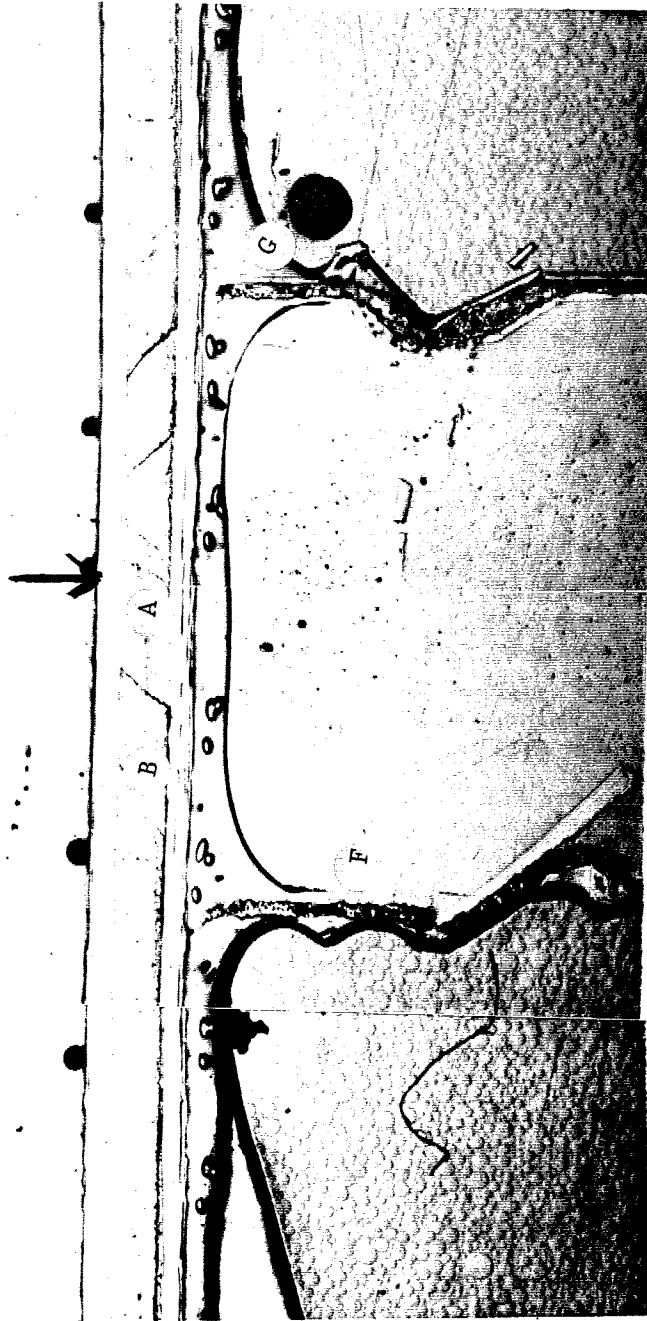


Figure 3.10. 0° Cross-Section 16694-3-2 (25X) Part B

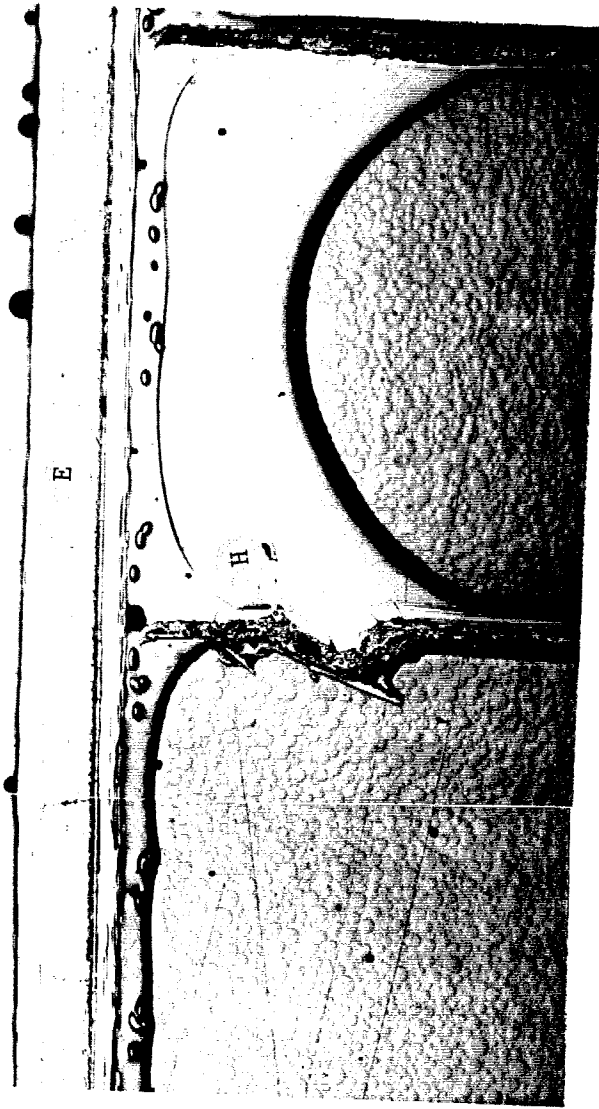


Figure 3.11. 0° Cross-Section 16694-3-2 (25X) Part C



Figure 3.12. 90° Cross-Section 16694-3-2 (25X)

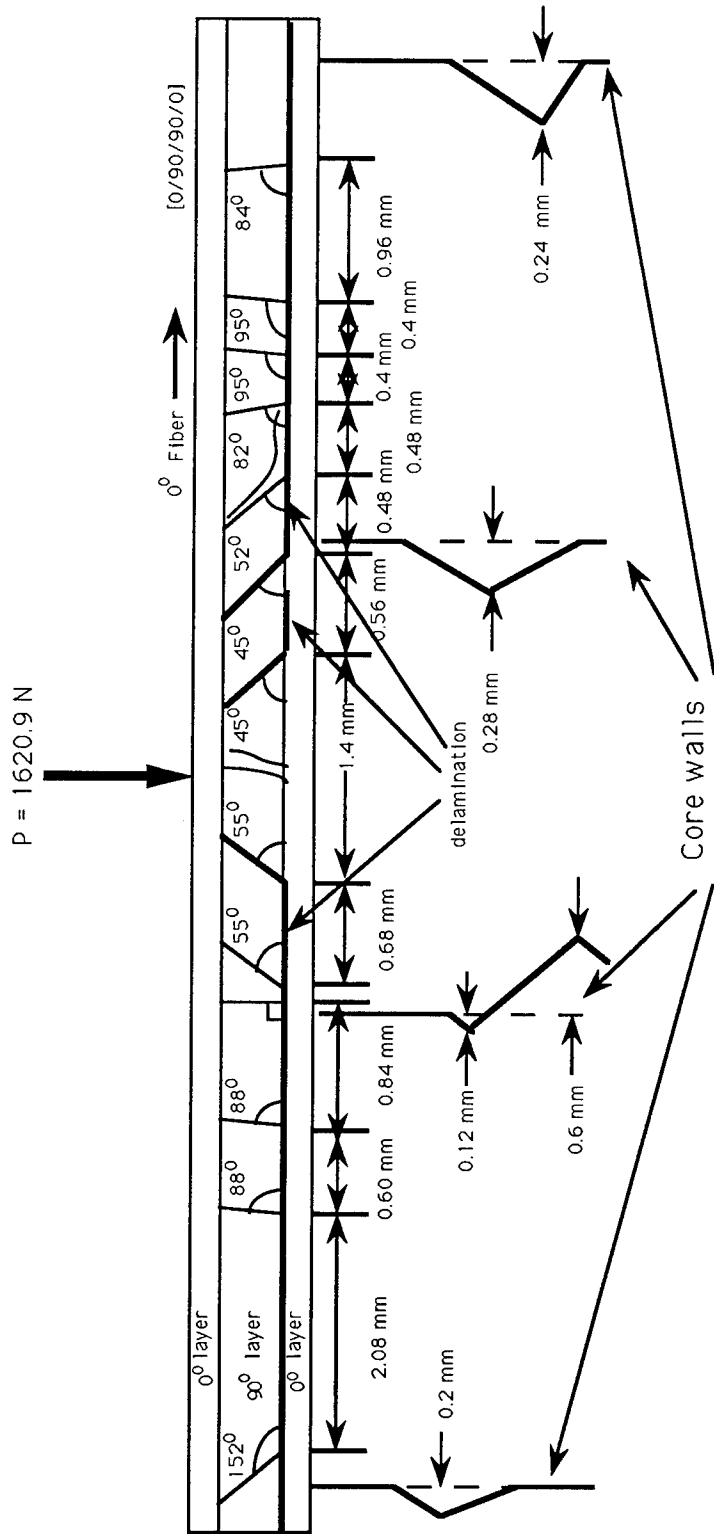


Figure 3.13. 0° Cross-Section Analysis 16694-3-2

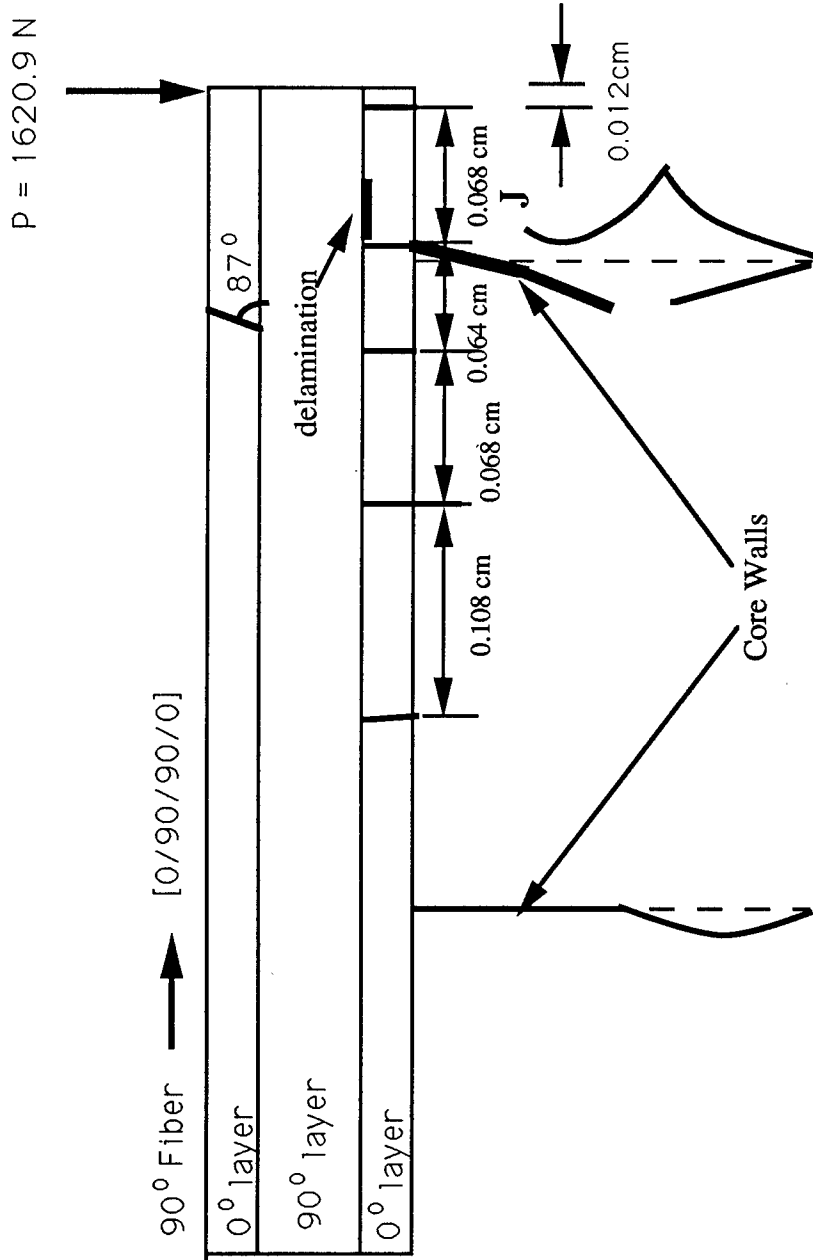


Figure 3.14. 90° Cross-Section Analysis 16694-3-2

represent the original position of the core walls while the solid lines represent the position of the core walls after delamination.

Underneath the impact site of the 0° cross-section, nearly vertical fine cracks exist (Figure 3.10 label A). As the distance to the left and right from the impact site increases the cracks take on angles between 45° and 55° (Figure 3.10, label B and C) pointed towards the impact site. As the distance from the impact site continues to increase, the cracks start to become vertical again. After this, two cracks to the left and right of the impact (not equidistant) take on large angles, approximately 152° (Figure 3.9, label D and Figure 3.11, label E). The above situation demonstrates a structure acting like a beam. Compressive stresses in the middle of the beam cause nearly vertical cracks coupled with in-plane shear stresses. The cracks away from the impact site are due to tension and bending. A crack at a 90° angle is due to bending while a crack at a 45° is due to in-plane shear stresses. The cracks at angles other than this are a combination of the two.

The delamination between the 0° and 90° plies at the bottom of the top face sheet begins approximately 0.7 mm (0.3 in) to the left and right away from the impact site (Figure 3.13). The mechanism of delamination can be looked at from the point of view of fracture and crack growth. Applying this analysis, Mode I and Mode II stresses both contribute to the loading at the tip of the delamination. Mode I, the "opening mode" results from normal stresses perpendicular to the plane of the delamination, while in-plane shear results in Mode II, the "sliding mode" [33]. According to Lammerant and Verpost [34], the Mode I component is due to the stress relaxation in the 90° layer which makes this layer bend away from the laminate when it is released from the laminate. In this case, the 90° layer is defined as the two 90° plies in the middle of the lay-up.

The upper portion of the core beneath the impact site in the 0° cross-section was crushed. A minimum of 0.4 mm (0.02 in) of the top of the core walls that experienced

crushing remained intact (Figure 3.10 label F and G, and Figure 3.11 label H) due to the adhesive. At each of the aforementioned labels, the adhesive covers the top portion of the core walls resulting in an arch-like formation. This implies that the adhesive plays a structural role by transferring loads. Damage of the core and/or adhesive contributes to the formation of the cracks and delamination in the face sheets. This is evident from the crack density. The crack density was obtained by counting the number of cracks in the first 10 cm (25X magnification) to the left and right of the impact site. The crack density to the right of the impact site, 0.9 cracks/cm, is greater than the crack density to the left of the impact site, 0.6 cracks/cm. The cell walls to the right of the impact site (Figure 3.10, label G) which received more damage instigates this imbalance. Notice that the top 1.28 mm of the cell wall directly to the left of the impact site (Figure 3.10 label F) remained intact. When the core wall did crush, below the top 1.28 mm, the deflection from the original position, resulting from the crush was less than that for the core wall directly to the right of the impact area (Figure 3.10, label G). Only the top 0.68 mm of this core wall remained intact. These two core walls, the ones directly to the left and right of the impact site (Figure 3.10, label G and F), contributed more to the crack density imbalance in the face sheets than the two core walls farther out to the left and right of the impact site (Figure 3.9, label I and Figure 3.11, label H). In this case, the cell wall to the left received more damage. This is partly due to the adhesive's structural role. The cell to the right received less damage because the adhesive settled down farther into the cell.

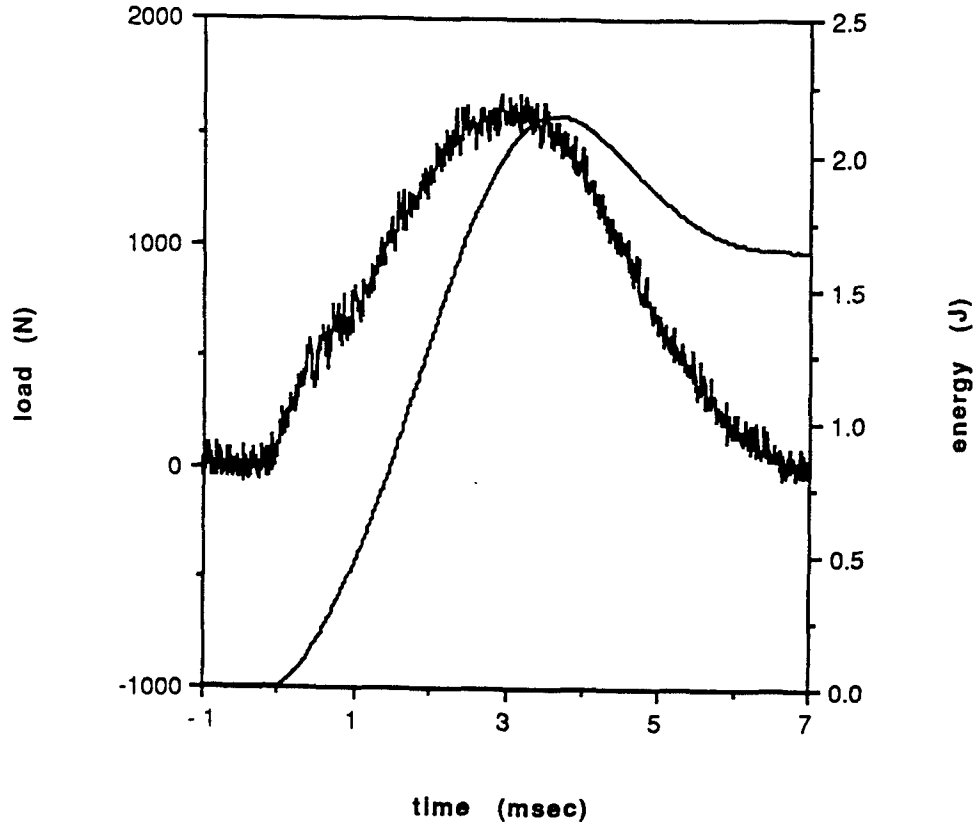
The location of the core walls with respect to the impact site is important in the case of a sandwich panel with thin face sheets. The core wall in the 90° cross-section was closer to the impact than any other (Figure 3.12, label J). This core wall received the most damage, crippling. As a result, the adhesive could not support the load and cracked.

(3) Impact Energy = 2.06 J (1.52 ft-lb)

The sandwich specimen was impacted at a drop height of 6.35 cm (2.5 in). The load curve for this test is presented in Figure 3.15. The details of the damage can be seen in the micrographs. The 0° and 90° cross-sections (Figures 3.16 and 3.17 respectively) give an overall view while Figures 3.18-3.22 give a more detailed view of the top portion of the sandwich panel.

The damage forms in a similar manner as the previous test. The damage forms near the top of the sandwich panel under the impact area. The bottom portion of the core and bottom face sheet again appear to be unaffected. There is more energy expended in the sandwich panel at this slightly higher impact energy than in the last specimen; therefore, there is more damage. Delamination again results between the 0° and 90° bottom plies. The length of the delamination changed a little from the 1.68 J; however, the opening of the delamination increased. This is because the stress contribution of Mode I loading has increased while the stress contribution due to Mode II loading has practically remained constant. In turn, there are more vertical cracks over the wider opened delamination. The crack density is still in the range of the last test; however, now the crack openings has increased away from the impact site (see Figures 3.23 and 3.24). The nearly vertical cracks (Figure 3.20, label A) underneath the impact area still remains and the openings have not increased much. The cracks to the left and right of the impact site (Figure 3.20, labels B and C) remain at similar angles and openings as the last tests. The crack opening increase begins to show in the cracks farther away from the impact site. As before, the cracks start to become vertical (Figure 3.20, label D and Figure 3.21, label E), but now the openings of the cracks are greater.

The upper portion of the core underneath the impact site in the 0° cross-section is again crushed; however, now the deflection in the core wall caused by the buckling has



Specimen ID - 16694-3-5	Max load - 1665.0 N (374.3 lb)
Impact Velocity - 1.06 m/s (3.49 ft/s)	Energy at Max Load - 1.970 J (1.453 ft-lb)
Impact Energy - 2.06 J (1.52 ft-lb)	Time - at Max load - 2.93 msec
Absorbed Energy - 1.646 J (1.214 ft-lb)	total - 6.61 msec
Max Disp. of Tup 0.242cm (0.0952 in)	Damage Area - 1.883 cm ² (0.292 in ²)
Damage Indent. - 0.018 cm (0.007 in)	Damage Radius - 1.01 cm (0.4 in)

Figure 3.15. Load and Energy from Dynatup for 4-ply at 6.35 cm (2.5 in) drop height



Figure 3.16. 0° Cross-Section 16694-3-5 (2.7 X)



Figure 3.17 90° Cross-Section 16694-3-5 (2.7 X)

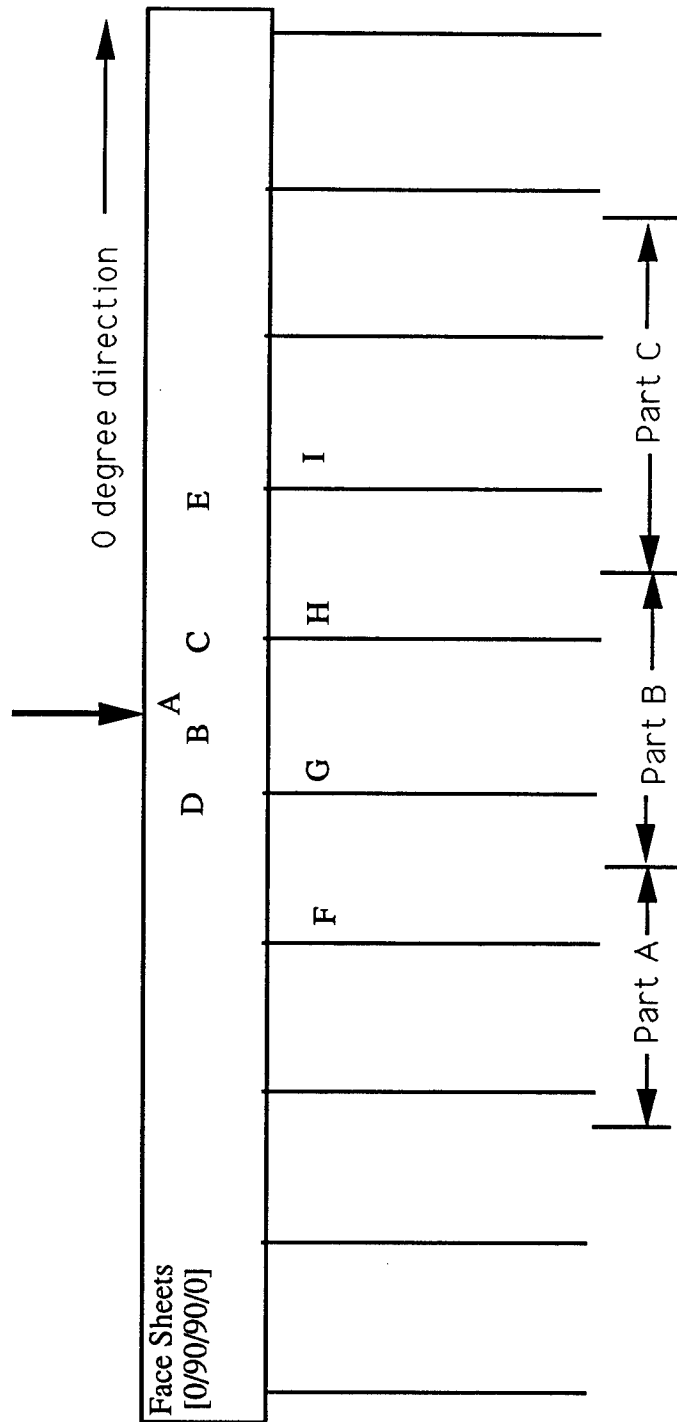


Figure 3.18. Guide to Micrograph of 0 Degree Cross-Section (25X) -16694-3-5

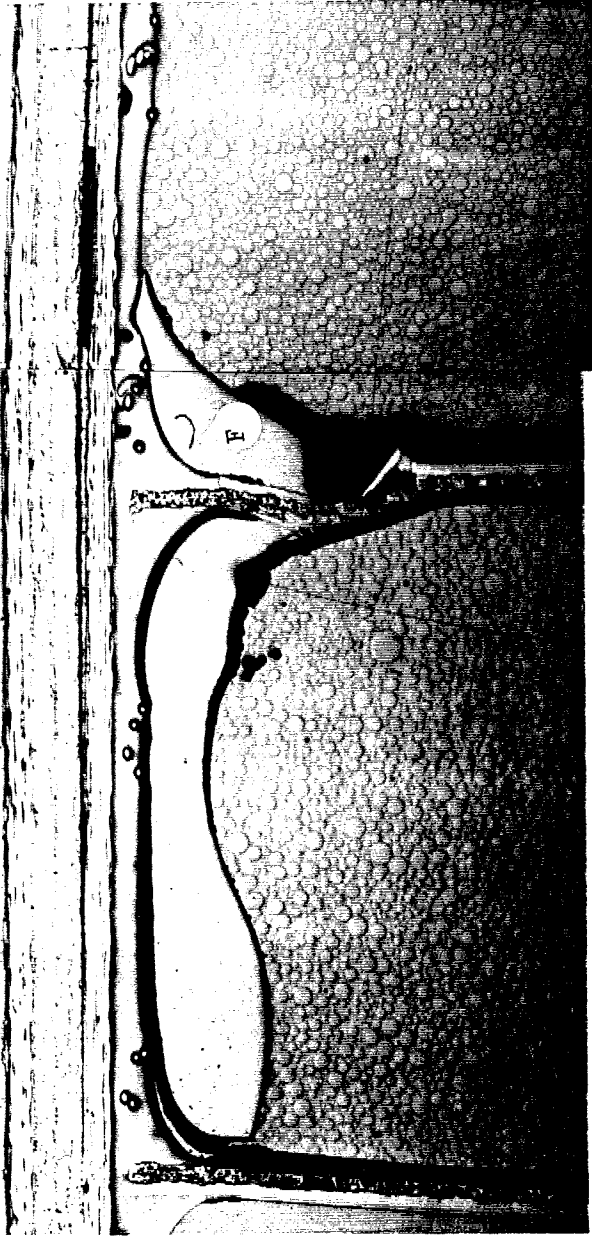


Figure 3.19. 0° Cross-Section 16694-3-5 (25X) Part A



Figure 3.20. 0° Cross-Section 16694-3-5 (25X) Part B

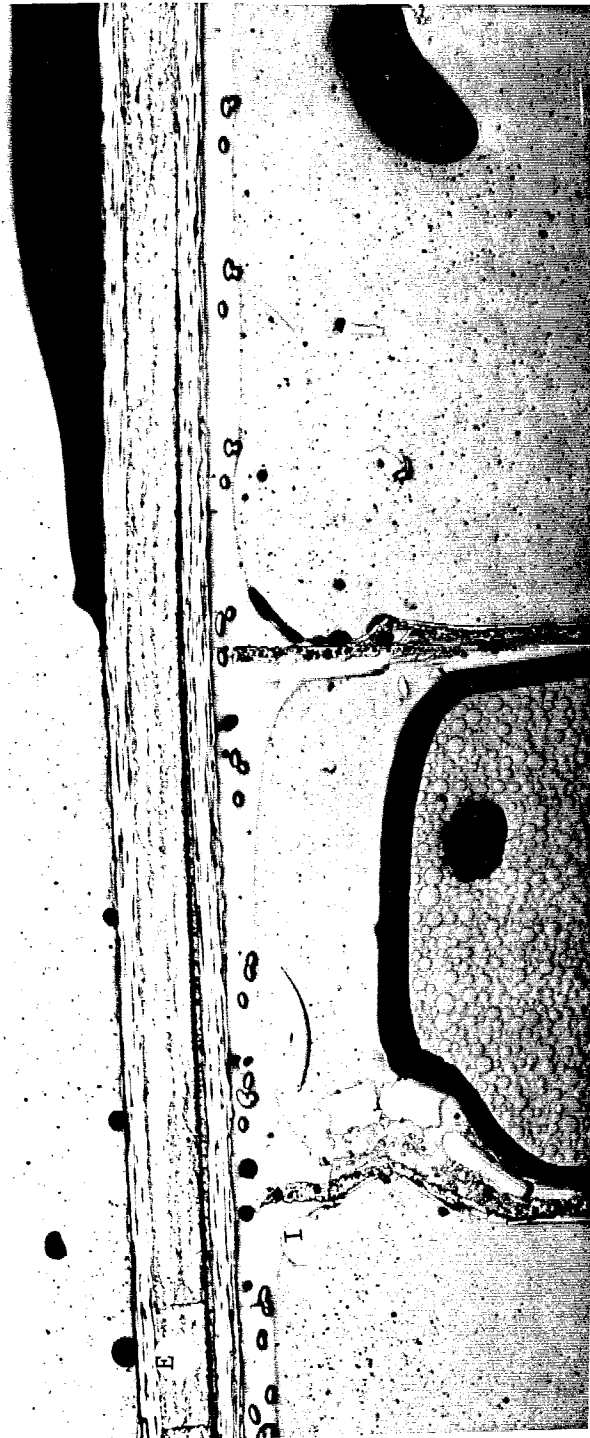


Figure 3.21. 0° Cross-Section 16694-3-5 (25X) Part C

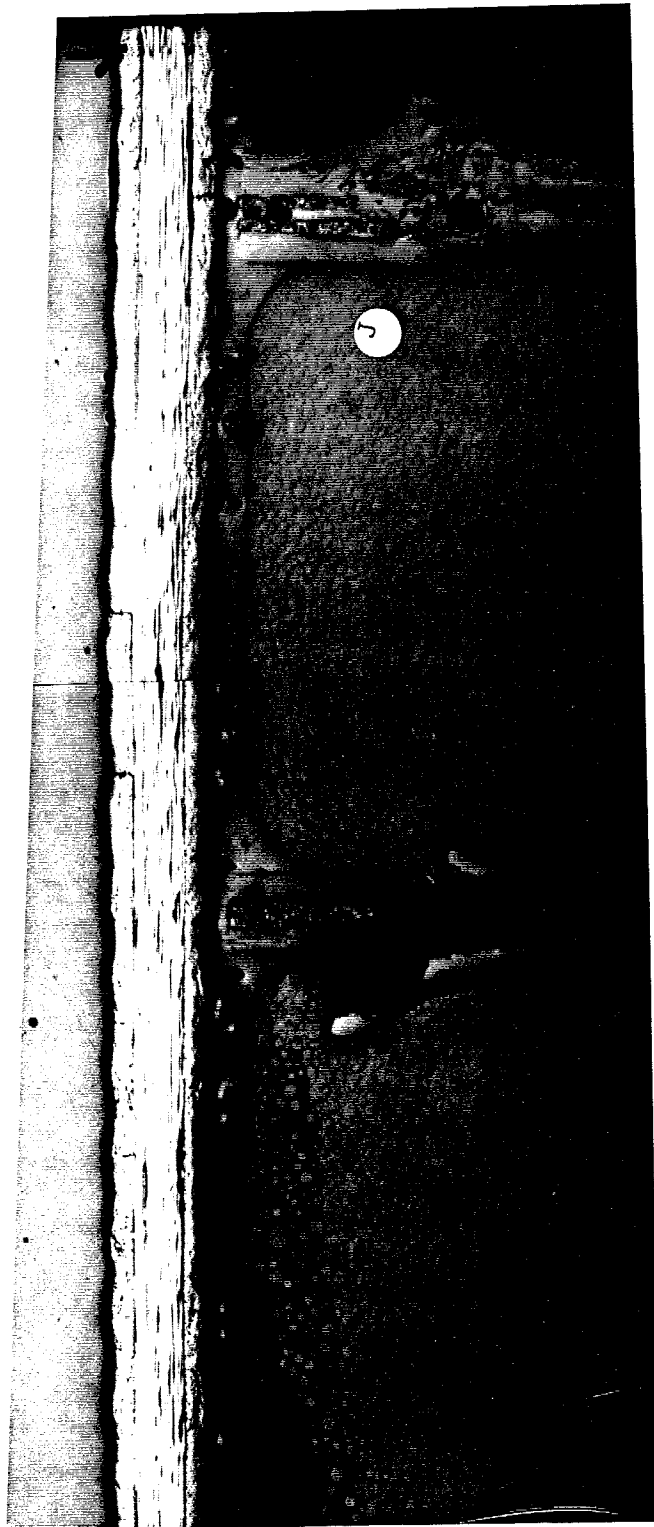


Figure 3.22. 90° Cross-Section 16694-3-5 (25X)

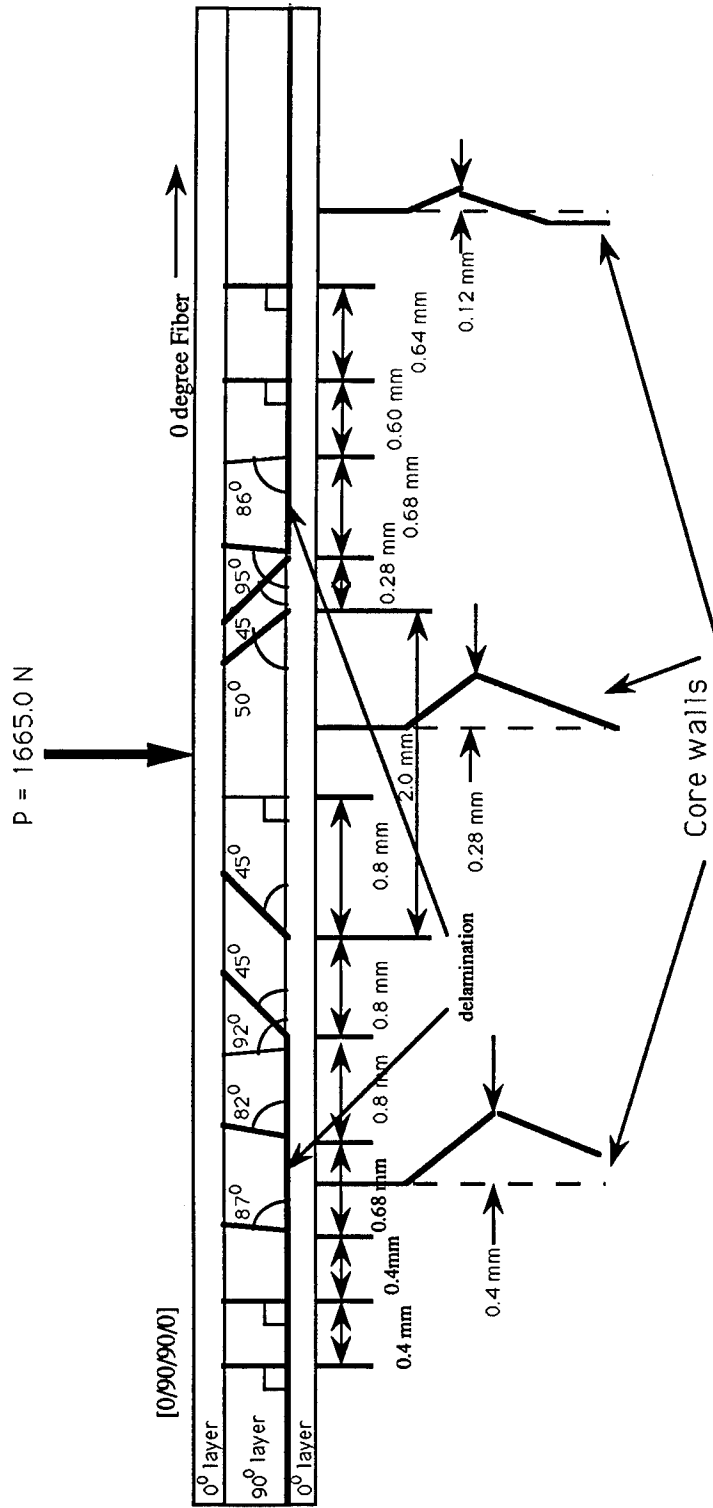


Figure 3.23. 0° Cross-Section Analysis 16694-3-5

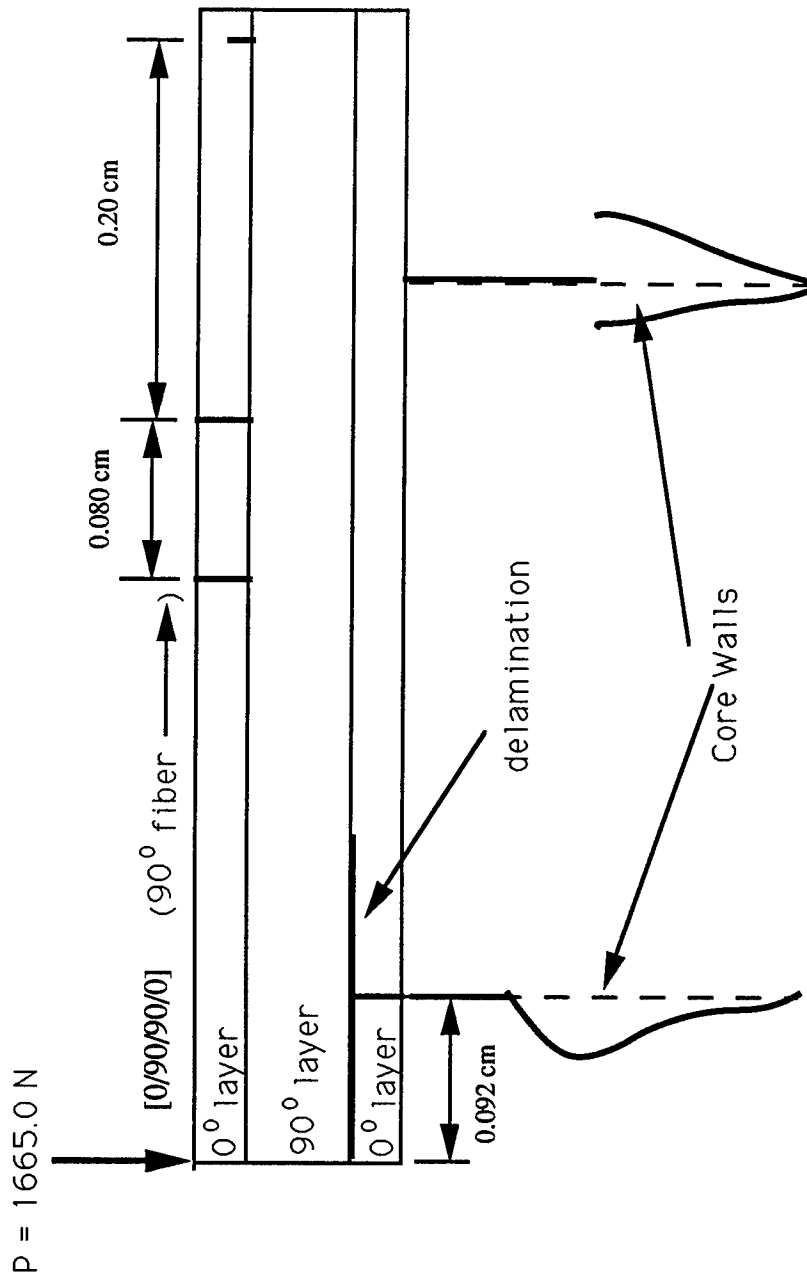


Figure 3.24. 90° Cross-Section Analysis 16694-3-5

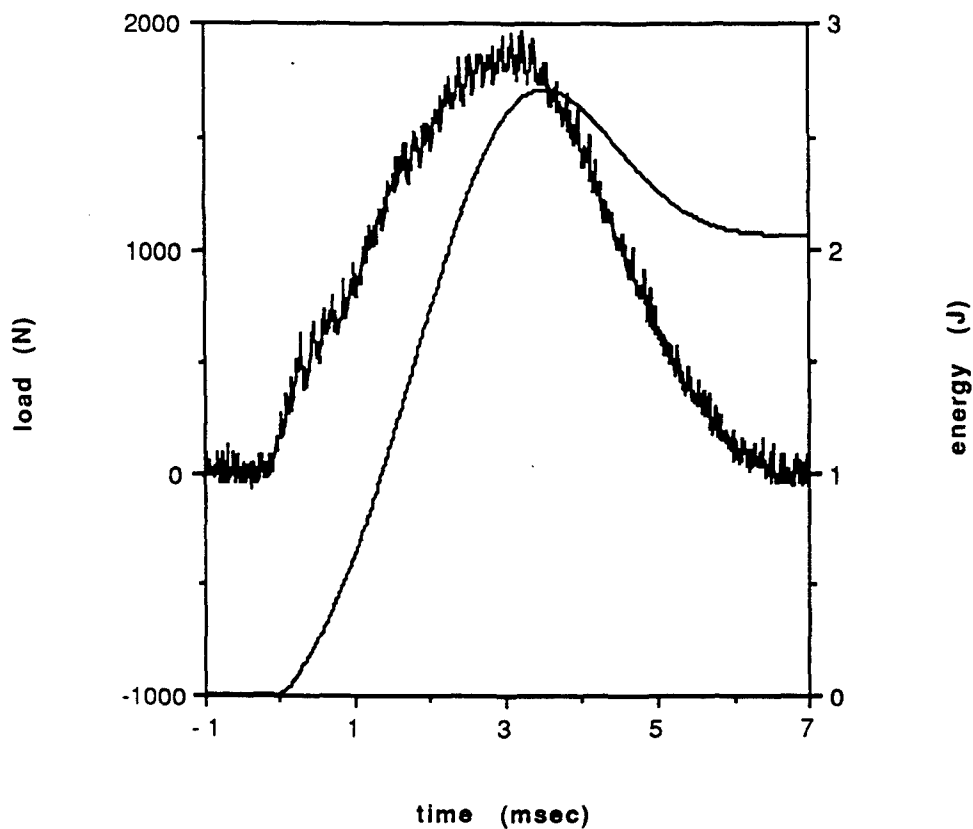
increased (Figure 3.20, label G and H and Figure 3.21, label I). The adhesive still performs its role of transferring the load. Minor cracks are present. The crack density above the damage core varies only by 0.1 crack/cm. Unlike the previous test, the core damage is more evenly distributed.

As in the last test, a core wall in the 90° cross-section was close to the impact site (Figure 3.22, label J), but the damage was more severe than it was at the lower impact energy. In this case, a core wall in the 0° cross-section (Figure 3.20, label H) was also close to the load. The impact load was distributed between the two core walls, resulting in less damage.

(4) Impact Energy = 2.62 J (1.93 ft-lb)

The sandwich specimen was impacted at a drop height of 7.62 cm (3.0 in). The load curve for this test is presented in Figure 3.25. The details of the damage can be seen in the micrographs. The 0° and 90° cross-sections (Figures 3.26 and 3.27 respectively) give an overall view while Figures 3.28-3.32 give a more detailed view of the top portion of the sandwich panel.

The resulting damage is similar to the two previous tests; however, there is more damage in the 90° cross-section to both the core and face sheet. The damage near the top of the sandwich is still concentrated beneath the impact area but spreads out farther. Unlike the previous tests, the core walls show signs of buckling and crippling in the bottom portion of the core. The bottom face sheet again appears to be unaffected. There is more energy dissipated in the impacted sandwich panel at this higher impact energy than in the last specimen; therefore, there is more damage. The delamination again appears between the 0° and 90° bottom plies. The length of the delamination and the opening of the delamination both increased. This is because the contribution due to



Specimen ID -16694-3-6	Max load - 1969.7 N (442.8 lb)
Impact Velocity - 1.20 m/s (3.94 ft/s)	Energy at Max Load - 2.672 J (1.971 ft-lb)
Impact Energy - 2.62 J (1.93 ft-lb)	Time - at Max load -3.28 msec
Absorbed Energy - 2.076 J (1.531 ft-lb)	total - 6.22 msec
Max Disp. of Tup 0.264cm (0.104 in)	Damage Area - 2.226 cm ² (0.345 in ²)
Damage Indent.- 0.025 cm (0.01 in)	Damage Radius - 1.01 cm (0.4 in)

Figure 3.25. Load and Energy from Dynatup for 4-ply at 7.62 cm (3.0 in) drop height

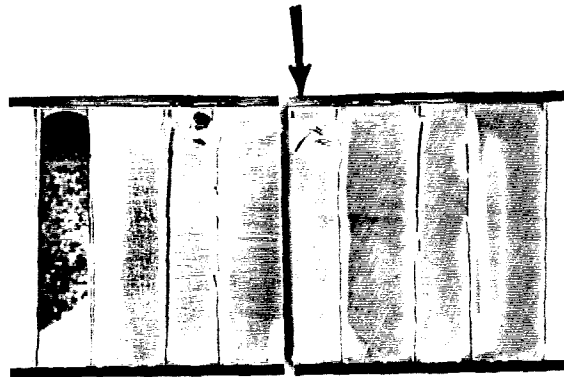


Figure 3.26. 0° Cross-Section 16694-3-6 (2.7 X)

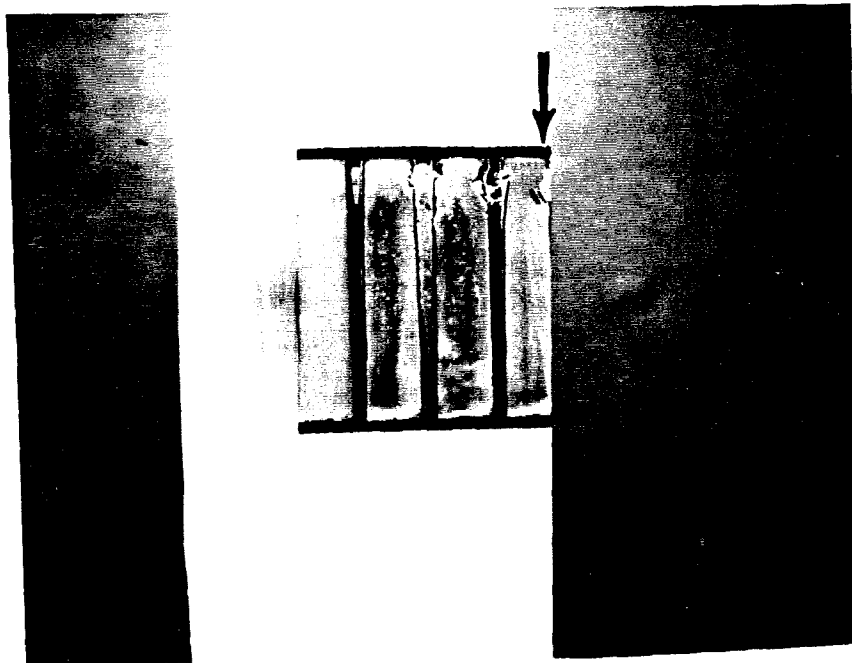


Figure 3.27. 90° Cross-Section 16694-3-6 (2.7 X)

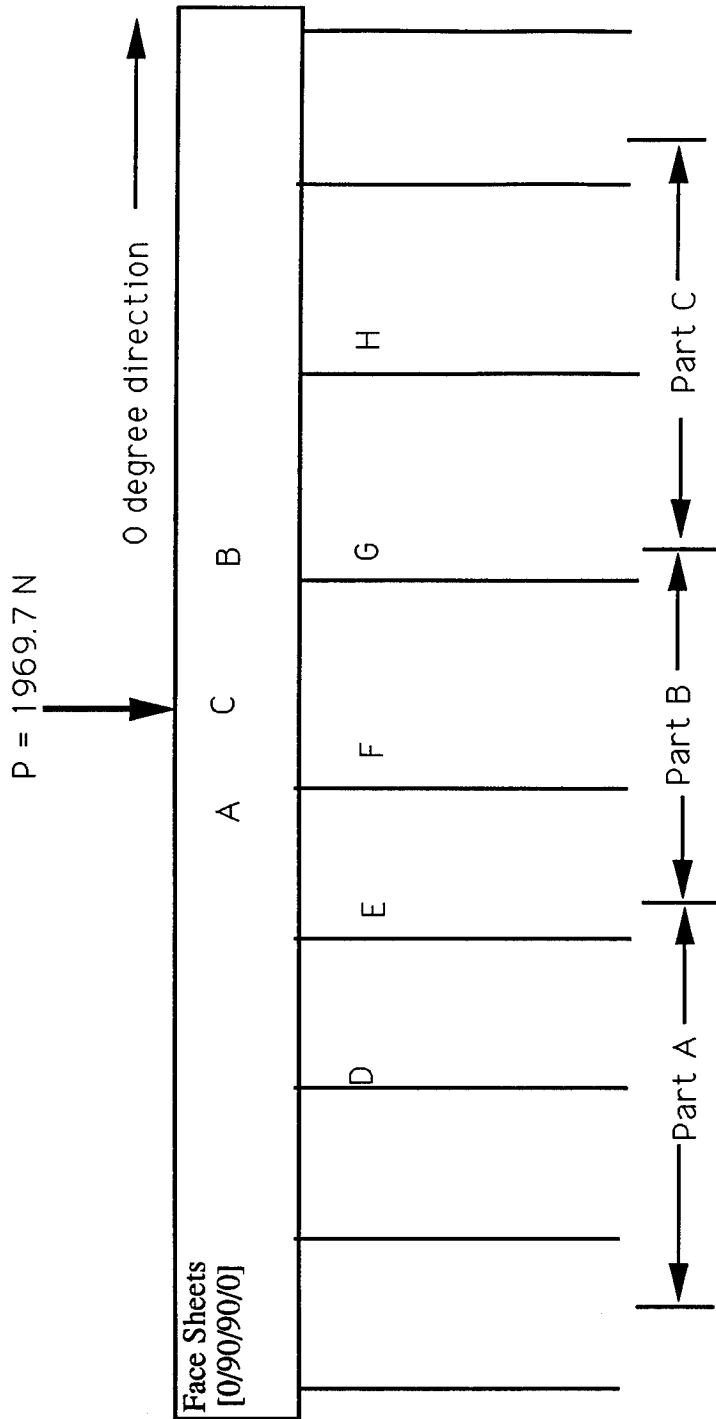


Figure 3.28. Guide to Micrograph of 0 Degree Cross-Section (25X) - 16694-3-6



Figure 3.29. 0° Cross-Section 16694-3-6 (25X) Part A

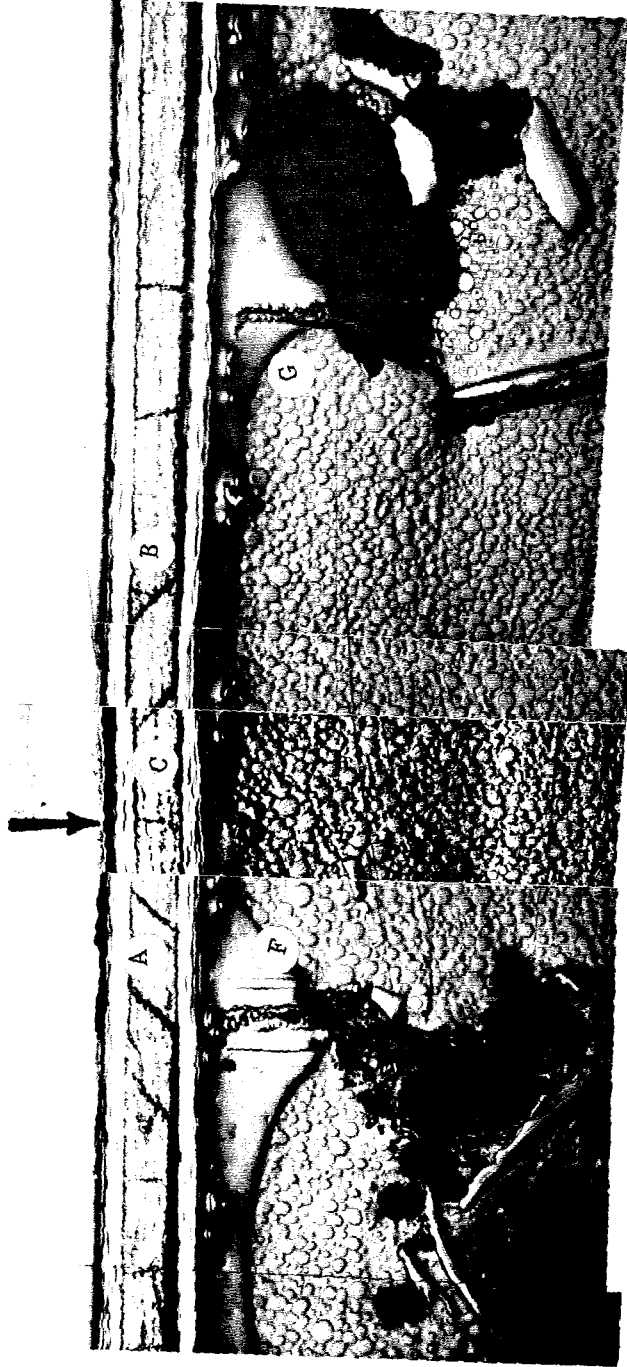


Figure 3.30. 0° Cross-Section 16694-3-6 (25X) Part B

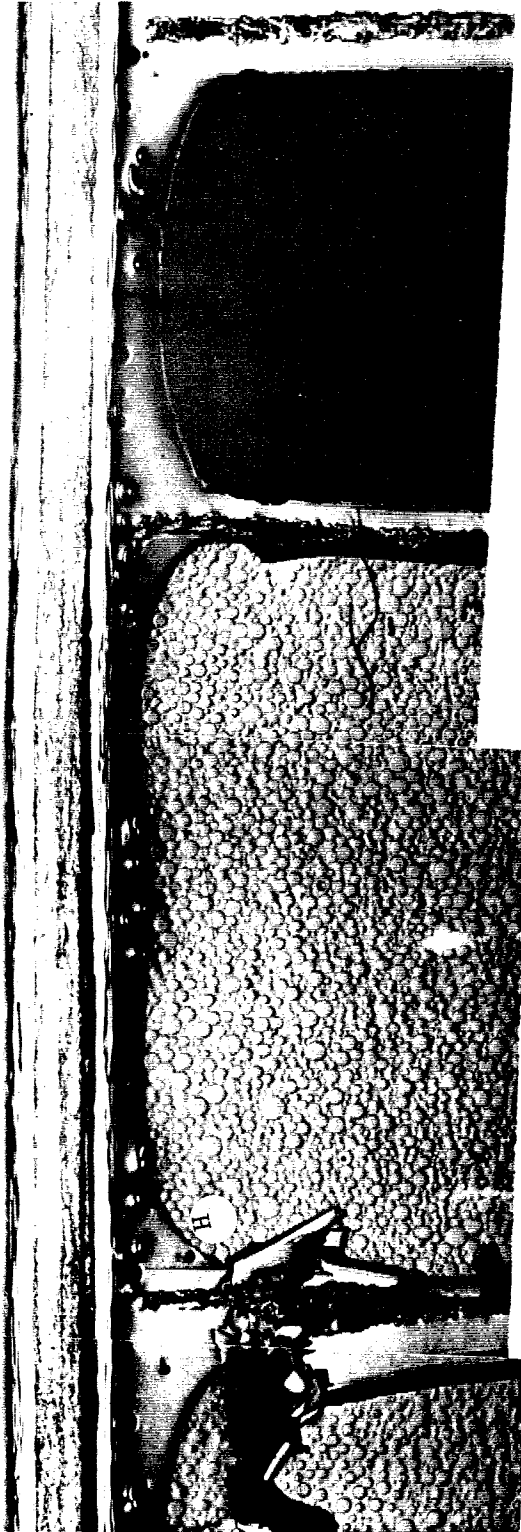


Figure 3.31. 0° Cross-Section 16694-3-6 (25X) Part C

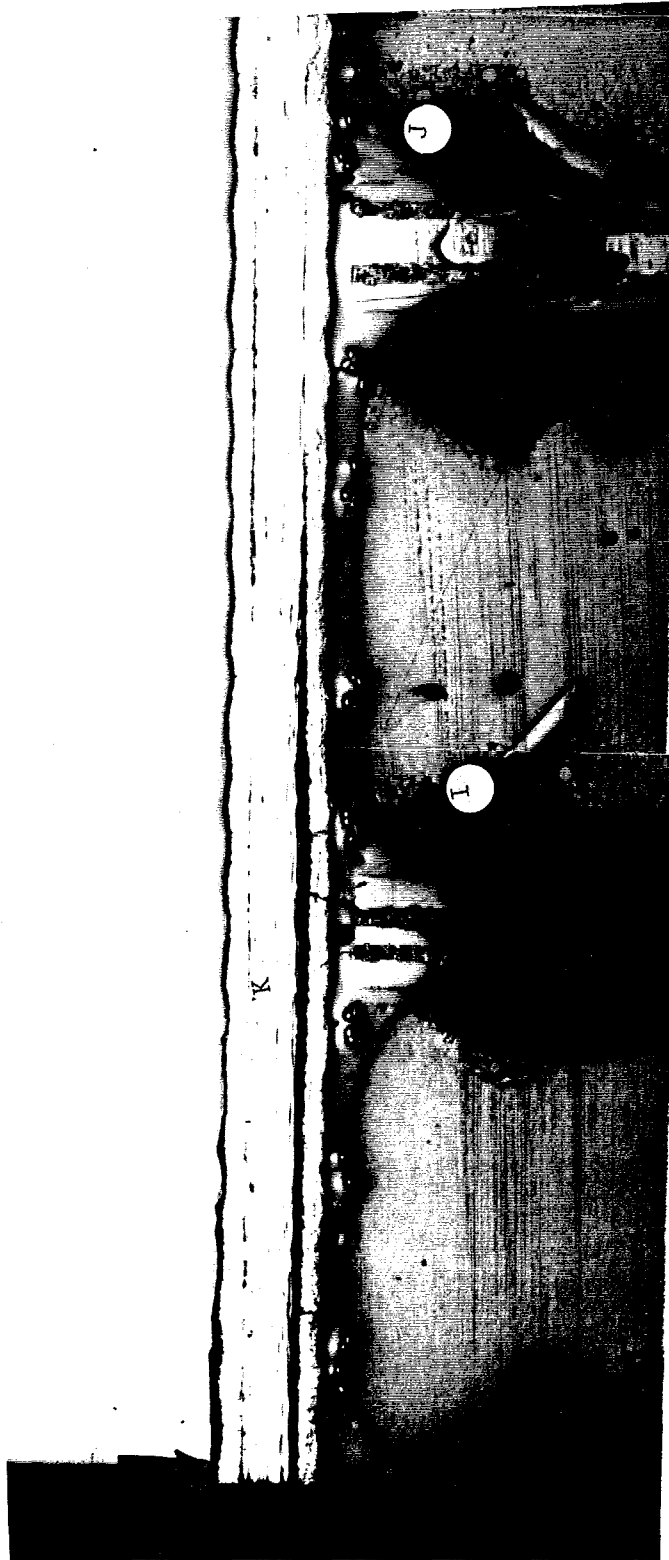


Figure 3.32. 90° Cross-Section 16694-3-6 (25X)

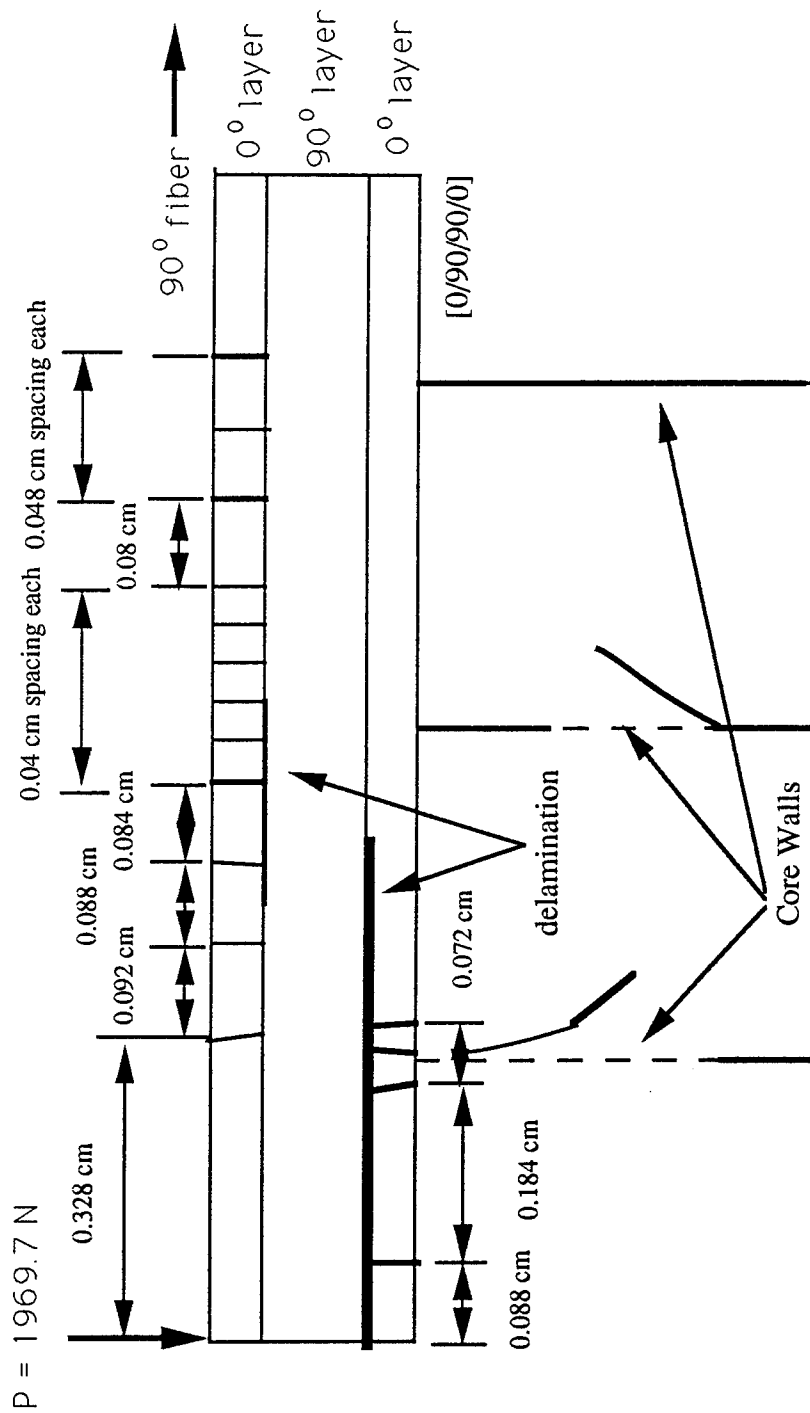


Figure 3.34. 90 degree Cross-Section Analysis 16694-3-6

both Mode I and Mode II loading has increased. In turn, the openings of the cracks directed in 90° and 45° angles has increased (See Figures 3.33 and 3.34). The nearly vertical crack underneath the impact area and the angled cracks to the left and right of the impact still remain and the openings have not increased much (Figure 3.30, label A, B, and C).

Figures 3.29 - 3.31, labels E-H, show that the upper portion of the core area underneath the impact site in the 0° cross-section are crippled. Minor cracks were present in the adhesive of the previous test. In this case, the adhesive remained intact, without any cracks, showing that it transferred the load from the face sheet to the core. The crack density of the face sheet to the left and right of the impact varied by 0.2 crack/cm. This again was due to the additional damage of the core on the side with the higher crack density.

In the previous test, the core wall in the 90° cross-section received the most damage while there was only minor damage in the face sheet. In this test, both the core and face sheet received major damage. The core walls crippled, and the face sheet delaminated between the bottom 0° and 90° plies (Figure 3.32 labels I - K). Cracks formed in the matrix and core also.

(5) C-scans

C-scans were taken of each impacted specimen except for Specimen ID 16694-3-1 which had a drop height of 3.81 cm (1.5 in). Figure 3.35 shows the area of damage captured by the C-scan. Because the face sheets are so thin, the Pulse-echo c-scan did not register a depth; nonetheless, this area took the shape of a peanut in each case.

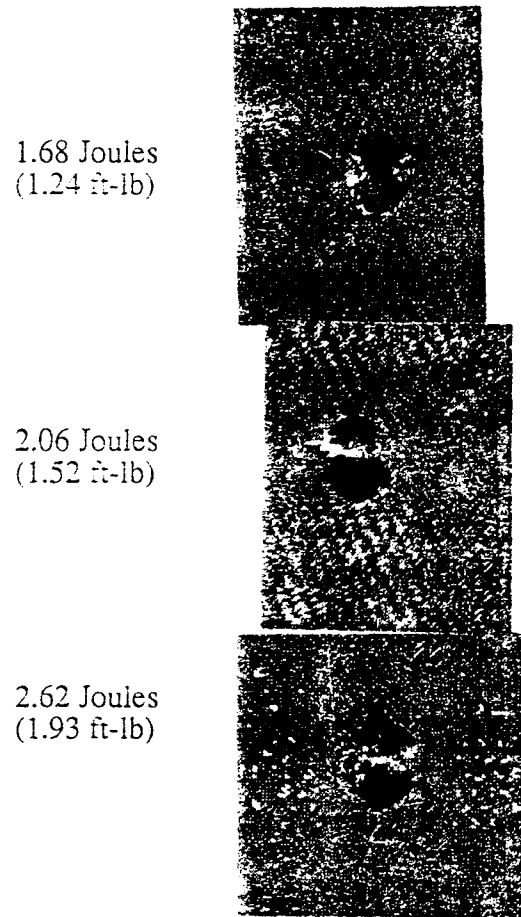


Figure 3.35. Puise-Echo C-Scans for Sandwich Panels with 4-Ply Face Sheets

The damage areas due to delamination in Figure 3.35, which are reduced by 33%, were measured using a planimeter. Figure 3.36 shows the damage area versus the impact energy and absorbed energy. The damage area increases as the energies increase. Figure 3.37 shows the nearly linear relationship between delamination length and damage area

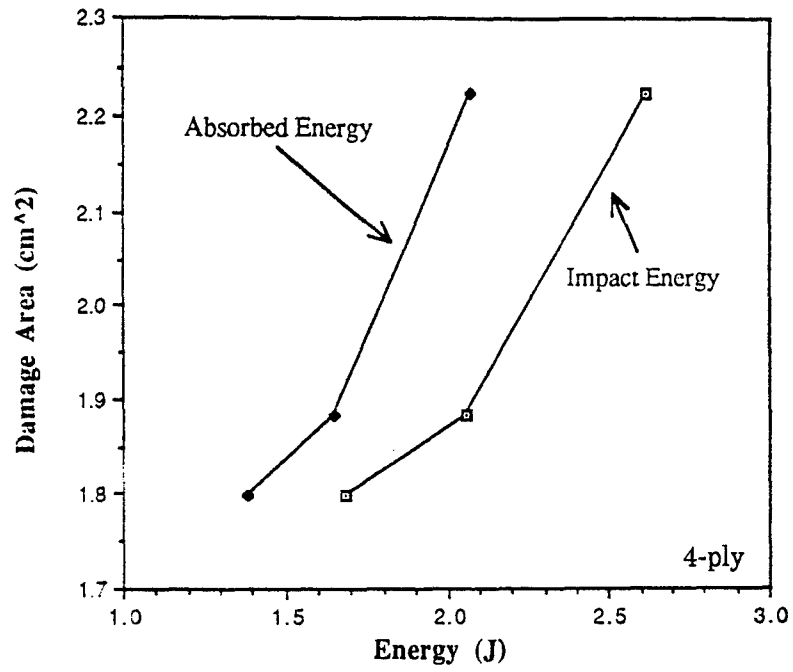


Figure 3.36. Damage Area vs Impact and Absorbed Energies - 4-ply

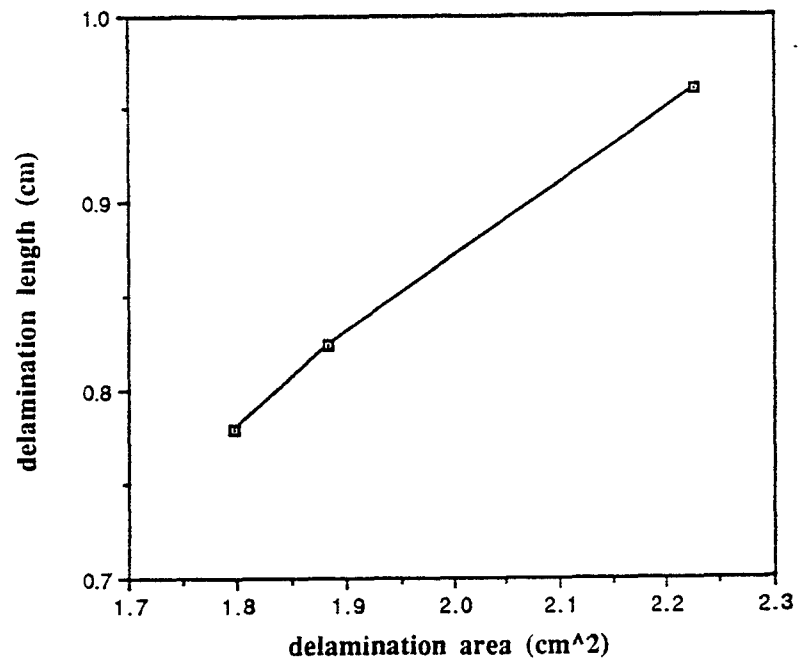


Figure 3.37. Delamination Length vs Delamination Area - 4-ply

(6) Additional Analysis

Figure 3.38 compares the energy curves for each test. The impact energy increases as the drop height increases in a linear manner. For example, as the drop height doubles from 3.81 cm (1.5 in) to 7.62 cm (3.0 in), the impact energy increases from 1.27 J (0.94 ft-lb) to 2.62 J (1.93 ft-lb). Figure 3.39 indicates that the absorbed energy also increases as the drop height increases in a similar manner as the impact energy does. Since the absorbed energy is an indication of the amount of damage in the sandwich panel, the damage increases as the drop height increases. Also, Figure 3.39 shows the difference between the absorbed energy and impact energy. This difference is the recovered elastic energy and it increases along with the drop height implying that, in this case, as the difference increases, so does the damage.

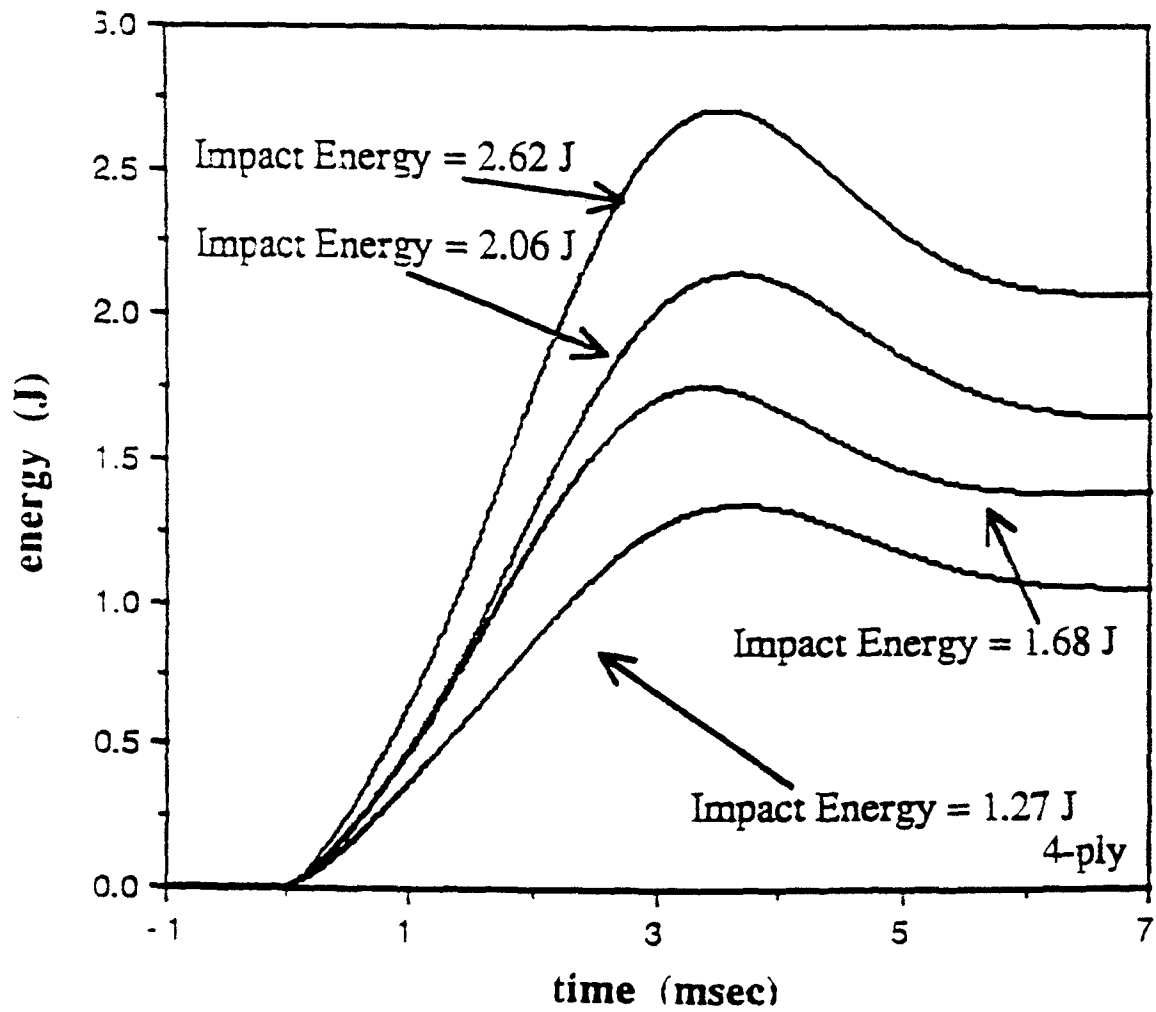


Figure 3.38. Comparison of Energy Curves for Sandwich Panels with 4-ply Face Sheets

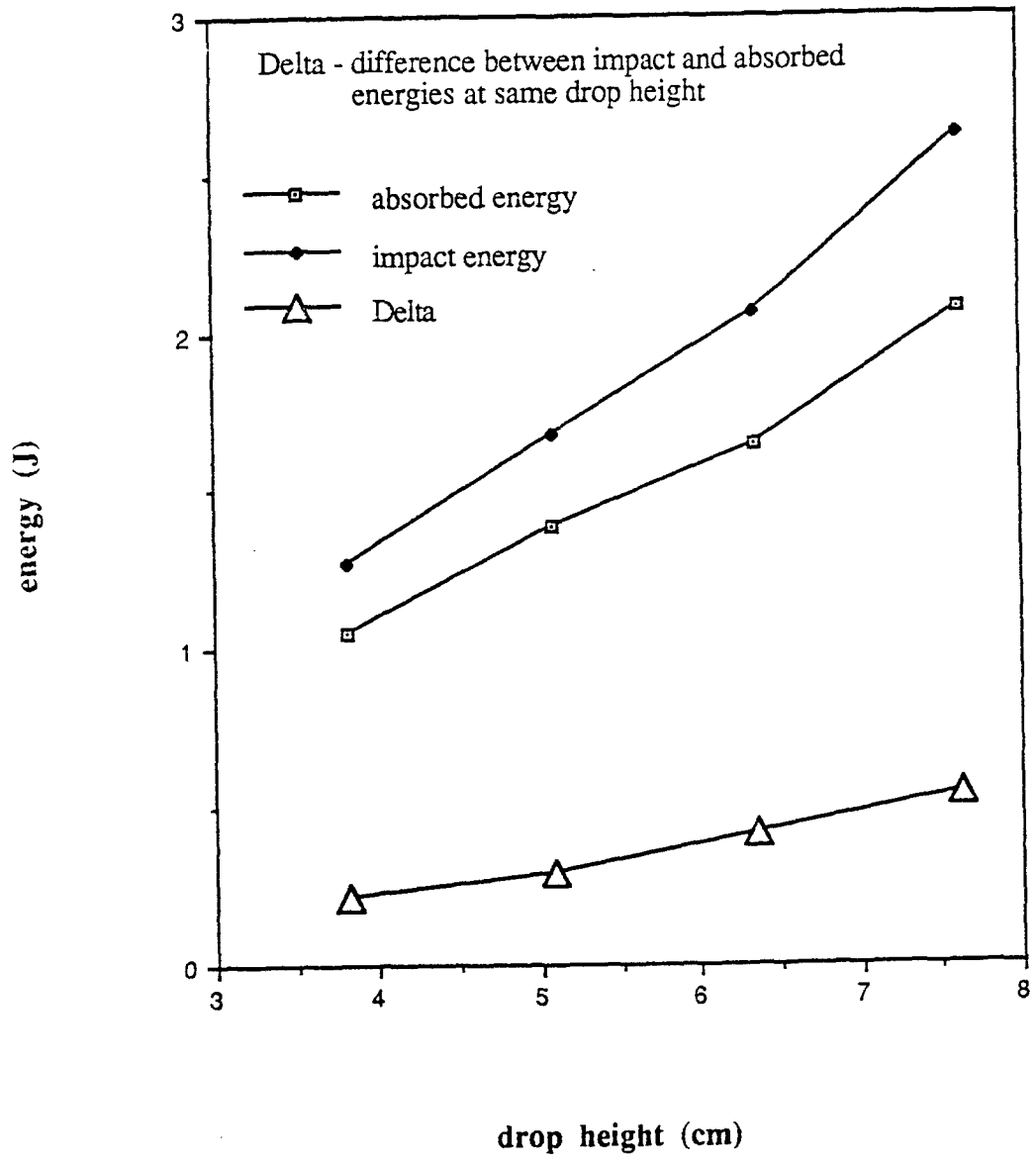


Figure 3.39. Comparison of Absorbed Energy and Impact Energy vs Drop Height for Sandwich Panels with 4-Ply Face Sheets

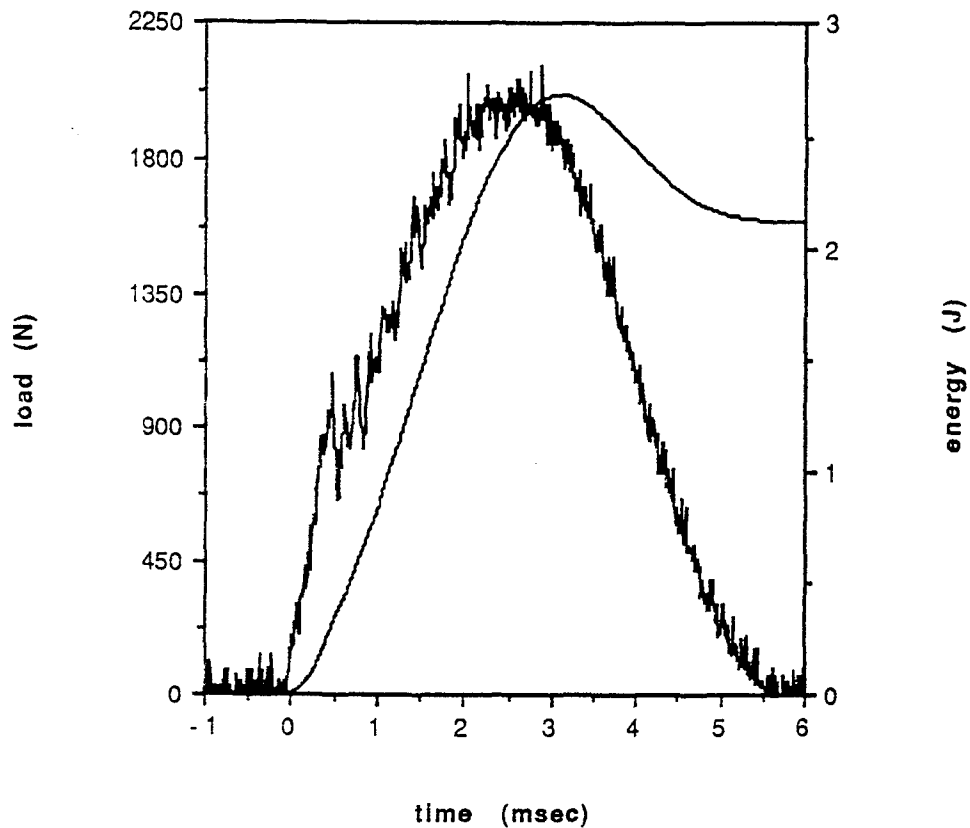
3.5 Sandwich Panels with 8-ply Face Sheets

The sandwich panels with 8-ply face sheets were subjected to low energy (velocity) impacts with drop heights ranging from 7.62 cm (3.0 in) to 10.16 cm (4.0 in). The load curves for the 8-ply face sheets are smoother than the load curves for the 4-ply face sheets because the ratio of the instrumental/background noise level to total impact load has decreased. In all tests, the first minor repeatable peaks are present until a load of approximately 1000 N (225 lb) is reached. This implies that at this point the sandwich panel no longer acts in an elastic manner. After this point, the load curves have a dramatic drop in each test. This is the initiation of damage. Recall that the point of damage initiation was 750 N (169 lb) for the 4-ply. Each case will be discussed in this section.

(1) Impact Energy = 2.60 J and 2.56 J

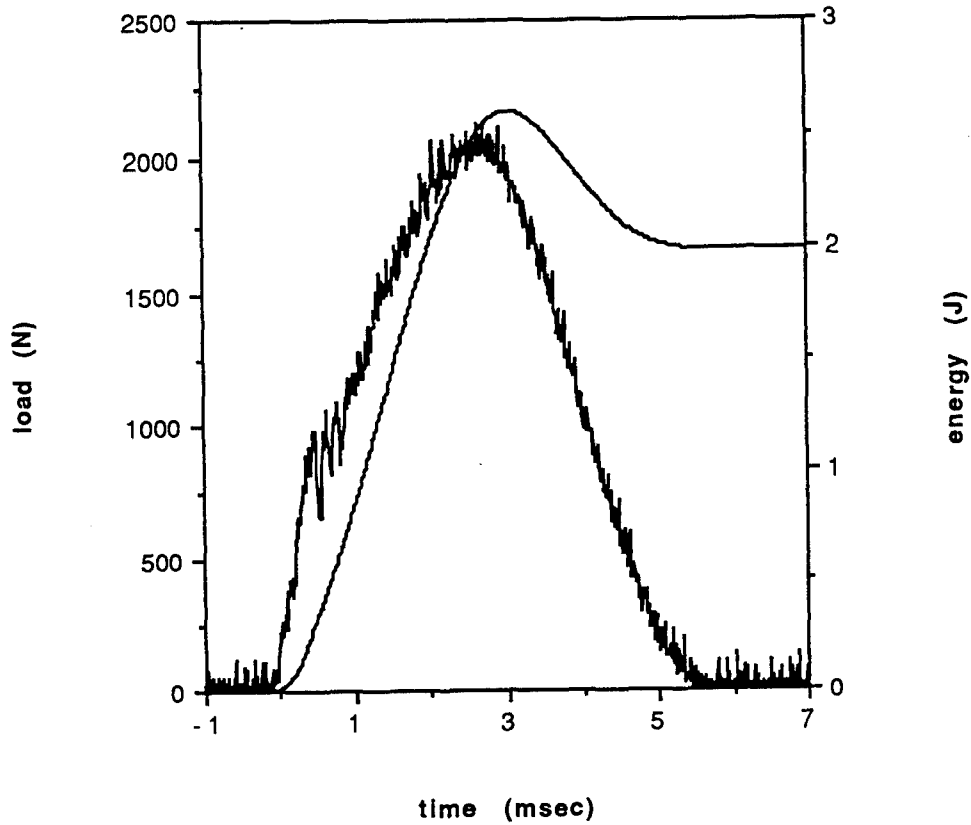
Two sandwich panels, 16892-2-1 and 16892-2-2 were impacted at a drop height of 7.62 cm (3.0 in) each. This was done to investigate the differences in reaction of panels under the same loading condition. As stated earlier, the location of the core wall with respect to the impact site played an important role in the development of cracks and delamination. This fact is supported throughout this section.

The load and energy curves for these two tests are presented in Figures 3.40 and 3.41. The maximum loads did not differ by much, 0.70%. However, the energy at maximum load differed by 5.65%. The absorbed energies differed by 6.34%, with more energy dissipated in specimen 16892-2-1. This implies that there may be more damage in this specimen. Though the amount of damage (absorbed energy) in the specimen increased as the impact energy increased, the impact energies only differed by 1.54%,



Specimen ID - 16894-2-1	Max load - 2106.7 N (473.6 lb)
Impact Velocity - 1.20 m/s (3.93 ft/s)	Energy at Max Load - 2.653 J (1.957 ft-lb)
Impact Energy - 2.60 J (1.92 ft-lb)	Time - at Max load - 2.90 msec
Absorbed Energy - 2.129 J (1.570 ft-lb)	total - 5.53 msec
Max Disp. of Tup 0.226cm (0.089 in)	Damage Area - 1.627 cm ² (0.252 in ²)
Damage Indent.- 0.015 cm (0.006 in)	Damage Radius - 0.08 cm (0.2 in)

Figure 3.40. Load and Energy from Dynatup for 8-ply at 7.62 cm (3.0 in) drop height



Specimen ID -16894-2-2

Impact Velocity - 1.18 m/s (3.86 ft/s)

Impact Energy - 2.52 J (1.86 ft-lb)

Total Energy - 1.994 J (1.471 ft-lb)

Max Disp. of Tup 0.220cm (0.086 in)

Damage Indent.- 0.015 cm (0.006 in)

Max load - 2121.4 N (476.9 lb)

Energy at Max Load - 2.503 J (1.846 ft-lb)

Time - at Max load - 2.65 msec

total - 5.45 msec

Damage Area - 1.627 cm² (0.252 in²)

Damage Radius - 0.08 cm (0.2 in)

Figure 3.41. Load and Energy from Dynatup for 8-ply at 7.62 cm (3.0 in) drop height

which is less than the difference in absorbed energies, an amount analogous to the amount of damage in the specimen. As expected, the difference between the impact velocities, 1.69% is close to the 1.54% difference in the impact energies.

The maximum load decreased as the total energy increased. Therefore, a higher maximum load does not always reflect more damage in the case of sandwich panels. Earlier, it was pointed out that the amount of damage that a panel was subjected to was dependent upon the location and damage of the core walls. As seen from the 0° cross-sections, Figures 3.42 and 3.43, the impact was at different points with respect to a core wall. The specimen that received the most damage was impacted closer to a core wall.

Figure 3.42 through 3.45 provide an overall view of the cross-sectioned damage area at 2.7 magnification. The damage is centered around the impact site. There is delamination in face sheets and core crushing/buckling/crippling in both the 0° and 90° cross-sections. The core walls appear to be damaged near the bottom portion of the core. There is no damage to the bottom face sheet.

Figure 3.46 through 3.51 show the 0° cross-sections of the impacted specimens. There is matrix cracking in the 90° plies and delamination at the bottom interface of each of the 0 and 90 plies (i.e. [0/90/delamination/0/90/90/delamination/0/90/delamination/0]) as shown in Figure 3.48, labels A- C and Figure 3.50, labels A - C.. The crack density at the top 90° ply of 16894-2-2 is higher than the other. The nearly vertical line(s) that was present in the 4-ply directly under the impact no longer exists.

Specimen 16894-2-1 was impacted over a core wall, Figure 3.48, label D This wall buckled near its top while the core walls to the left and right continued to receive loading, Figure 3.47, label E and Figure 3.48. label F. They (label E and F) crippled. Figure 3.47, label G and Figure 3.48, label H point out the vertical cracks, due to bending, above the core walls in the face sheet.



Figure 3.42. 0° Cross-Section 16894-2-1 (2.7 X)



Figure 3.43. 0° Cross-Section 16894-2-2 (2.7 X)

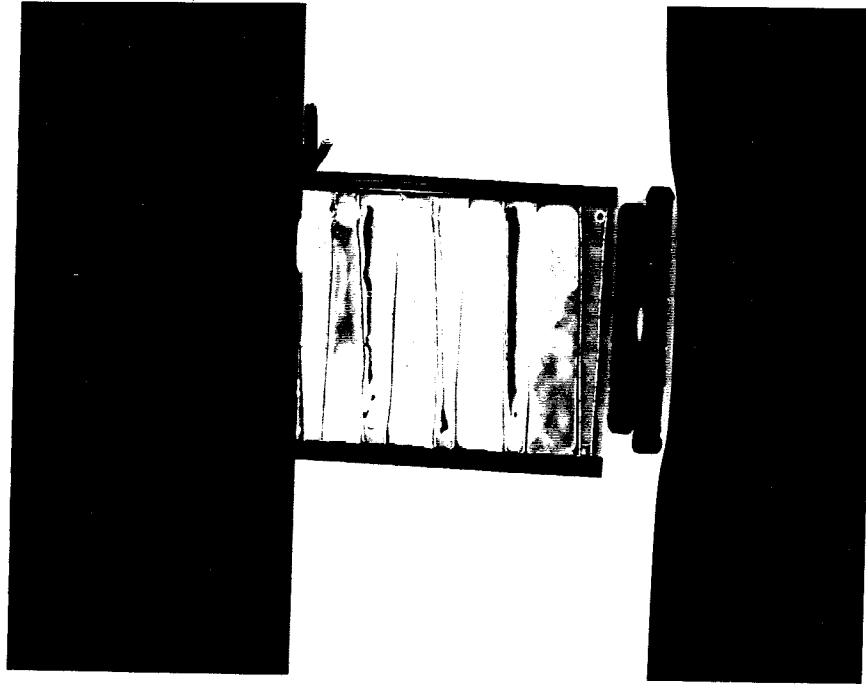


Figure 3.44. 90° Cross-Section 16894-2-1 (2.7 X)

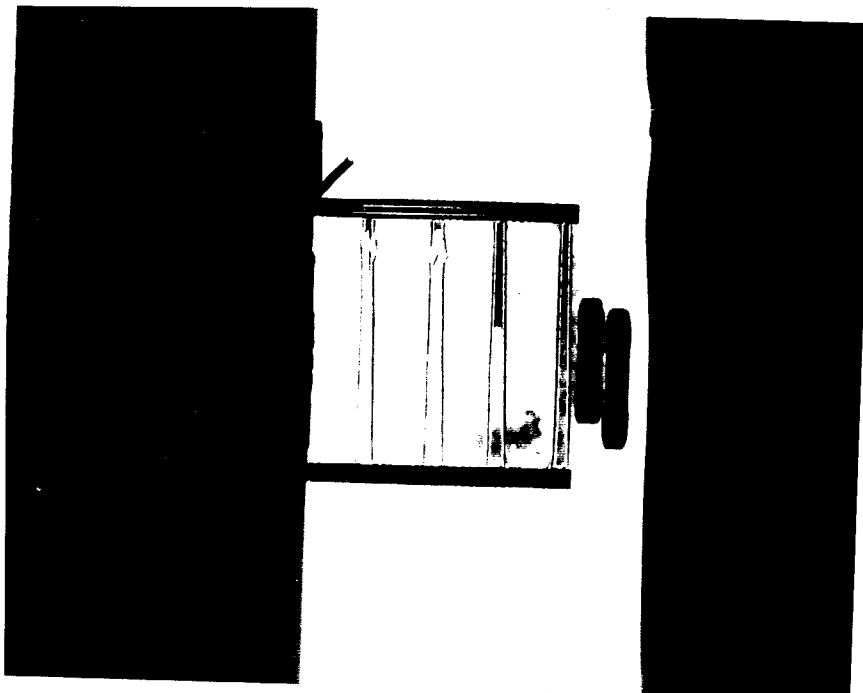


Figure 3.45. 90° Cross-Section 16894-2-2 (2.7 X)

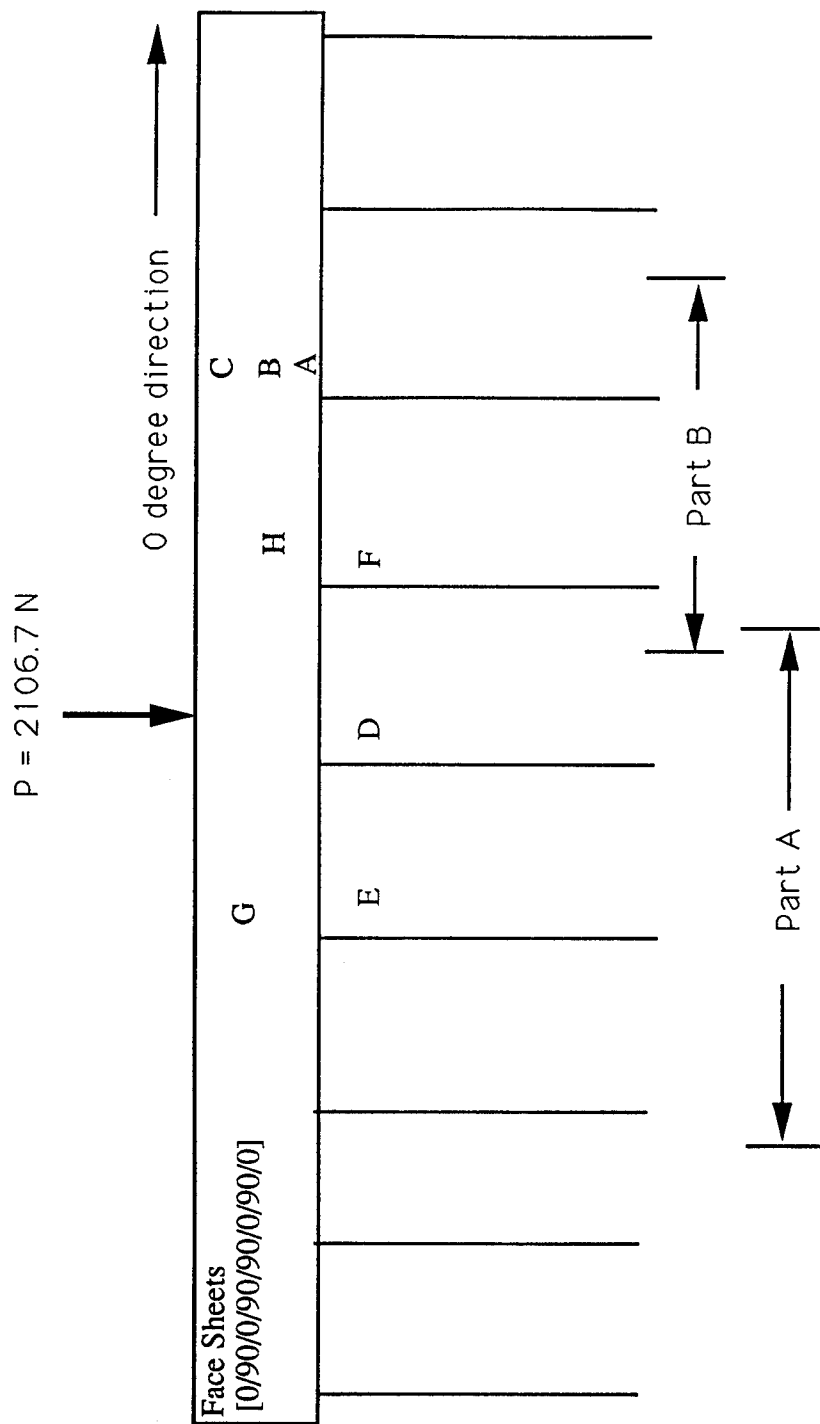


Figure 3.46. Guide to Micrograph of 0 Degree Cross-Section (25X) -16894-2-1

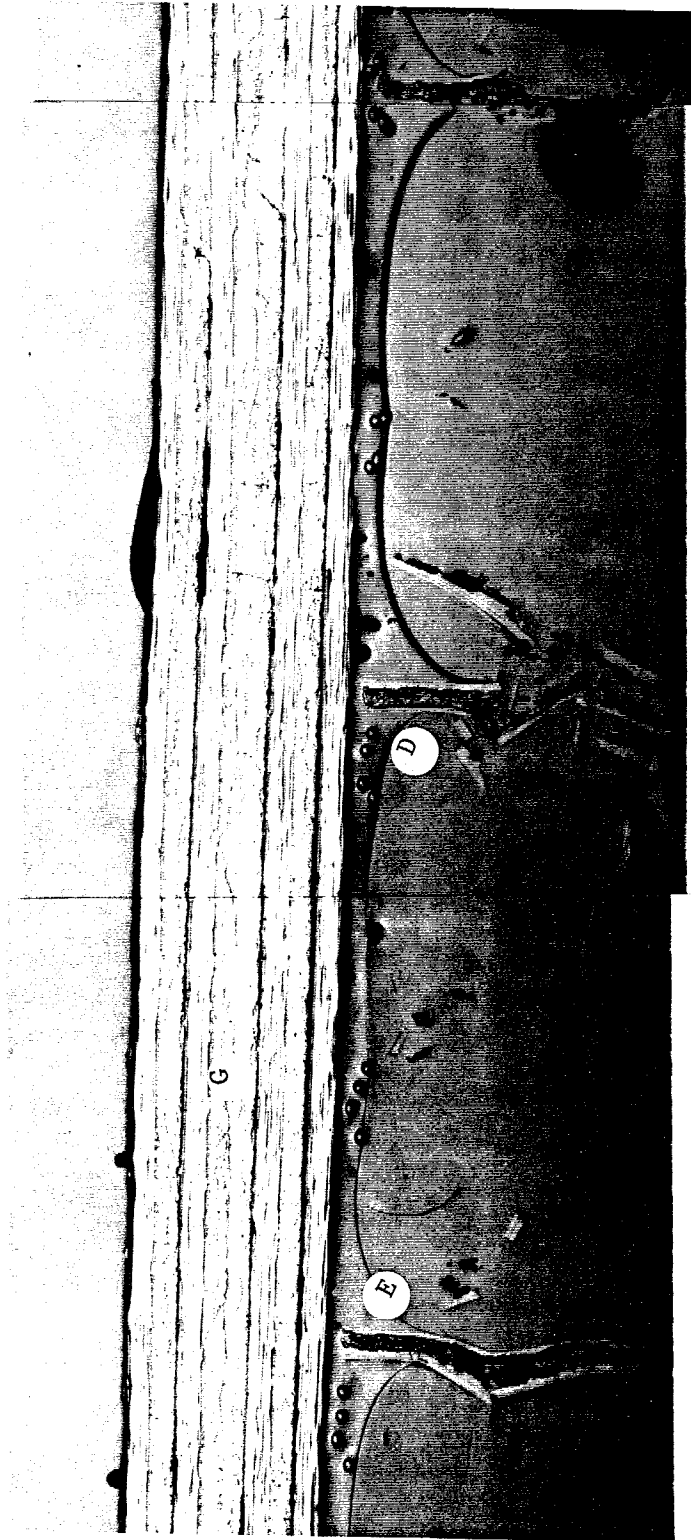


Figure 3.47. 0° Cross-Section 16894-2-1 (25X) Part A

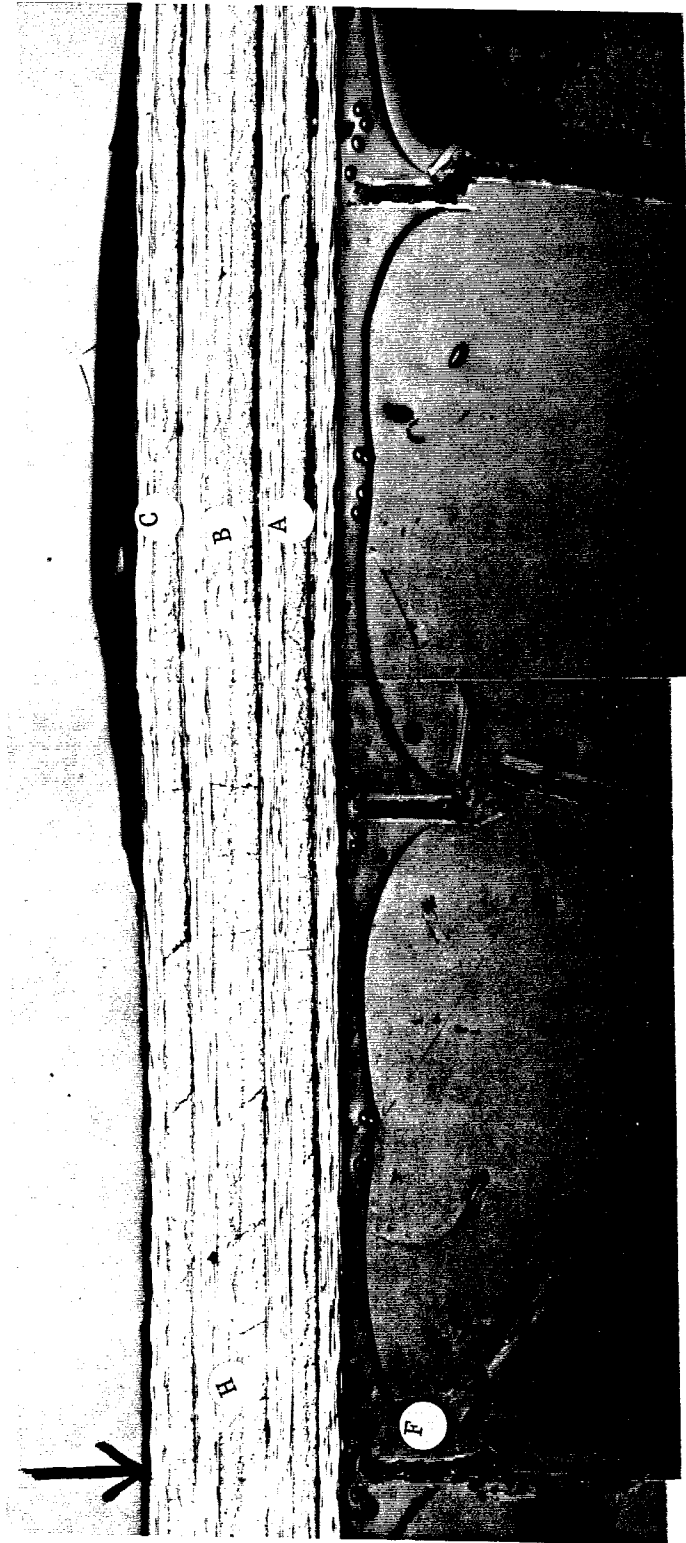


Figure 3.48. 0° Cross-Section 16894-2-1 (25X) Part B

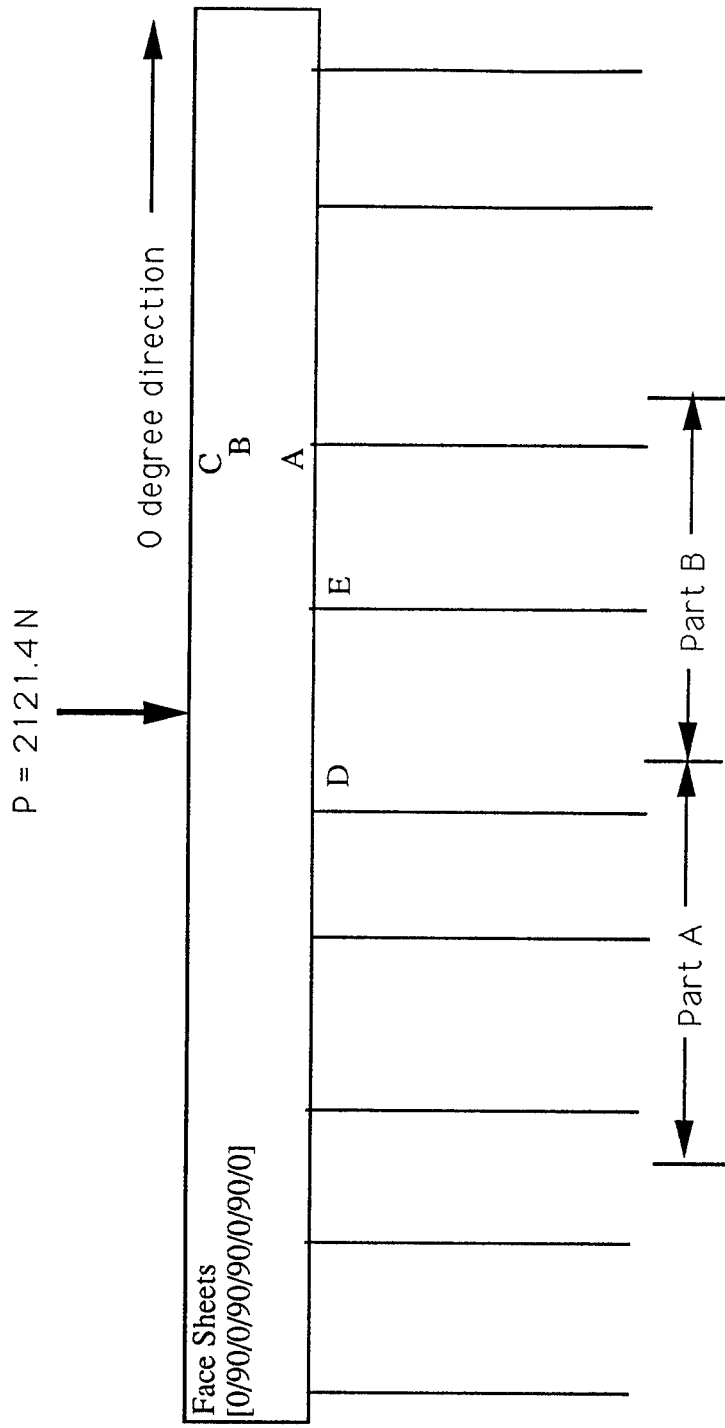


Figure 3.49. Guide to Micrograph of 0 Degree Cross-Section (25X) -16894-2-2

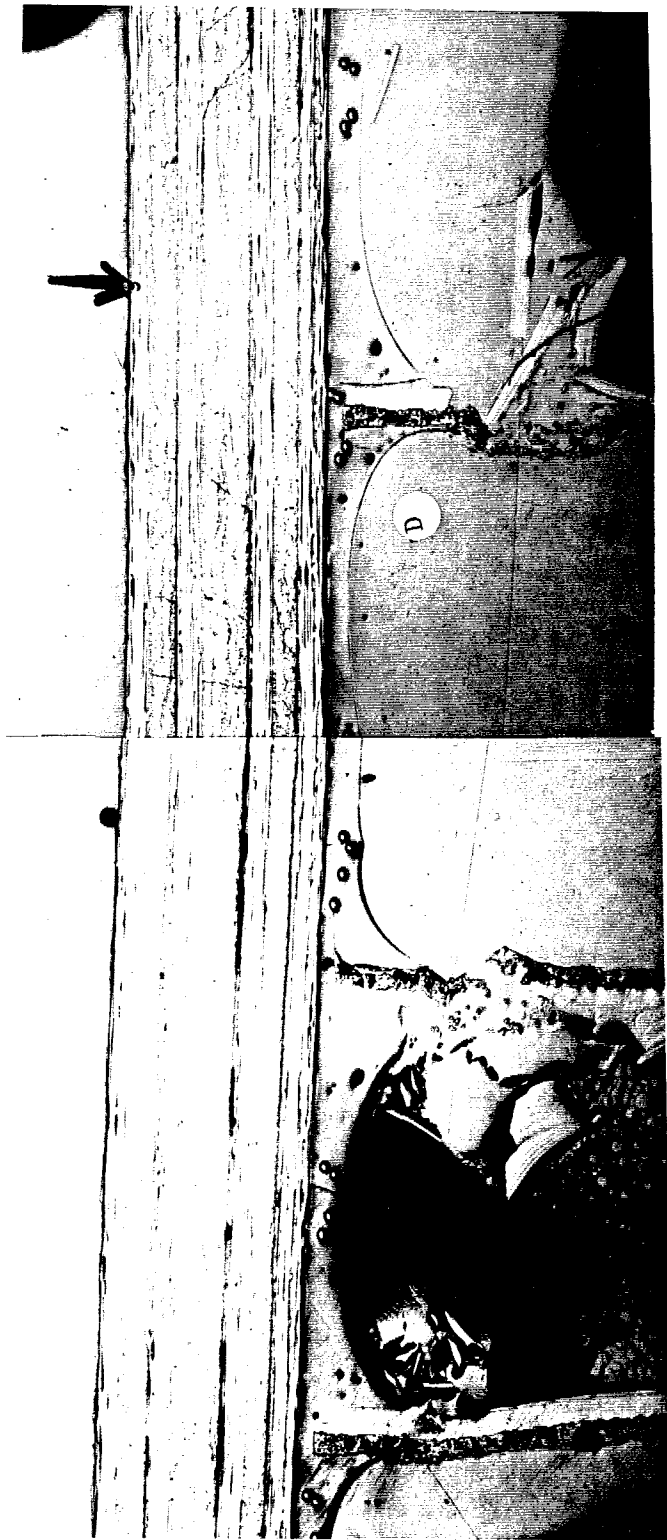


Figure 3.50. 0° Cross-Section 16894-2-2 (25X) Part A



Figure 3.51. 0° Cross-Section 16894-2-2 (25X) Part B



Figure 3.52. 90° Cross-Section 16894-2-1 (25X)



Figure 3.53. 90° Cross-Section 16894-2-2 (25X)

Specimen 16894-2-2 was impacted in between core walls, Figure 3.50, label D and Figure 3.51, label E. The core wall close to the impact (Figure 3.50, label D) received the most damage.

There was a significant amount of delamination in the 90° cross-section. These are shown in Figures 3.52-3.53. There were long delaminations at the bottom (Figure 3.52, label I and 3.53, label I) and a few short delaminations at the top of the 0/90 interface (Figure 3.52, label J and 3.53, label J). Lammerant and Verpost [34] experienced this phenomenon in the face sheets they impacted. They observed that the higher delamination is directed towards the middle of the laminate (back towards the impact site) while the delamination at the lower interface is directed away from the center as in Figure 3.54.

The micrograph of 16894-2-1 shows that the crack densities to the right and left of the impact site in the middle 90° layer is larger than the crack density in the top and bottom 90° plies. Again, this is attributed to the core positioning. A similar crack formation is seen in the micrograph of 16894-2-2.

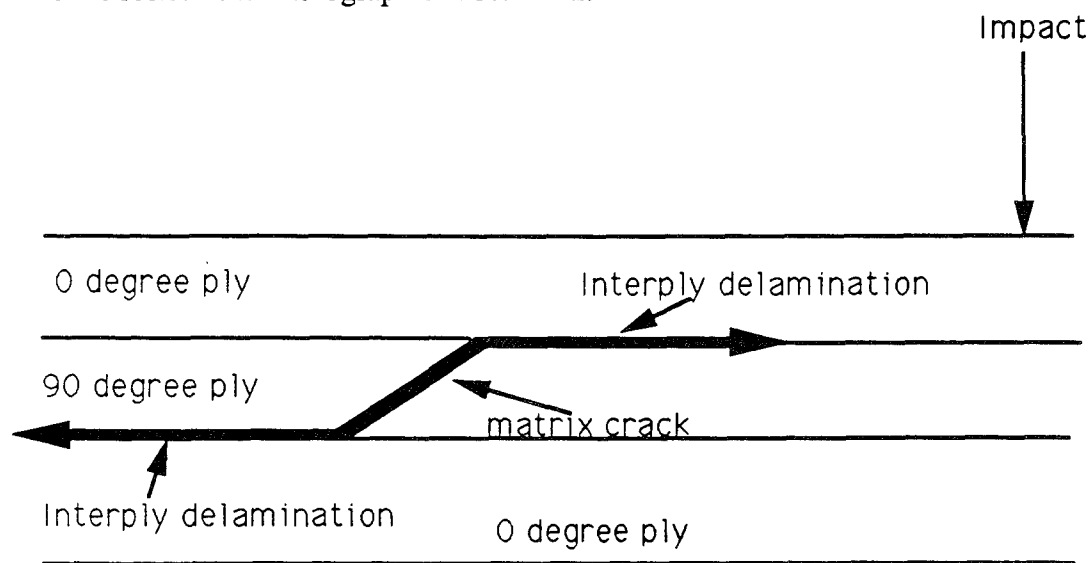


Figure 3.54. Direction of Delamination Enlargement

(2) Impact Energy = 3.05 J (2.25 ft-lb)

The sandwich specimen was impacted at a drop height of 8.89 cm (3.5 in). The load curve is shown in Figure 3.55. The impact energy, absorbed energy and maximum load have increased from the previous tests as did the damage area. The first significant drop in the load curve occurs at approximately 800 N, which is in the same range as previous test. The details of the damage can be seen in the micrographs. The 0° and 90° cross-sections (Figure 3.56 and 3.57) show an overall view while Figures 3.58-3.63 give a more detailed view of the top portion of the sandwich specimen.

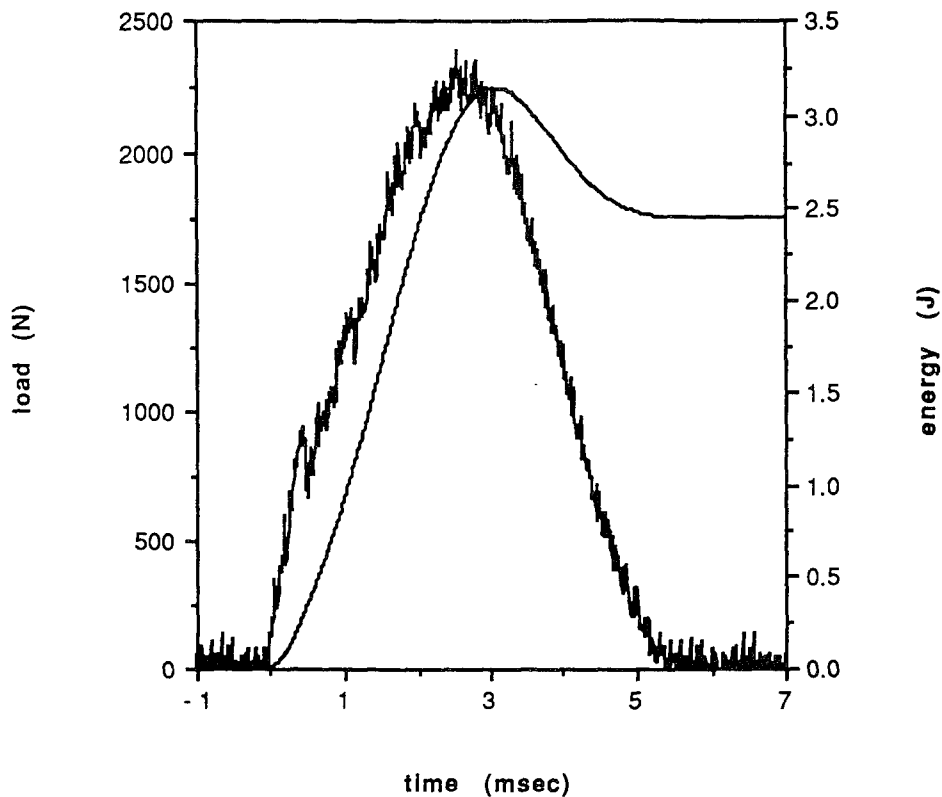
From the overview, it is apparent that there is a significant amount of delamination in the top face sheet. The core cripples at the top in both the 0° and 90° cross-sections. The delamination in the 90° cross-section appears to have bigger openings than the delamination in 0° cross-section. The bottom area of the core and the face sheet appear to be unaffected by the impact.

The higher magnification shows that the cracks and delamination form in a similar manner as previous tests. The angled cracks to the left and right of the impact are once again present, as are the vertical cracks near the impact area.

Cracks are also present in the adhesive in 0° cross-section. These cracks are not present in the 90° cross-section; however the openings of the delamination is larger in the 90° cross-section. This implies that the adhesive did not transfer as much load in the 90° cross-section as it did in the 0° cross-section

(3) Impact Energy = 3.35 J

The sandwich specimen was impacted at a drop height of 10.16 cm (4.0 in). The load and energy curves are shown in Figure 3.64. In this case, the load curve drops at



Specimen ID -16894-2-3	Max load - 2391.8 N (537.7 lb)
Impact Velocity - 1.30 m/s (4.26 ft/s)	Energy at Max Load - 2.954 J (2.179 ft-lb)
Impact Energy - 3.05 J (2.25 ft-lb)	Time - at Max load - 2.55 msec
Absorbed Energy - 2.451 J (1.808 ft-lb)	total 5.38 msec
Max Disp. of Tup 0.246cm (0.097 in)	Damage Area - 1.798 cm ² (0.279 in ²)
Damage Indent.- 0.017 cm (0.007 in)	Damage Radius - 0.51 cm (0.2 in)

Figure 3.55. Load and Energy from Dynatup for 8-ply at 8.89 cm (3.5 in) drop height

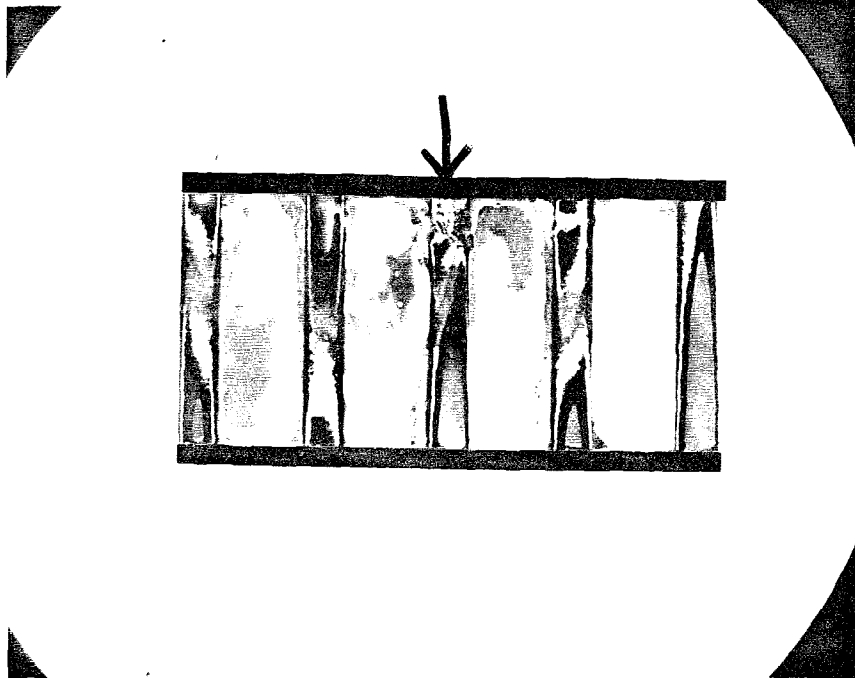


Figure 3.56. 0° Cross-Section 16894-2-3 (2.7 X)



Figure 3.57. 90° Cross-Section 16894-2-3 (2.7 X)

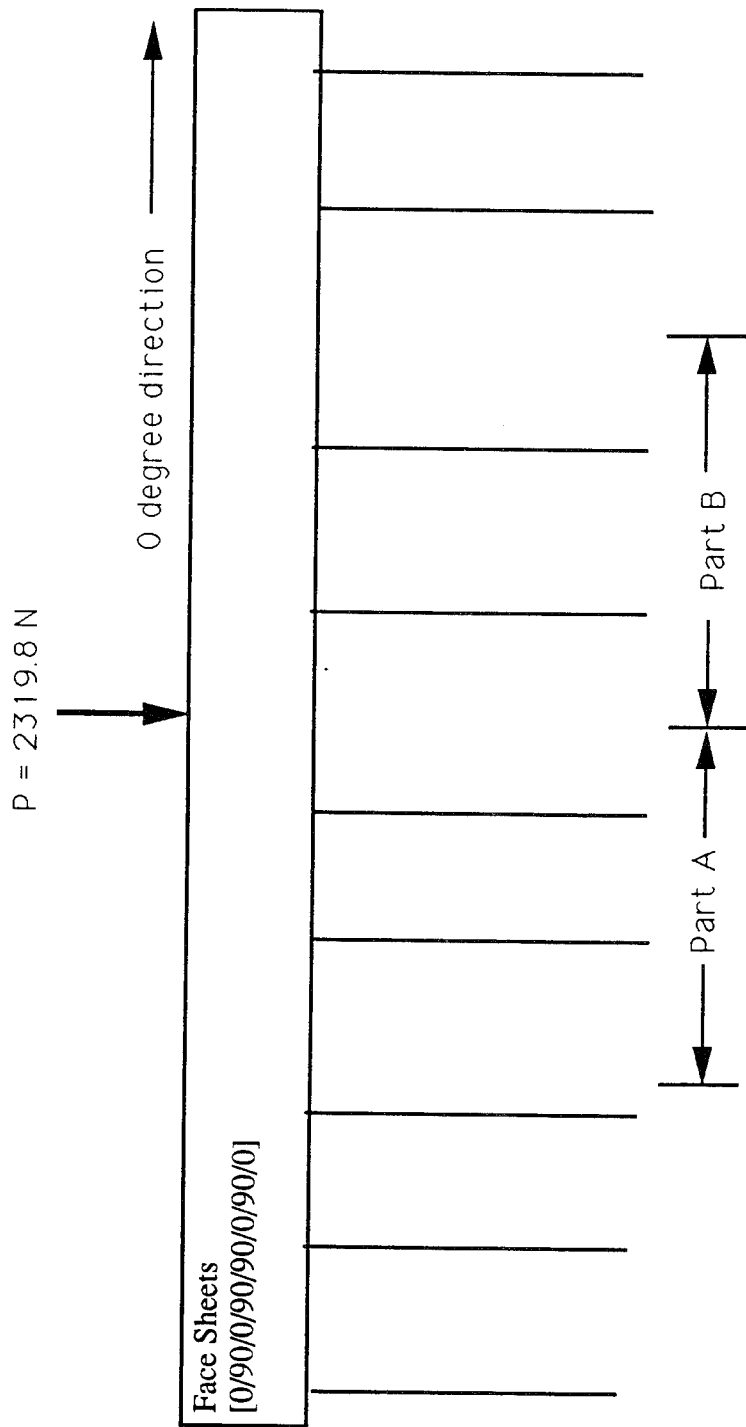


Figure 3.58. Guide to Micrograph of 0 Degree Cross-Section (25X) -16894-2-3

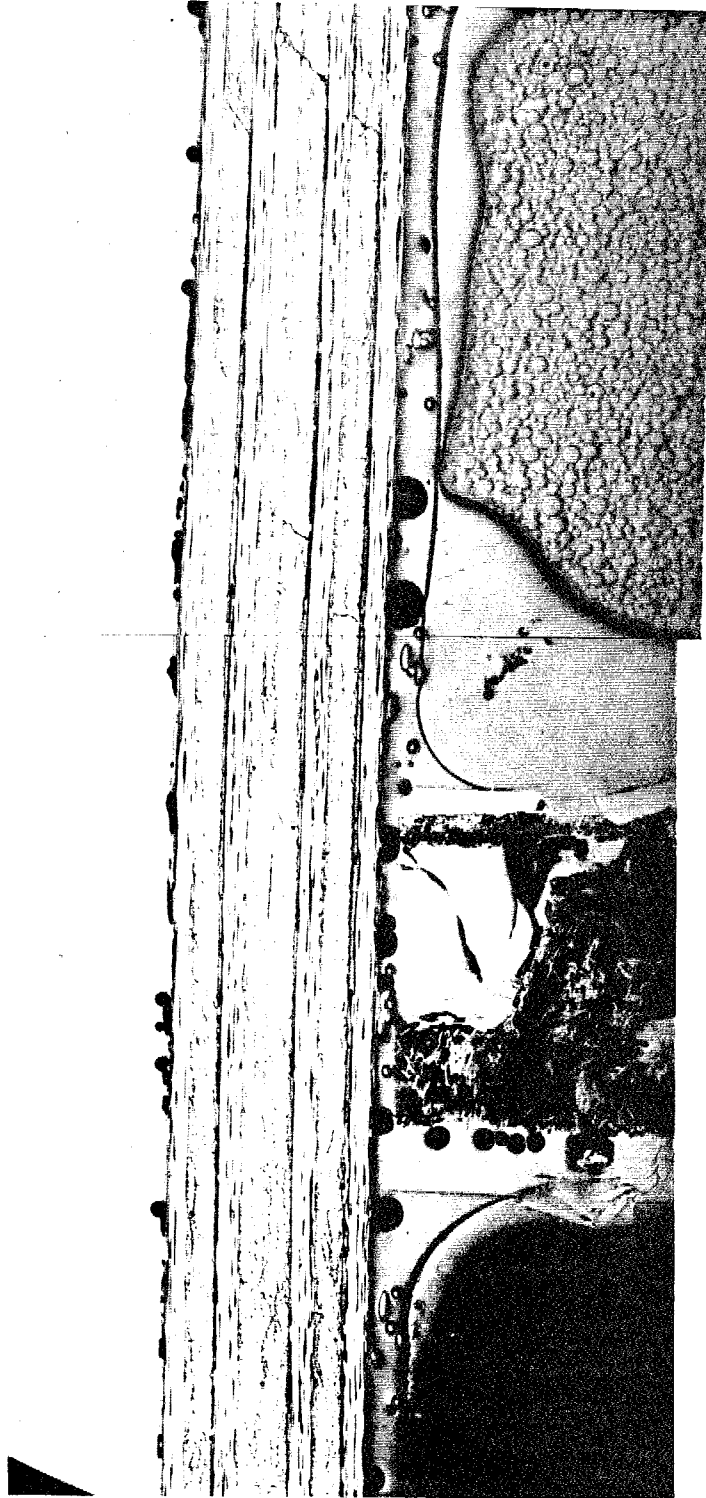


Figure 3.59. 0° Cross-Section 16894-2-3 (25X) Part A



Figure 3.60. 0° Cross-Section 16894-2-3 (25X) Part B

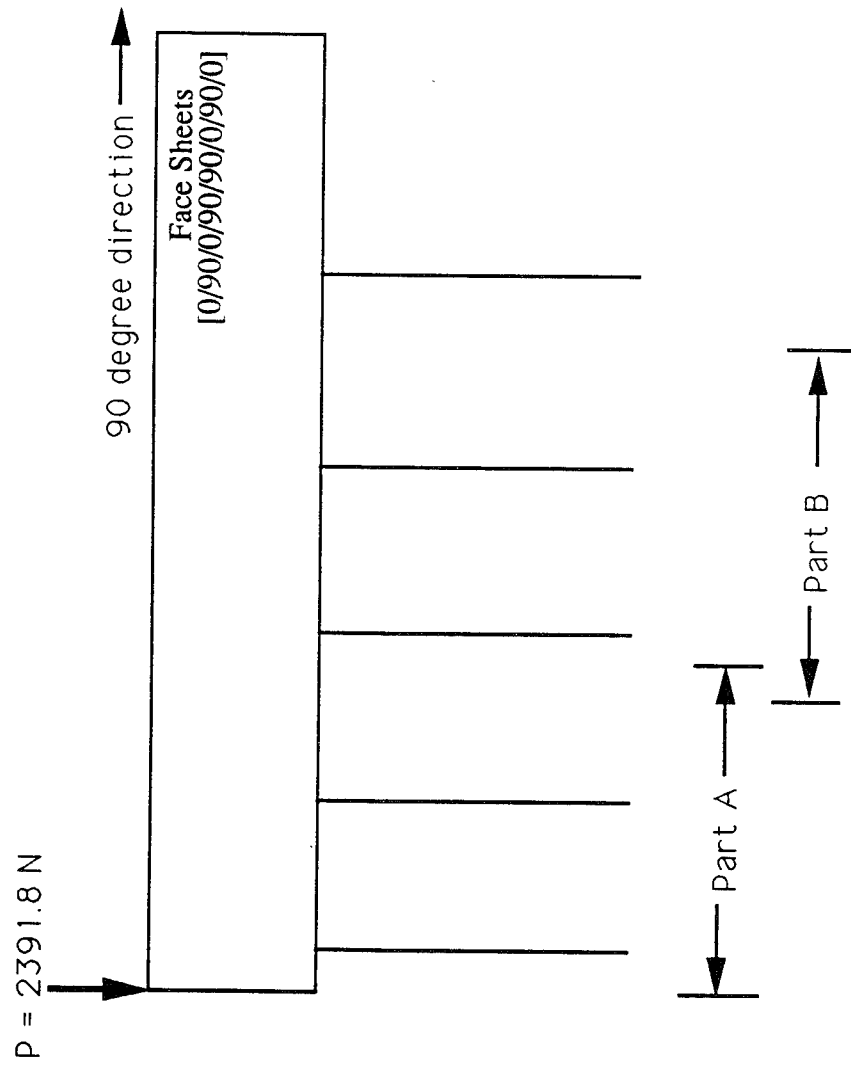


Figure 3.61. Guide to Micrograph of 90 Degree Cross-Section (25X) - 16894-2-2

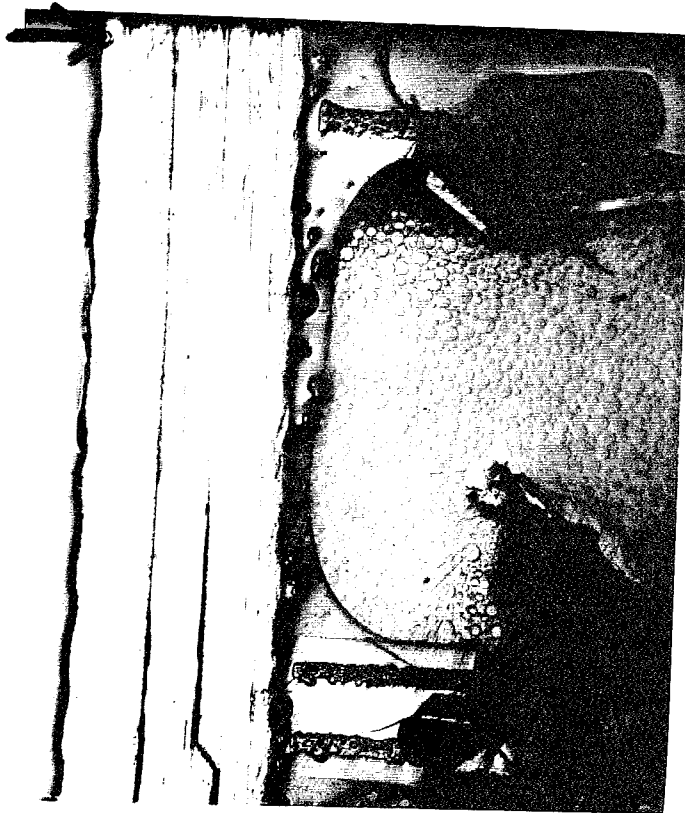


Figure 3.62. 90° Cross-Section 16894-2-3 (25X) Part A

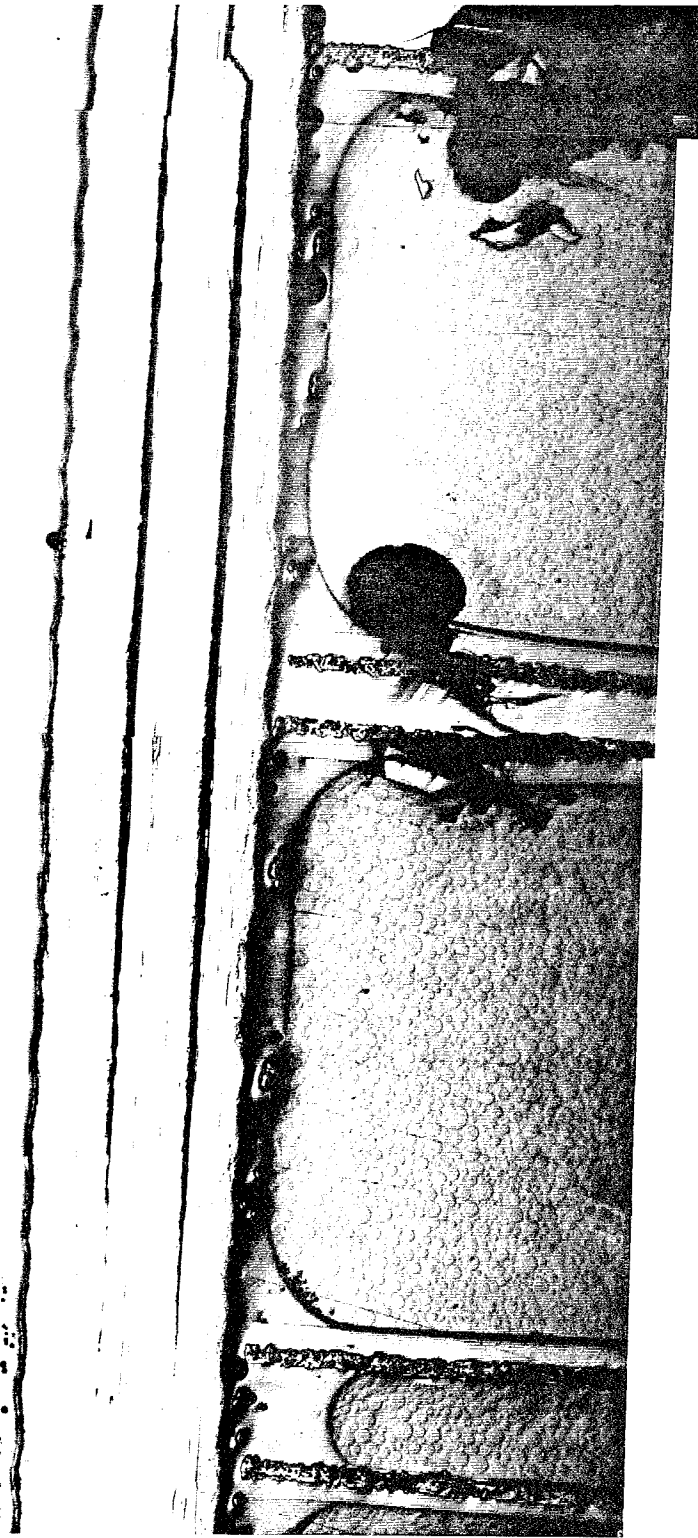
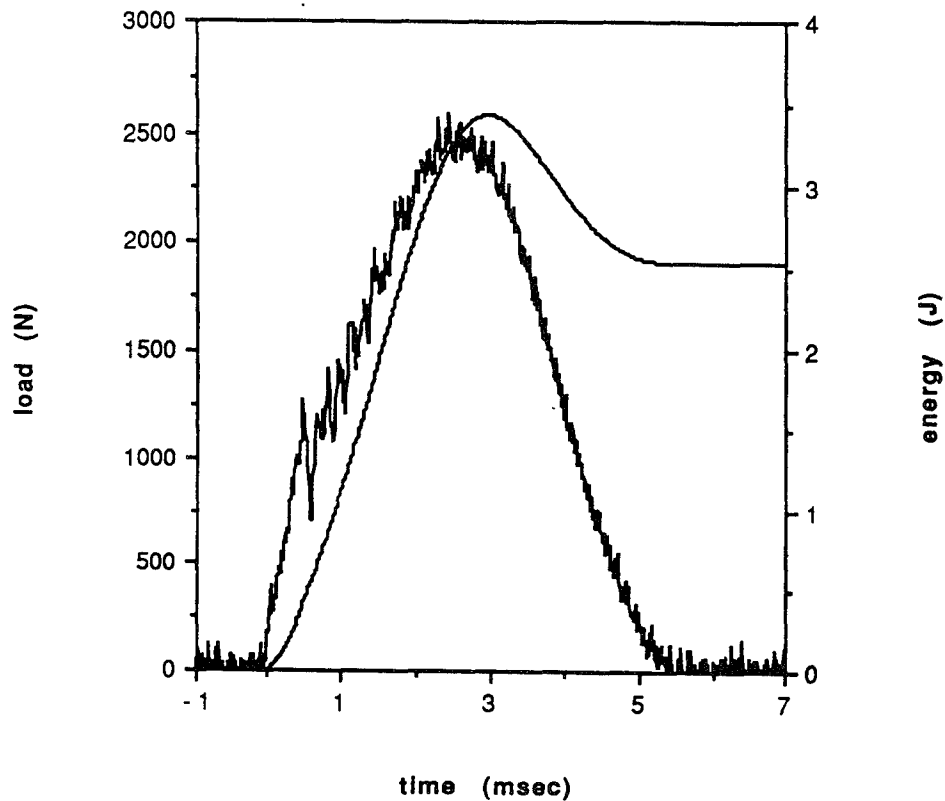


Figure 3.63. 90° Cross-Section 16894-2-3 (25X) Part B

approximately 1200 N. This value is higher than the previous test; however, it is still in the general range. The impact energy, absorbed energy and maximum load have increased from the previous test. The damage area also increased. The details of the damage can be seen in the micrographs. The 0° and 90° cross-sections (Figure 3.65 and 3.66) show an overall view while Figure 3.67-3.73 provide a more detailed view.

In the previous test, delamination with large openings only formed in the 90° cross-sections. In this instance, the delamination has large openings in both the 0° and 90° cross-sections. The specimen was impacted near core walls in both the 90° and 0° cross-section. When this occurred in one of the 4-ply tests (Specimen ID 16694-3-5), the impact load was distributed between the core walls, resulting in less damage of the core (See Section 3.3.3). Though the specimen received a significant amount of damage based on the delamination and crack openings, delamination length and core crippling at this impact level, the results from the 4-ply test imply that the damage would have been more severe if were not for the support offered by the core walls. The bottom core area and face sheet again appear to be unaffected by the impact.

The delamination travels as shown in Figure 3.54. With the increase in impact energy, the higher interface delamination has openings just as large as the lower interface (Figure 3.69, labels A and B). In the previous test, the lower interface delamination had wider openings than the higher. The cracks angled towards the impact are again present. As the distance from the impact increases, the cracks take on vertical angles. In the case of the 4-ply, at the higher impact energies, only vertical cracks were over the delamination (Figure 3.20, label E). In this case, vertical and angled cracks developed over the delamination (Figure 3.70, label C). As the impact energy increased in the 8-ply test more cracks developed at the bottom 90° ply (Figure 3.69, label D). The 90° cross-section (Figure 3.73 and 3.74) did not change much from the previous test.



Specimen ID -16894-2-6	Max load - 2596.0 N (583.6lb)
Impact Velocity - 1.36 m/s (4.46 ft/s)	Energy at Max Load - 3.215 J (2.371 ft-lb)
Impact Energy - 3.35 J (2.47 ft-lb)	Time - at Max load - 2.45 msec
Absorbed Energy - 2.530 J (1.866 ft-lb)	total - 5.37 msec
Max Disp. of Tup 0.248cm (0.098 in)	Damage Area - 2.140 cm ² (0.332 in ²)
Damage Indent.- 0.030 cm (0.012 in)	Damage Radius - 0.64 cm (0.25 in)

Figure 3.64. Load and Energy from Dynatup for 8-ply at 10.16 cm (4.0 in) drop height

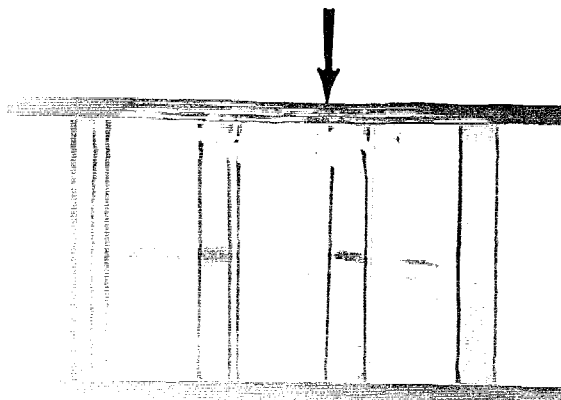


Figure 3.65. 0° Cross-Section 16894-2-6 (2.7 X)

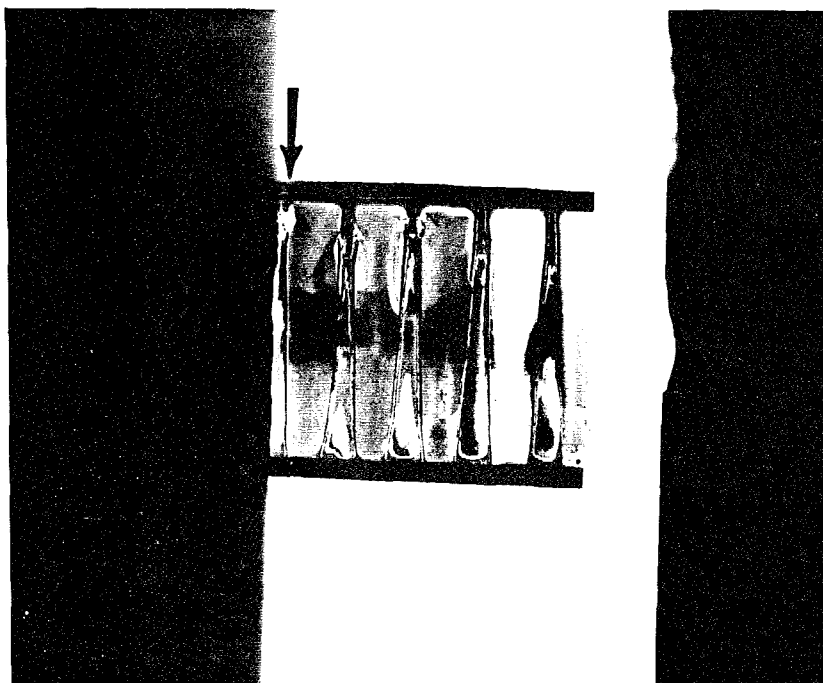


Figure 3.66. 90° Cross-Section 16894-2-6 (2.7 X)

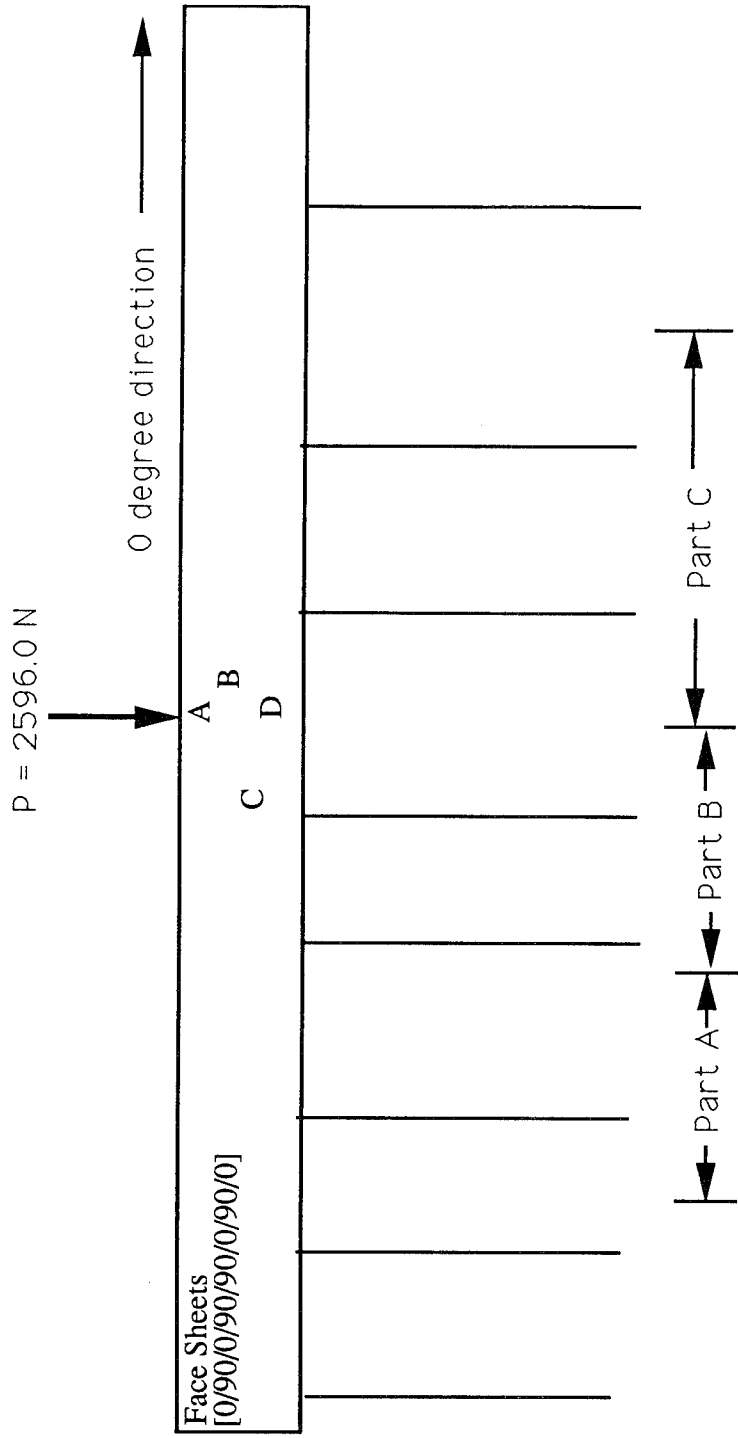


Figure 3.67. Guide to Micrograph of 0 Degree Cross-Section (25X) -16894-2-6

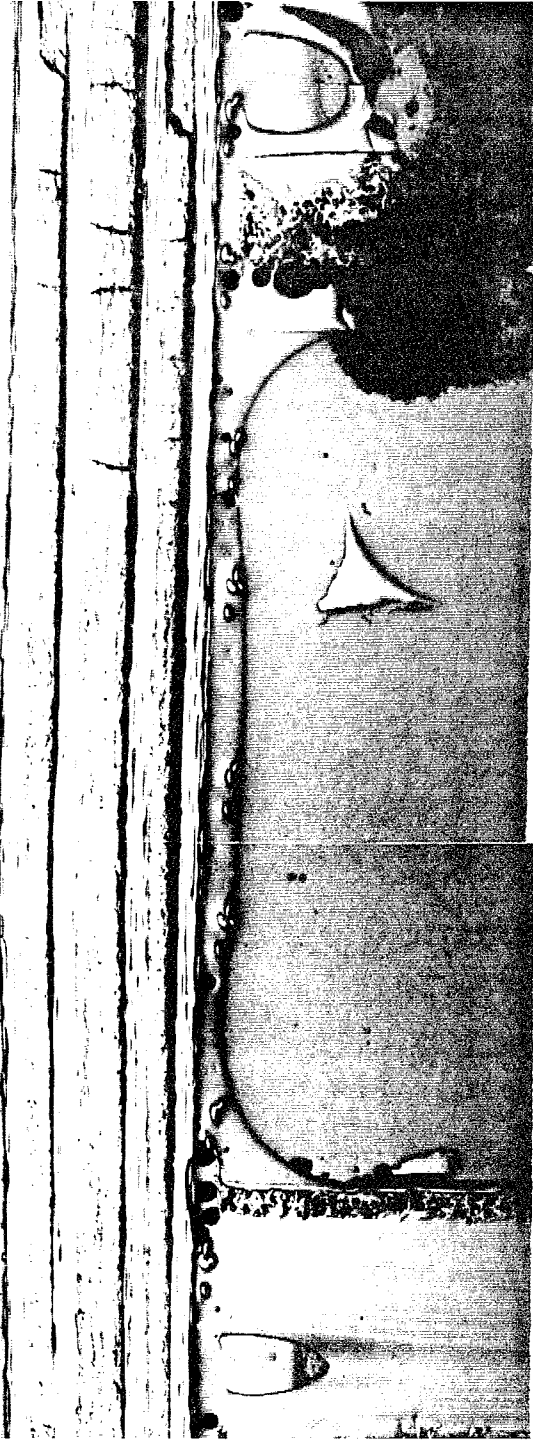


Figure 3.68. 0° Cross-Section 16894-2-6 (25X) Part A

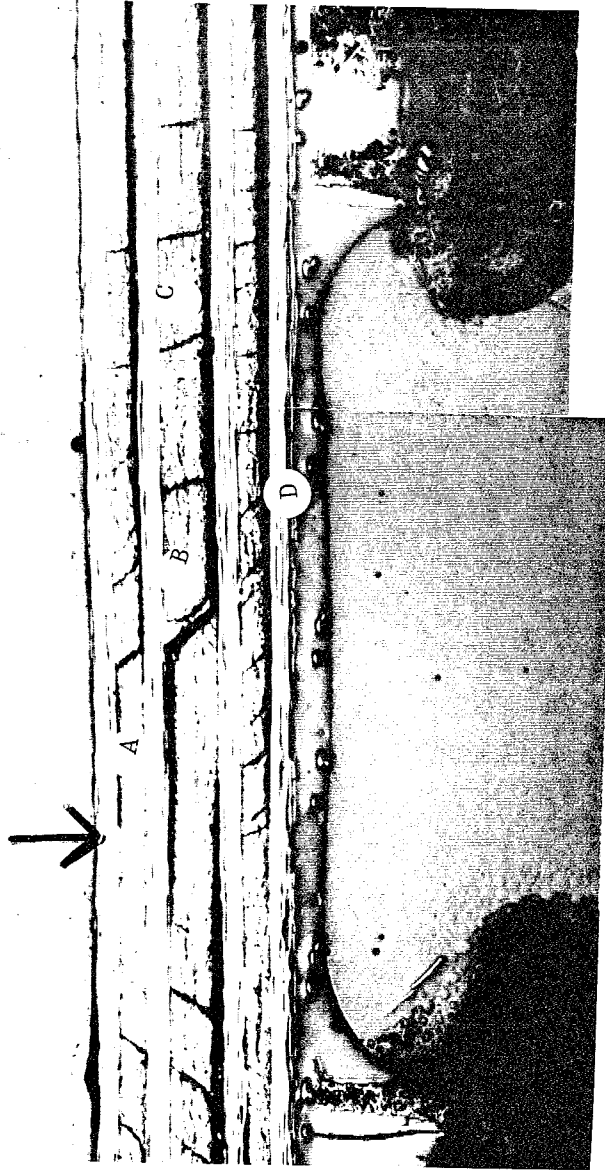


Figure 3.69. 0° Cross-Section 16894-2-6 (25X) Part B



Figure 3.70. 0° Cross-Section 16894-2-6 (25X) Part C

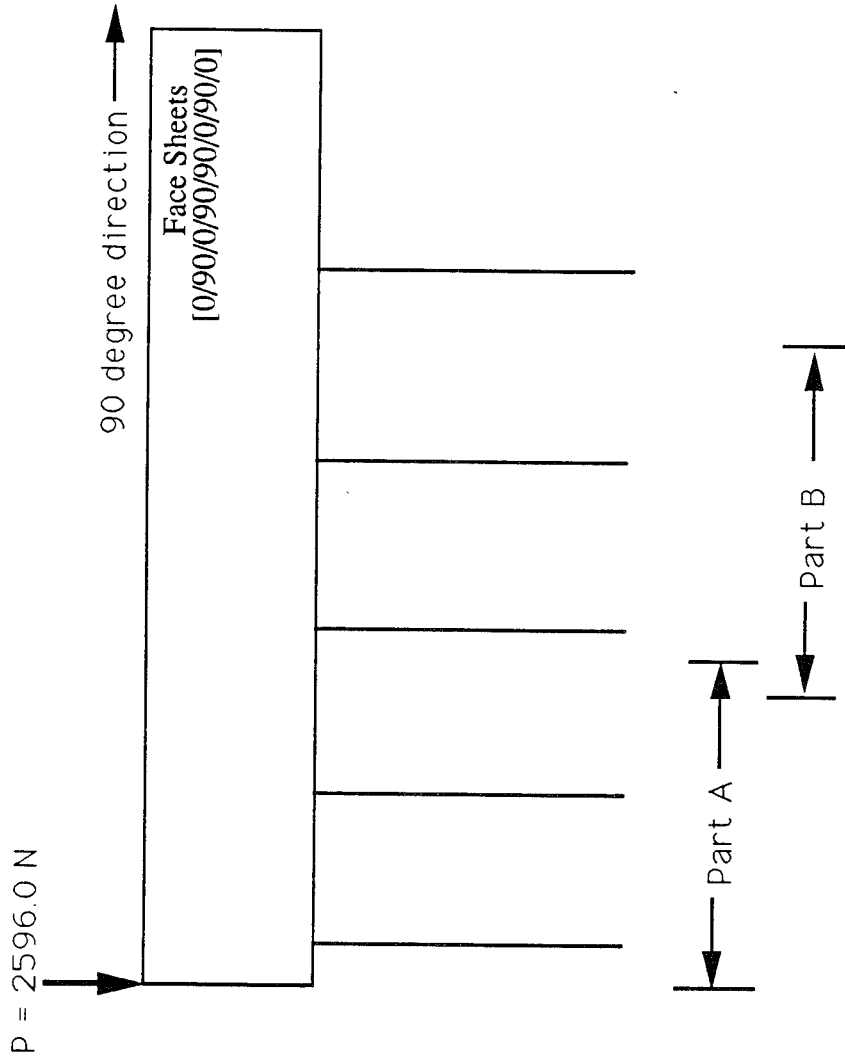


Figure 3.71. Guide to Micrograph of 90 Degree Cross-Section (25X) - 16894-2-6



Figure 3.72. 90° Cross-Section 16894-2-6 (25X) Part A

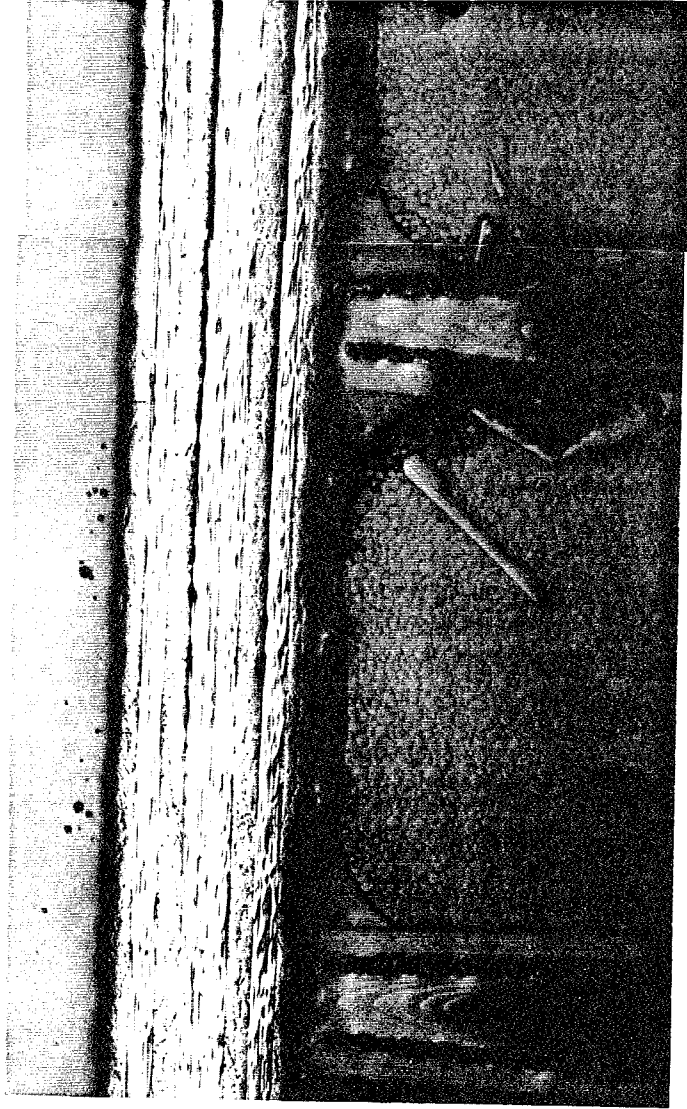


Figure 3.73. 90° Cross-Section 16894-2-6 (25X) Part B

(4) C-scan

Pulse echo c-scans were taken of each impacted specimen. Figure 3.74 shows the area of damage captured by the C-scan. The shapes changed from impact to impact. Some were oblong while others took the diamond shape like in the 4-ply sandwich panels.

2.60 Joules
(1.92 ft-lb)



2.52 Joules
(1.86 ft-lb)

3.05 Joules
(2.25 ft-lb)



3.35 Joules
(2.47 ft-lb)



Figure 3.74. Pulse-Echo C-scans for Sandwich Panels with 8-ply Face Sheets

The damage shown in Figure 3.74 is due to delamination in the face sheet and the size is reduced by 33%. Figure 3.75 shows the damage area versus the impact energy and absorbed energy. The damage area increases as the energies increases in a similar manner as that seen in the 4-ply.

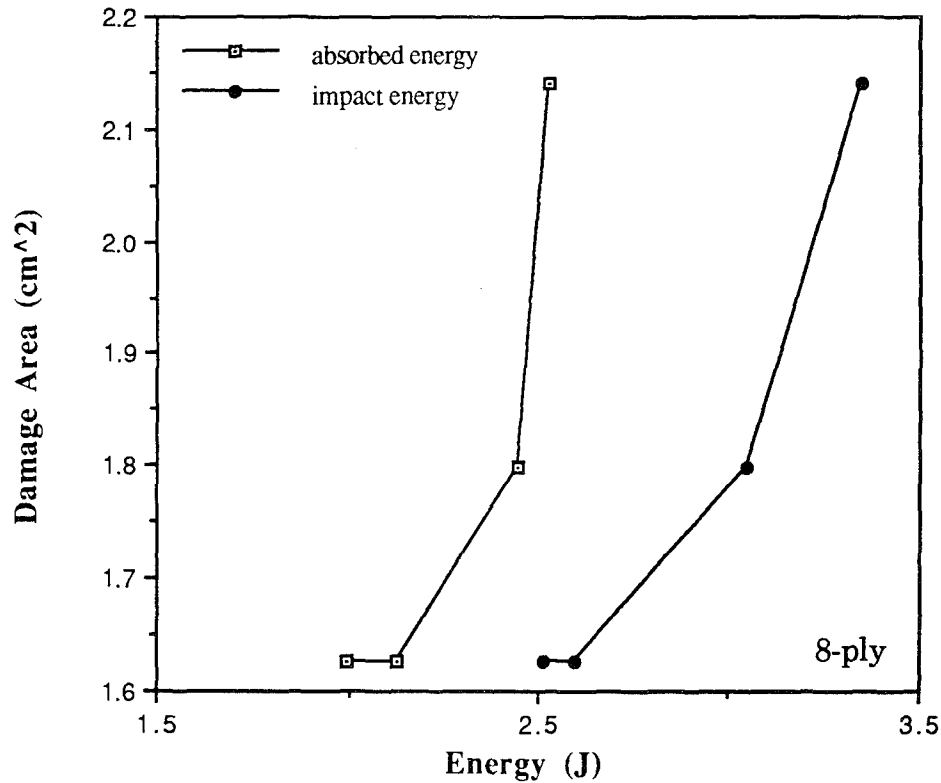


Figure 3.75. Damage Area vs Impact and Absorbed Energies - 8-ply

(5) Additional Analysis

Figure 3.76 compares the energy curves for each test while Figure 3.77 compares the load curves for the highest and lowest impact energy. Note that the peak energy values occur around the same time. Also, the total time of event, as shown in the load curves are approximately the same for this test series. The test with an impact energy level of 3.35 J had a drop in the load curve at approximately 1200 N. Although 1200 N is

in the general range, this was a higher value than the other test. Nonetheless, the initial drops occur at the same time and dip down to approximately the same value.

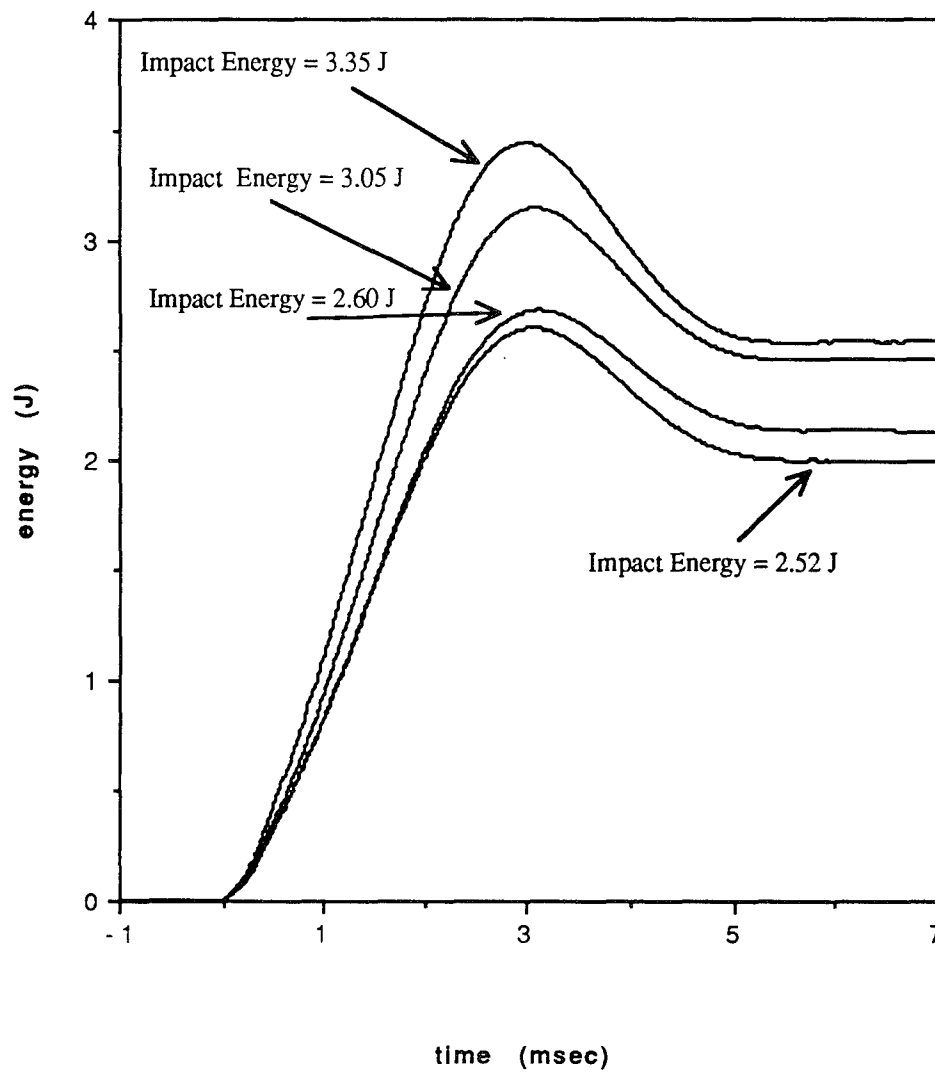


Figure 3.76. Comparison of Energy Curves for Sandwich Panels with 8-ply Face Sheets

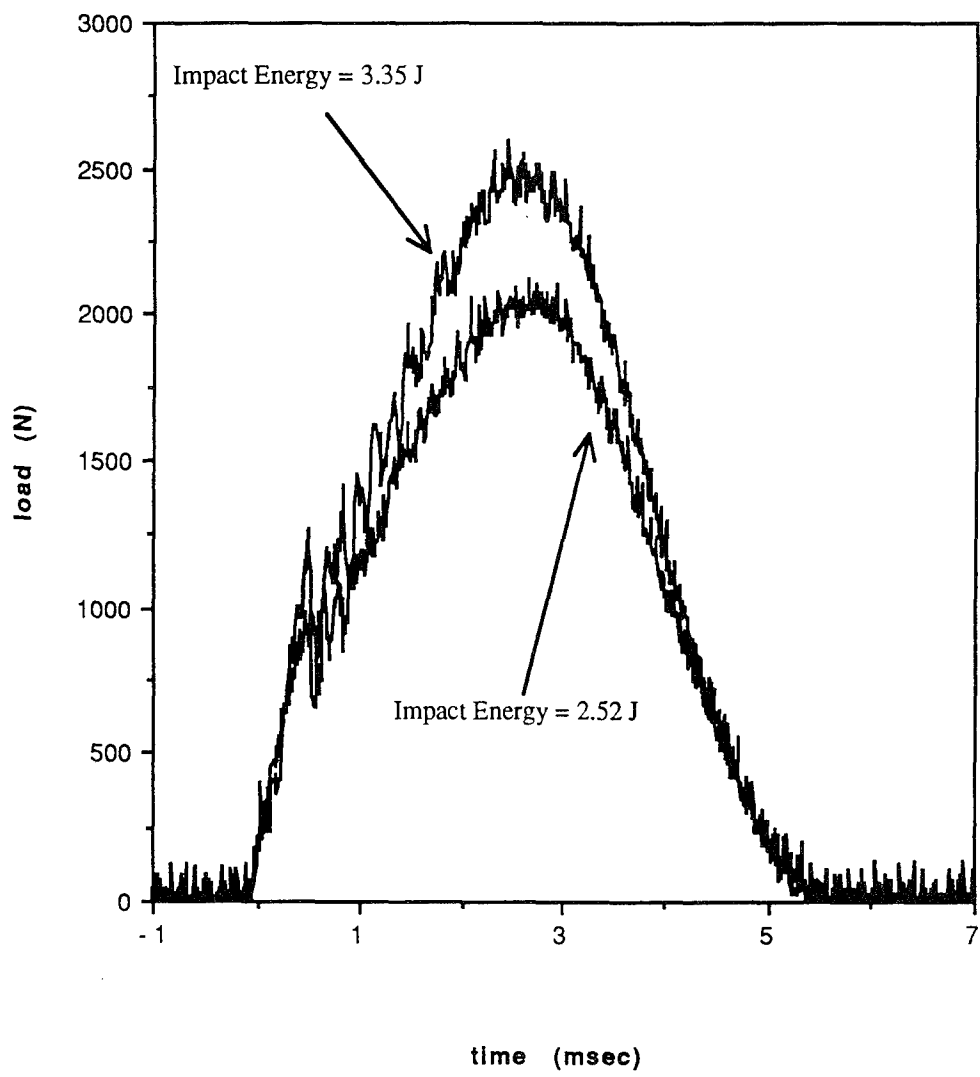


Figure 3.77. Comparison of Load Curves for Various Impact Energies for Sandwich Panels with 8-ply Face Sheets

Figure 3.78 shows the difference between the absorbed energy and impact energy. As in the 4-ply test series, the differences (recovered elastic energy) increase with drop height. Figure 3.79 compares the recovered elastic energy for the 4-ply and 8-ply tests.

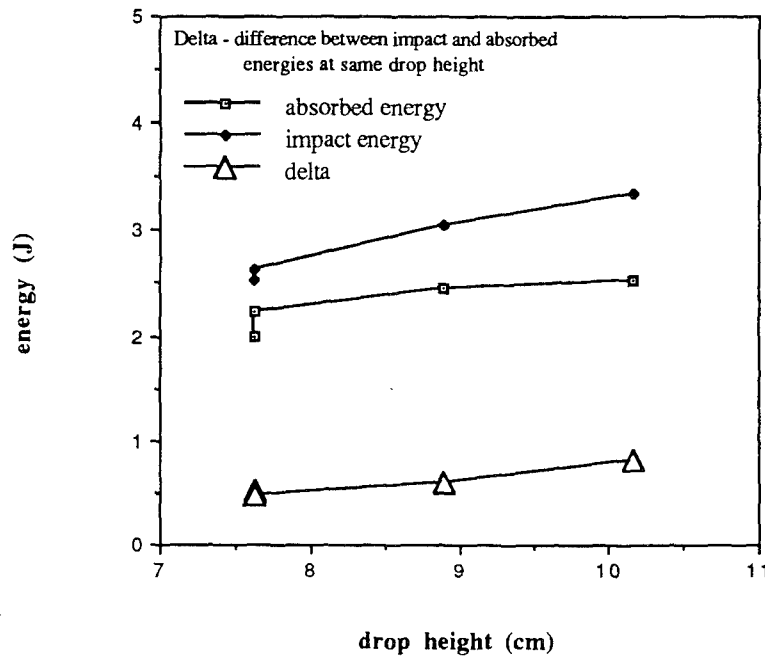


Figure 3.78. Comparison of Absorbed Energy and Impact Energy vs Drop Height for Sandwich Panels with 8-ply Face Sheets

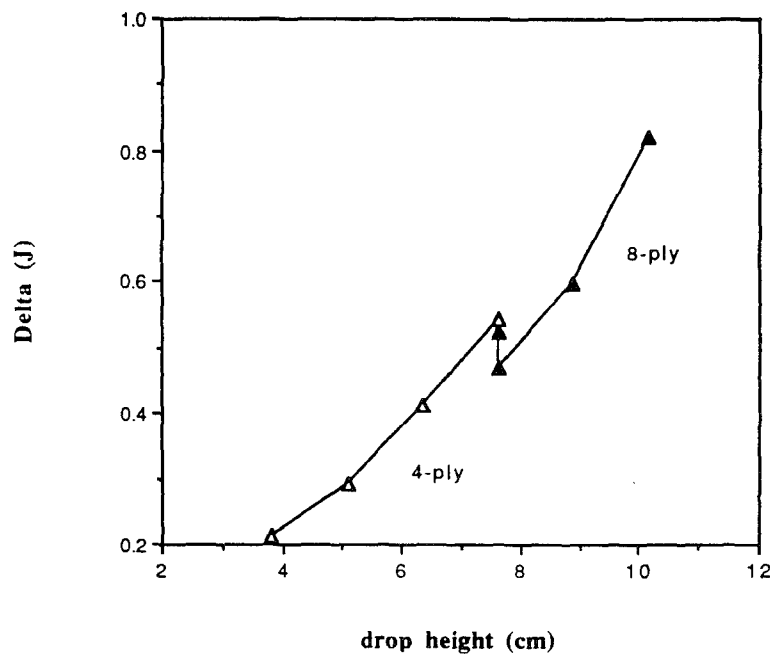


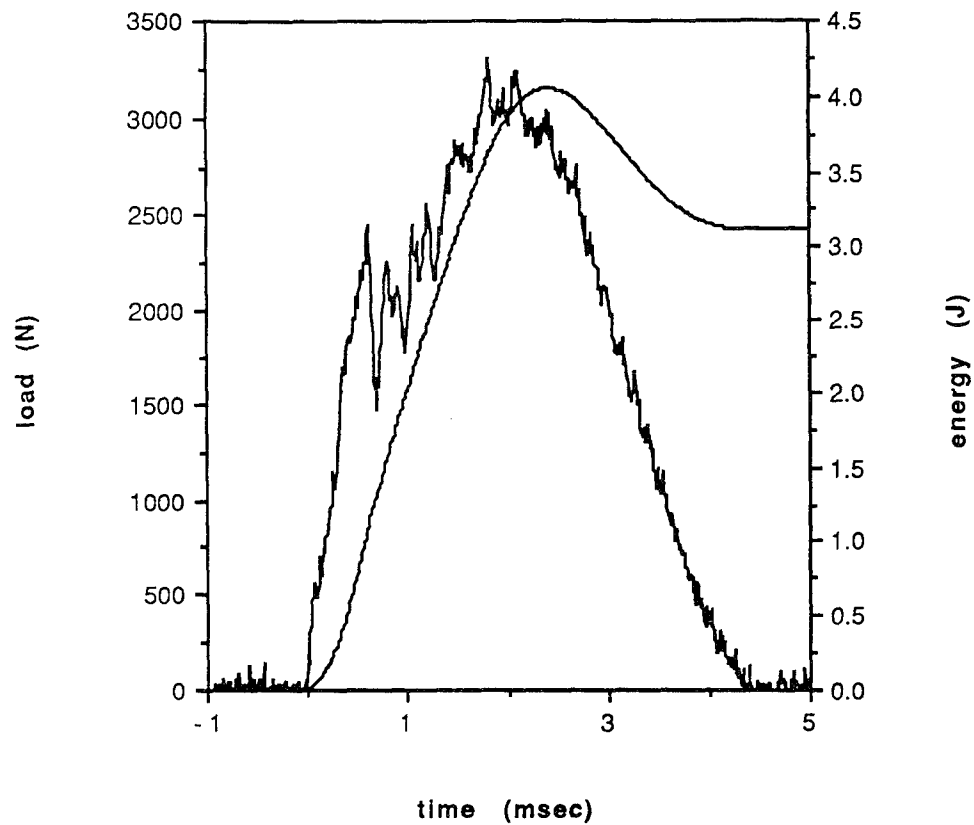
Figure 3.79. Comparison of Recovered Elastic Energy for 4-ply and 8-ply Test Series

3.6 Sandwich Panels with 16-ply Face Sheets

The sandwich panels with 16-ply face sheets were subjected to low energy (velocity) impacts with drop heights ranging from 11.43 cm (4.5 in) to 16.51 cm (6.5 in). The smoothness of the load curve has improved over the last test due to the decrease in the ratio of instrumental/background noise level to impact load. In all test, the first minor repeatable peaks are present until a load of approximately 2500 N (562 lb) is reached. This implies that at this point the sandwich panel no longer acts in an elastic manner. After this point, the load curve has a dramatic dip in each test. This is the initiation of damage such as crushing and ply delamination. Recall that the approximate point of damage initiation is 750 N (169 lb) for the 4-ply and 1000 N (225 lb) for the 8-ply. The load and energy curves for each test will be presented; however, only the micrographs for the highest and lowest impact levels will be presented.

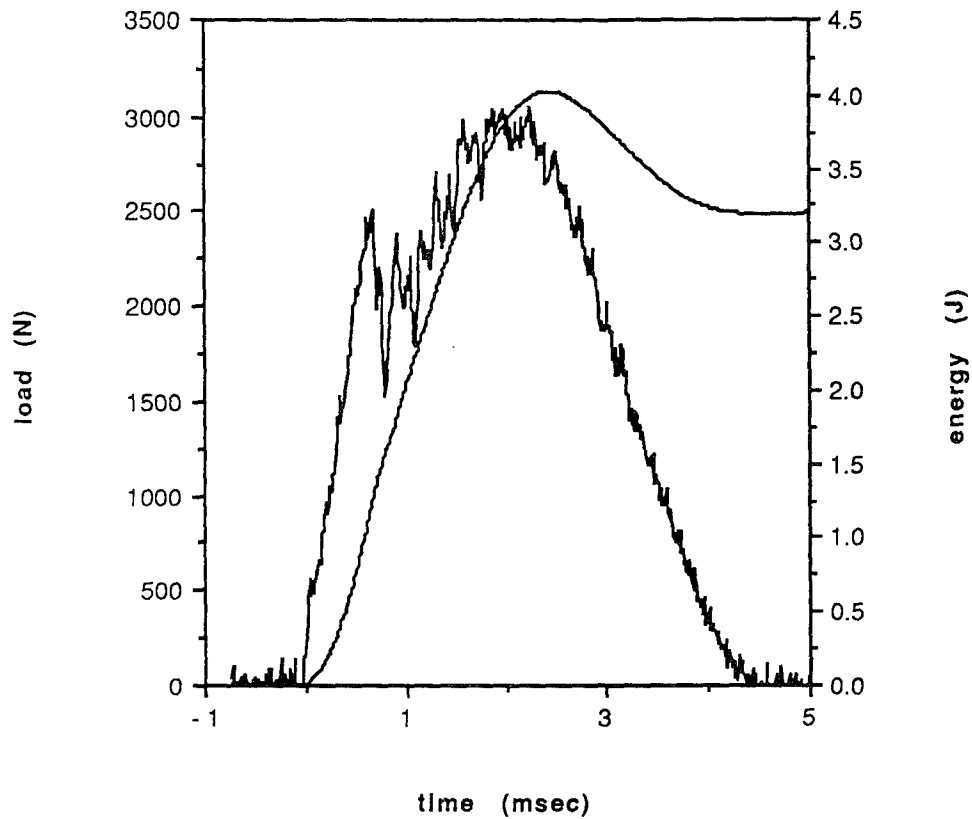
(1) Impact Energy = 3.95 J and 3.97 J

The load and energy curves for sandwich panels with 16-ply face sheets at a drop height of 11.43 cm (4.5 in) are shown in Figures 3.80 and 3.81. Two tests (Specimen ID 17294-1-1 and 17294-1-2) were performed at this drop height. Though the maximum load values differ by 7.5% (3304.6 N for the first test and 3057.7 N for the second), the impact energies and impact velocities varied by 0.5% and 0.2%. The absorbed energies differed by 2.7%. The test with the higher maximum load (Specimen ID 17294-1-1) resulted in an energy at maximum load lower than the impact energy while Specimen ID 17294-1-2 resulted in an energy at maximum load slightly higher than the impact energy. Furthermore, the time to maximum load of the 17294-1-1 occurred earlier. Notice how the load curve settles at the top for an elapsed time at a range of values around the



Specimen ID -17294-1-1	Max load - 3304.6 N (742.9 lb)
Impact Velocity - 1.48 m/s (4.85 ft/s)	Energy at Max Load - 3.628 J (2.676 ft-lb)
Impact Energy - 3.97 J (2.93 ft-lb)	Time - at Max load - 1.84 msec
Absorbed Energy - 3.109 J (2.293 ft-lb)	total - 4.33 msec
Max Disp. of Tup 0.2121 cm (0.0835 in)	Damage Area - 2.055 cm ² (0.318 in ²)
Damage Indent.- 0.013m (0.005 in)	Damage Diameter- 0.76 cm (0.3 in)

Figure 3.80. Load and Energy from Dynatup for 16-ply at 11.43 cm (4.5 in) drop height



Specimen ID - 17294-1-2	Max load - 3057.7 N (687.4 lb)
Impact Velocity - 1.48 m/s (4.84 ft/s)	Energy at Max Load - 3.982 J (2.937 ft-lb)
Impact Energy - 3.95J (2.91 ft-lb)	Time - at Max Load - 2.26 msec
Absorbed Energy - 3.192 J (2.354 ft-lb)	total - 4.38 msec
Max Disp. of Tup 0.2103 cm (0.0828 in)	Damage Area - 2.055 cm ² (0.318 in ²)
Damage Indent.- 0.015 cm (0.006 in)	Damage Diameter - 0.76 cm (0.3 in)

Figure 3.81. Load and Energy from Dynatup for 16-ply at 11.43 cm (4.5 in) drop height

maximum load for 17294-1-2 while the load curve for 17294-1-1 fluctuates more during this same time range. Overall, the tests compared favorably, including the damage area.

Figures 3.82-3.85 provide an overall view of the cross-sectioned damage area at 2.7 magnification. The damage is centered around the impact site. There is delamination in the face sheets along with crushing/buckling/crippling of the core. There appears to be more core damage in 17294-1-2 while there appears to be more delamination in 17294-1-1 in the 90° cross-sections. The delamination openings appear to be larger and the core crippling appears to be more severe in 17294-1-2.

The closer look at the 25X micrographs, Figures 3.86 - 3.93 confirms the above. The core walls of 17294-1-1 in the 90° cross-section are slightly crushed (Figure 3.93, label A and B) whereas the core walls of 17294-1-2 in the 90° cross section are crippled (Figure 3.95, label C, D and E). As shown in Figure 3.93, the delamination in 17294-1-1 extends to across the impact site in both higher and lower interfaces while the delamination in 17294-1-2, Figure 3.95, does not extend as far under the impact site. Overall, there are only 4 matrix cracks in specimen 17294-1-2 while there are 36 matrix cracks in 17294-1-1. This difference again is attributed to the location of the core walls with respect to the impact site. Specimen 17294-1-1 is impacted in the middle of 2 core walls resulting in more face sheet damage and less core damage. Specimen 17294-1-1 is impacted directly over a core wall resulting in more damage to the core wall and less damage to the face sheets.

A close-up of the 0° cross-section shows that interply delamination forms at each point of different ply orientation (as it did in the 8-ply sandwich panels). The pattern of delamination and cracks are similar for the two tests; however the openings are larger in 17294-1-1. This specimen also had more face sheet damage in the 90° direction.

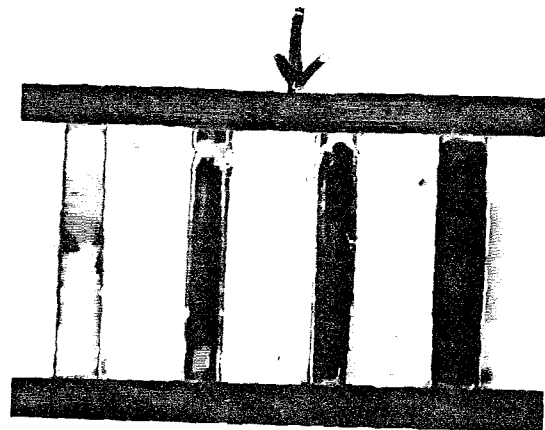


Figure 3.82. 0° Cross-Section 17294-1-1 (2.7 X)

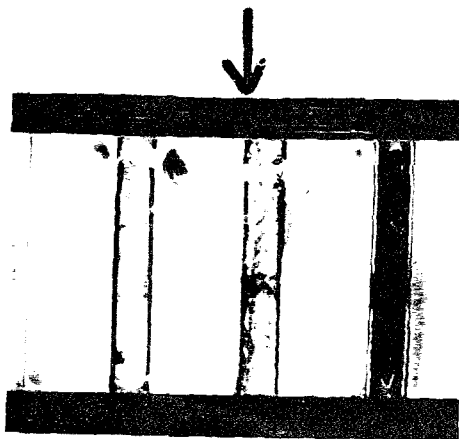


Figure 3.83. 0° Cross-Section 17294-1-2 (2.7 X)

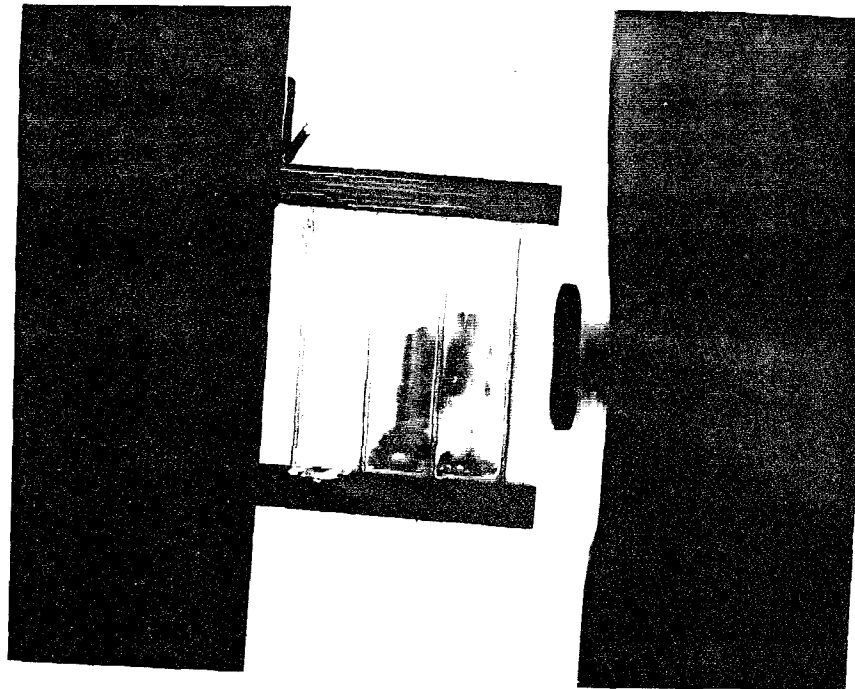


Figure 3.84. 90° Cross-Section 17294-1-1 (2.7 X)

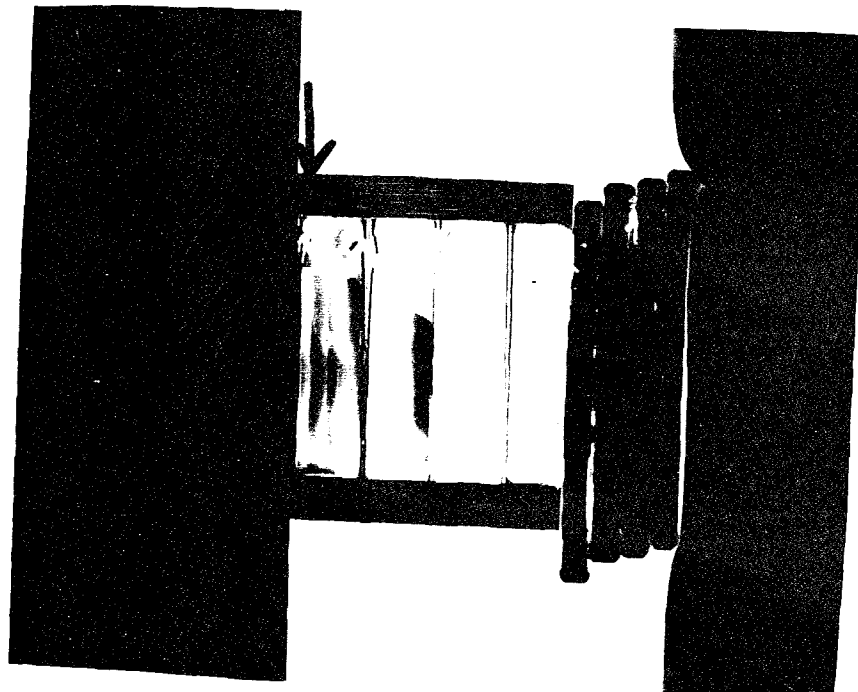


Figure 3.85. 90° Cross-Section 17294-1-2 (2.7 X)

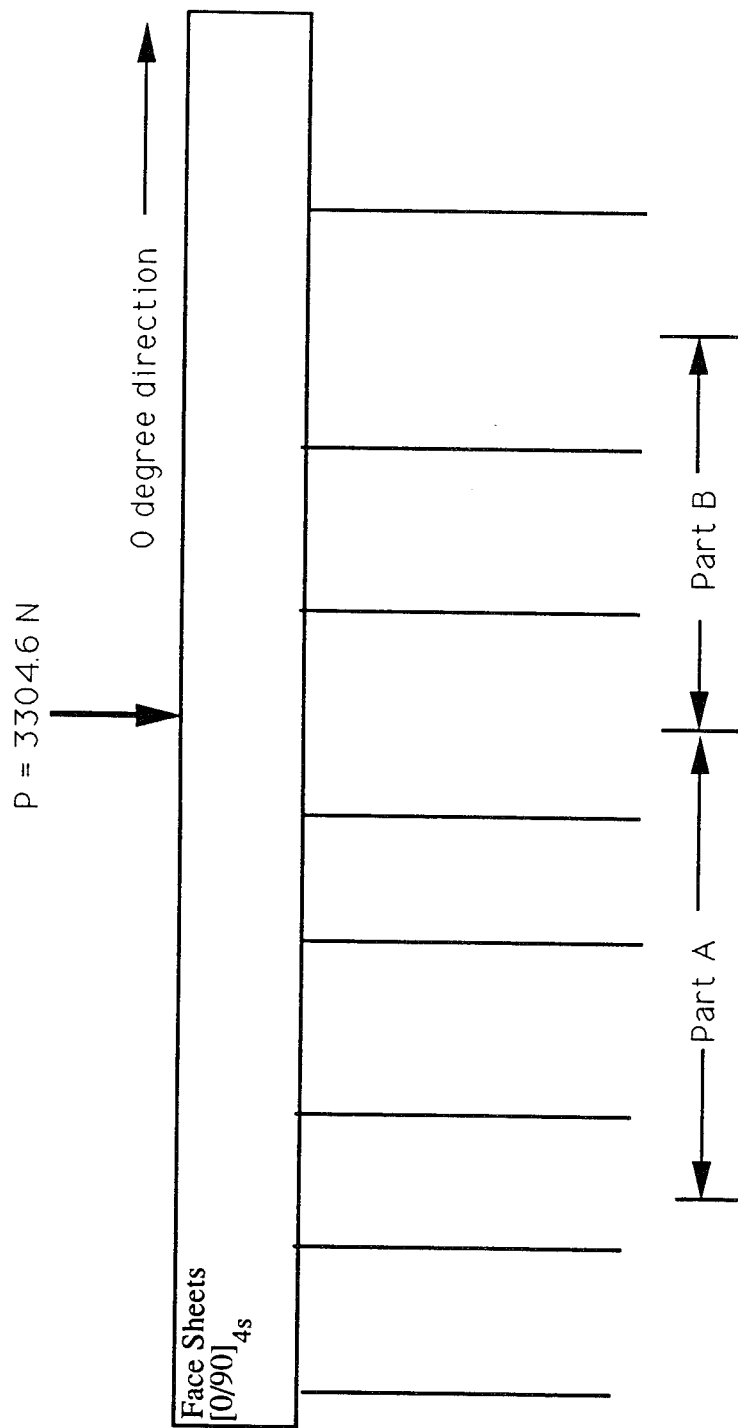


Figure 3.86. Guide to Micrograph of 0 Degree Cross-Section (25X) - 17294-1-1

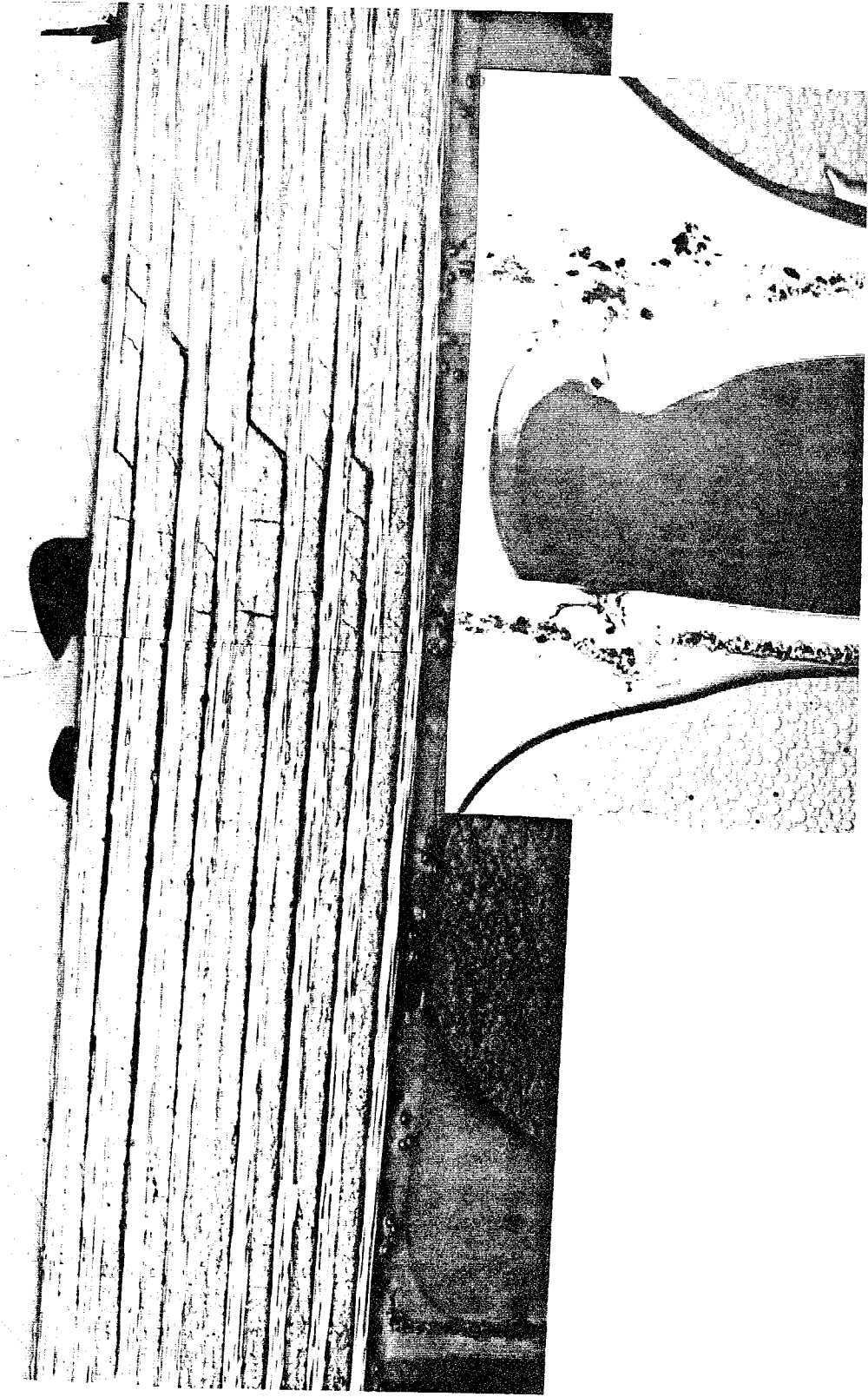


Figure 3.87. 0° Cross-Section 17294-1-1 (25X) Part A

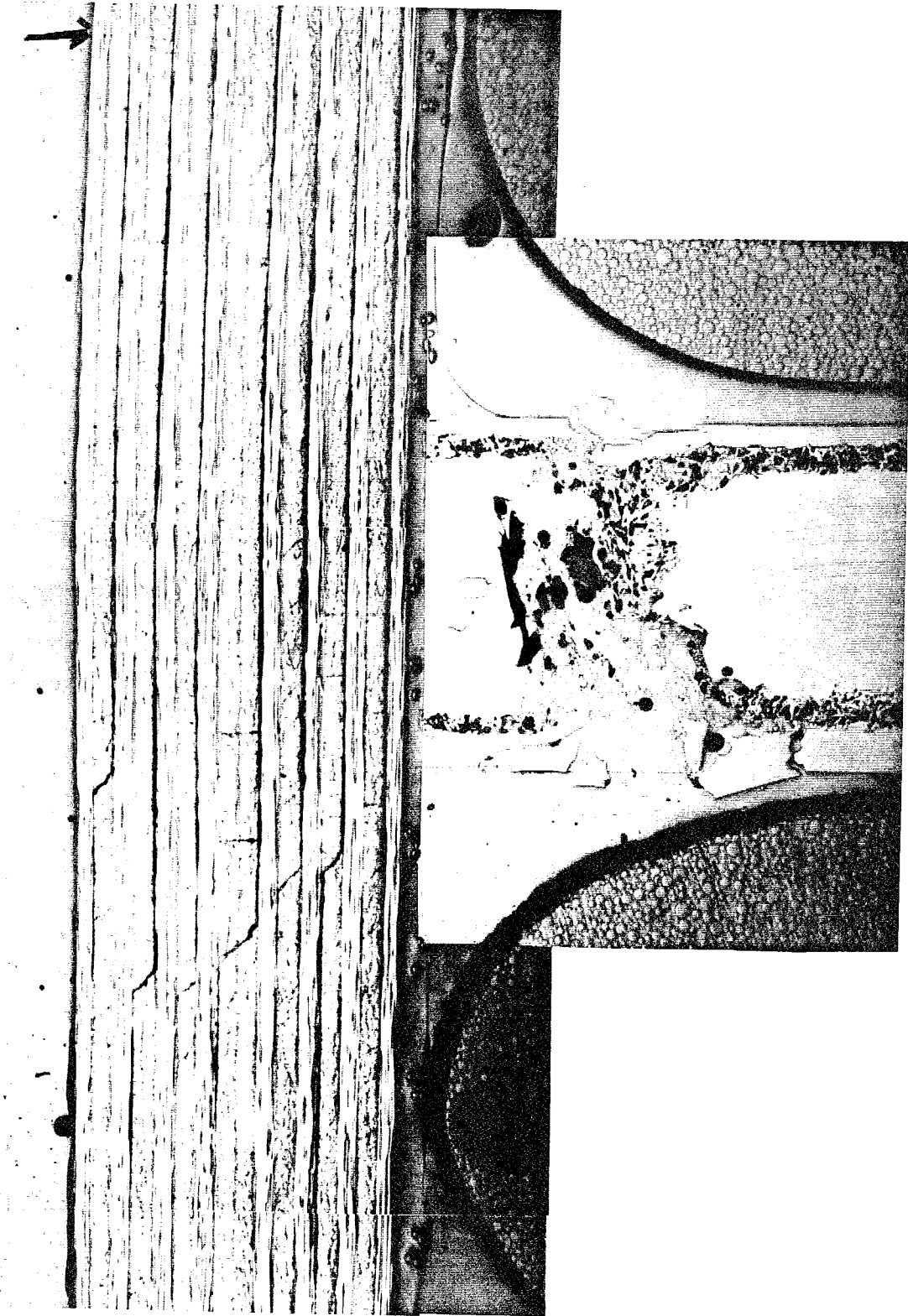


Figure 3.88. 0° Cross-Section 17294-1-1 (25X) Part B

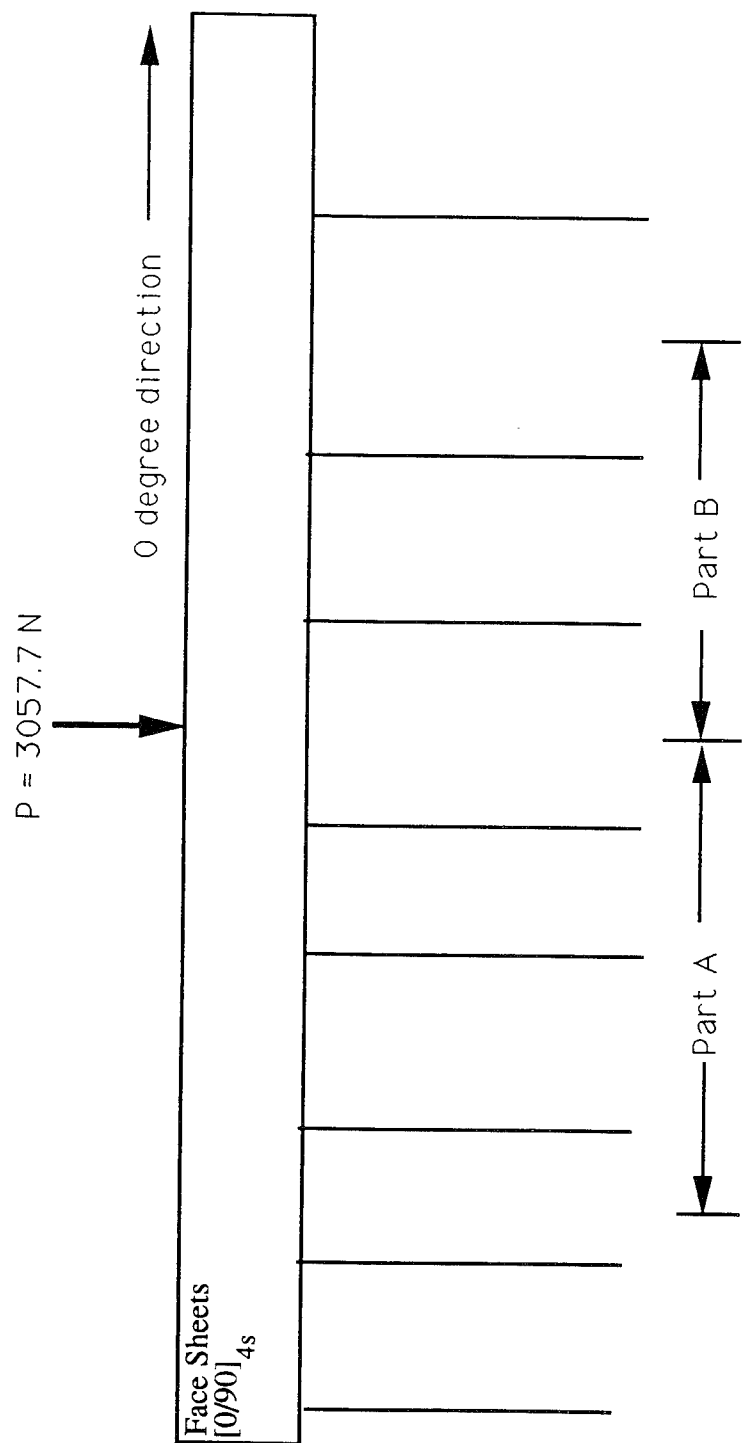


Figure 3.89. Guide to Micrograph of 0 Degree Cross-Section (25X) -17294-1-2

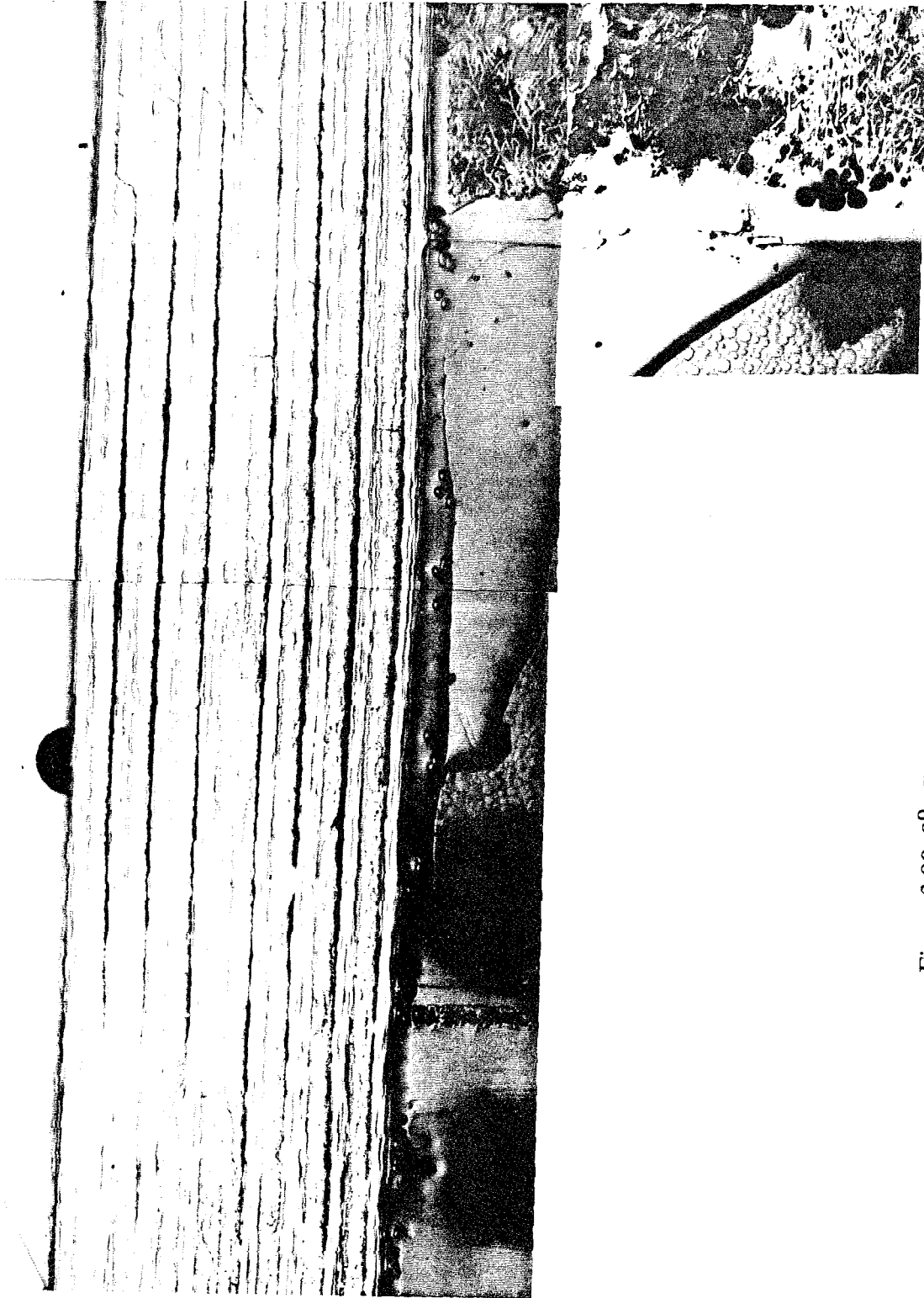


Figure 3.90. 0° Cross-Section 17294-1-2 (25X) Part A



Figure 3.91. 0° Cross-Section 17294-1-2 (25X) Part B

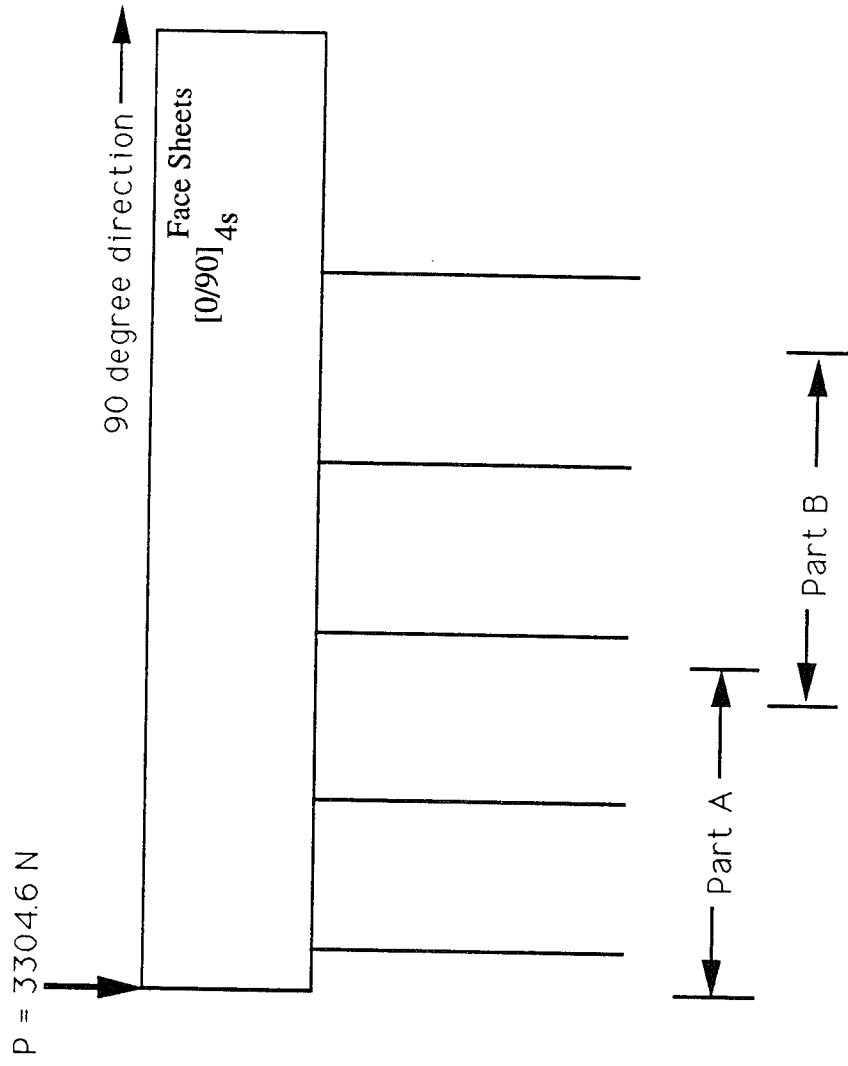


Figure 3.92. Guide to Micrograph of 90 Degree Cross-Section (25X) - 17294-1-1

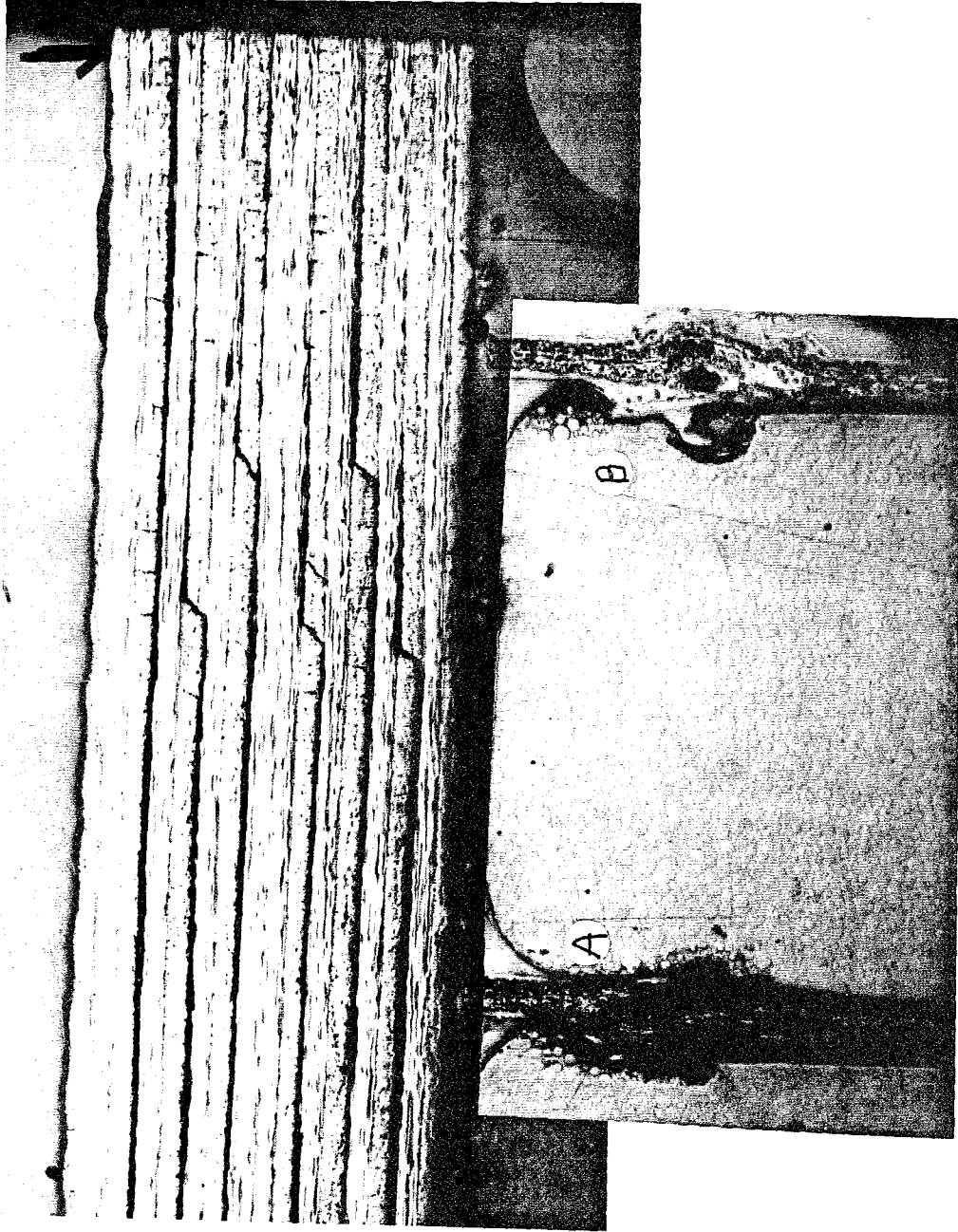


Figure 3.93. 90° Cross-Section 17294-1-1 (25X) Part A

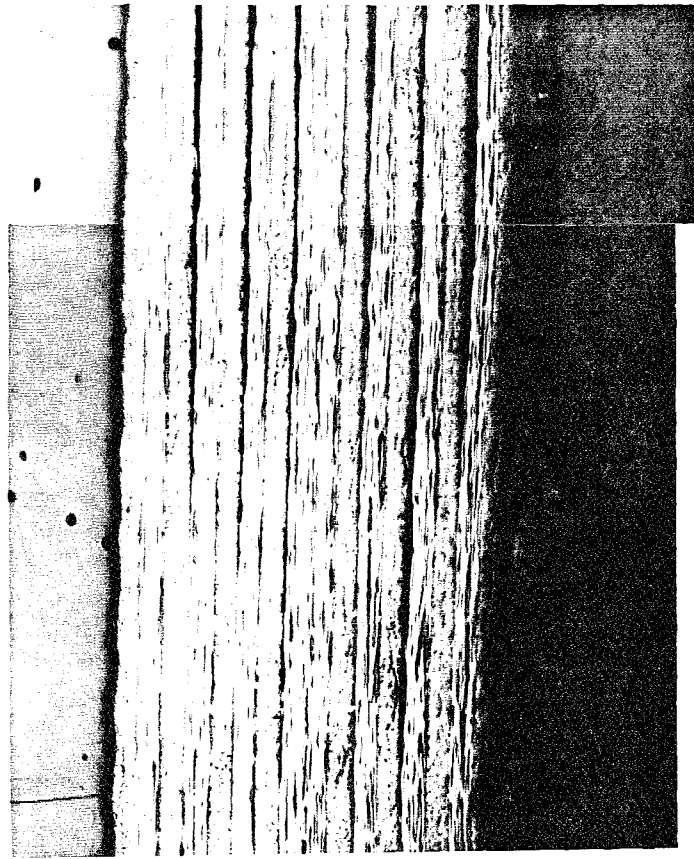


Figure 3.94. 90° Cross-Section 17294-1-1 (25X) Part B

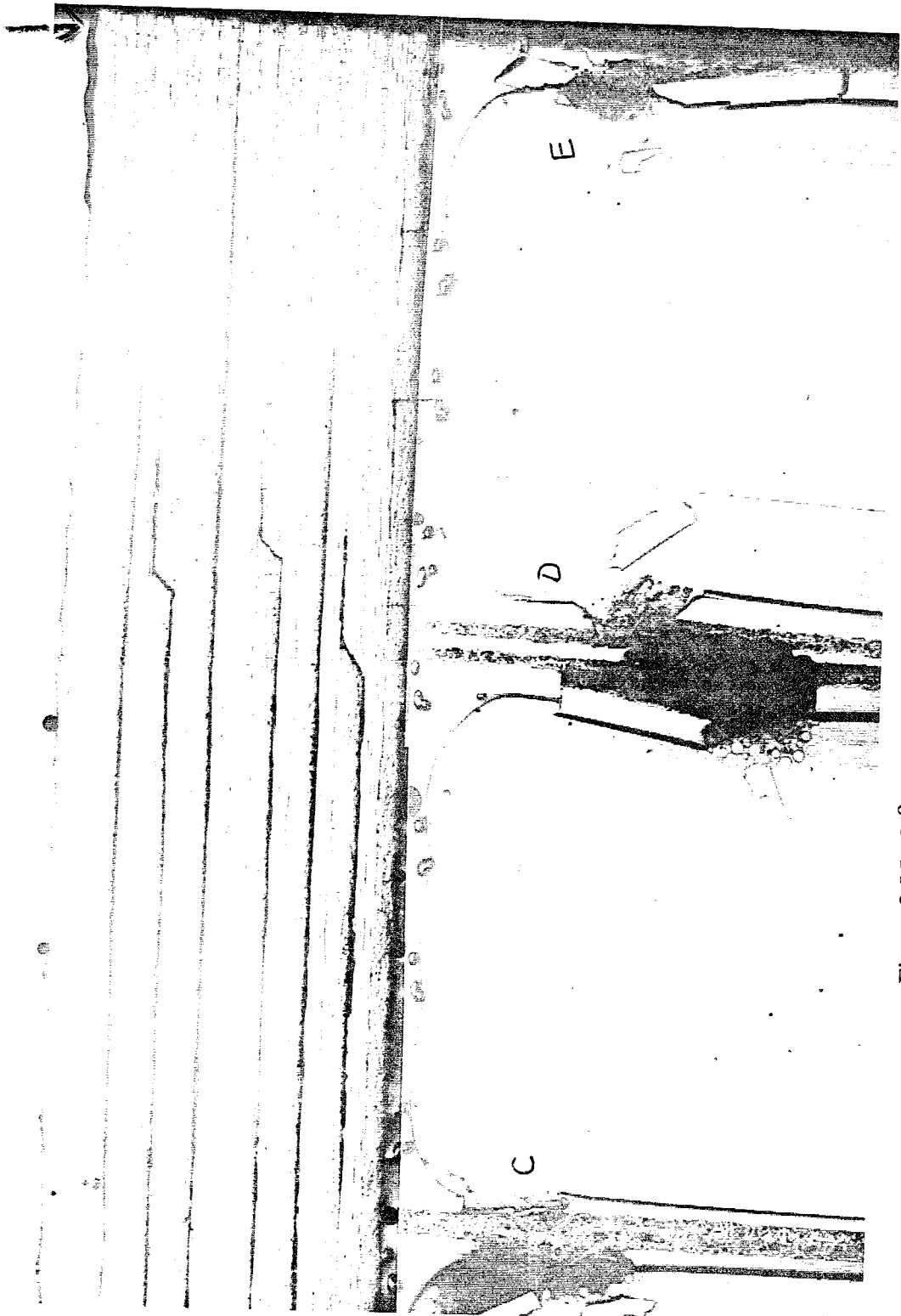


Figure 3.95. 90° Cross-Section 17294-1-2 (25X)

(2) Impact Energy = 4.26 J (3.14 ft-lb)

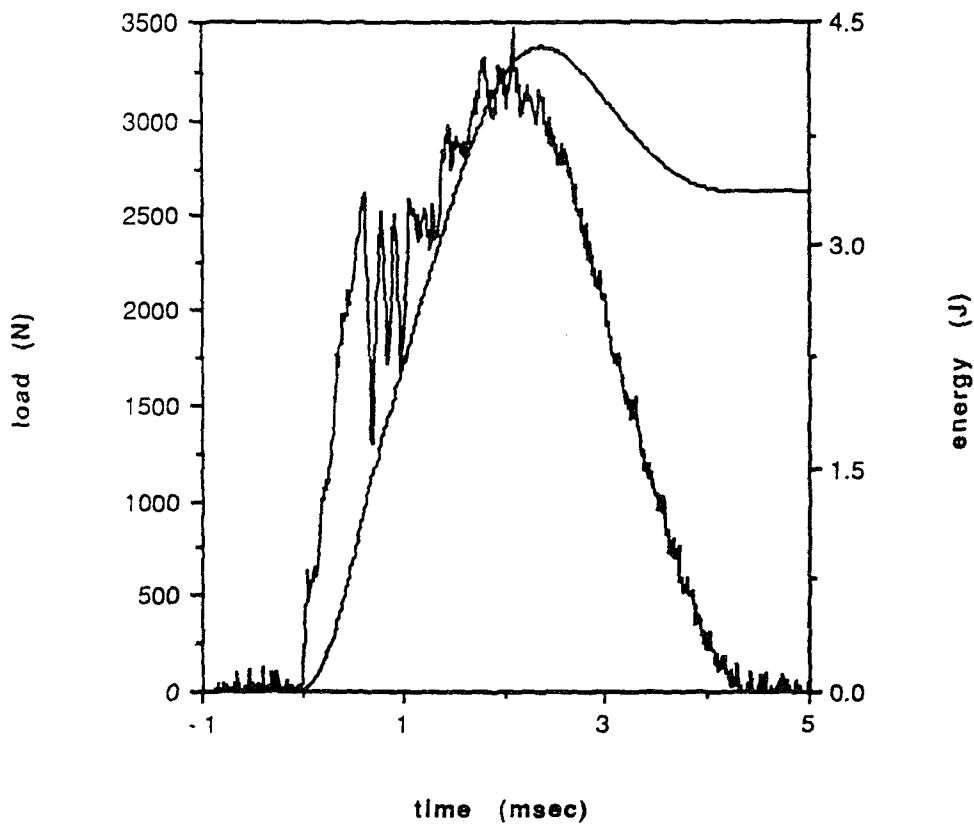
The sandwich panel was impacted at a drop height of 12.70 cm (5.0 in). The load and energy curves are shown in Figure 3.96. A drastic drop in the load curve occurs at approximately 2700 N. In this test, the drop is more drastic than the previous test. The load drops down to approximately 1250 N, resulting in a drop of 1450 N. This drop is over half of the 2700 N. Following the drop, two more drastic drops occur. Notice that they do not reload above the 2700 N. After fractions of a millisecond, the load reaches 2700 N. A similar behavior occurs in the previous test. The maximum load and absorbed energy increase at this higher impact energy.

(3) Impact Energy = 4.85 J (3.58 ft-lb)

The sandwich panel was impacted at a drop height of 13.97 cm (5.5 in). The load and energy curves are shown in Figure 3.97. A drastic drop in the load curve occurs at approximately 2900 N. Thus far, as the drop height has increased, the load of damage initiation has increased slightly. For example, the first drop in the load curve has increased from 2500 N to 2900 N as the drop height has increased from 11.43 cm (4.5 in) to 13.97 cm (5.5 in). In each case, the load curve continues to drop and reload for a few times to a load value less than the damage initiation level. Once again, the maximum load and absorbed energy increase with an increase in impact energy.

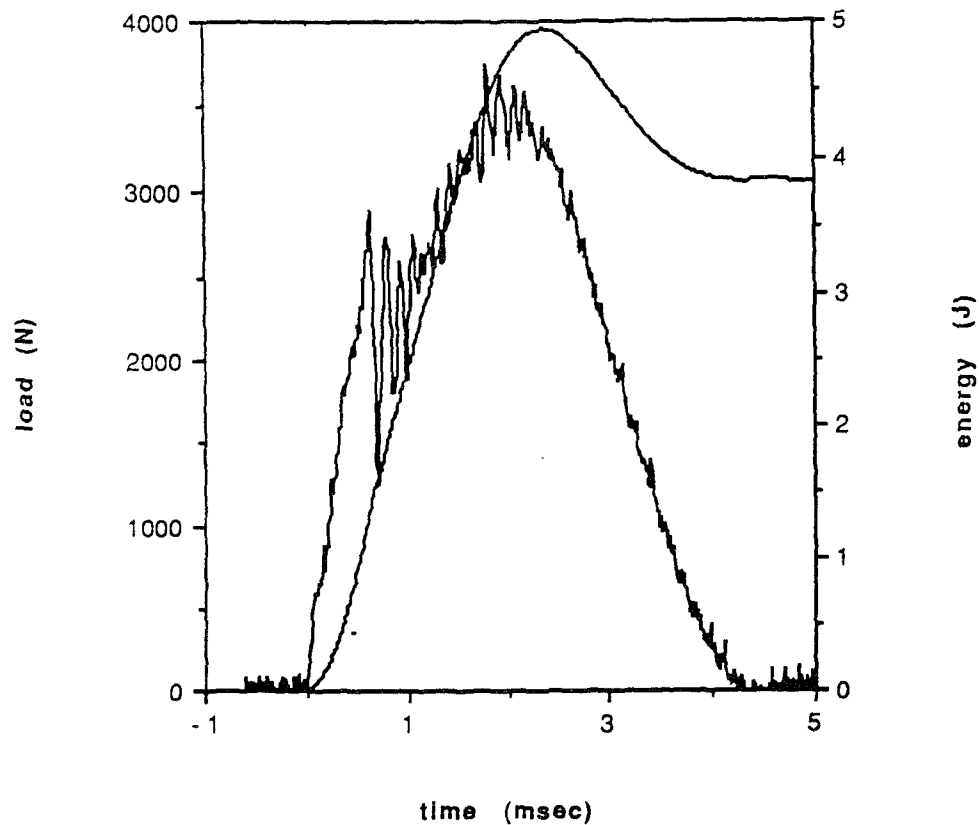
(4) Impact Energy = 5.21 J (3.84 ft-lb)

The sandwich panel was impacted at a drop height of 15.24 cm (6.0 in). The load and energy curves are shown in Figure 3.98. A drastic drop in load occurs at



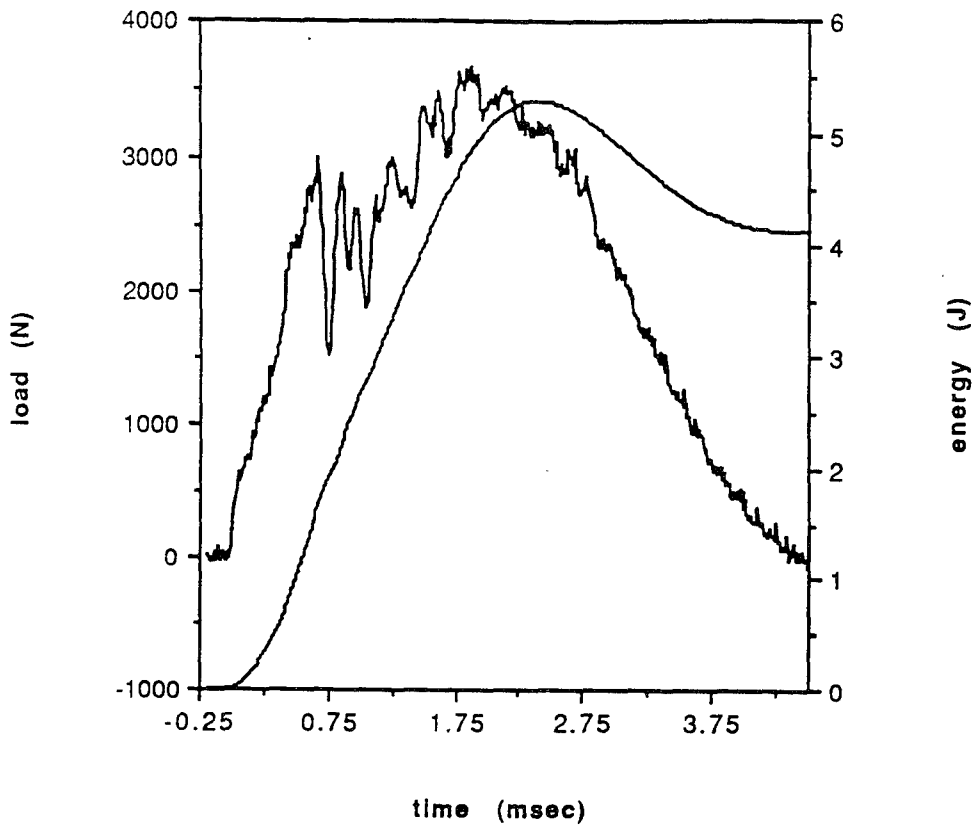
Specimen ID -17294-1-3	Max load - 3473.2 N (780.8 lb)
Impact Velocity - 1.53 m/s (5.02 ft/s)	Energy at Max Load - 4.225 J (3.116 ft-lb)
Impact Energy - 4.26 J (3.14 ft-lb)	Time - at Max Load - 2.11 msec
Absorbed Energy - 3.364 J (2.481 ft-lb)	total - 4.26 msec
Max Disp. of Tup 0.2154 cm (0.0848 in)	Damage Area - 1.9691 cm ² (0.305 in ²)
Damage Indent.- 0.018 cm (0.007 in)	Damage Diameter - 0.76 cm (0.3 in)

Figure 3.96. Load and Energy from Dynatup for 16-ply at 12.70 cm (5.0 in) drop height



Specimen ID -17294-1-4	Max load - 3747.2 N (842.4 lb)
Impact Velocity - 1.63 m/s (5.36 ft/s)	Energy at Max Load - 4.409 J (3.252 ft-lb)
Impact Energy - 4.85J (3.58 ft-lb)	Time - at Max Load - 1.81 msec
Absorbed Energy - 3.829 J (2.824 ft-lb)	total - 4.24 msec
Max Disp. of Tup 0.2310 cm (0.0909 in)	Damage Area - 2.140 cm ² (0.332 in ²)
Damage Indent.- 0.018 cm (0.007 in)	Damage Diameter - 1.02 cm (0.4 in)

Figure 3.97. Load and Energy from Dynatup for 16-ply at 13.97 cm (5.5 in) drop height



Specimen ID -17294-1-5	Max load - 3669.8 N (825.0 lb)
Impact Velocity - 1.69 m/s (5.56 ft/s)	Energy at Max Load - 4.852 J (3.579 ft-lb)
Impact Energy - 5.21J (3.84 ft-lb)	Time - at Max Load - 1.88 msec
Absorbed Energy - 4.126 J (3.043 ft-lb)	total - 4.36 msec
Max Disp. of Tup 0.2392 cm (0.0942 in)	Damage Area - 2.654 cm ² (0.411 in ²)
Damage Indent.- 0.020 cm (0.008 in)	Damage Diameter - 1.02 cm (0.4 in)

Figure 3.98. Load and Energy from Dynatup for 16-ply at 15.24 cm (6.0 in) drop height

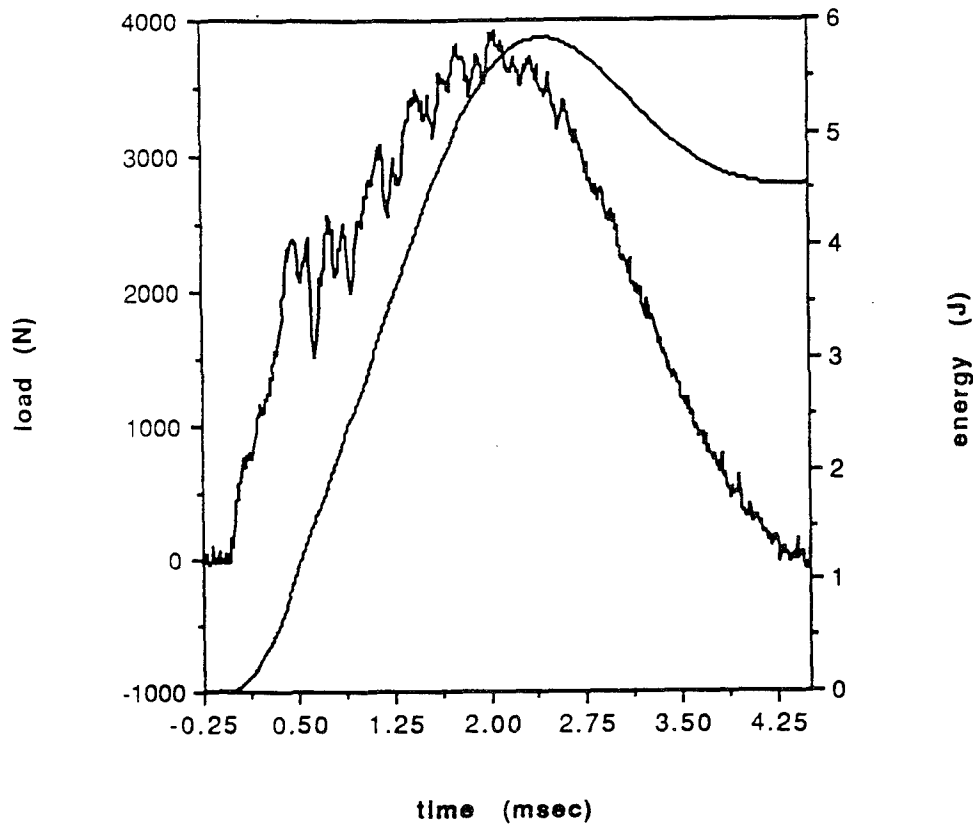
approximately 3000 N. Once again, the initiation of major damage occurs at a higher value than the previous test. The absorbed energy increased; however, the maximum load did not increase. At a drop height of 13.97 cm (5.5 in) the maximum load is 3747.2 N (842.4 lb) while the maximum load for a drop height of 15.24 cm (6.0 in) is 3669.8 N (825.0 lb). This situation also occurred in the thinner face sheets.

(5) Impact Energy = 5.74 J (4.23 ft-lb)

The sandwich specimen was subjected to low velocity impact at a drop height of 16.51 in (6.5 in). The load and energy curves for this test are shown in Figure 3.99. The load curve drops at approximately 2400 N (540 lb). Unlike the previous cases, damage initiates at a lower value than the previous test. The trend had been an increase in the load that initiates damage as the drop height increases. Also, in the earlier test, it took approximately two peaks in the load curve before reaching above the load value of damage initiation. This did not occur. A continuous cycle of damage and reloading occurs until the maximum load is reached. The damage caused by this cycle can be seen in the micrographs.

Figures 3.100 and 3.101 show the over-all view of the damaged specimen. There is a large amount of delamination compared to the delamination seen in the lower energy level. The core crushes, buckles and cripples. There appears to be more delamination of the face sheet in the 0° cross-section than in the 90° cross-section. The core appears to be damaged more in then 0° cross-section.

A closer examination of the micrographs are shown in Figures 3.102 - 3.108. The openings of the cracks and delamination have increased as well as the length of delamination. There is also an increase in delamination at the higher 0°-90° interface.



Specimen ID - 17294-1-6	Max load - 3914.0 N (879.9 lb)
Impact Velocity - 1.78 m/s (5.83 ft/s)	Energy at Max Load - 5.591 J (4.124 ft-lb)
Impact Energy - 5.74 J (4.23 ft-lb)	Time - at Max Load - 2.07 msec
Absorbed Energy - 4.530 J (3.341 ft-lb)	total - 4.28 msec
Max Disp. of Tup 0.2584 cm (0.1017 in)	Damage Area - 2.740 cm ² (0.424 in ²)
Damage Indent.- 0.023 cm (0.009 in)	Damage Diameter - 1.27 cm (0.5 in)

Figure 3.99. Load and Energy from Dynatup for 16-ply at 16.51 cm (6.5 in) drop height

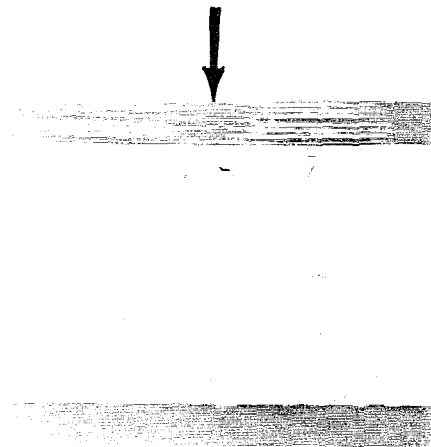


Figure 3.100. 0° Cross-Section 17294-1-6 (2.7 X)

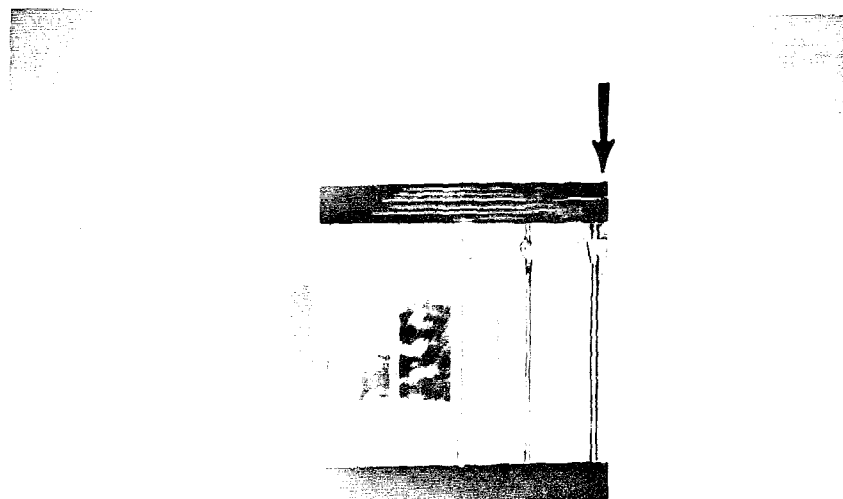


Figure 3.101. 90° Cross-Section 17294-1-6 (2.7 X)

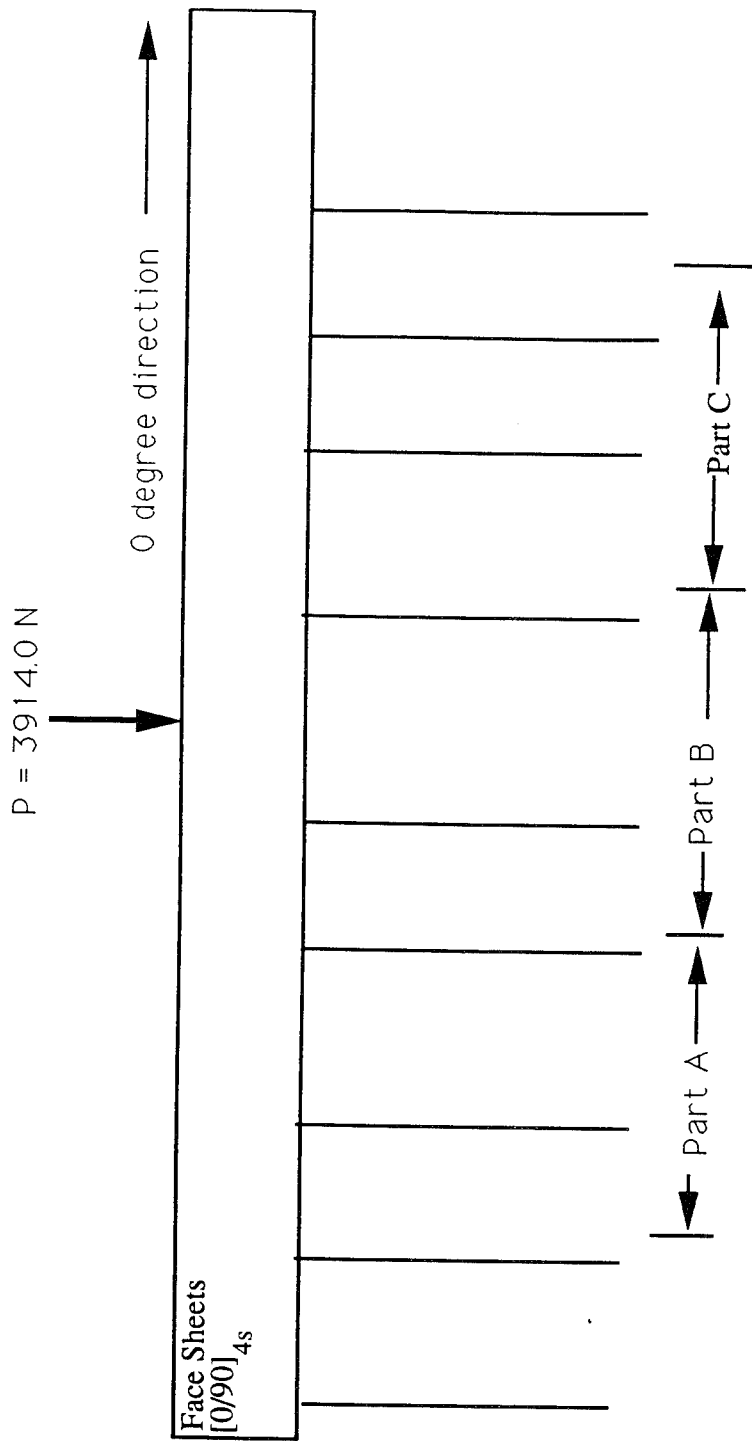


Figure 3.102. Guide to Micrograph of 0 Degree Cross-Section (25X) - 17294-1-6

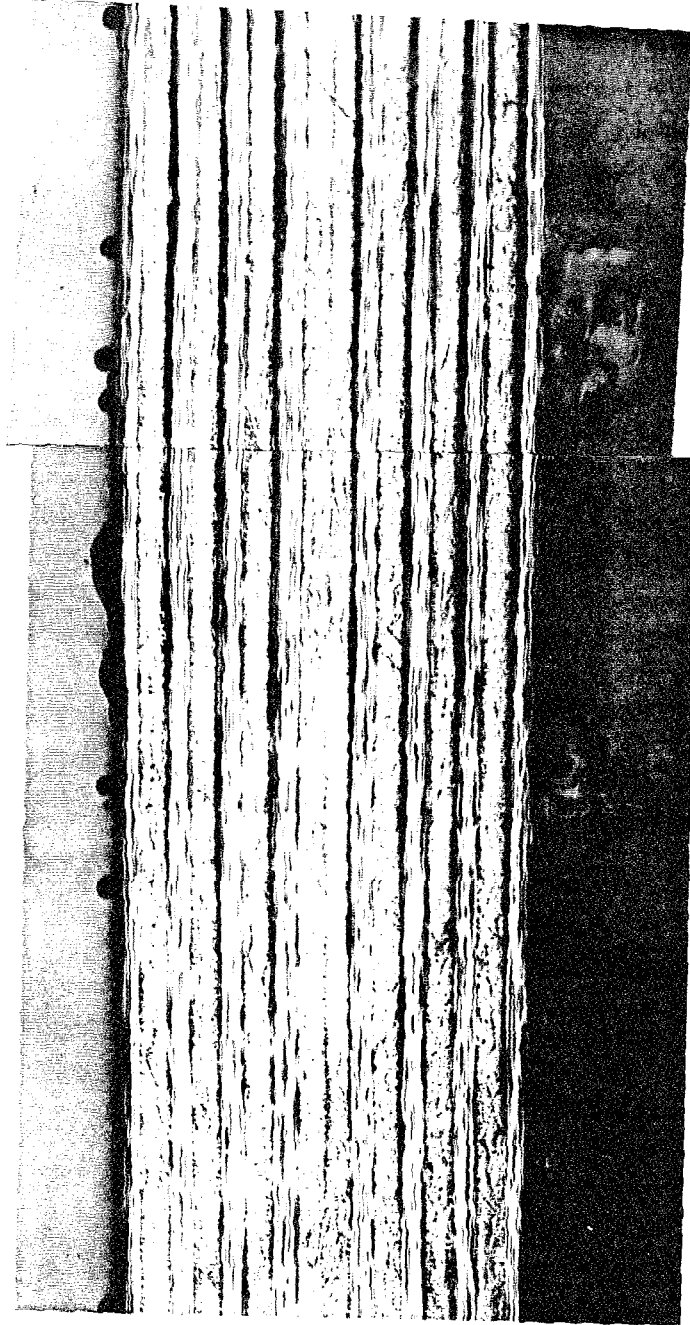


Figure 3.103. 0° Cross-Section 17294-1-6 (25X) Part A

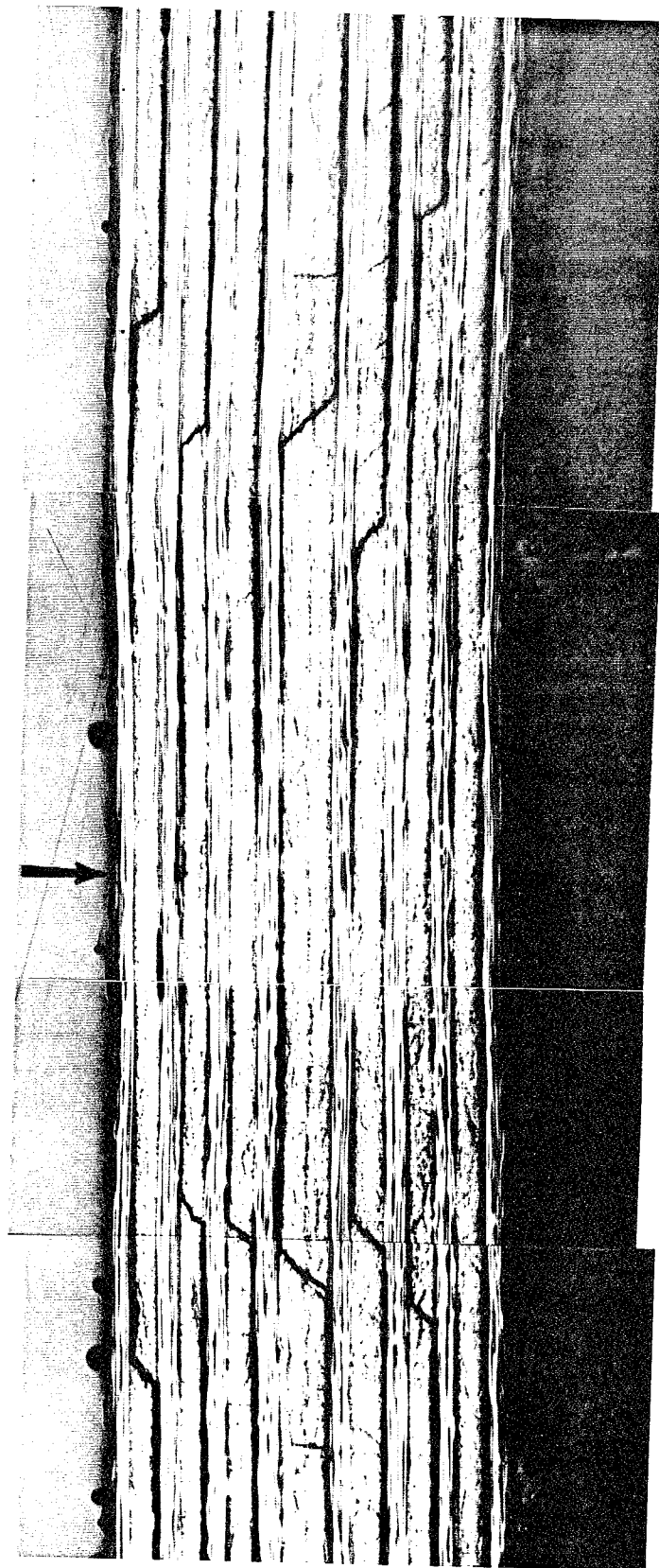


Figure 3.104. 0° Cross-Section 17294-1-6 (25X) Part B

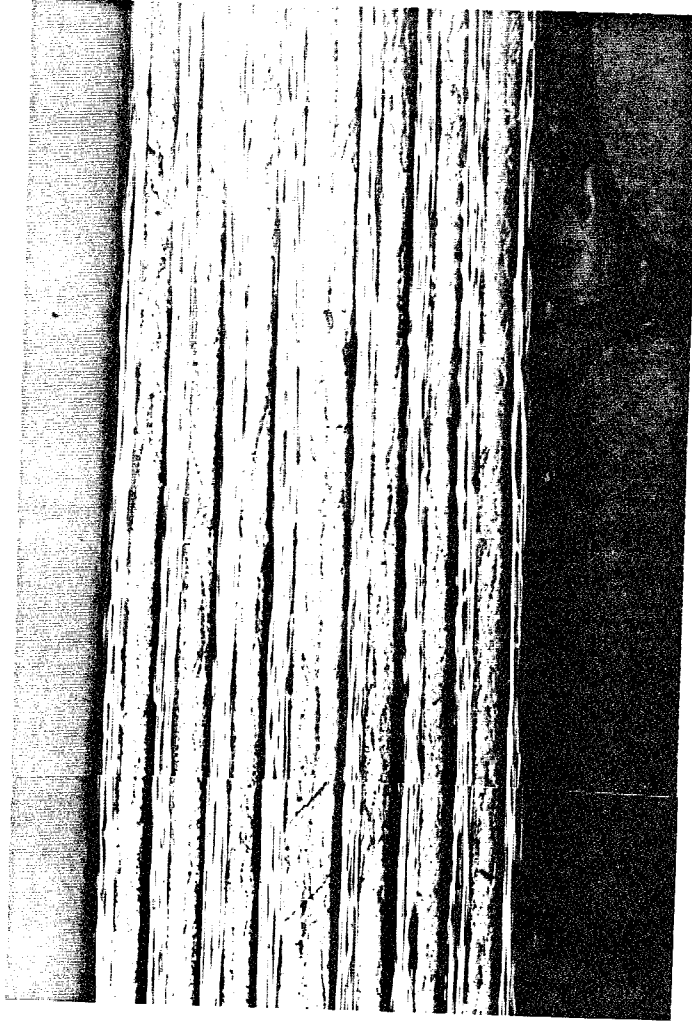


Figure 3.105. 0° Cross-Section 17294-1-6 (25X) Part C

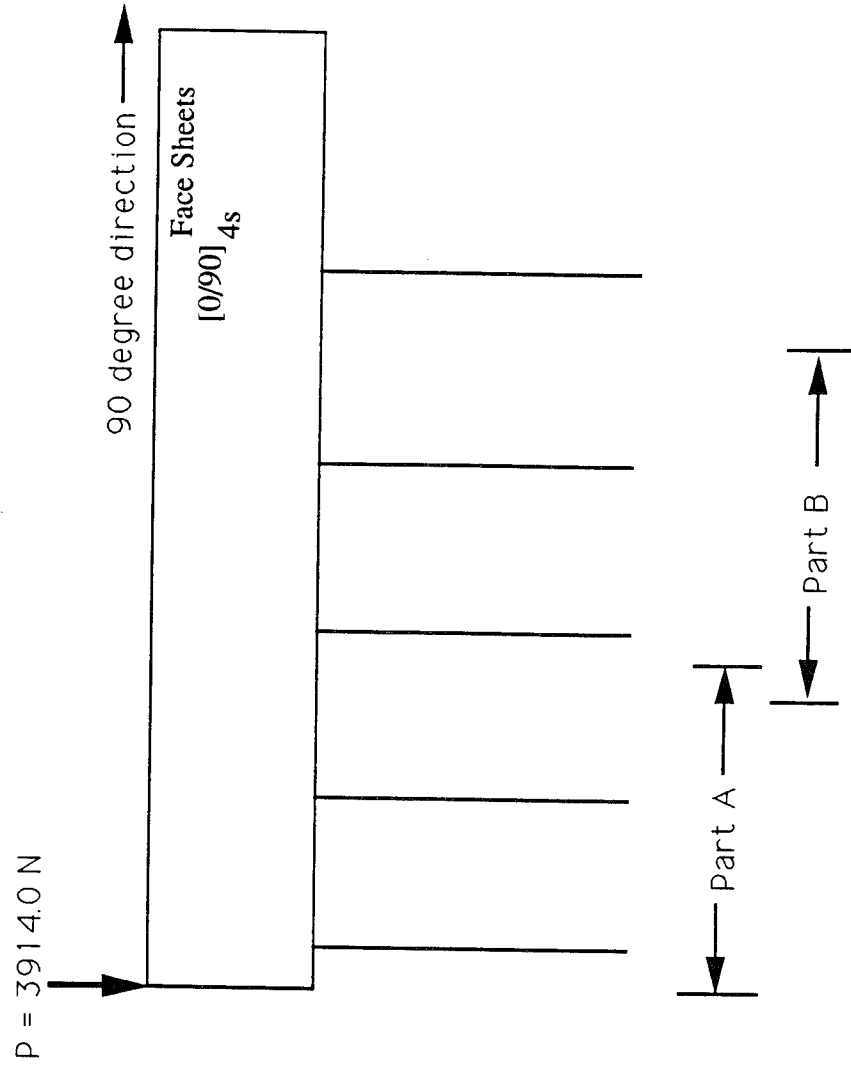


Figure 3.106. Guide to Micrograph of 90 Degree Cross-Section (25X) - 17294-1-6

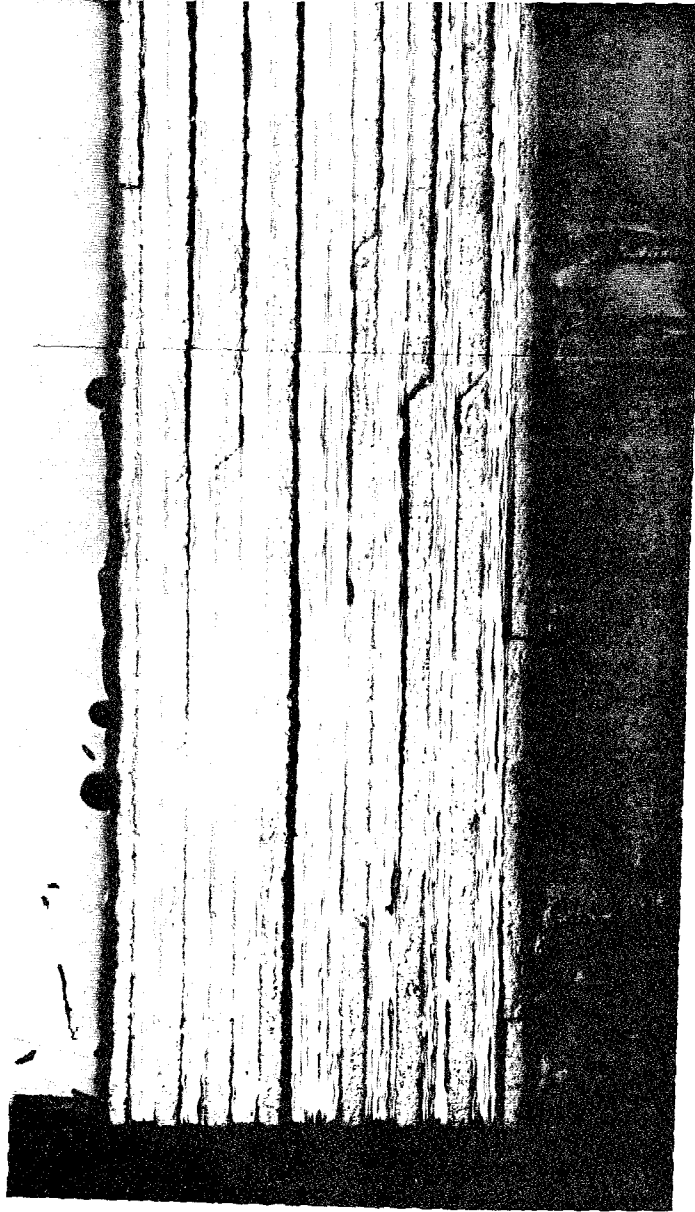


Figure 3.107. 90° Cross-Section 17294-1-6 (25X) Part A

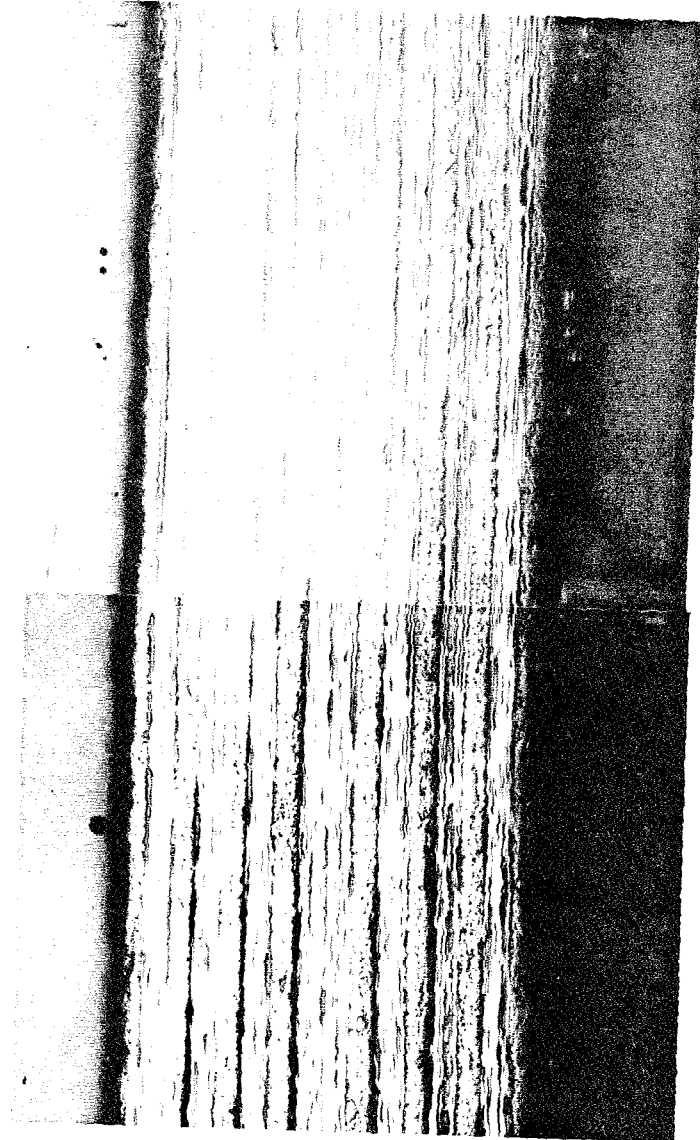


Figure 3.108. 90° Cross-Section 17294-1-6 (25X) Part B

The vertical cracks that formed at the lower energy are found only at a few locations; therefore, there are less cracks. A delamination with a large opening is present between the 0° ply and 90° middle layer. This was present at the lower impact energy; however, the opening was not as large. In all cases, the core crushed, buckled or crippled. The adhesive remained in tact.

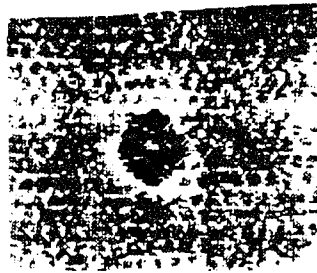
(6) C-Scans

C-scans were taken of each impacted specimen. Figure 3.109 shows the area of damage due to delamination of the face sheets captured by the Pulse-echo C-scans. The area, which is reduced 33%, took the shape of a diamond. The higher the impact energy the more prominent the damage resembled the square shape. Figure 3.110 shows the damage area versus the impact energy and absorbed energy. The damage area decreases as the impact energy increases from 3.95 J (2.91 ft-lb) to 4.26 J (3.14 ft-lb); otherwise, the damage areas increase as the energies. In this situation, the damage area is smaller; however, the permanent indentation depth is larger. This two-dimensional measure may be a good measure to look at but is not a good judge of failure in all cases. At the higher impact energies, the damage area appears to start leveling off. According to Bucinell, et al [35], this implies that the delaminations are only formed during the elastic response phase of an impact event. Once the response transitions to the plastic phase, all energy goes into creating damage directly under the impactor. This is also supported by the micrographs. Furthermore, Figure 3.54 illustrates this point. As the impact energy increases, the delamination length grows in a direction towards the impact site.

3.95 Joules
(2.91 ft-lb)



4.26 Joules
(3.14 ft-lb)



4.85 Joules
(3.58 ft-lb)



5.21 Joules
(3.84 ft-lb)



5.74 Joules
(4.23 ft-lb)



Figure 3.109. Pulse-Echo C-scans for Sandwich Panels with 16-ply Face Sheets

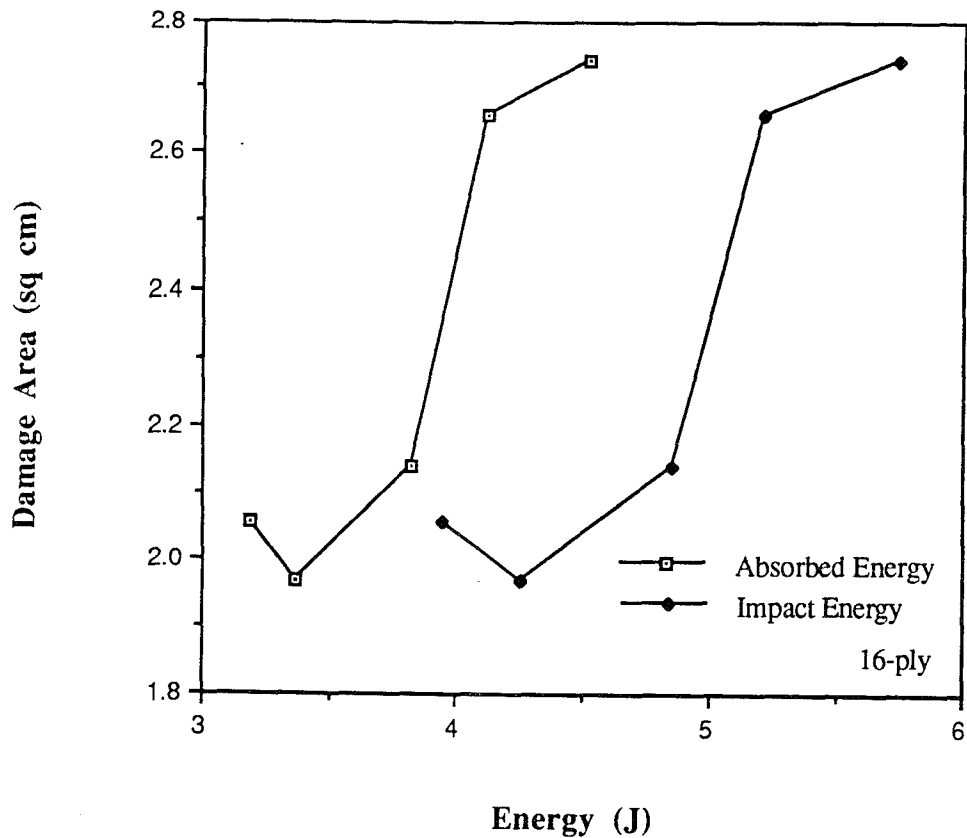


Figure 3.110. Damage Area vs Impact and Absorbed Energies - 16-ply

(7) Additional Analysis

Figure 3.111 compares the energy curves for various impact energies. Figure 3.112 compares the load curves for the highest and lowest impact energies. As in the previous test with thinner face sheets, the peak energy values occur at approximately the same time. From Figure 3.112, it is apparent that the time of event is approximately the same regardless of the impact energy level. The initial drop in the load curves also occurs around the same time. This also happened in the previous test series.

Figure 3.113 shows the difference between the absorbed and impact energy. As in the previous test, the differences, which are the amount of recovered elastic energy, increased with drop height. Since the absorbed energy signifies the amount of

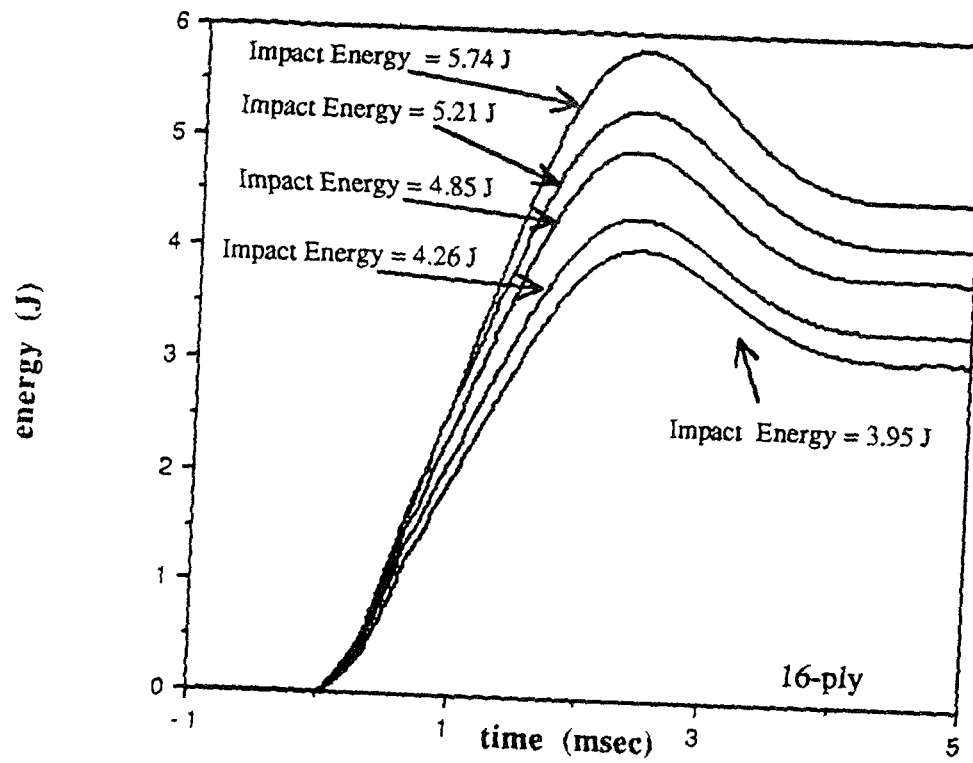


Figure 3.111. Comparison of Energy Curves for Sandwich Panels with 16-ply Face Sheets

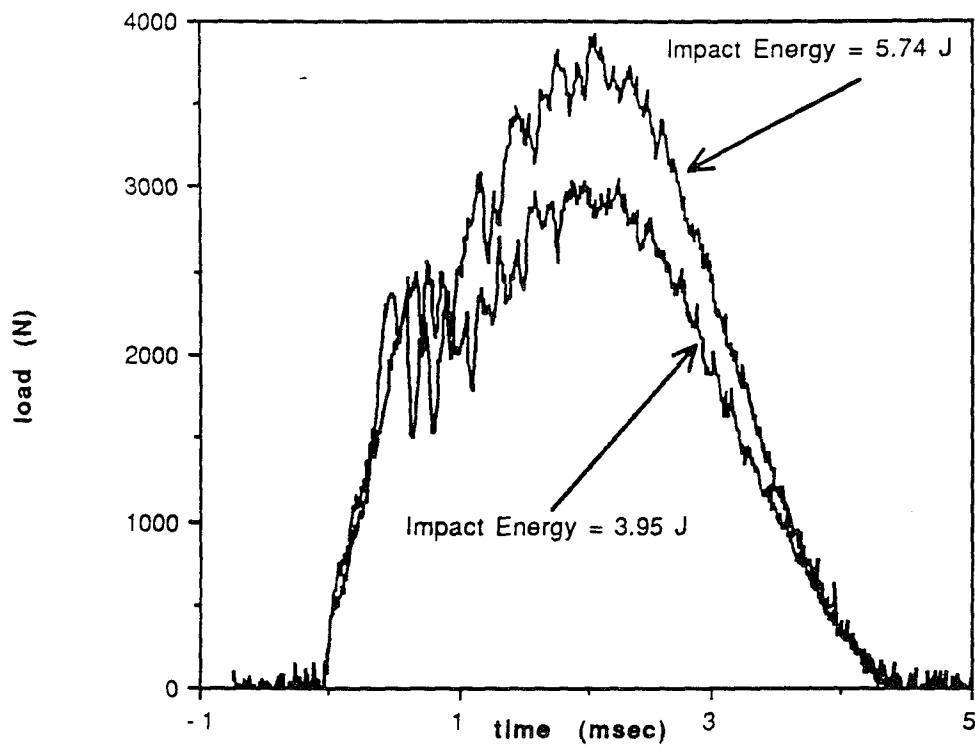


Figure 3.112. Comparison of Load Curves for Sandwich Panels with 16-ply Face Sheets

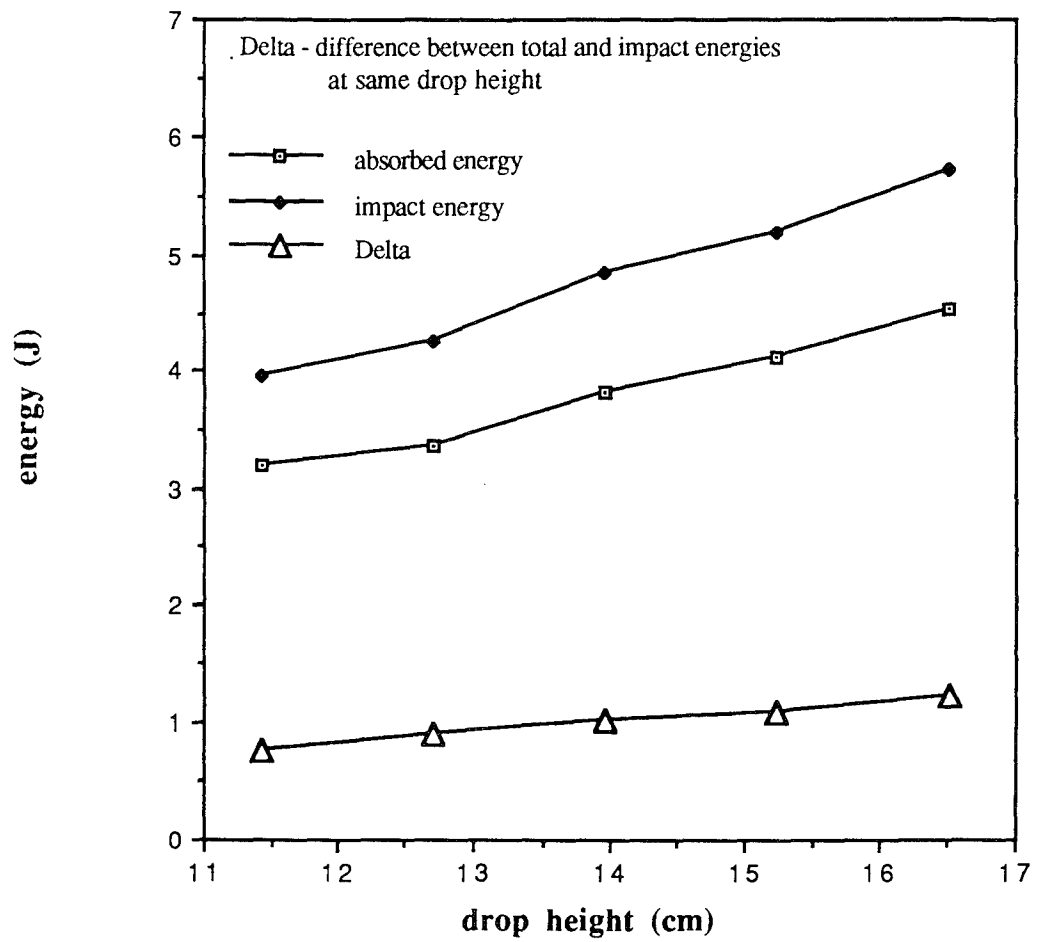


Figure 3.113. Comparison of Absorbed Energy and Impact Energy vs Drop Height for Sandwich Panels with 16-ply Face Sheets

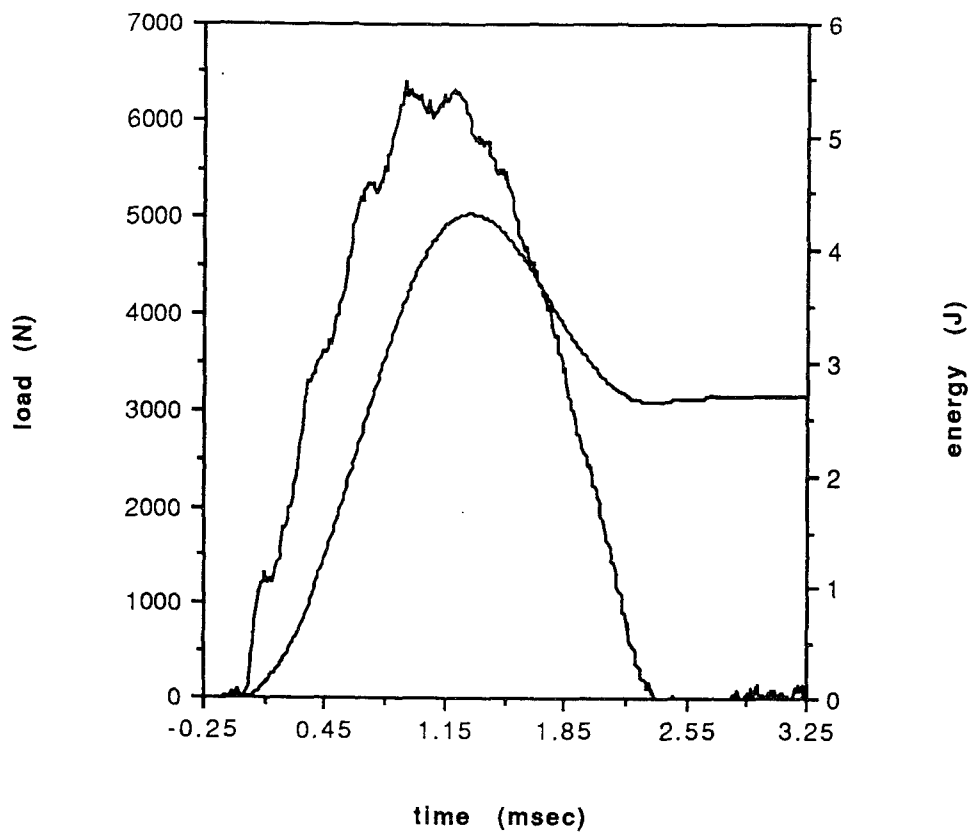
damage in the sandwich panel, the damage increases as the drop height increases. Also, Figure 3.113 shows that the difference between the absorbed energy and impact energy increases along with the drop height implying that as the difference increases, so does the damage.

3.7 Sandwich Panels with 32-ply Face Sheets

The sandwich panels with 32-ply face sheets were subjected to low energy (velocity) impacts with drop heights ranging from 12.70 cm (5.0 in) to 16.51 cm (6.5 in). In this test series, the approximate threshold impact energy was identified. This is the finite level of impact energy where damage does not occur in the sandwich panel; however, a slight increase in this level of impact results in damage of the panel. It is dependent upon the thickness of the sandwich panel, stacking sequence, impactor shape, boundary conditions, etc. For the sandwich panel with 32 ply face sheets used in this test series, this value is approximately 3.5 J (2.6 ft-lb). The associated maximum load is approximately 6228 N (1400 lb). The load and energy curves for each test will be discussed; however, only the micrographs for the 4.70 J (3.47 ft-lb) and 5.17 J (3.81 ft-lb) impact energies will be presented.

(1) Impact Energy = 4.27 J (3.15 ft-lb)

The sandwich specimen was impacted at a drop height of 12.70 cm (5.0 in). The load curve for this test is presented in Figure 3.114. Because delamination of the face sheet was not picked up by the C-scan, micrographs were not taken. However, there is a small amount of damage in the specimen as noted by the energy verse time curve. The 2.64 J (1.95 ft-lb) of energy was absorbed by the specimen. This energy may have gone into matrix cracking and slight delamination since core crushing was not a major factor. Note that a drastic drop in the load curve is not present in this test.



Specimen ID -17594-1-5	Max load - 6377.0 N (1433.6 lb)
Impact Velocity - 1.53 m/s (5.03 ft/s)	Energy at Max Load - 3.537 J (2.609 ft-lb)
Impact Energy - 4.27J (3.15 ft-lb)	Time - at Max Load - 0.92 msec
Absorbed Energy - 2.644 J (1.950 ft-lb)	total - 2.37 msec
Max Disp. of Tup 0.1247 cm (0.0491 in)	Damage Area - n/a
Damage Indent.- n/a	Damage Diameter - n/a

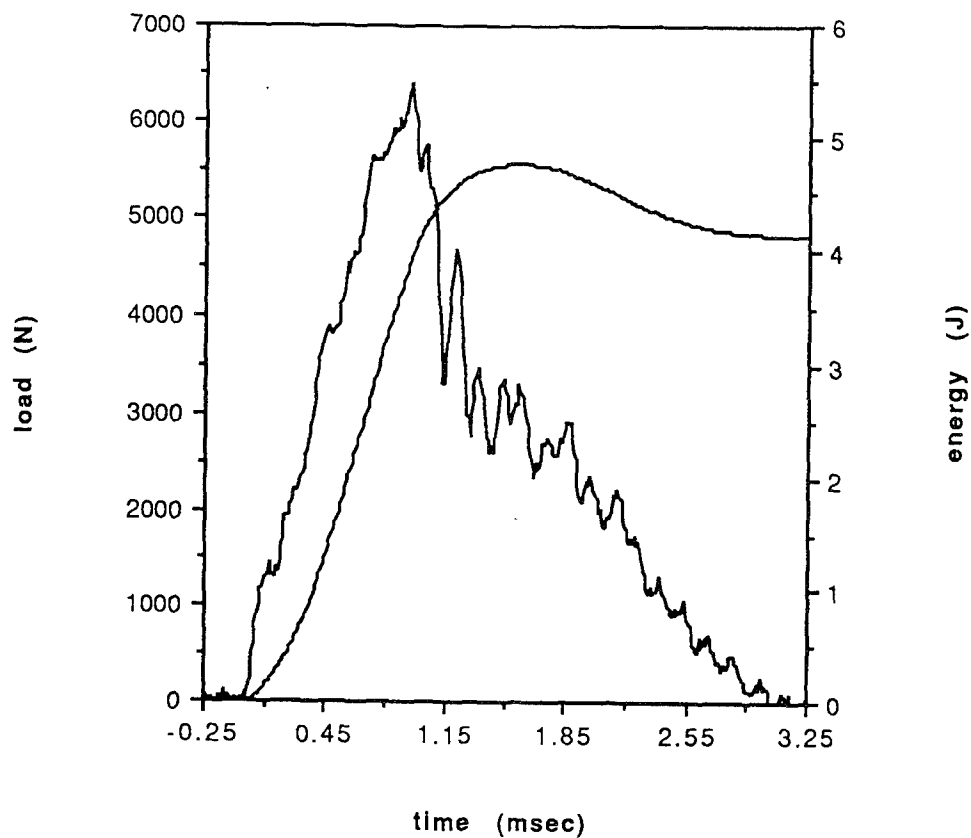
Figure 3.114. Load and Energy from Dynatup for 32-ply at 12.70 cm (5.0 in) drop height

(2) Impact Energy = 4.70 J (3.47 ft-lb)

The sandwich specimen was impacted at a drop height of 13.97 cm (5.5 in). The load and energy versus time curves are shown in Figure 3.115. Unlike the previous load curve, a drastic drop did occur. Unlike all previous tests, this drastic drop occurred at the maximum load. What is interesting about this maximum load is that it is the same as the maximum load of the previous test where there was no drastic drop in the load curve. The impact energy, impact velocity, and energy at maximum load all increased over the last test. This again shows that the impact energy value describes the event better than the maximum load value. The absorbed energy increased by 36% thereby creating delamination that was picked up by the C-scans.

The overall view at 2.7 magnification of the damage area is presented in Figures 3.116 and 3.117. There is crushing/buckling/crippling of the core and delamination of the face sheet as shown in the 0° cross-section. The core wall closest to the impact is damaged in the 90° cross-section. There is also delamination of the face sheet.

Figures 3.118 - 3.121 shows the 25X micrographs of the specimens. The delamination in the 90° cross-section extends under the impact site. Where this occurs, there is also delamination in the 0° cross-section. An example of this situation can be seen in Figure 3.121, label A and Figure 3.120, label B. The angles in the vertical direction that were present in the thinner face sheets are no longer present. This means that in-plane shear stress is the denominating factor in the failure mechanism. Most crack angles are 60° or less; however, there are some crack angles around 78° showing that there still is some bending coming into play. These cracks appear mostly at the bottom 90° layer, Figure 3.119, label C.



Specimen ID - 17594-1-6b	Max load - 6377.0 N (1433.6 lb)
Impact Velocity - 1.61 m/s (5.28 ft/s)	Energy at Max Load - 3.944 J (2.909 ft-lb)
Impact Energy - 4.70 J (3.47 ft-lb)	Time - at Max Load - 0.96 msec
Absorbed Energy - 4.137 J (3.051 ft-lb)	total - 3.05 msec
Max Disp. of Tup 0.1404 cm (0.0553 in)	Damage Area - 3.3388 cm ² (0.5175 in ²)
Damage Indent.- 0.005 cm (0.002 in)	Damage Diameter - 0.77 cm (0.30 in)

Figure 3.115. Load and Energy from Dynatup for 32-ply at 13.91 cm (5.5 in) drop height

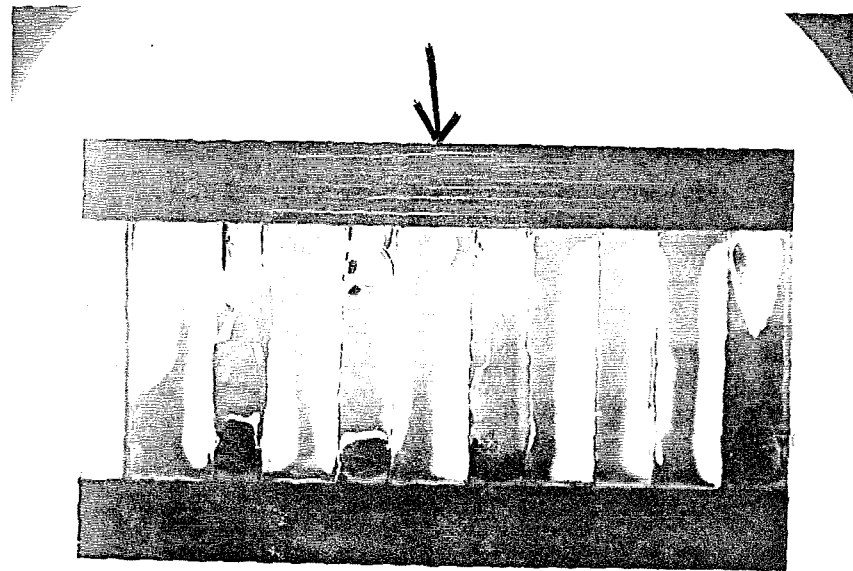


Figure 3.116. 0° Cross-Section 17594-1-6b (2.7 X)

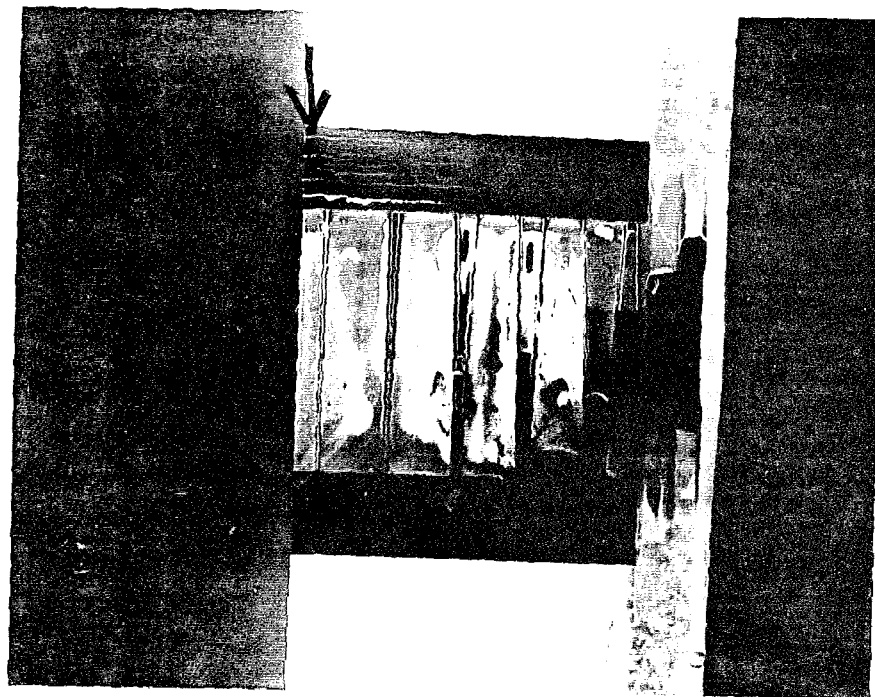


Figure 3.117. 90° Cross-Section 17594-1-6b (2.7 X)

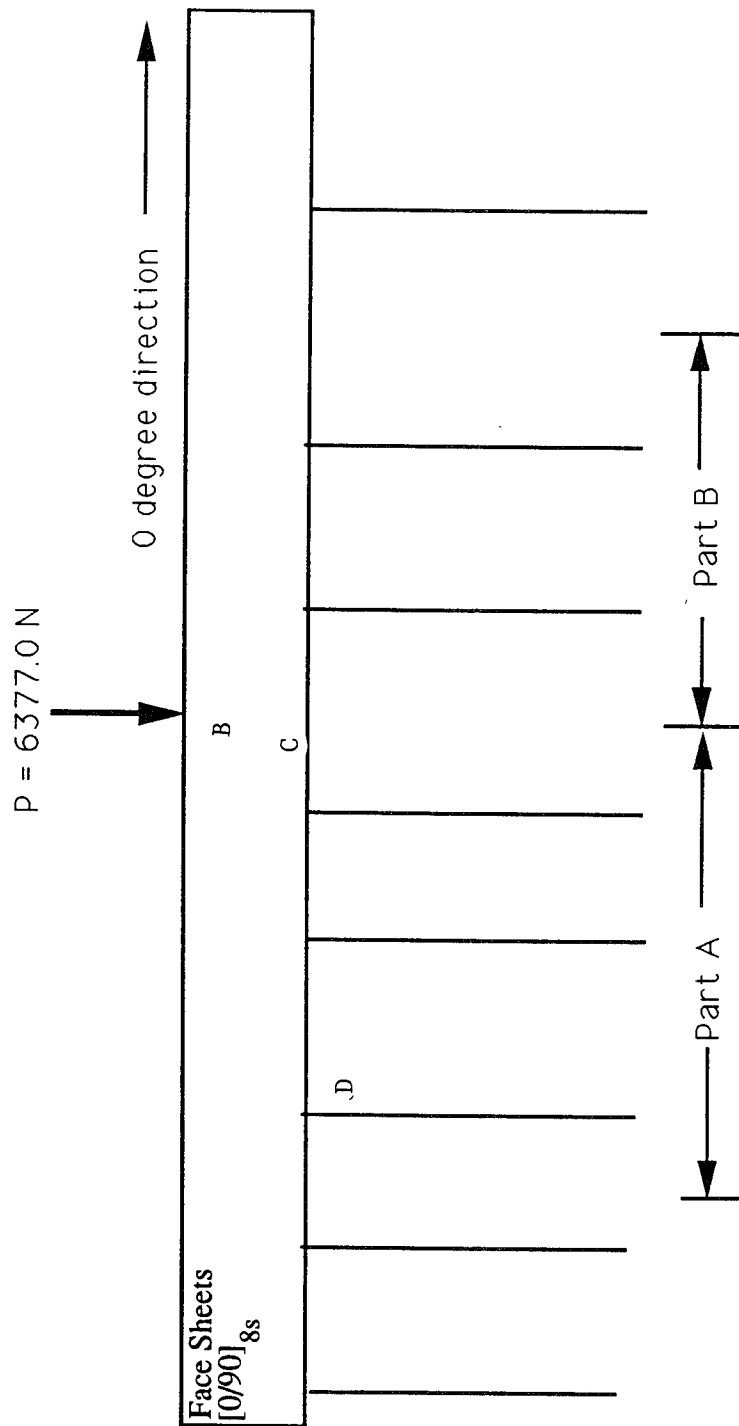


Figure 3.118. Guide to Micrograph of 0 Degree Cross-Section (25X) -17594-1-6

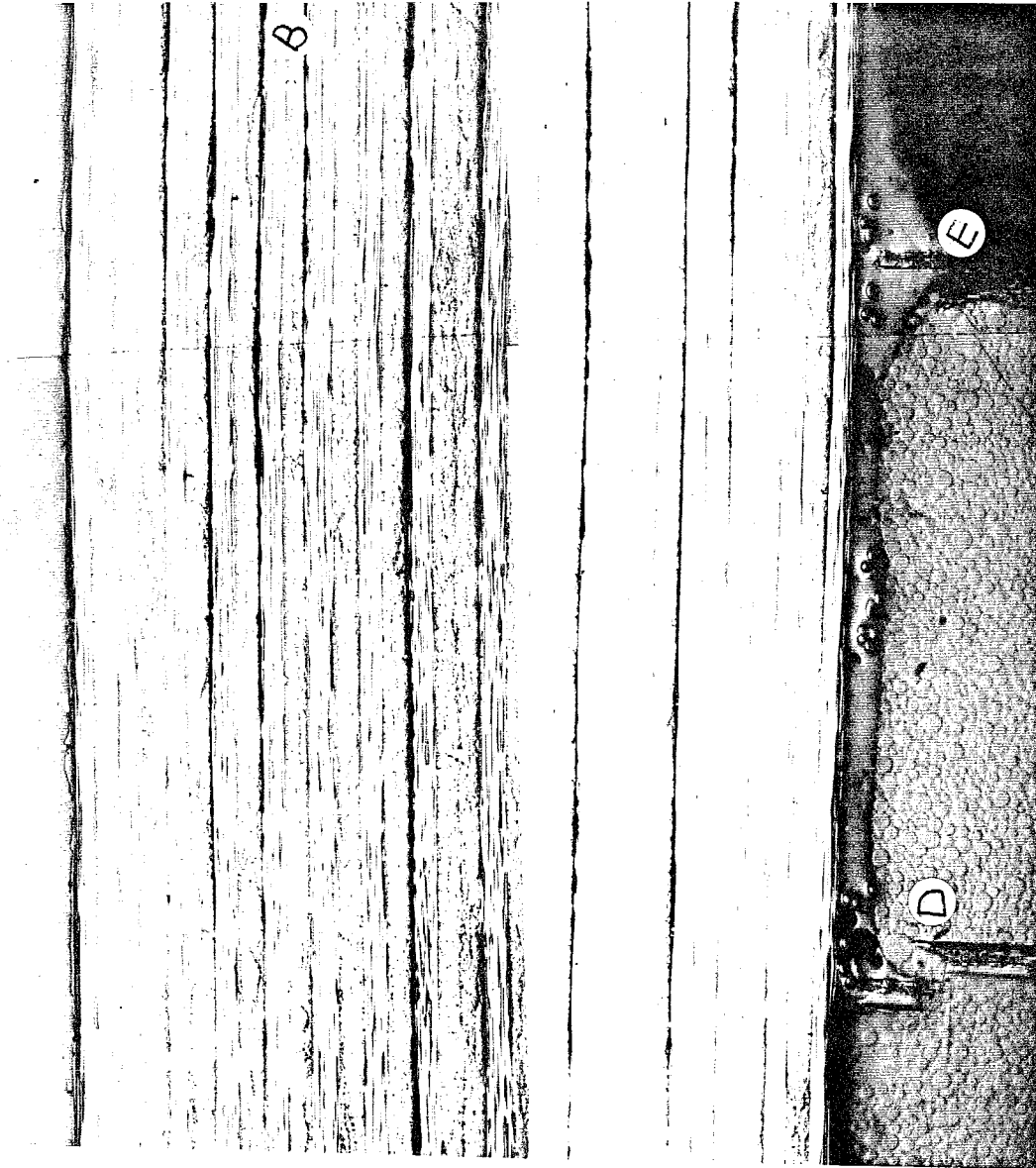


Figure 3.119. 0° Cross-Section 17594-1-6 (25X) Part A

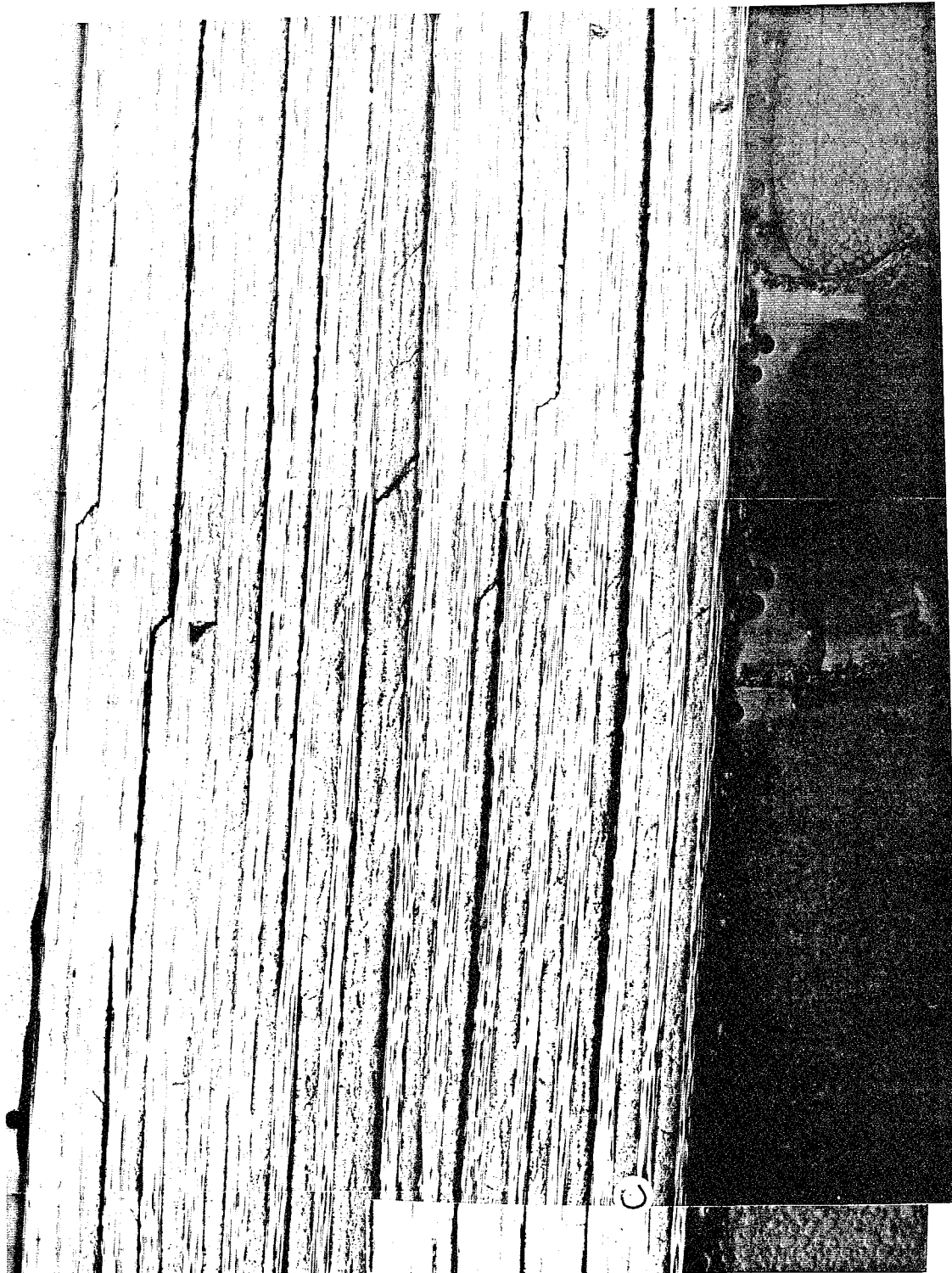


Figure 3.120. 0° Cross-Section 17594-1-6 (25X) Part B

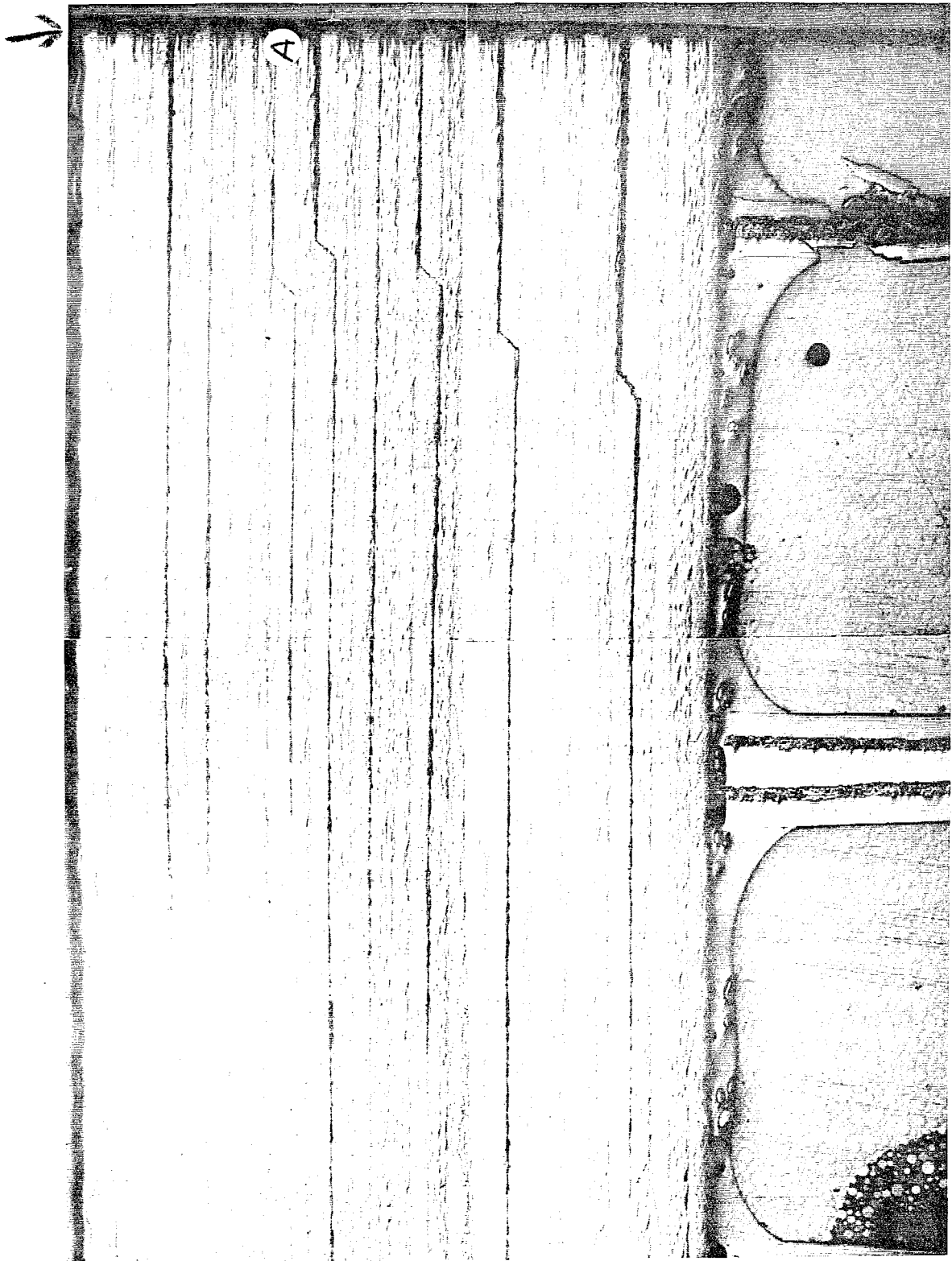


Figure 3.121. 90° Cross-Section 17294-1-6 (25X)

The adhesive does not drip far down into the cells. In fact, the point where the adhesive stops is where the damage to the cell walls starts (Figure 3.119, label D). There are also small holes in the adhesive (Figure 3.120, label E). Because the adhesive transfers load, the holes contribute to the damage of the core and face sheet.

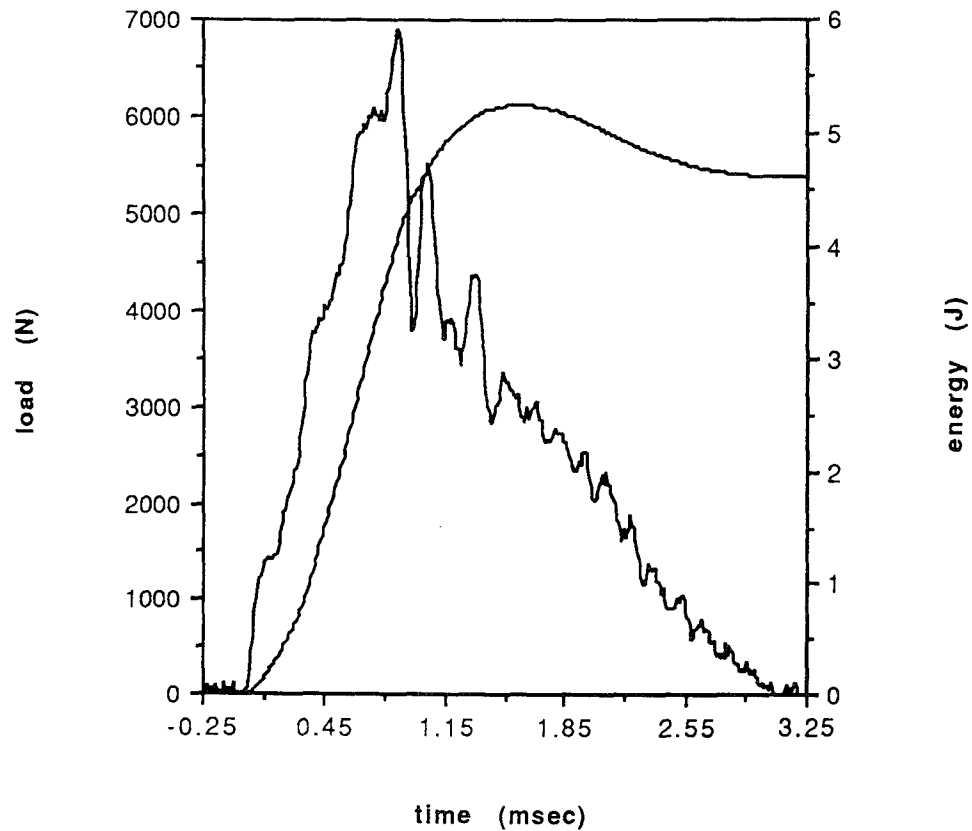
(3) Impact Energy = 5.18 J and 5.17 J

The load and energy curves for sandwich panels with 32-ply face sheets at a drop height of 15.24 cm (6.0 in) are shown in Figures 3.122 and 3.123. Two tests (Specimen ID 17594-1-1 and 17594-1-2) were performed at this height. Though the maximum load values differ by 8.2% (6888.1 N for first test and 6320.0 N for the second test), the impact energies varied by 0.2%. The impact velocities were equivalent. The absorbed energies differed by 3.4%.

The load and energy curves just about overlap each other until approximately 6000 N, then the load curves deviate (Figure 3.124). The load curve of the second test dips to 5500 N while the load curve of the first test continues to load to the maximum load value after a minor peak. After reaching maximum load, the load curves drop approximately the same amount. The curves go back to zero in a similar manner.

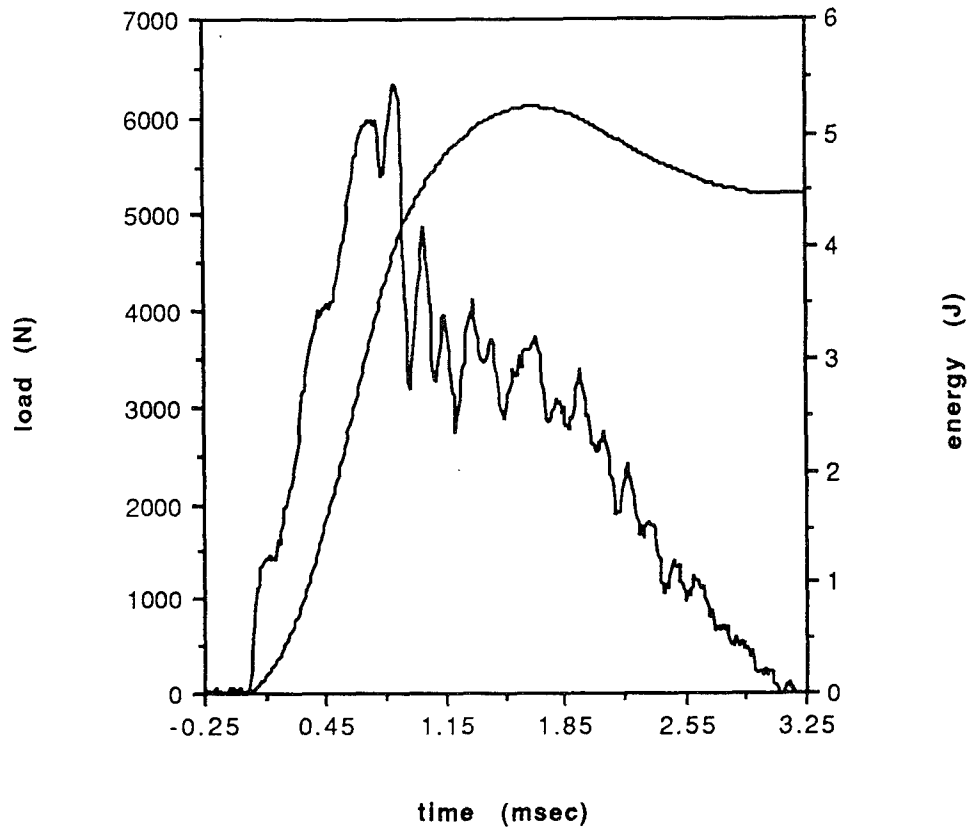
The overall views of the damaged area of the specimens are shown in Figure 3.125 - 3.128. The damage is centered beneath the impact site. There is crippling in the core wall. Some delamination extends across the impact site.

Figures 3.129 - 3.142 are the damaged cross-sections at 25 magnification. Fine cracks are present in 17294-1-1 in the bottom 90° ply (Figure 3.131, label A). These cracks are present in 17294-1-2 (Figure 3.134, label B); however, the crack openings are larger. Referring to 17294-1-1, delamination is present under these cracks to the right of impact (Figure 3.130, label C) but not to the left (Figure 3.132, label D). In 17294-1-2,



Specimen ID -17594-1-1	Max load - 6888.1 N (1548.5 lb)
Impact Velocity - 1.69 m/s (5.54 ft/s)	Energy at Max Load - 4.034 J (2.975 ft-lb)
Impact Energy - 5.18 J (3.82 ft-lb)	Time - at Max Load - 0.87 msec
Absorbed Energy - 4.608 J (3.399 ft-lb)	total - 3.06 msec
Max Disp. of Tup 0.1460 cm (0.0576 in)	Damage Area - 4.6231 cm ² (0.7166 in ²)
Damage Indent.- 0.013 cm (0.005 in)	Damage Diameter - 1.02 cm (0.40 in)

Figure 3.122. Load and Energy from Dynatup for 32-ply at 15.24 cm (6.0 in) drop height



Specimen ID -17594-1-2	Max load - 6320.0 N (1420.8 lb)
Impact Velocity - 1.69 m/s (5.54 ft/s)	Energy at Max Load - 3.962 J (2.922 ft-lb)
Impact Energy - 5.17 J (3.81 ft-lb)	Time - at Max Load - 0.86 msec
Absorbed Energy - 4.455 J (3.286 ft-lb)	total - 3.10 msec
Max Disp. of Tup 0.1505 cm (0.0592 in)	Damage Area - 4.6231 cm ² (0.7166 in ²)
Damage Indent.- 0.010 cm (0.004 in)	Damage Diameter - 1.02 cm (0.40 in)

Figure 3.123. Load and Energy from Dynatup for 32-ply at 15.24 cm (6.0 in) drop height

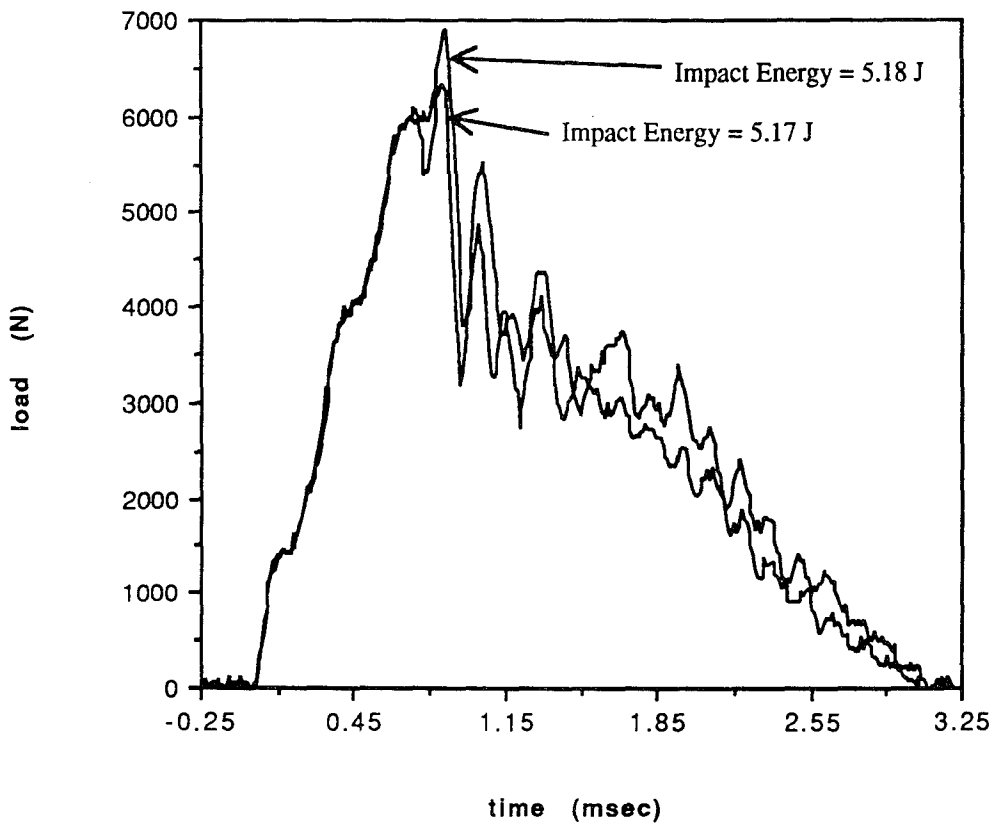


Figure 3.124. Comparison of Load Curves with Impact Energies = 5.18 and 5.17 J for 32-ply

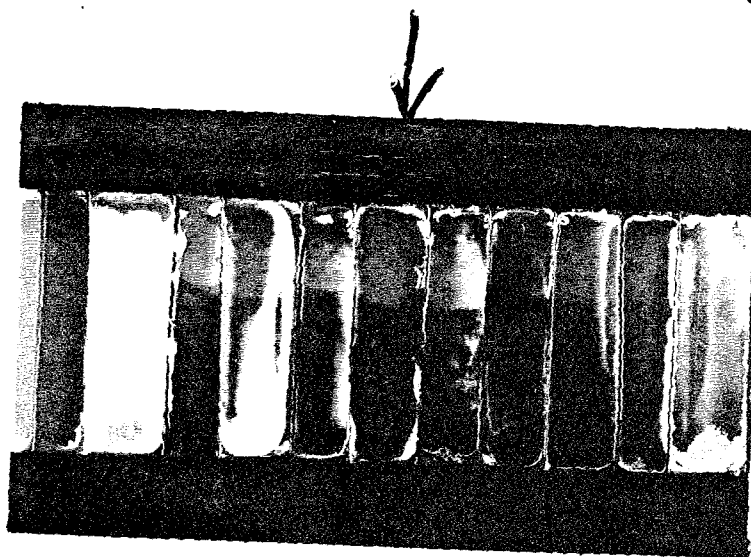


Figure 3.125. 0° Cross-Section 17594-1-1 (2.7 X)

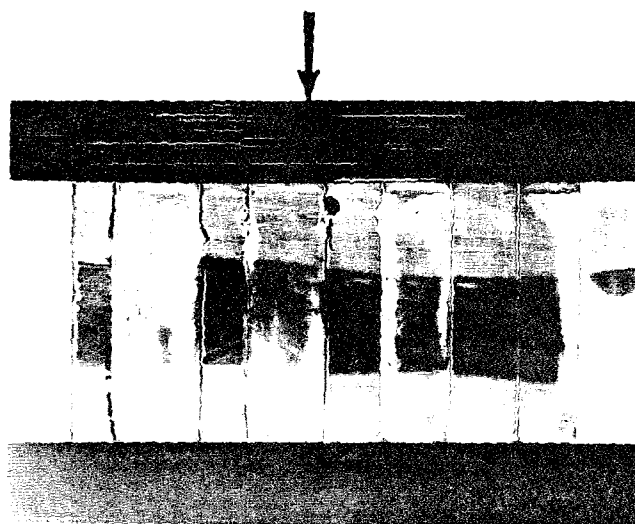


Figure 3.126. 0° Cross-Section 17594-1-2 (2.7 X)

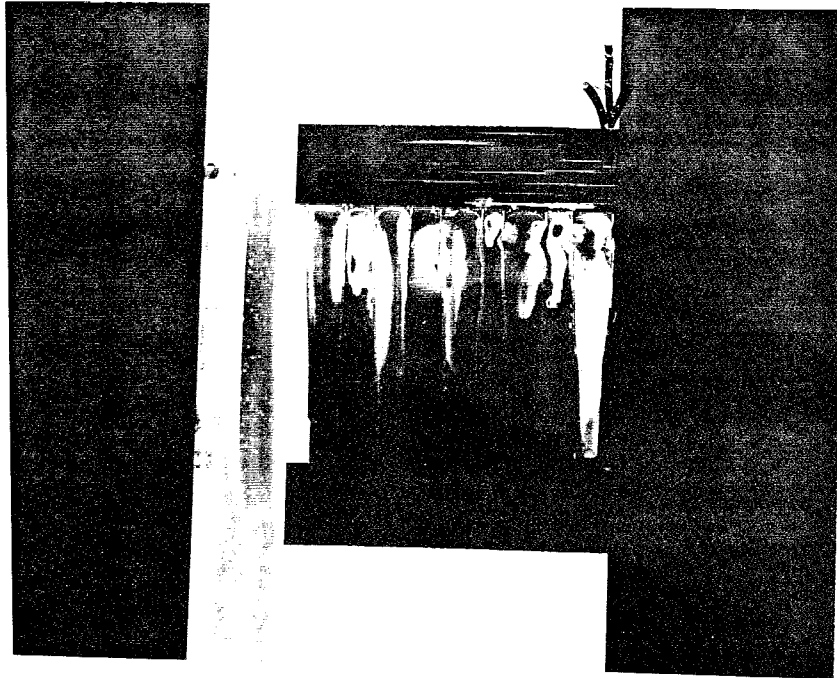


Figure 3.127. 90° Cross-Section 17594-1-1 (2.7 X)



Figure 3.128. 90° Cross-Section 17594-1-2 (2.7 X)

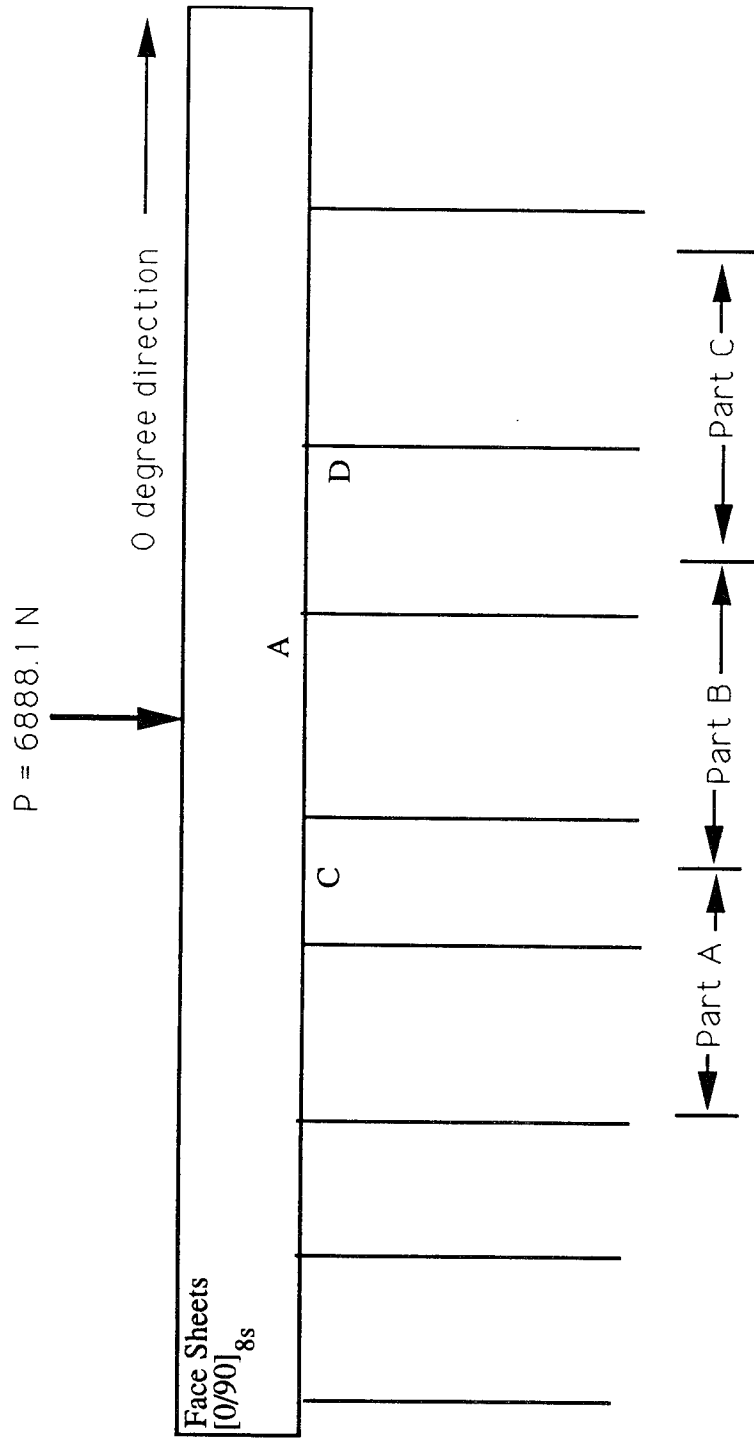


Figure 3.129 Guide to Micrograph of 0 Degree Cross-Section (25X) -17594-1-1

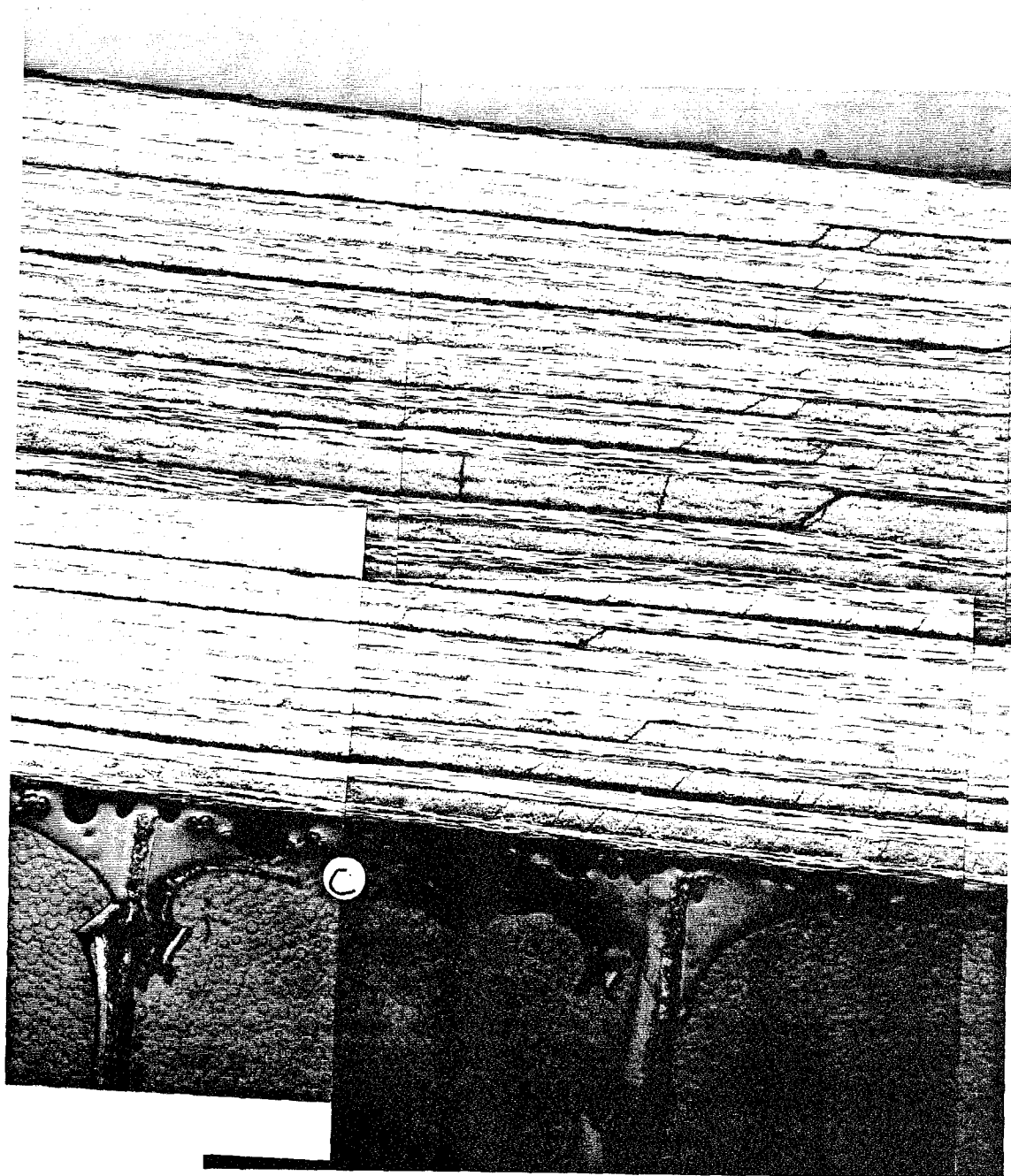


Figure 3.130. 0° Cross-Section 17594-1-1 (25 X) Part A

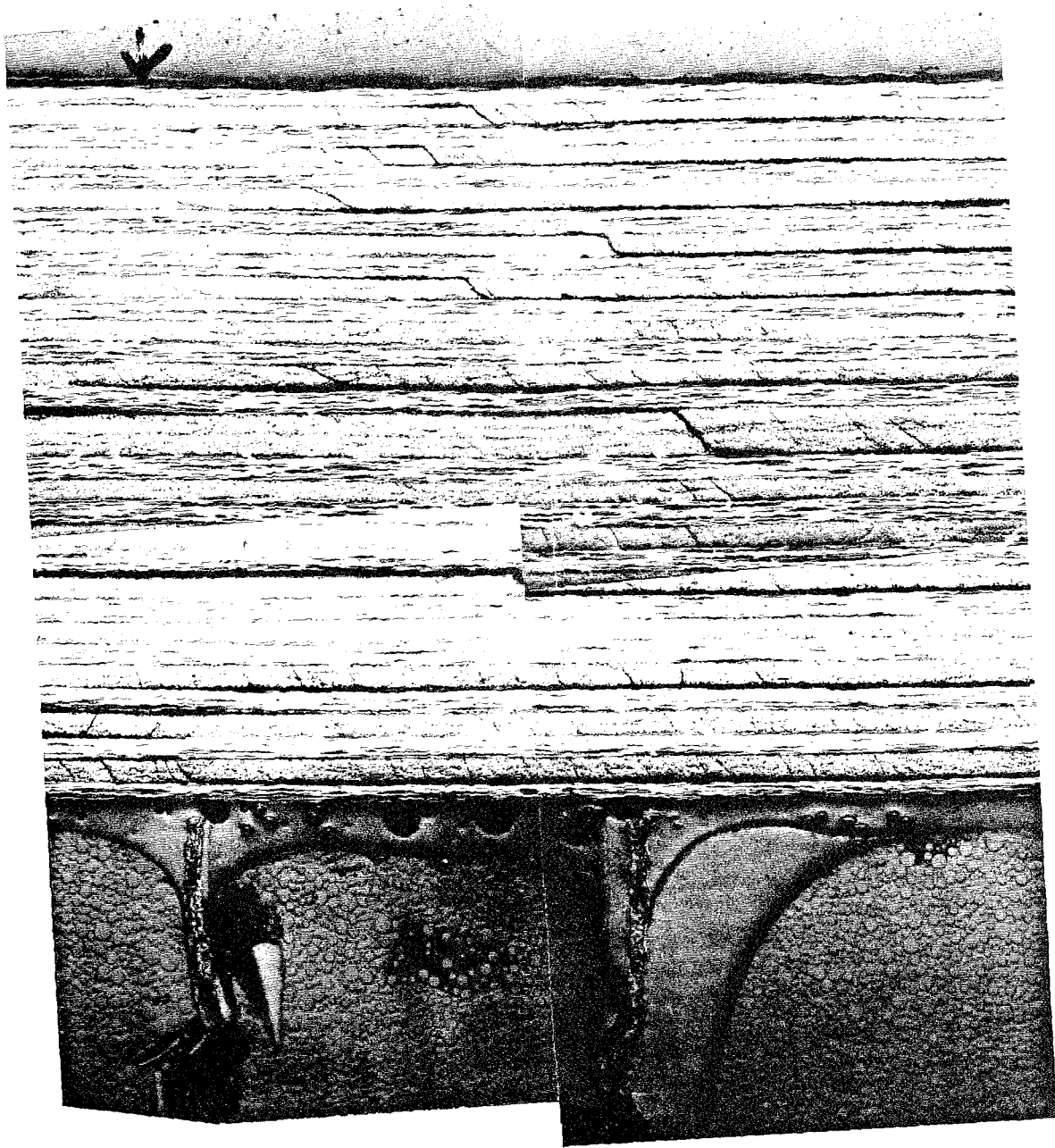


Figure 3.131. 0° Cross-Section 17594-1-1 (25 X) Part B

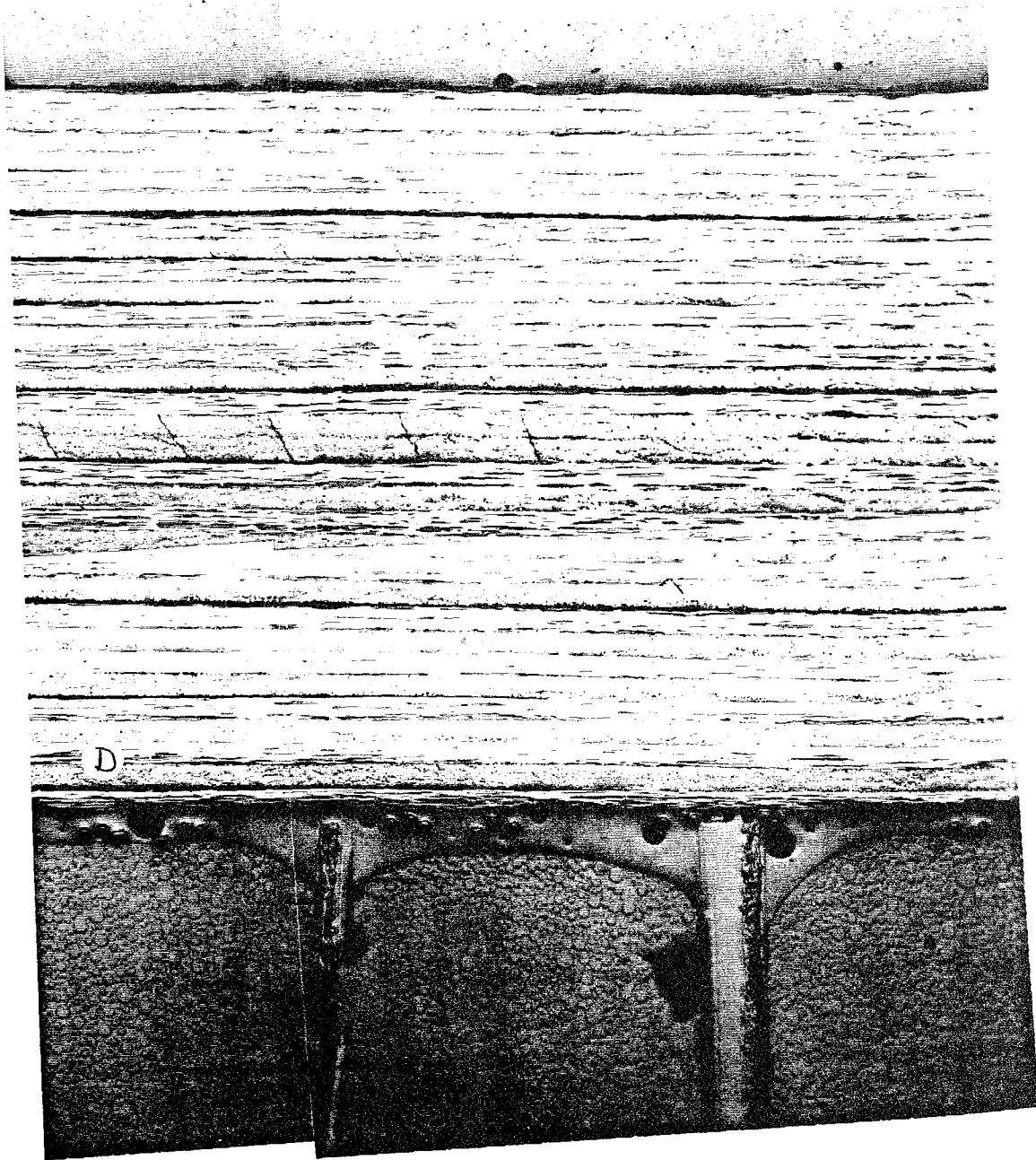


Figure 3.132 0° Cross-Section 17594-1-1 (25 X) Part C

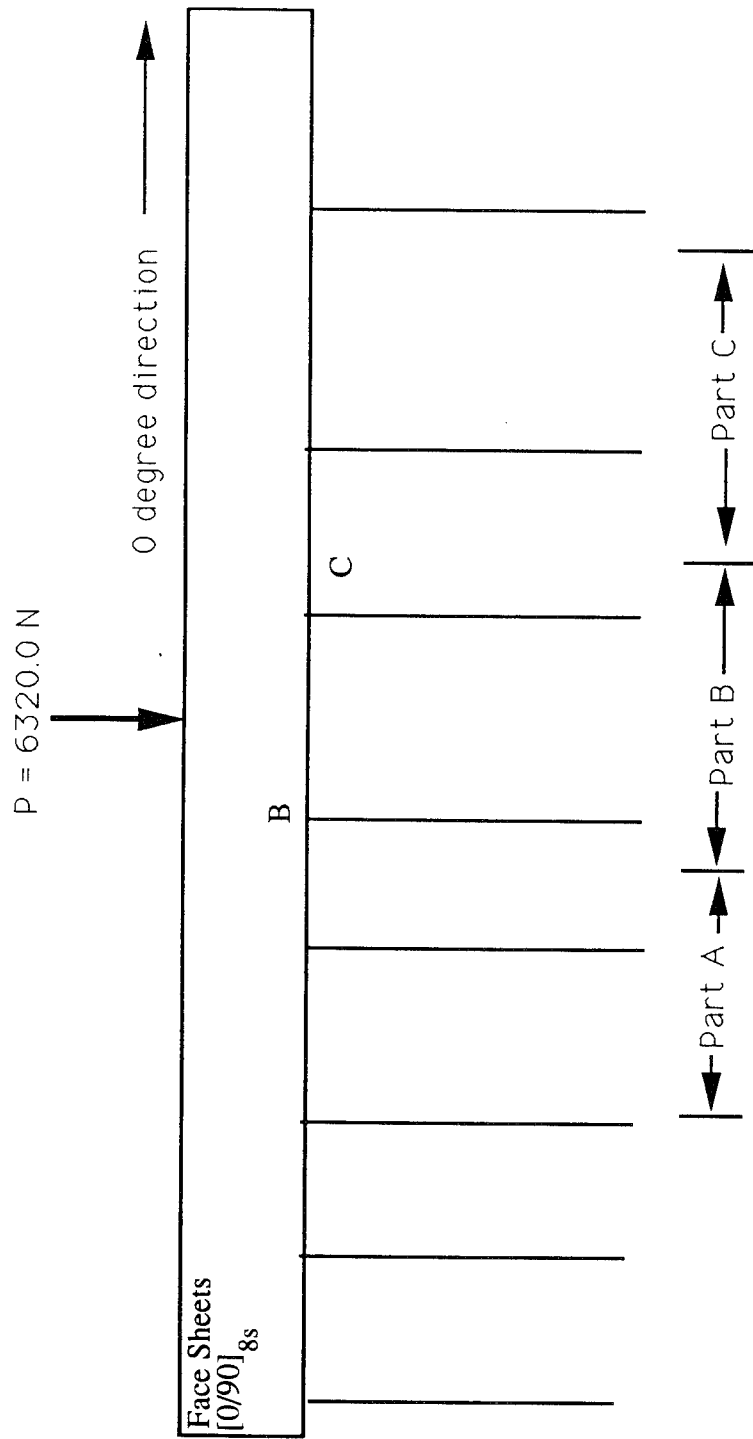


Figure 3.133. Guide to Micrograph of 0 Degree Cross-Section (25X) -17594-1-2

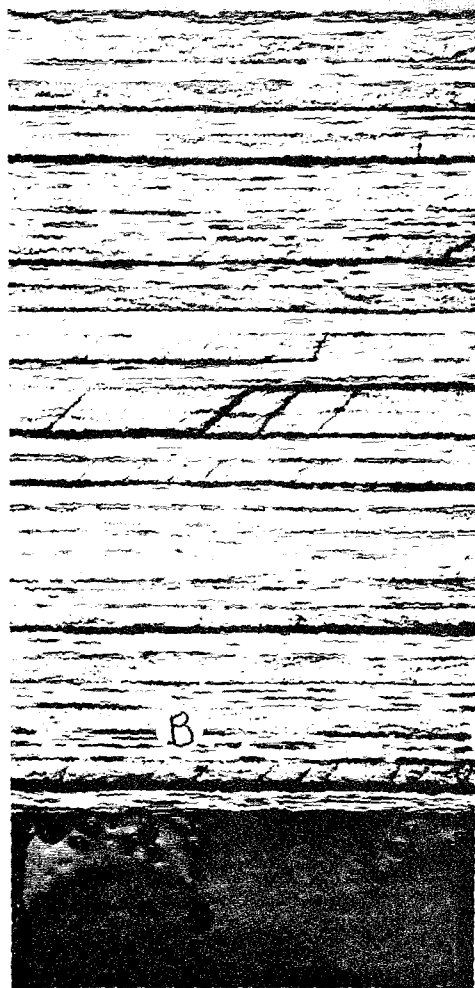


Figure 3.134. 0° Cross-Section 17594-1-2 (25 X) Part A

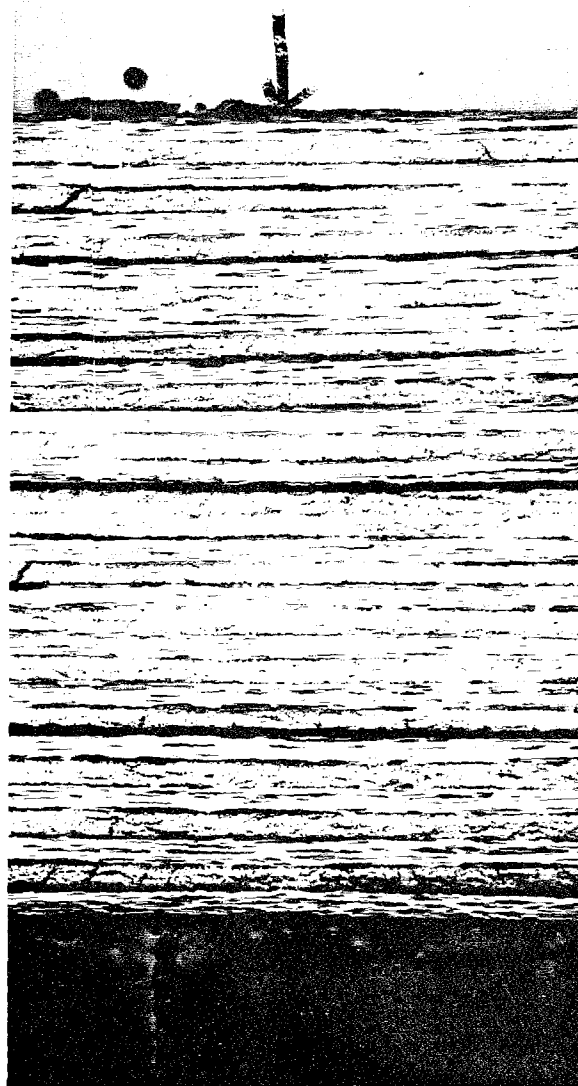


Figure 3.135. 0° Cross-Section 17594-1-2 (25 X) Part B

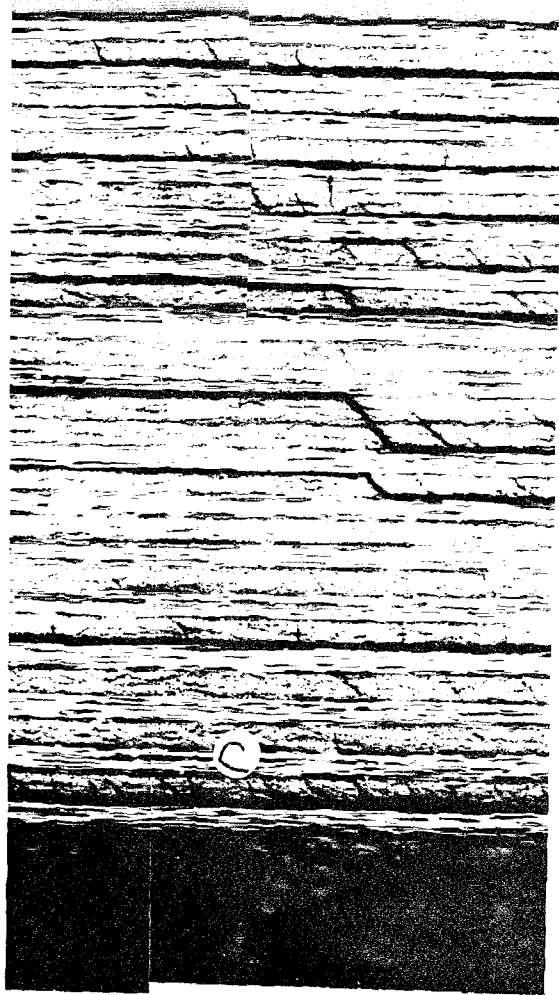


Figure 3.136. 0° Cross-Section 17594-1-2 (25 X) Part C

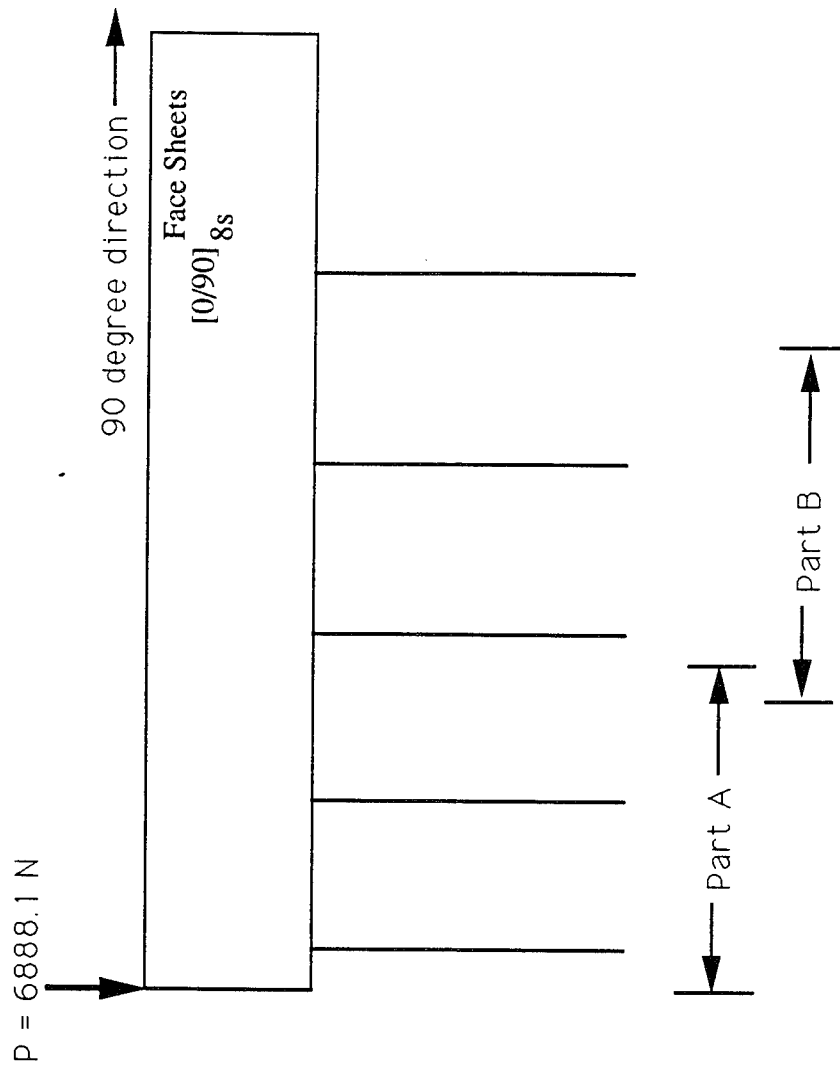


Figure 3.137. Guide to Micrograph of 90 Degree Cross-Section (25X) - 17194-1-1

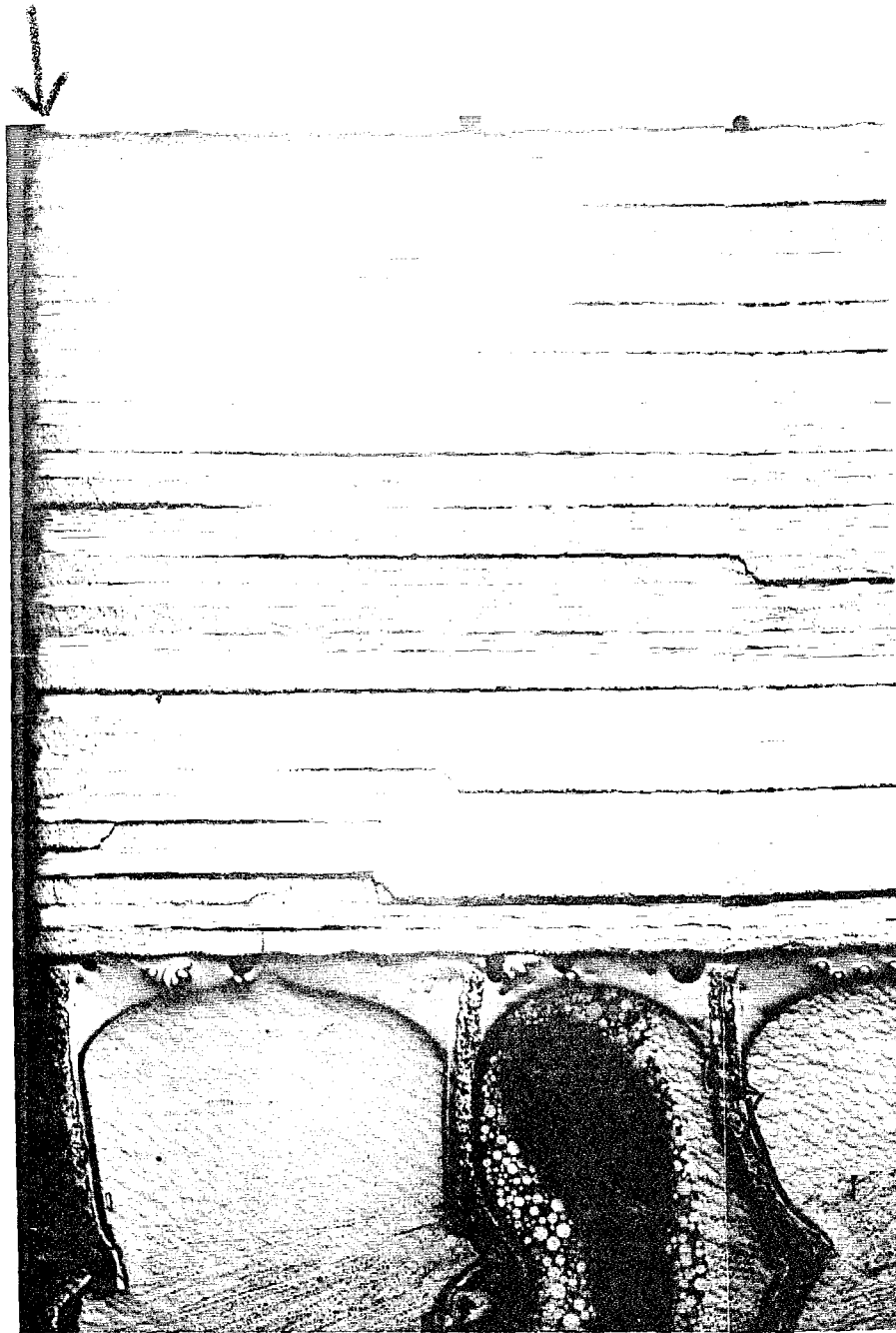


Figure 3.138. 90° Cross-Section 17594-1-1 (25 X) Part A

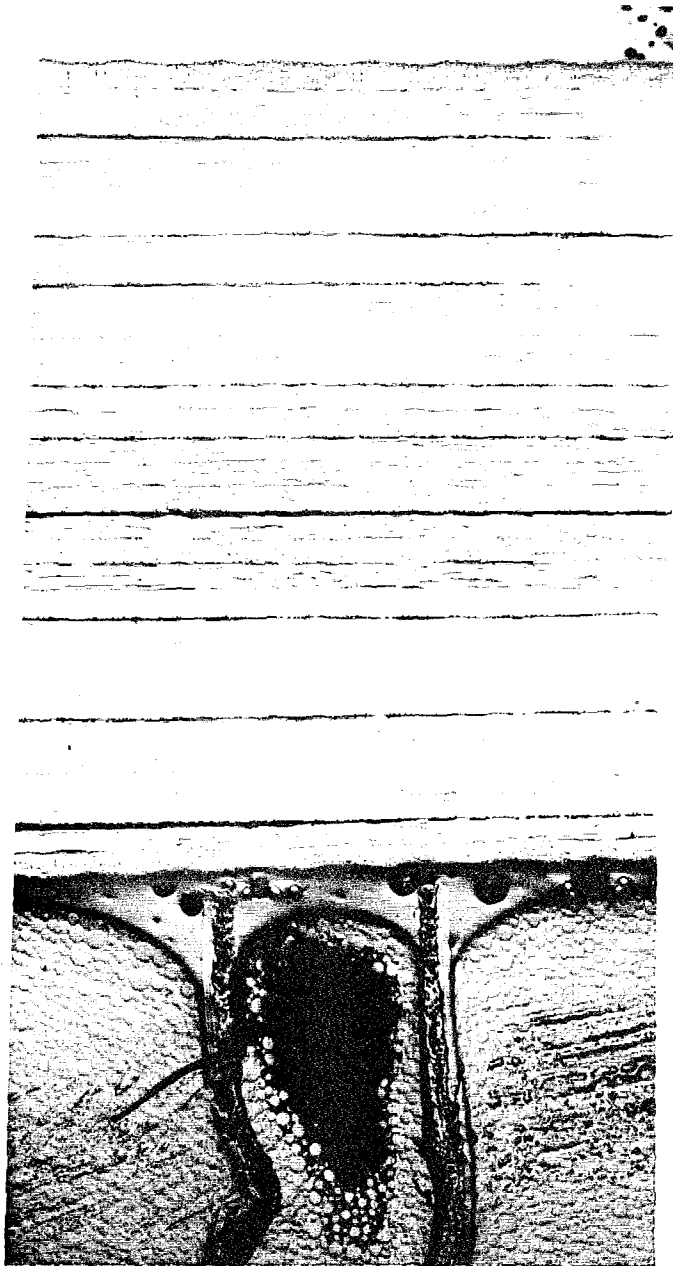


Figure 3.139. 90° Cross-Section 17594-1-1 (25 X) Part B

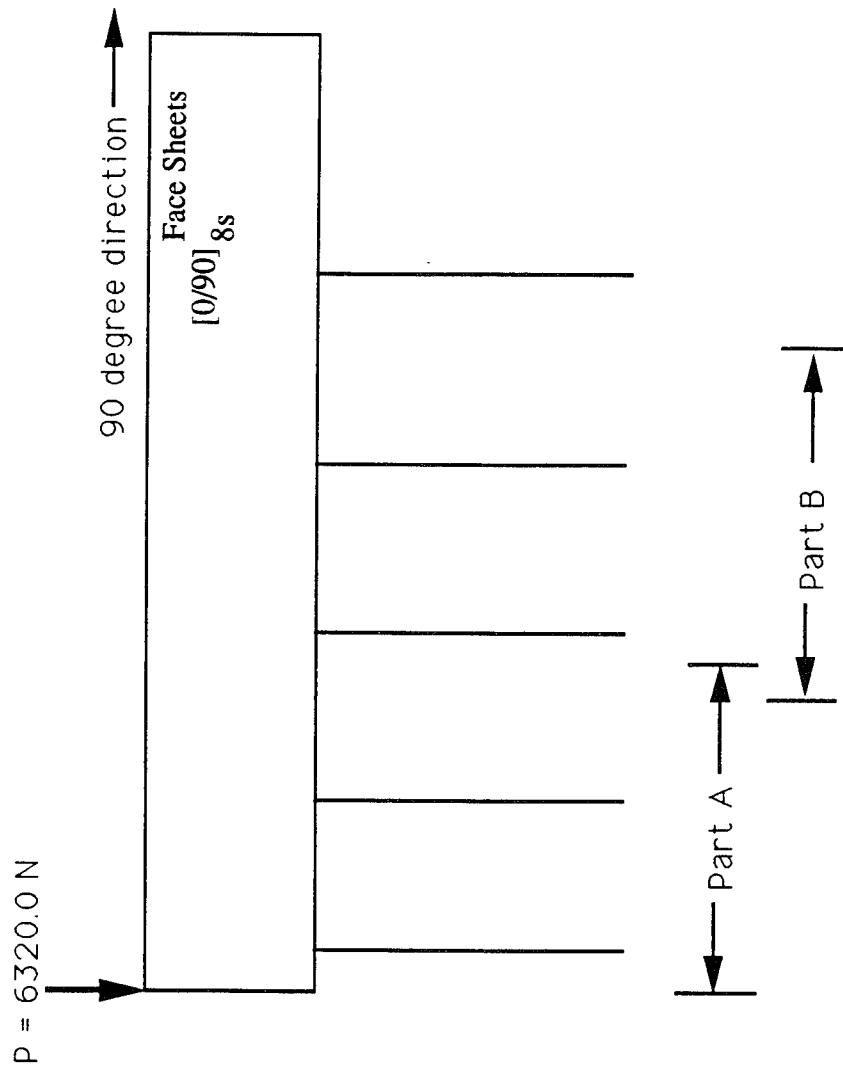


Figure 3.140. Guide to Micrograph of 90 Degree Cross-Section (25X) - 17294-1-2

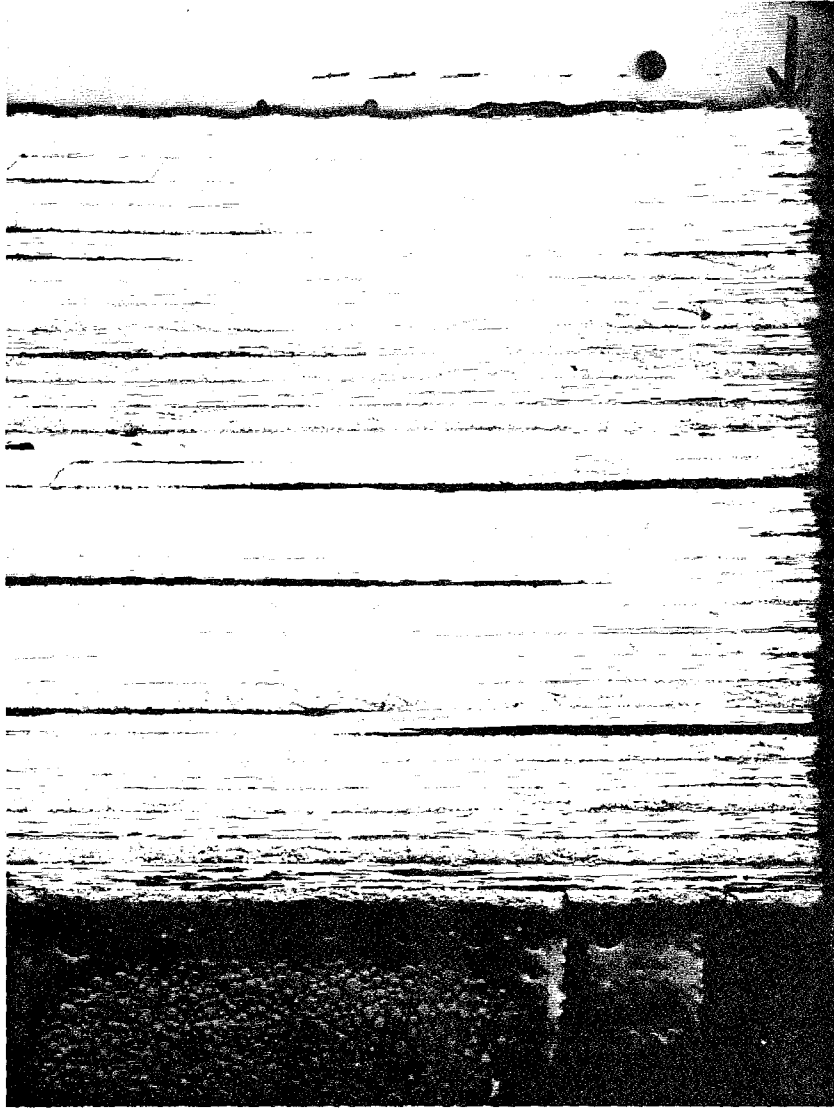


Figure 3.141. 90° Cross-Section 17594-1-2 (25 X) Part A

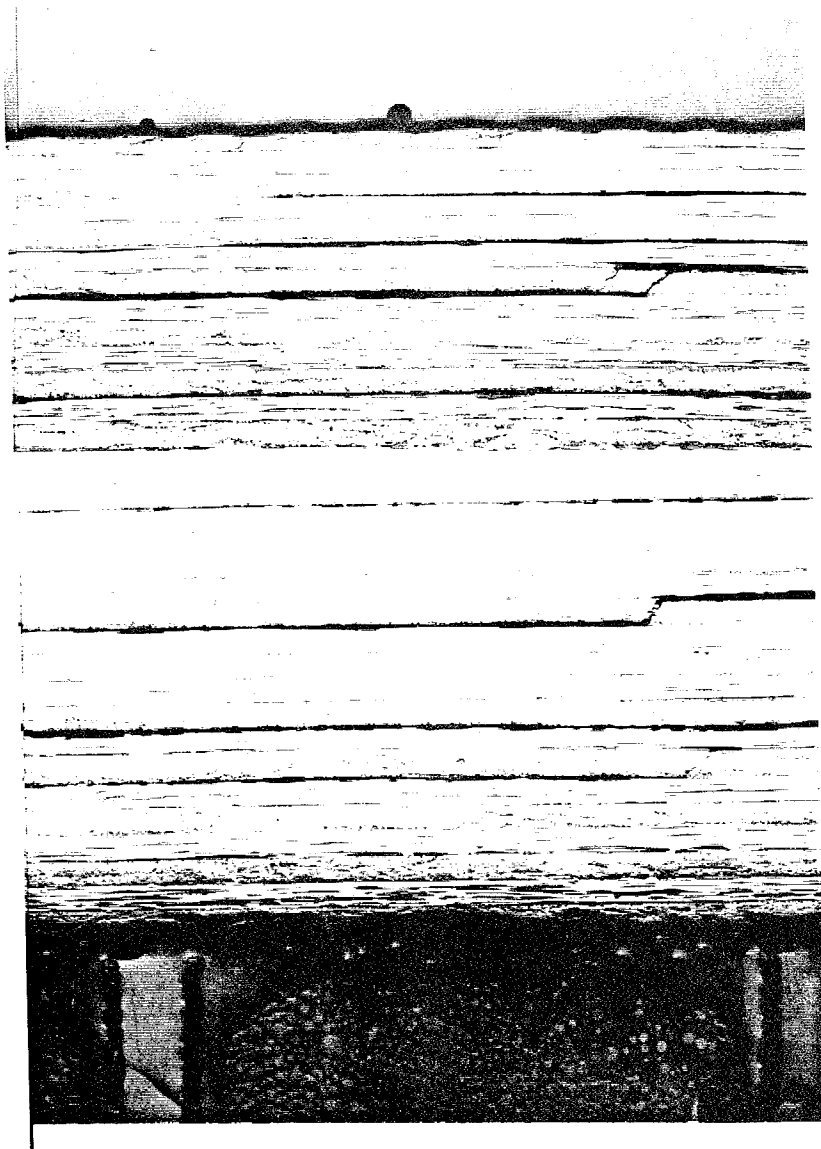


Figure 3.142. 90° Cross-Section 17594-1-2 (25 X) Part B

the delamination is present on both sides. This may be due to the adhesive which has incomplete spots in its layer in this case (Figure 3.135, label E).

(4) Impact Energy = 5.67 J (4.18 ft-lb)

The sandwich panel was impacted at a drop height of 16.51 cm (6.5 in). The load and energy curves are shown in Figure 3.143. A drastic drop in the load curve occurs at the maximum load value of 6718.1 N. This value is less than test 17594-1-1; however, there is more energy absorbed by the specimen. The curve is similar to the previous test.

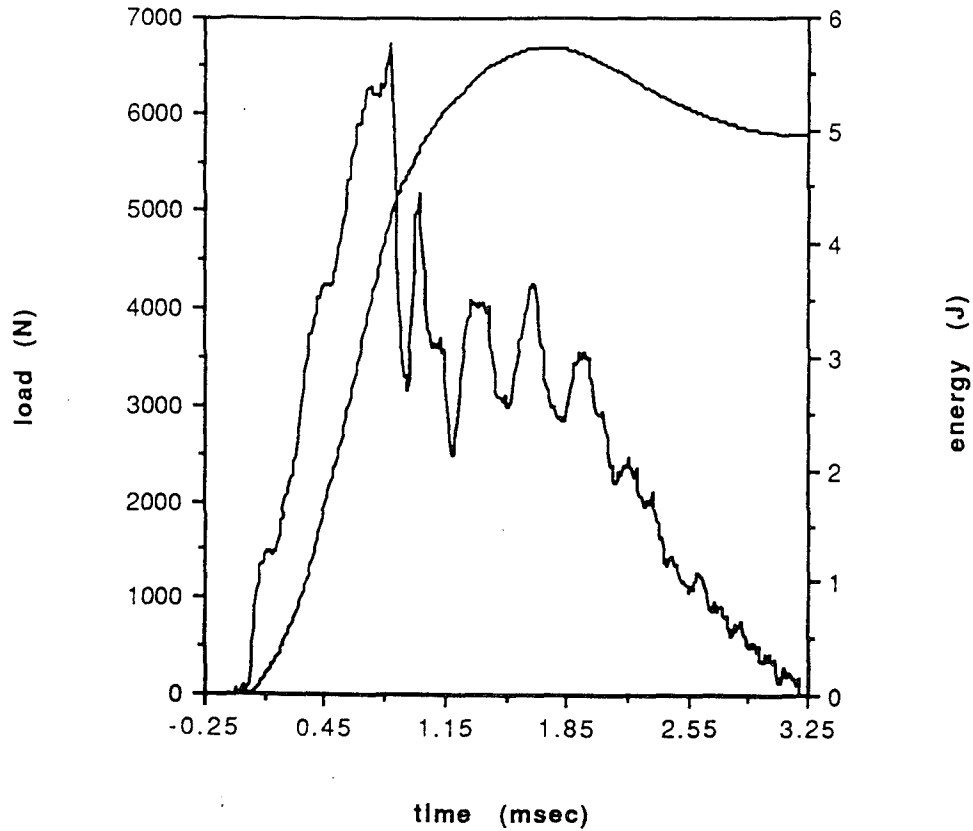
(5) C-scans

C-scans were taken of each impacted specimen that had delamination. Figure 3.144 shows the area of damage picked up by the pulse-echo C-scan. As shown previously, excluding the 16-ply, the damage area increases as the impact area increases (Figure 3.145).

(6) Additional Analysis

Figure 3.146 compares the energy curves for various impact energies. Figure 3.147 compares the load curves for three energy levels. The same characteristics as were found in previous test series again occur here. One minor exception is the time of event for the load curve for an impact energy of 4.27 J. The total time is shorter than the other tests. It took less time because the sandwich specimen did not lose its stiffness because there was no major damage.

Figure 3.148 shows the difference between the absorbed and impact energies. In



Specimen ID -17594-1-3	Max load - 6718.1 N (1510.3 lb)
Impact Velocity - 1.77 m/s (5.80 ft/s)	Energy at Max Load - 4.196 J (3.095 ft-lb)
Impact Energy - 5.67 J (4.18 ft-lb)	Time - at Max Load - 0.84 msec
Absorbed Energy - 4.455 J (3.286 ft-lb)	total - 3.22 msec
Max Disp. of Tup 0.2154 cm (0.0848 in)	Damage Area - 5.1368 cm ² (0.7962 in ²)
Damage Indent.- 0.013 cm (0.005 in)	Damage Diameter - 0.77 cm (0.30 in)

Figure 3.143. Load and Energy from Dynatup for 32-ply at 16.51 cm (6.5 in) drop height

4.70 Joules
(3.47 ft-lb)



5.18 Joules
(3.81 ft-lb)



5.67 Joules
(4.18 ft-lb)



Figure 3.144. Pulse-Echo C-scans for Sandwich Panels with 32-ply Face Sheets

previous tests, the difference increased as the drop height increased. This did not occur in this test. There is a large difference in the test series that did not have a large drop in the load curve. To further investigate the behavior of the energies associated with the impacts, the absorbed energy, impact energy and energy maximum load were compared in Figure 3.149. Generally, the energy maximum load is larger than the absorbed energy. This did not occur at the lowest drop height. This is because the amount of energy absorbed by the specimen was not large enough to cause major damage.

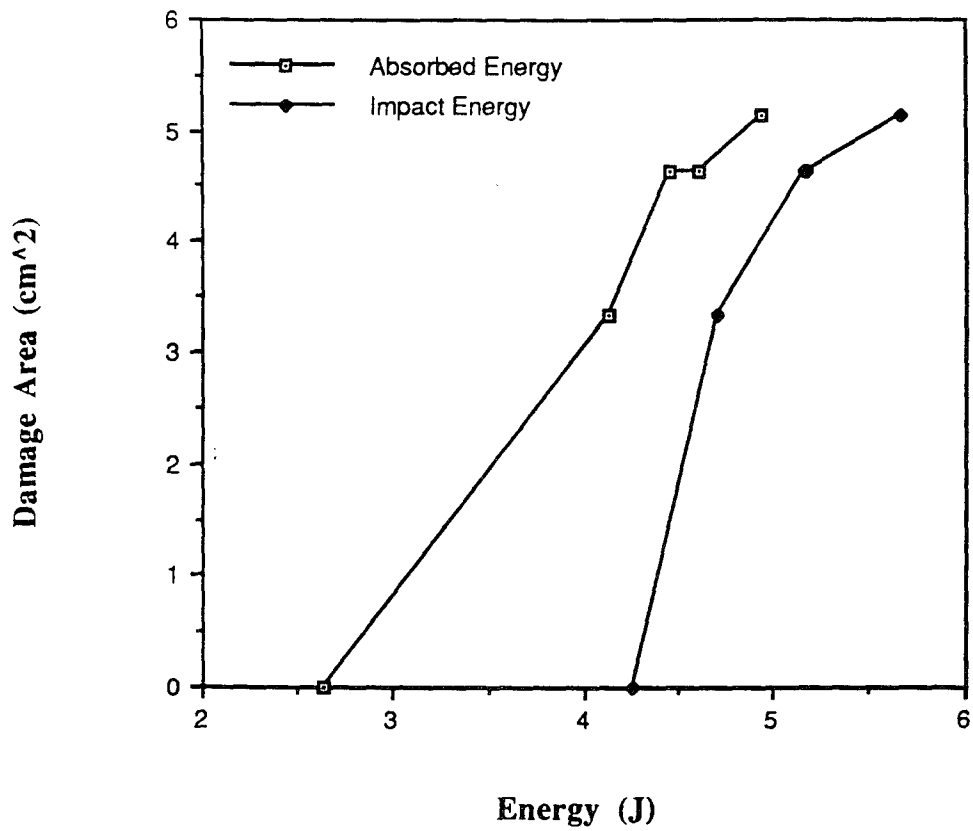


Figure 3.145. Damage Area vs Impact and Absorbed Energies - 32-ply

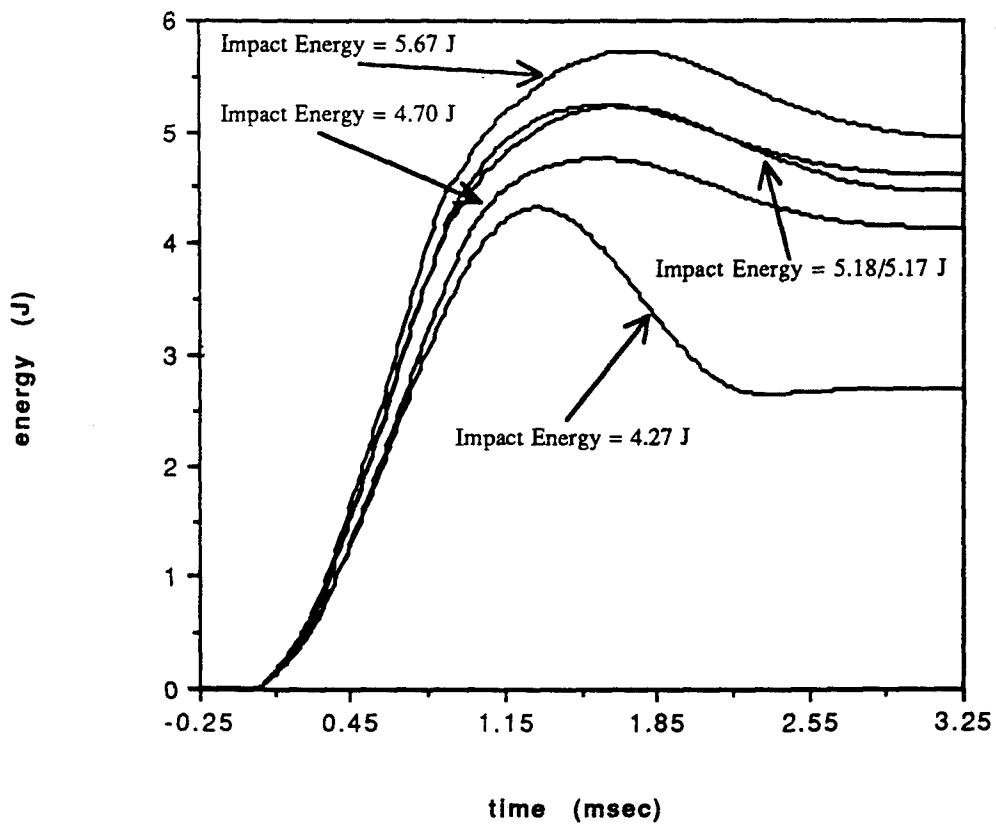


Figure 3.146. Comparison of Energy Curves for Sandwich Panels with 32-ply Face Sheets

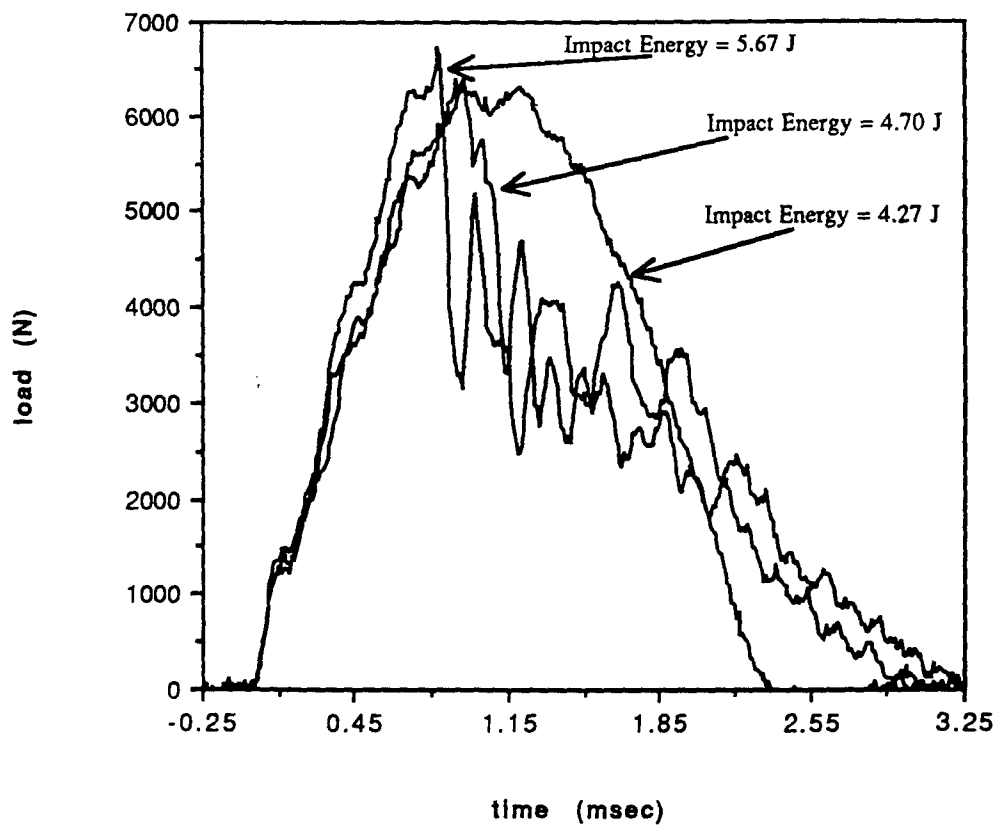


Figure 3.147. Comparison of Load Curves for Sandwich Panels with 32-ply Face Sheets

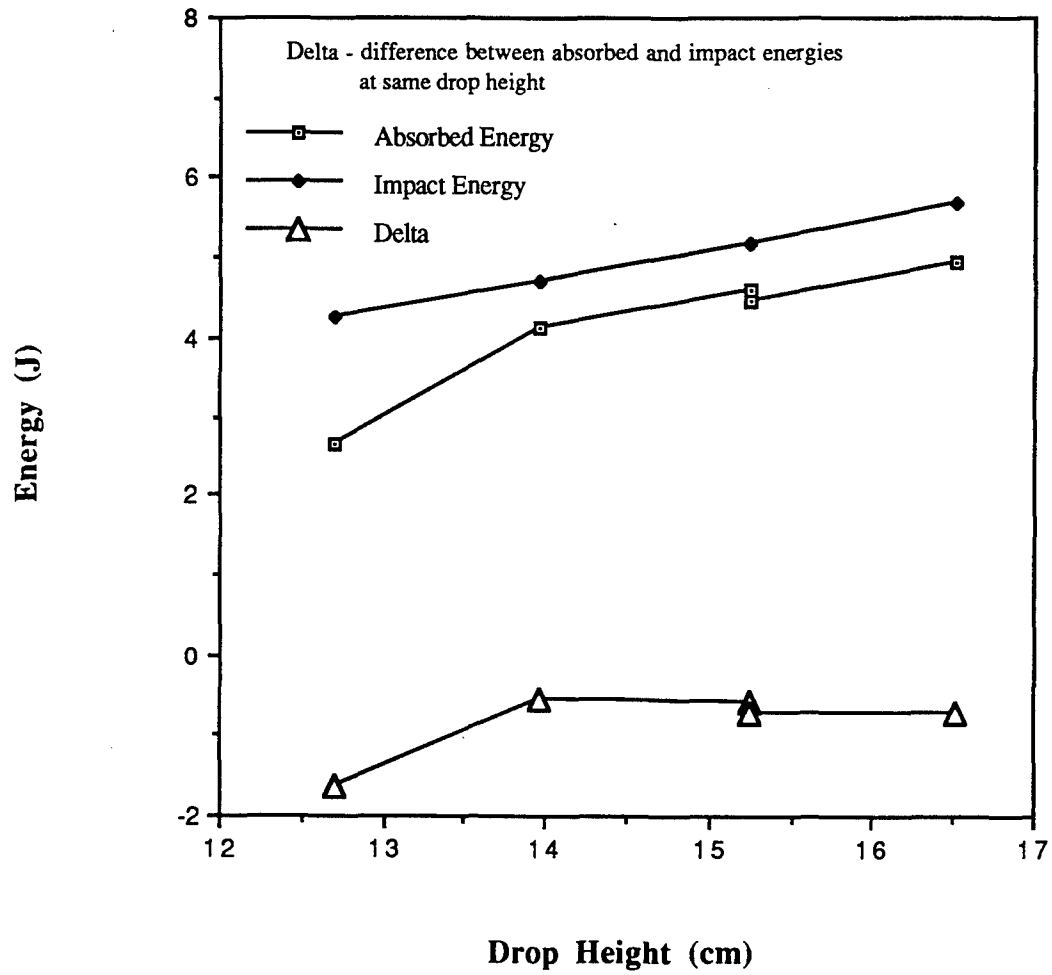


Figure 3.148. Comparison of Absorbed Energy and Impact Energy vs Drop Height for Sandwich Panels with 32-ply Face Sheets

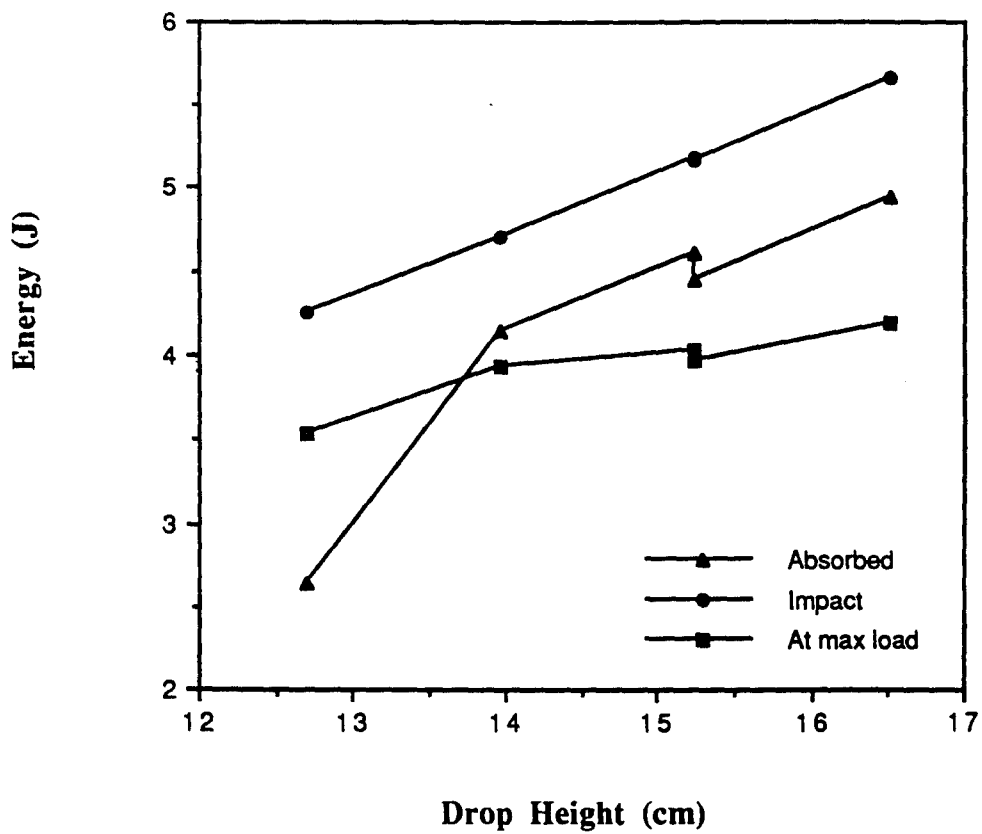


Figure 3.149. Comparison of Absorbed Energy, Impact Energy and Energy at Maximum Load for Sandwich Panels with 32-ply Face Sheets

3.8 Sandwich Panels with 48-ply Face Sheets

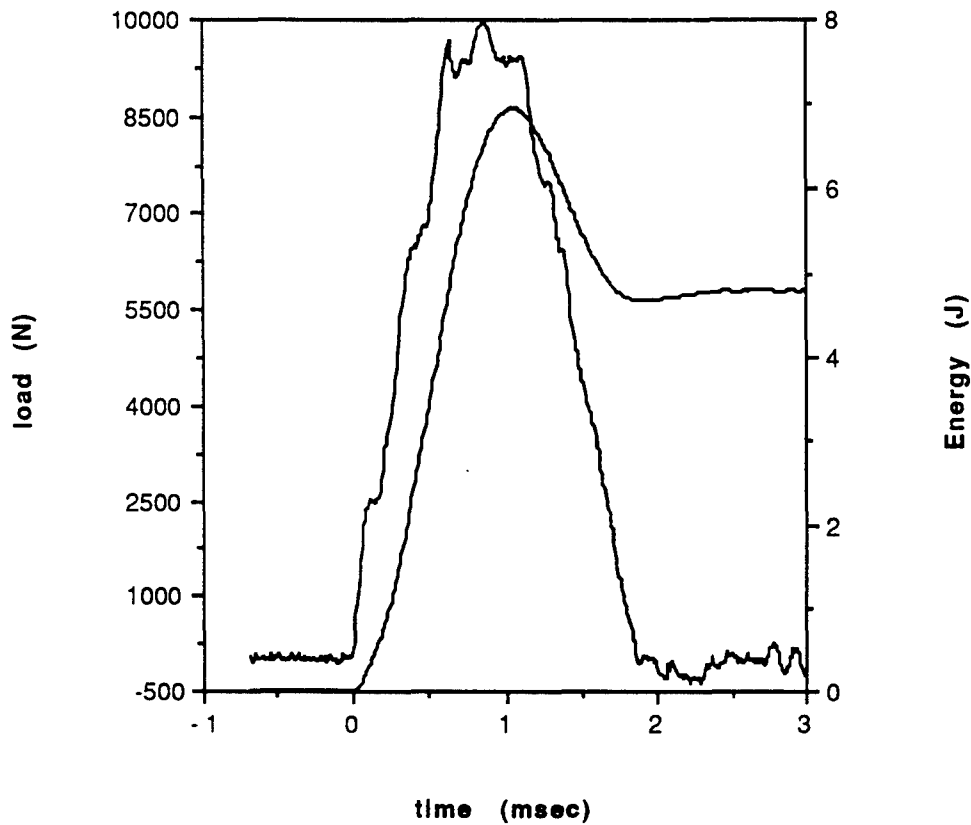
The sandwich panels with 48-ply face sheets were subjected to low energy (velocity) impacts with drop heights ranging from 20.32 cm (8.0 in) to 27.94 cm (11.0 in). The approximate threshold impact energy is approximately 6 J (4 ft-lb). The associated maximum load is 10,500 N (2361 lb). The load and energy curves for each test will be discussed; however, only the micrographs for the 7.78 J (5.74 ft-lb) and 9.67 J (7.13 ft-lb) impact energies will be presented.

(1) Impact Energy = 6.89 J (5.08 ft-lb)

The load and energy curves for a sandwich panel with 48-ply face sheets at a drop height of 20.32 cm (8.0 in) are shown in Figure 3.150. Note the repeatable jumps in the early part of the load-time curve. This characterizes the natural frequency phenomena eluded to previously. According to the results from the pulse-echo C-scans, there was no delamination of the face sheets ; however, there is a small amount of damage in the specimen as noted by the energy versus time curve. A total of 4.678 J (3.450 ft-lb) of energy was absorbed by the specimen in this test. This energy may have gone into matrix cracking. Note that a drastic drop in the load curve is not present in this test. Only a slight dip at the top exists.

(2) Impact Energy = 7.78 J (5.74 ft-lb)

The sandwich panel was subjected to low velocity impact at a drop height of



Specimen ID -18294-2-6	Max load - 9978.7 N (2243.3 lb)
Impact Velocity - 1.95 m/s (6.39 ft/s)	Energy at Max Load - 6.428 J (4.741 ft-lb)
Impact Energy -6.89 J (5.08 ft-lb)	Time - at Max Load - 0.86 msec
Absorbed Energy - 4.678 J (3.450 ft-lb)	total - 1.87 msec
Max Disp. of Tup 0.1295 cm (0.0510 in)	Damage Area - n/a
Damage Indent.- n/a	Damage Diameter - n/a

Figure 3.150. Load and Energy from Dynatup for 48-ply at 20.32 cm (8.0 in) drop height

of 22.86 cm (9.0 in). The load and energy curves are presented in Figure 3.151. The impact energy, absorbed energy and energy at maximum load all increased. Though a drastic peak does not exist in the load curve, there is energy dissipated, an increase of 9.6% over the pervious test. A small delamination area was picked up by the C-scan.

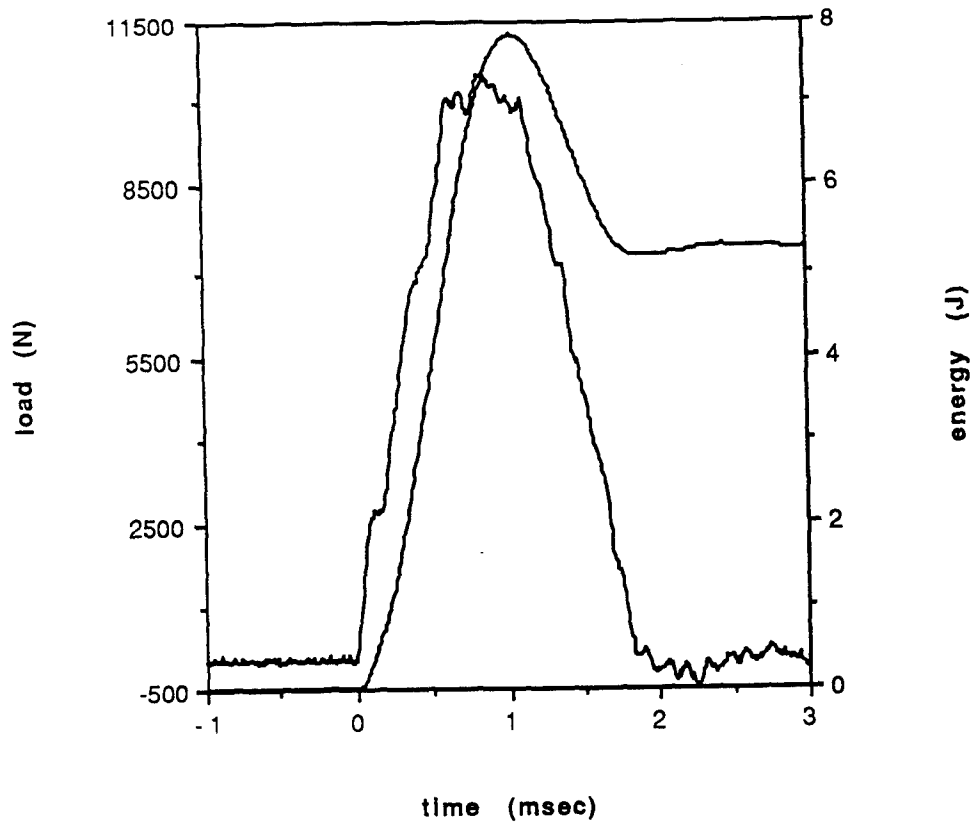
Figures 3.152 and 3.153 show an overall view of the impact area. The only apparent damage is a fine delamination. The core does not receive any damage. The top face sheet is acting like a plate on an elastic foundation. The damage area is further magnified in Figures 3.154 and 3.155. As shown in the 0° cross-section, a fine delamination exists 0.114 cm (.045 in) down from the impact (Figure 3.154, label A). The delamination has traveled away and towards the impact site. A fine delamination also exists at this same spot in the 90° cross-section (Figure 3.155, label B). Only one crack, the crack between the delamination is apparent in the entire damaged area.

(3) Impact Energy = 8.84 J (6.52 ft-lb)

The sandwich panel was impacted at a drop height of 25.4 cm (10.0 in.). The load and energy curves are shown in Figure 3.156. At this energy level, a drastic drop in the load curve results at approximately 11200 J (2500 lb). A total energy of 6.587 J (4.858 ft-lb) is absorbed by the specimen. This is an increase of 21% over the last test. Results from the C-scan shows that there is a significant amount more of delamination area.

(4) Impact Energy = 9.67 J (7.13 ft-lb)

The sandwich specimen was impacted at a drop height of 27.94 cm (11.0 in). The load curve for this test is presented in Figure 3.157. After the repeatable peaks in the load



Specimen ID -18294-2-2 Max load - 10498.7 N (2360.2 lb)
 Impact Velocity - 2.06 m/s (6.79 ft/s) Energy at Max Load - 7.151 J (5.274 ft-lb)
 Impact Energy - 7.78 J (5.74 ft-lb) Time - at Max Load - 0.84 msec
 Absorbed Energy - 5.177 J (3.818 ft-lb) total - 1.94 msec
 Max Disp. of Tup 0.1366 cm (0.0538in) Damage Area - 0.1712cm² (0.0265 in²)

Figure 3.151. Load and Energy from Dynatup for 48-ply at 22.86 cm (9.0 in) drop height

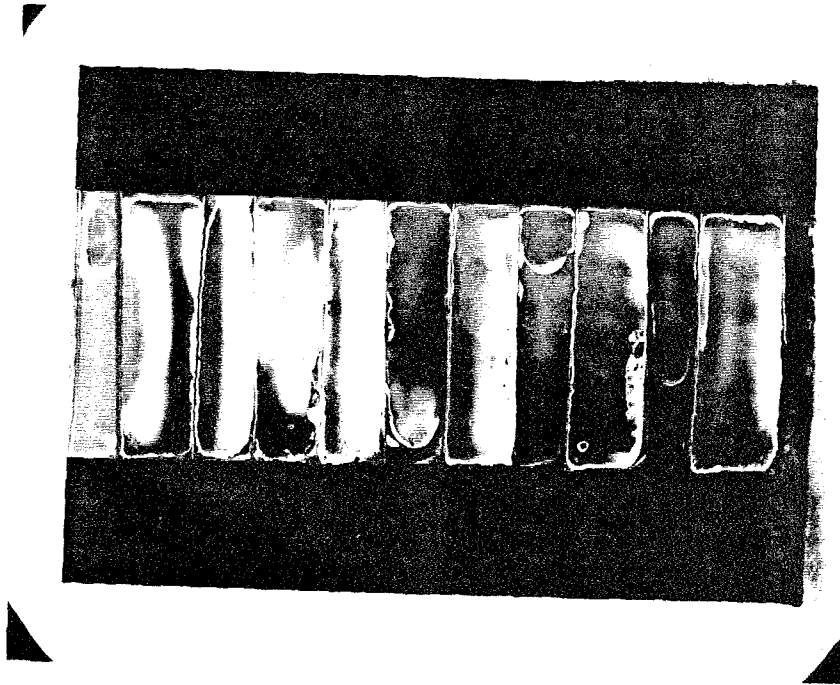


Figure 3.152. 0° Cross-Section 18294-2-2 (2.5 X)

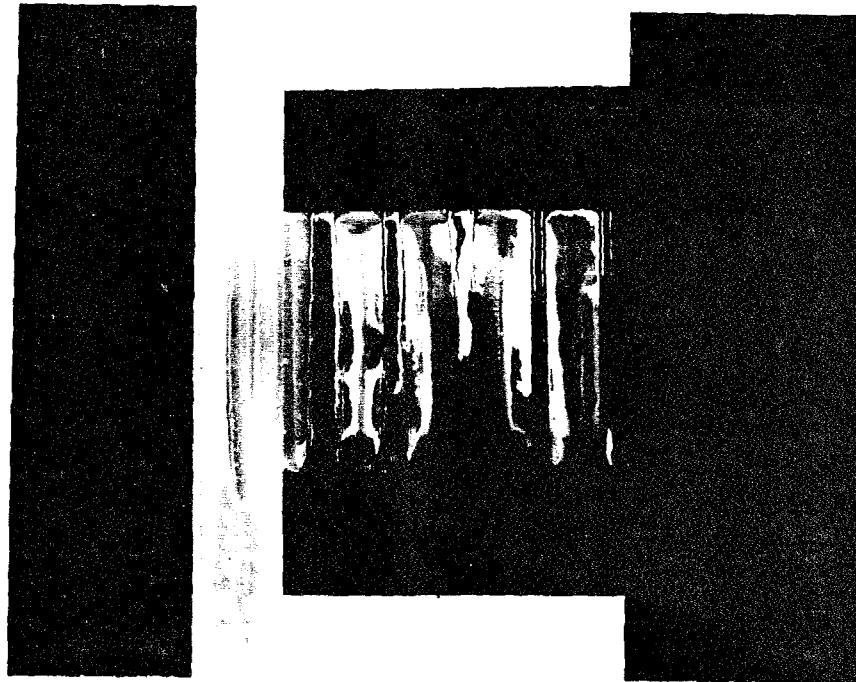


Figure 3.153. 90° Cross-Section 18294-2-2 (2.5 X)

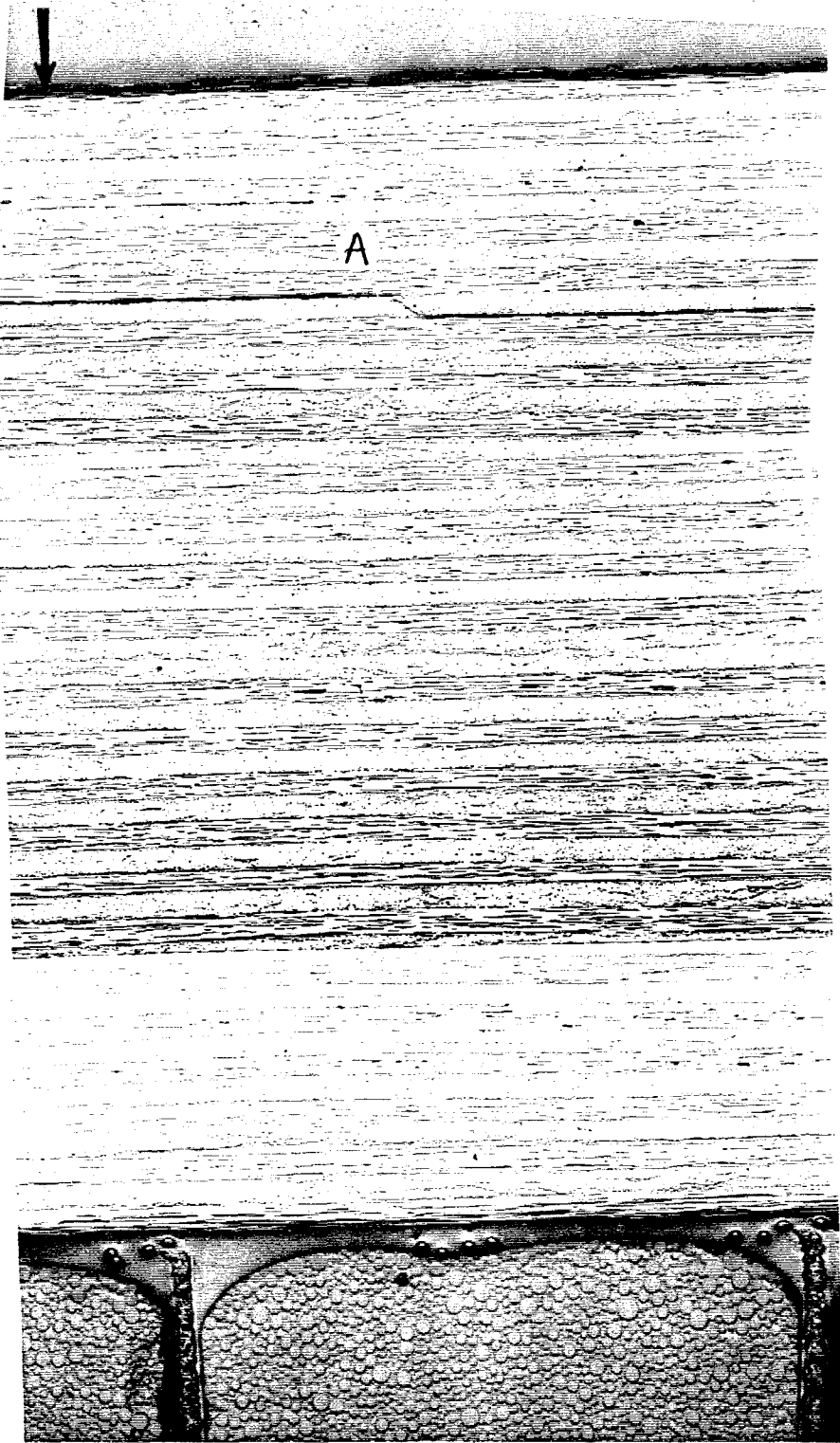


Figure 3.154. 0° Cross-Section 18294-2-2 (25 X)

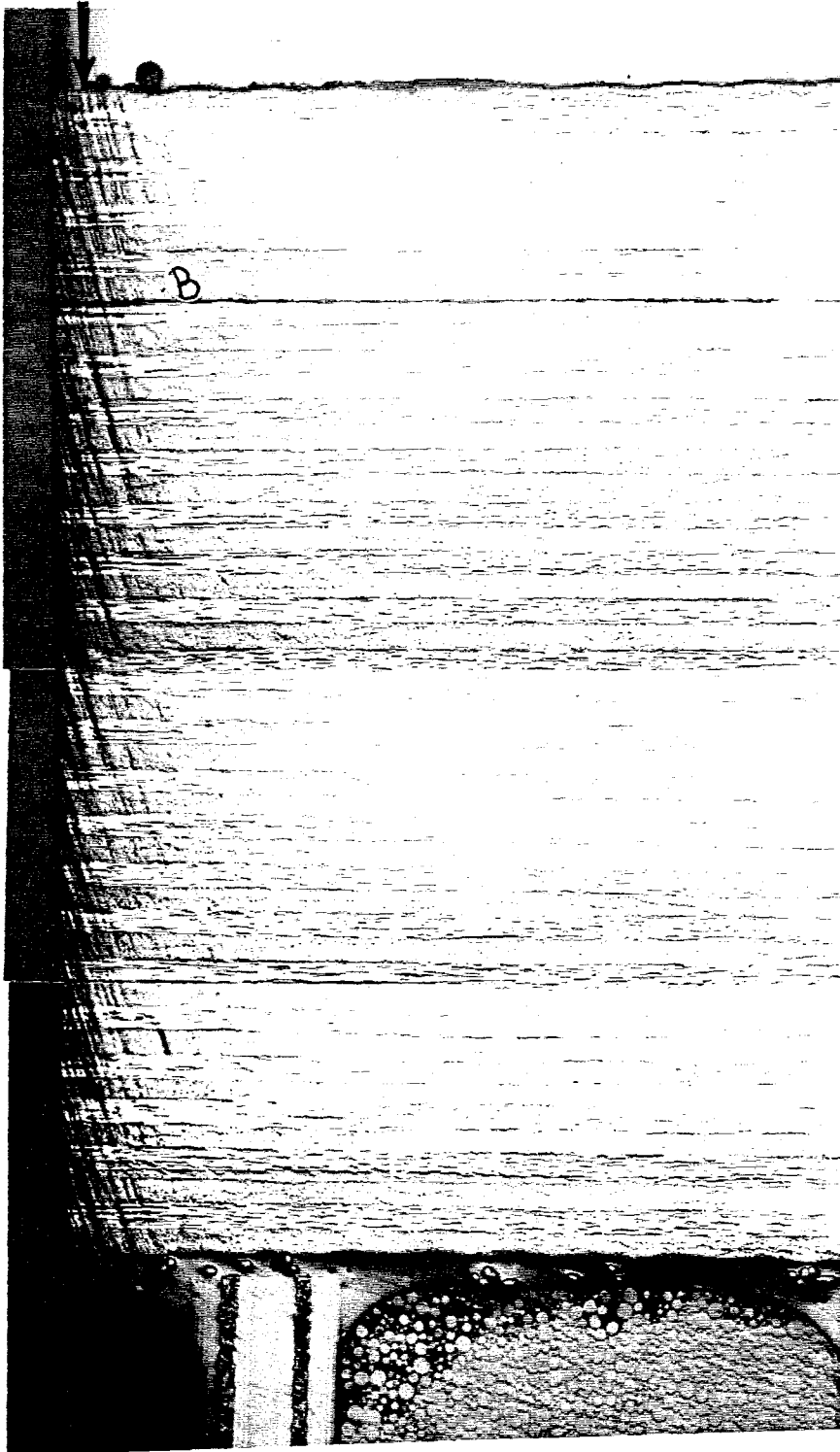
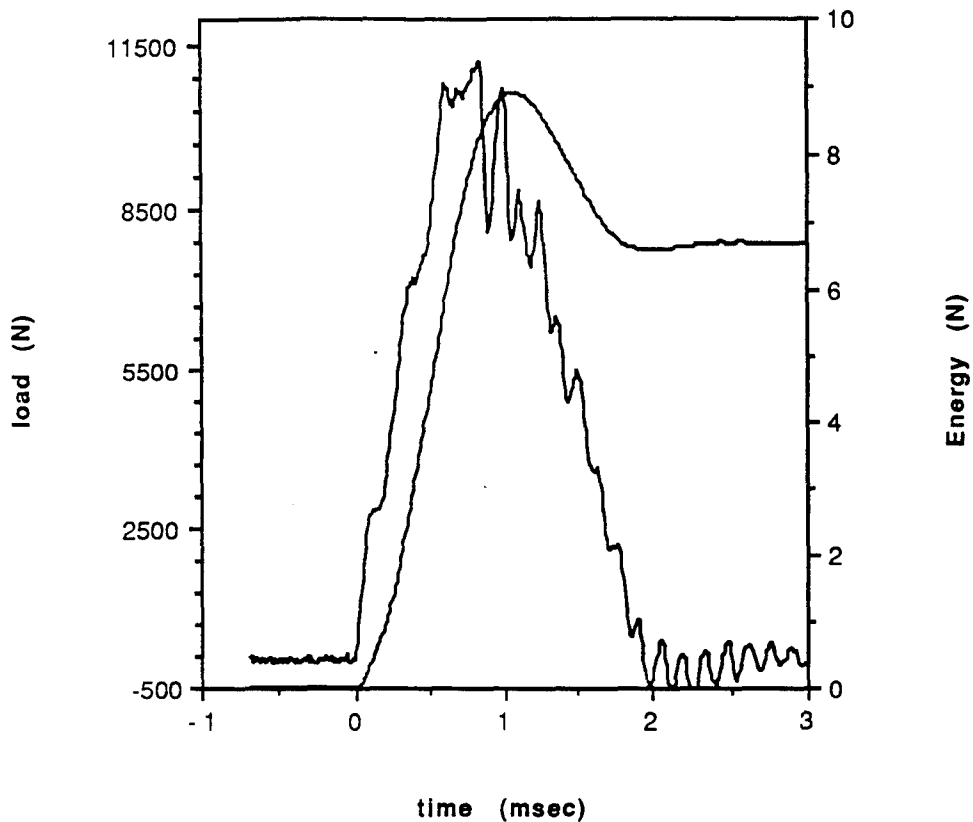
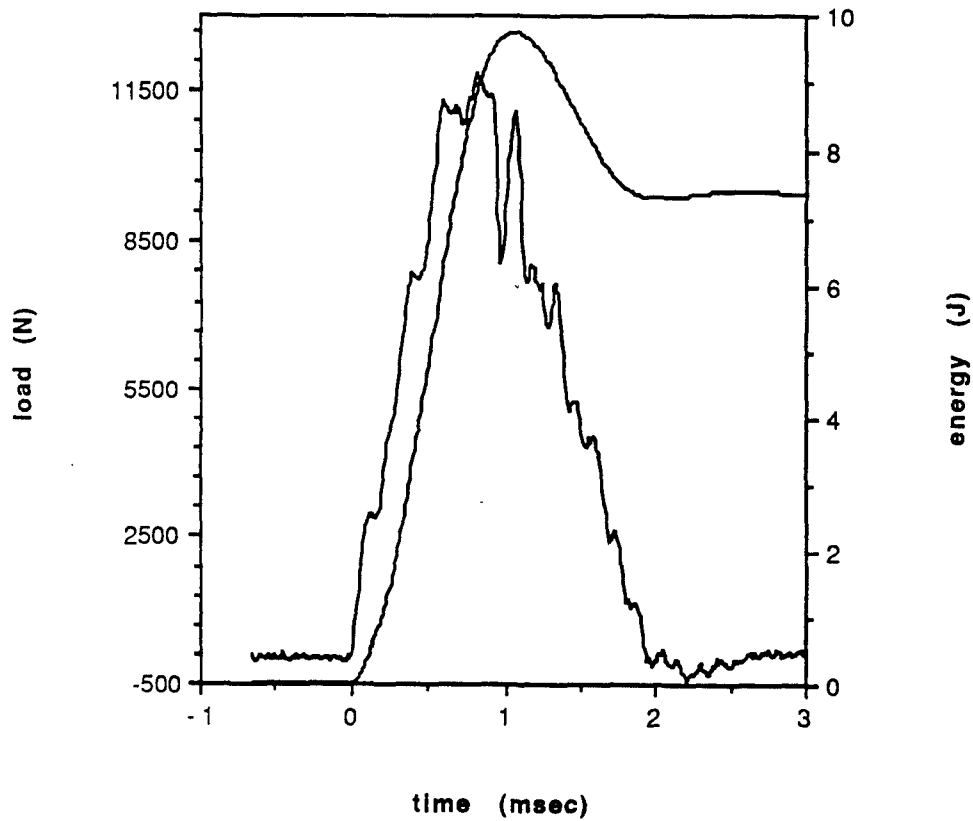


Figure 3.155. 90° Cross-Section 18294-2-2 (25 X)



Specimen ID - 18294-2-5	Max load - 11210.9 N (2520.3 lb)
Impact Velocity - 2.21 m/s (7.24 ft/s)	Energy at Max Load - 8.256 J (6.089 ft-lb)
Impact Energy - 8.84 J (6.52 ft-lb)	Time - at Max Load - 0.85 msec
Absorbed Energy - 6.587 J (4.858 ft-lb)	total - 1.95 msec
Max Disp. of Tup 0.1444 cm (0.0538in)	Damage Area - 6.1574 cm ² (0.9544 in ²)

Figure 3.156. Load and Energy from Dynatup for 48-ply at 25.40 cm (10.0 in) drop height



Specimen ID -18294-2-4 Max load - 11808.7 N (2654.7 lb)
 Impact Velocity - 2.31 m/s (7.58 ft/s) Energy at Max Load - 8.837 J (6.518 ft-lb)
 Impact Energy -9.67 J (6.52 ft-lb) Time - at Max Load - 0.83 msec
 Absorbed Energy - 7.311 J (5.392 ft-lb) total - 1.95 msec
 Max Disp. of Tup 0.1522 cm (0.0599 in) Damage Area - 6.6778 cm² (1.0351in²)

Figure 3.157. Load and Energy from Dynatup for 48-ply at 27.94 cm (11.0 in) drop height

curve that exist in each of the test in this series, a drastic drop occurs at . There is an 11% increase in the absorbed energy. The maximum load also increases.

The overall view of the impacted area, Figures 3.158 and 3.159, shows that there is delamination in the upper face sheet while everything else stays intact. The 25 magnification is shown in Figures 3.160 - 3.163. At the lower impact, a fine delamination resulted at the top of the face sheet. In this case, a fine delamination with wider openings exists at the top and also at the middle 90° layer. This implies that the damage first occurs at the top layer. A rigid structure subjected to low velocity impact acts in this manner. The damage originated from high contact stresses on the impact surface.

(5) C-scans

C-scans were taken of each specimen that had delamination. Figure 3.164 shows the area of damage picked up by the pulse-echo C-scan. The damage area increases as the impact energy increases (Figure 3.165).

(6) Additional Analysis

Figure 3.166 compares the energy curves for various impact energies. Figure 3.167 compares the load curves for the highest and lowest impact energies. The same characteristics in previous test series are observed. Figure 3.168 shows the difference between absorbed and impact energies. As in the 32-ply face sheet test series, the difference did not increase as the drop height increased implying that the elastic energy recovered remains constant and that all of the additional impact energy is absorbed resulting in more damage.

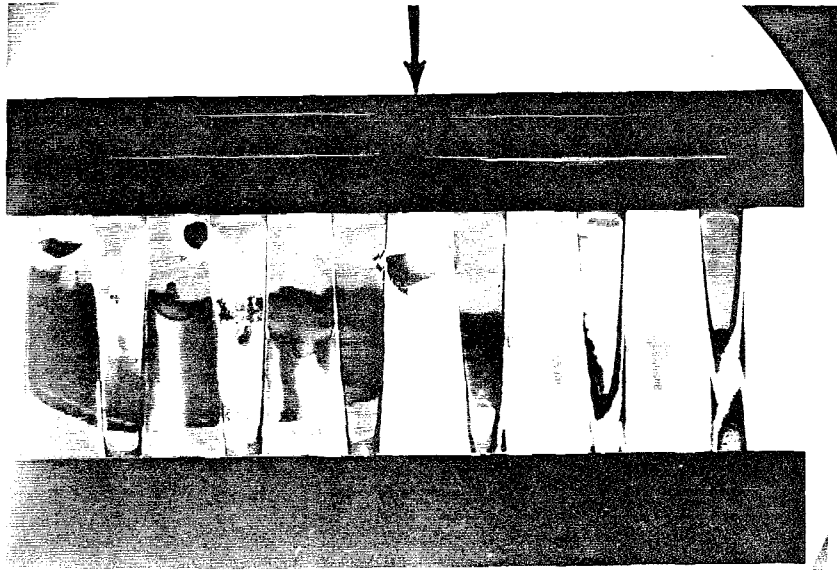


Figure 3.158. 0° Cross-Section 18294-2-4 (2.5 X)

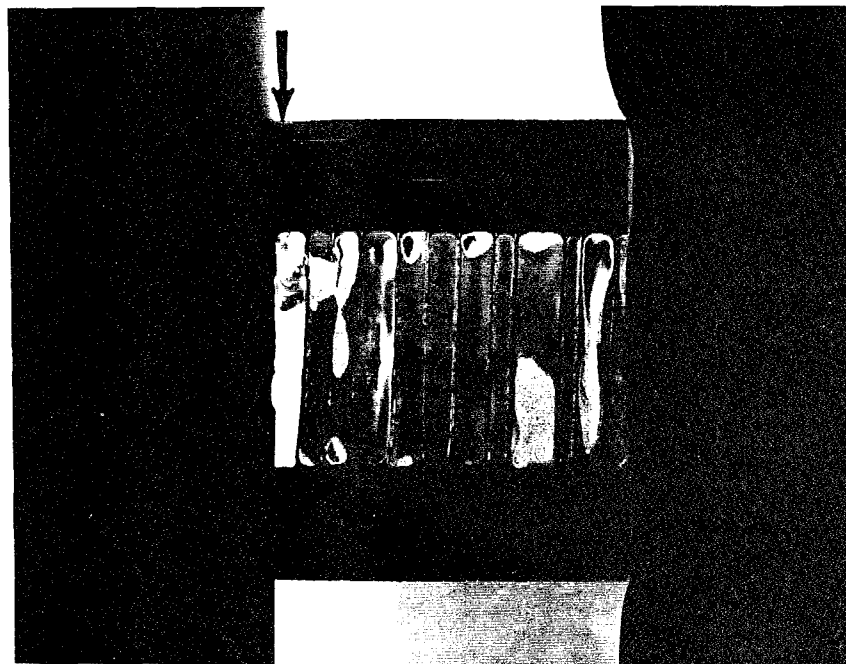


Figure 3.159. 90° Cross-Section 18294-2-4 (2.5 X)

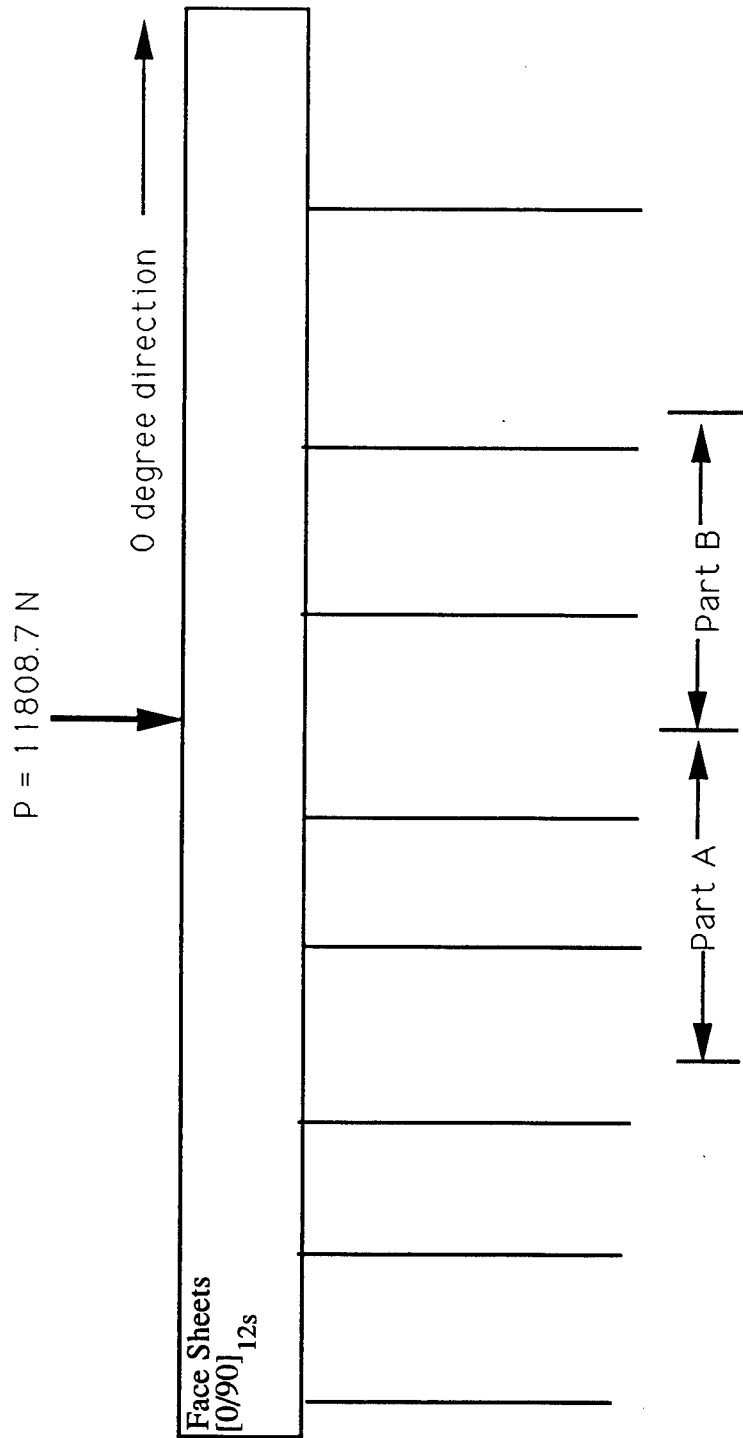


Figure 3.160. Guide to Micrograph of 0 Degree Cross-Section (25X) -18294-2-4

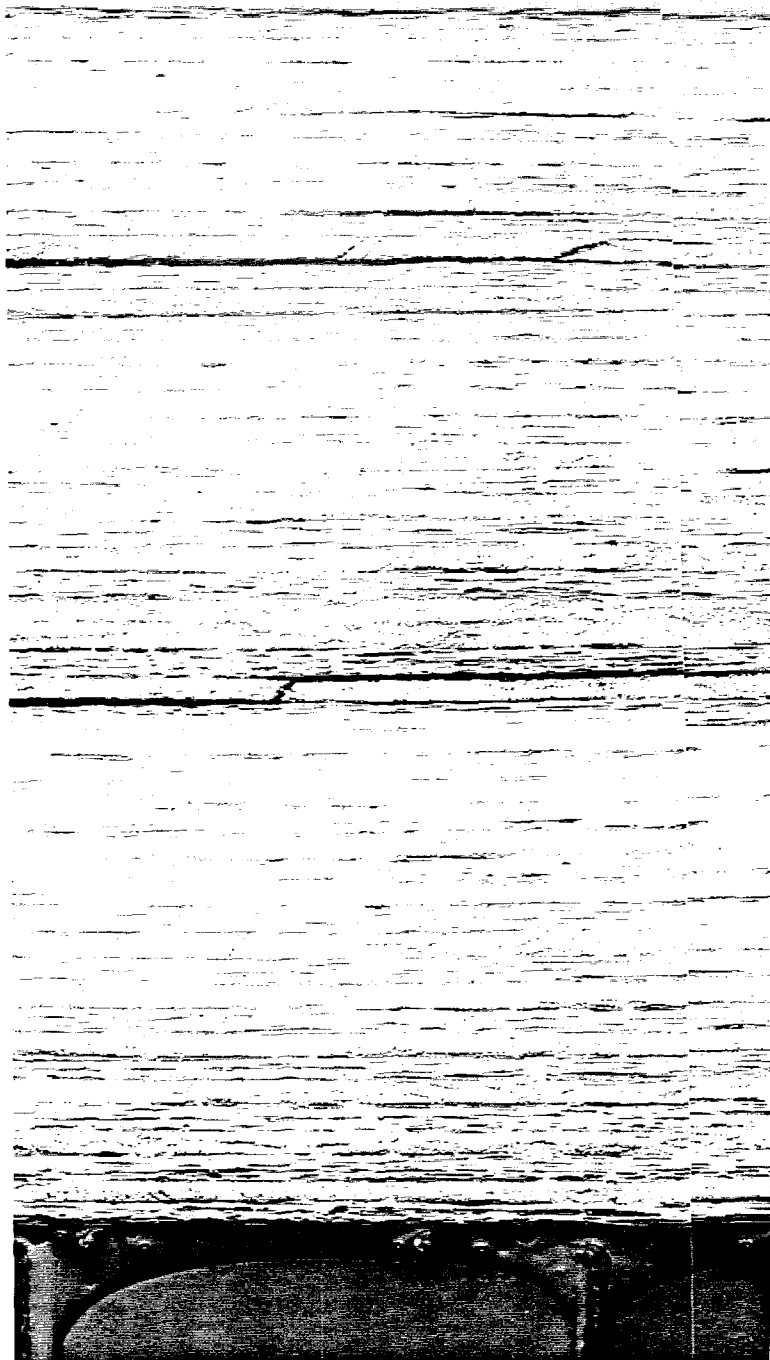


Figure 3.161. 0° Cross-Section 18294-2-4 (25 X) Part A

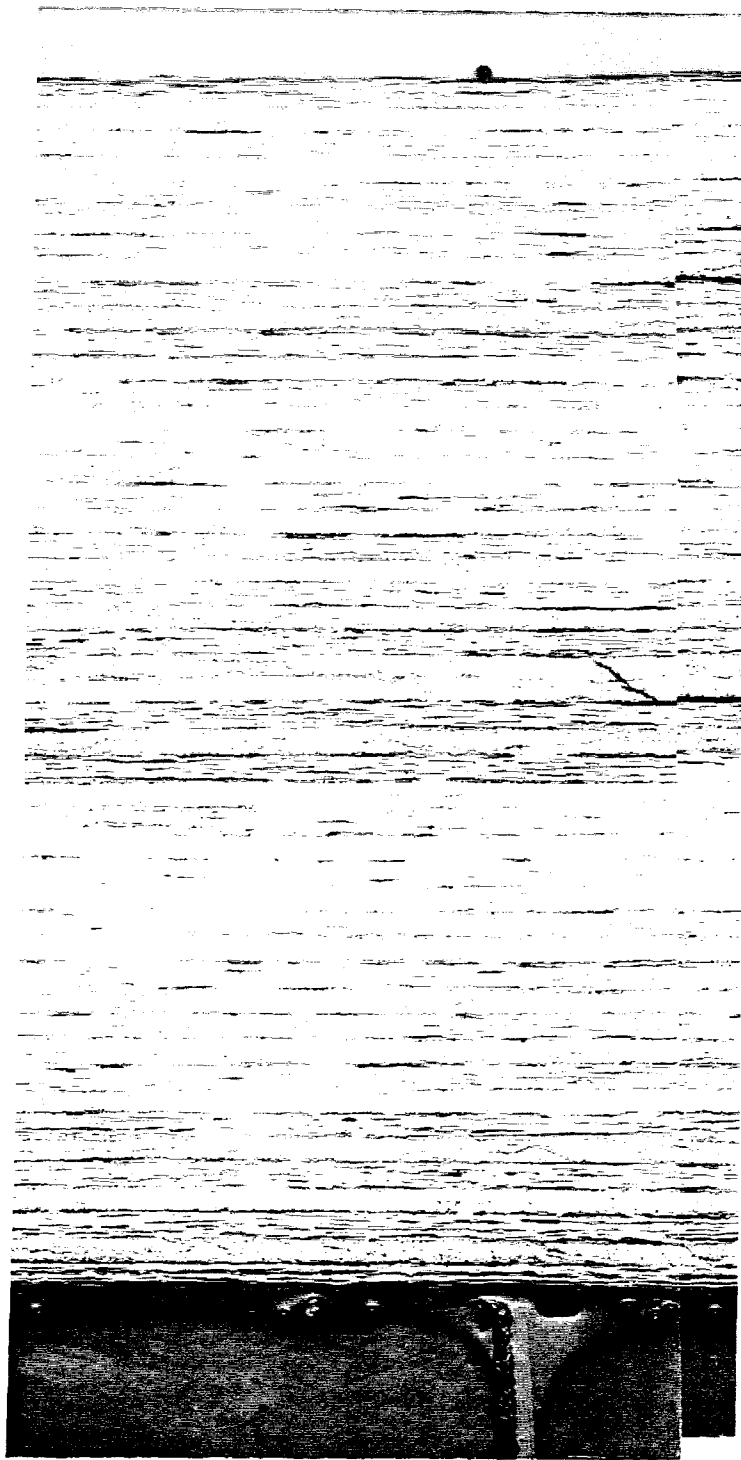


Figure 3.162. 0° Cross-Section 18294-2-4 (25 X) Part B

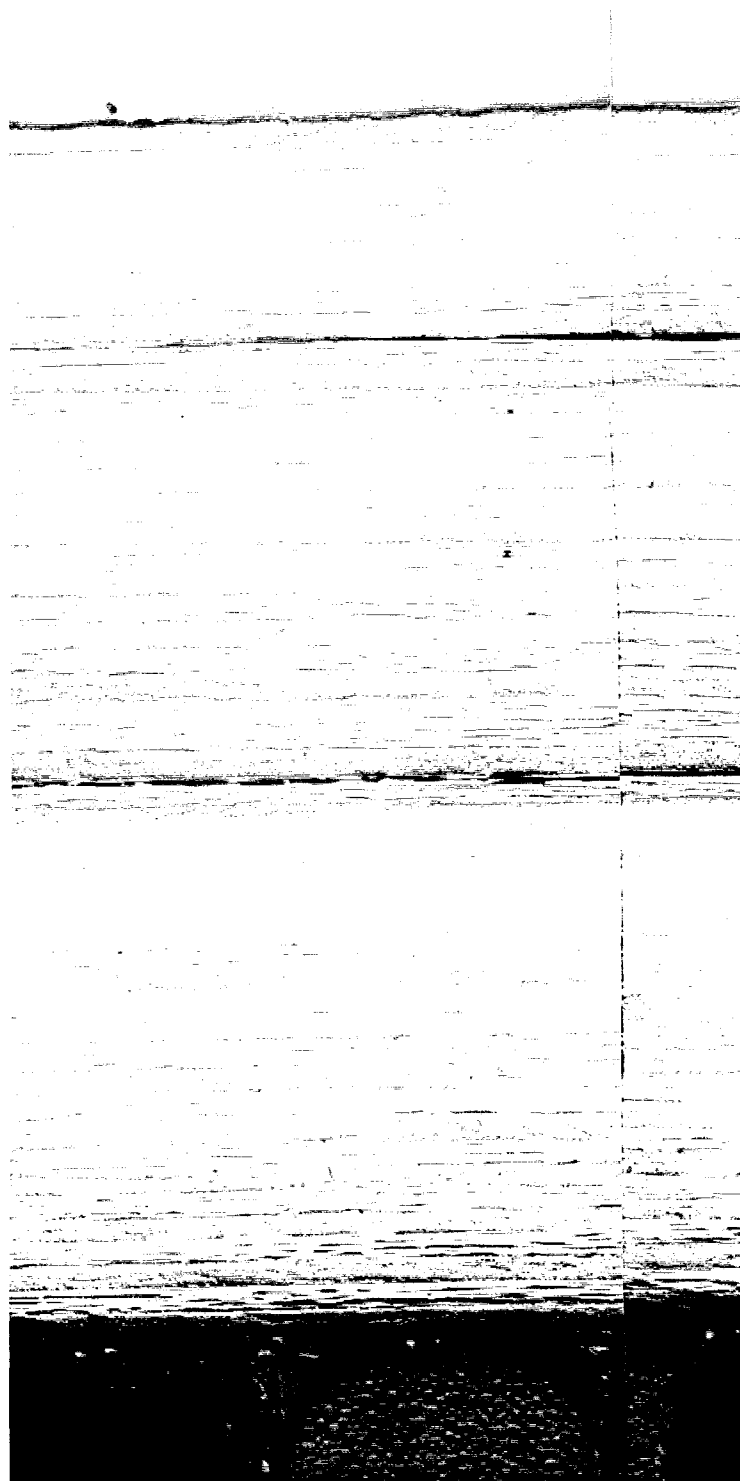


Figure 3.163. 90° Cross-Section 18294-2-4 (25 X)

7.78 Joules
(5.74 ft-lb)



8.84 Joules
(6.52 ft-lb)



9.67 Joules
(7.13 ft-lb)

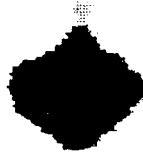


Figure 3.164 Pulse-Echo C-scans for Sandwich Panels with 48-ply Face Sheets

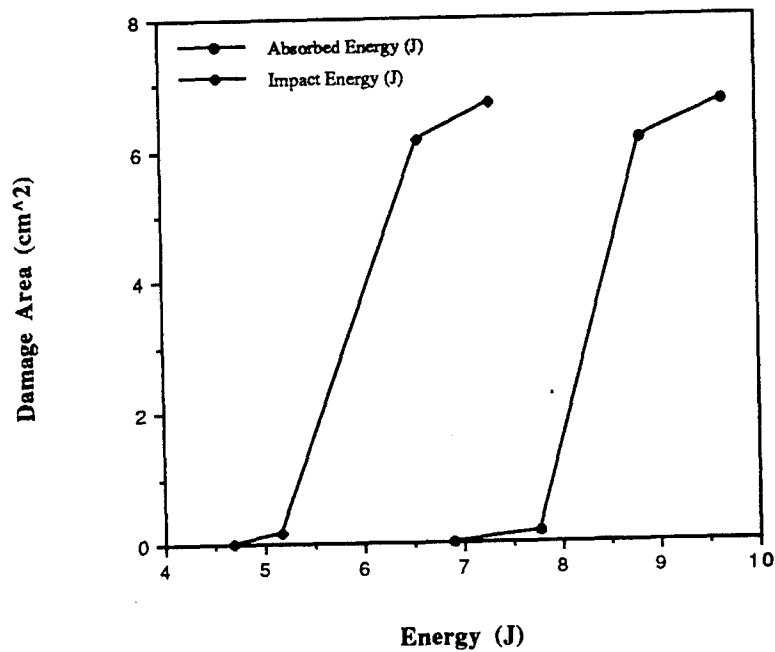


Figure 3.165. Damage Area vs Impact and Absorbed Energies - 48-ply

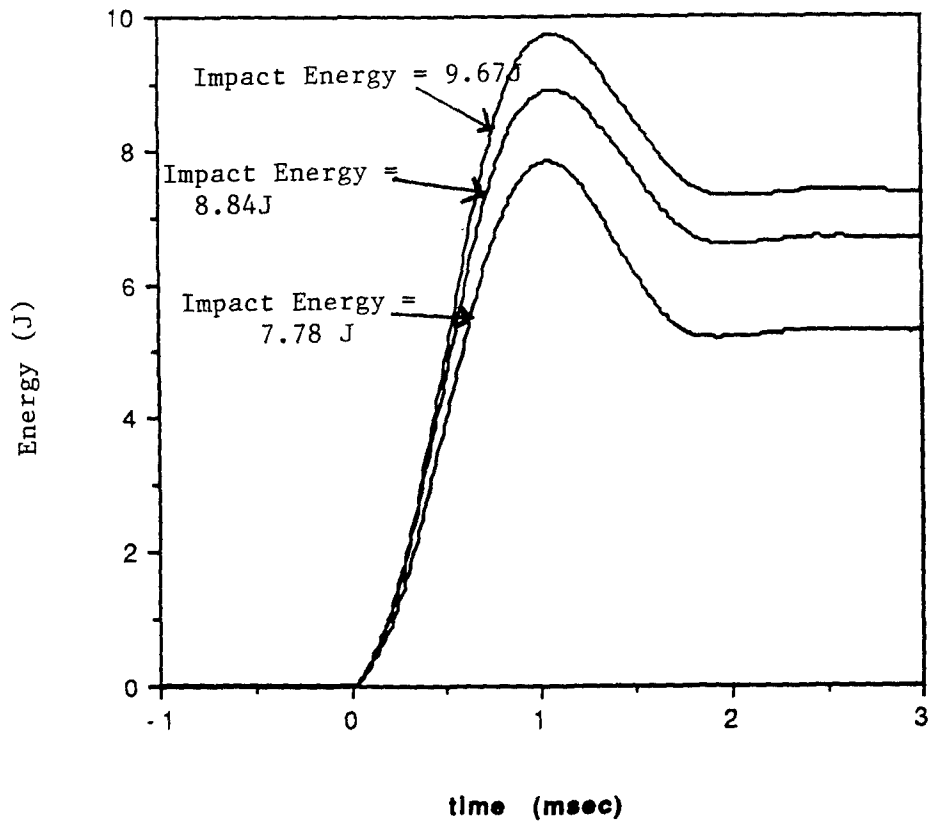


Figure 3.166 Comparison of Energy Curves for Sandwich Panels with 48-ply Face Sheets

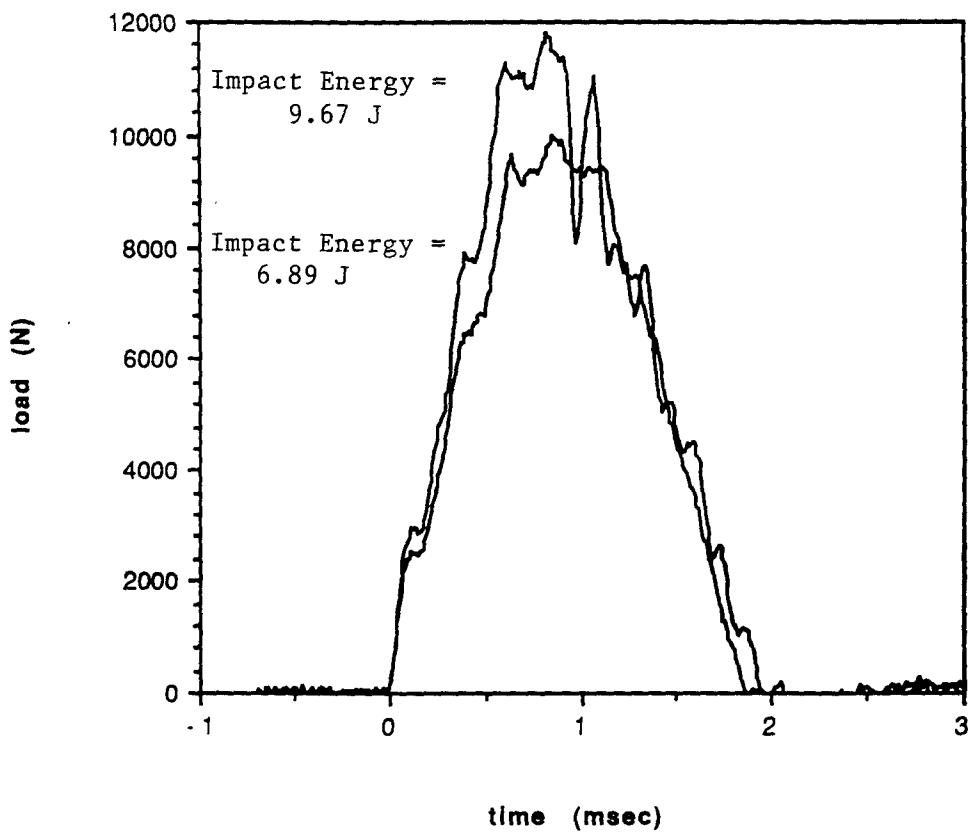


Figure 3.167 Comparison of Load Curves for Sandwich Panels with 48-ply Face Sheets

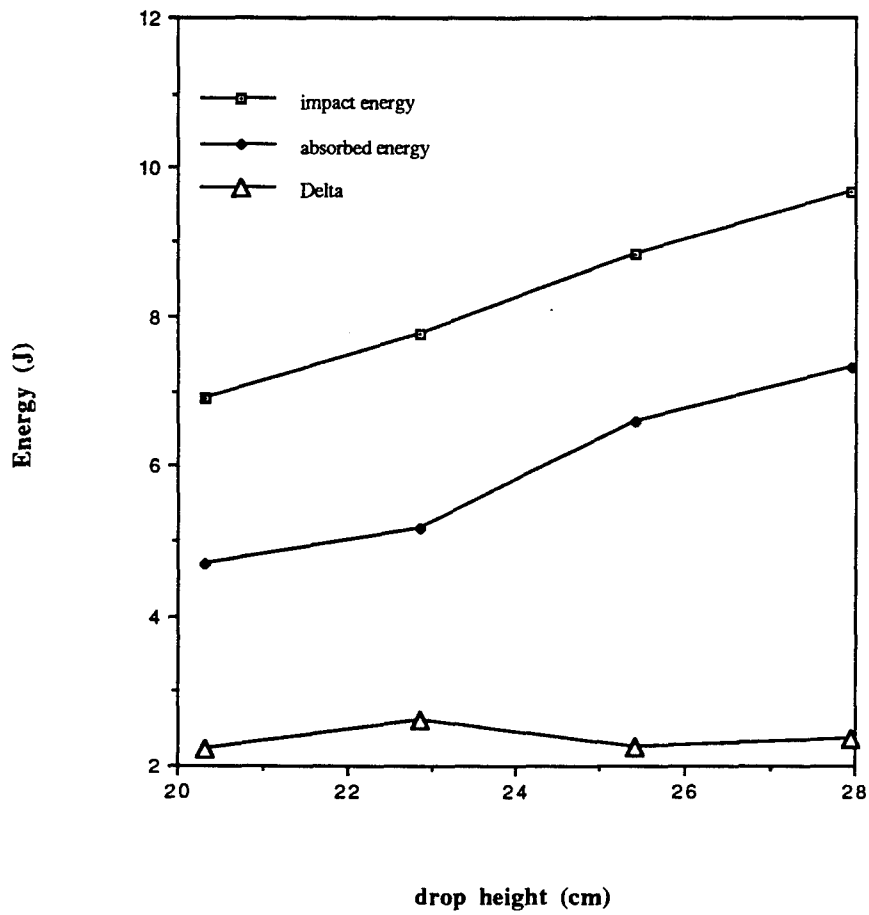


Figure 3.168. Comparison of Absorbed Energy and Impact Energy for Sandwich Panels with 48-ply Face Sheets

3.9 Comparison of Sandwich Panels with Different Face Sheet Thicknesses

The sandwich panels with 4-ply and 8-ply face sheets were each impacted at a drop height of 7.62 cm (3.0 in). Also, the 16-ply and 32-ply were each impacted at drop heights of 12.7 cm (5.0 in), 13.97 cm (5.5 in) and 15.24 cm (6.0 in). This section investigates the effect of doubling the face sheet thickness of sandwich panels impacted at the same drop height based on the load and energy curves, and delamination area. Because the impacts were at nearly equivalent impact energies, the load and energy curves were divided by the number of plies in order to examine the impact on a per ply basis.

Sandwich panels with 4-ply and 8-ply face sheets were impacted at a drop height of 7.62 cm (3.0 in) resulting in impact energy values of 2.62 J (1.93 ft-lb) and 2.60 J (1.92 ft-lb) respectively. The comparison of the load curves are shown in Figures 3.169 and 3.170. The sandwich panel with 4-ply face sheets had more applied load per ply than the sandwich panel with 8-ply face sheets which may imply more damage per ply. As shown in Figure 3.171, the sandwich panel with 8-ply face sheets absorbed 3% more energy at the end of impact than the sandwich panel with 4-ply face sheets; however on a per ply basis (Figure 3.172), the sandwich panel with 4-ply face sheets absorbed 49% more energy than the 8-ply. This implies that the sandwich panel with 4-ply face sheets received more damage. Results from the pulse-echo C-scans show that the damage area due to delamination of the 4-ply sandwich panel was 27% more than the damage area of the 8-ply.

Figures 3.169 - 3.172 show that the time of event for the impact of the sandwich panel with 8-ply face sheets decreased when compared with the sandwich panel with 4-ply face sheets. This occurred throughout testing. In each test series of constant face sheet thickness, the time of event for impact was in the same range. Figure 3.173 and

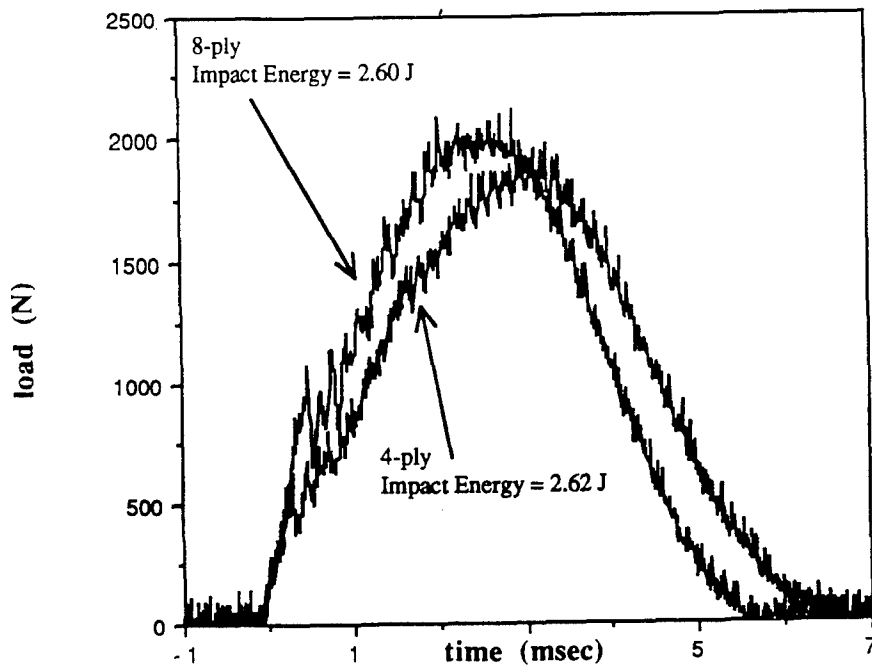


Figure 3.169. Comparison of Load Curves of Sandwich Panels with 4-ply and 8-ply Face Sheets at a drop height of 7.62 cm (3.0 in)

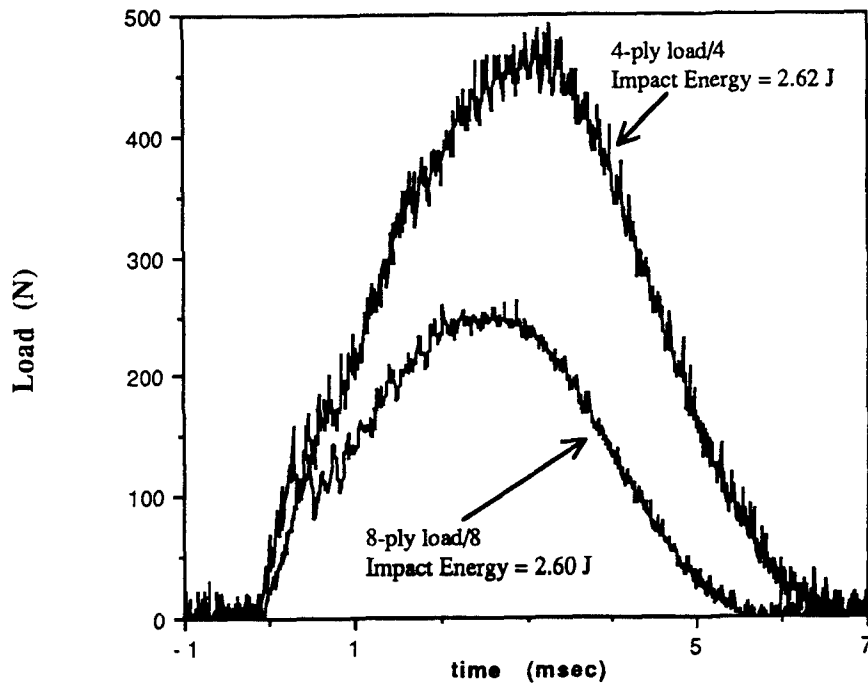


Figure 3.170. Comparison of Load Curves (per ply) of Sandwich Panels with 4-ply and 8-ply Face Sheets at a Drop Height of 7.62 cm

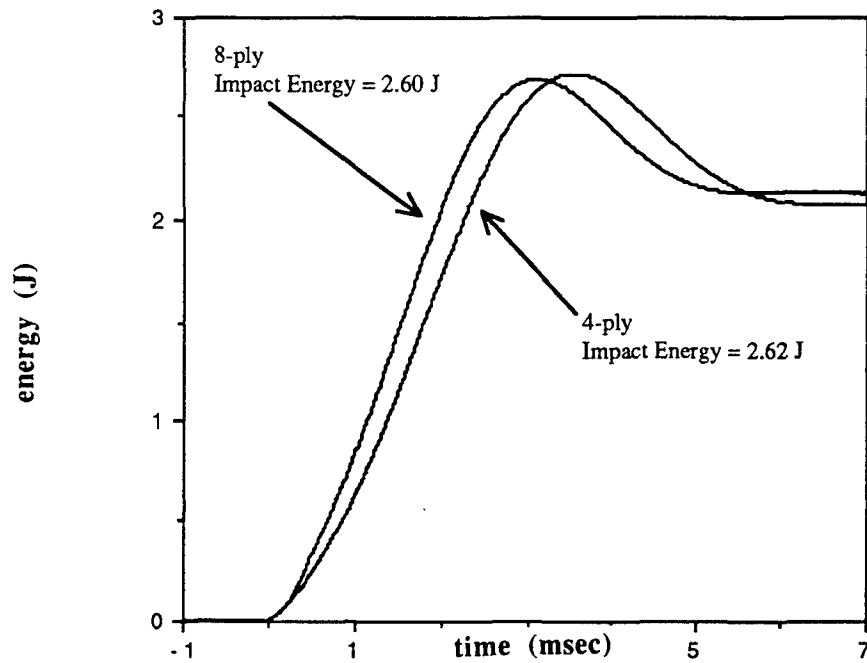


Figure 3.171. Comparison of Energy Curves of Sandwich Panels with 4-ply and 8-ply Face Sheets at a drop height of 7.62 cm (3.0 in)

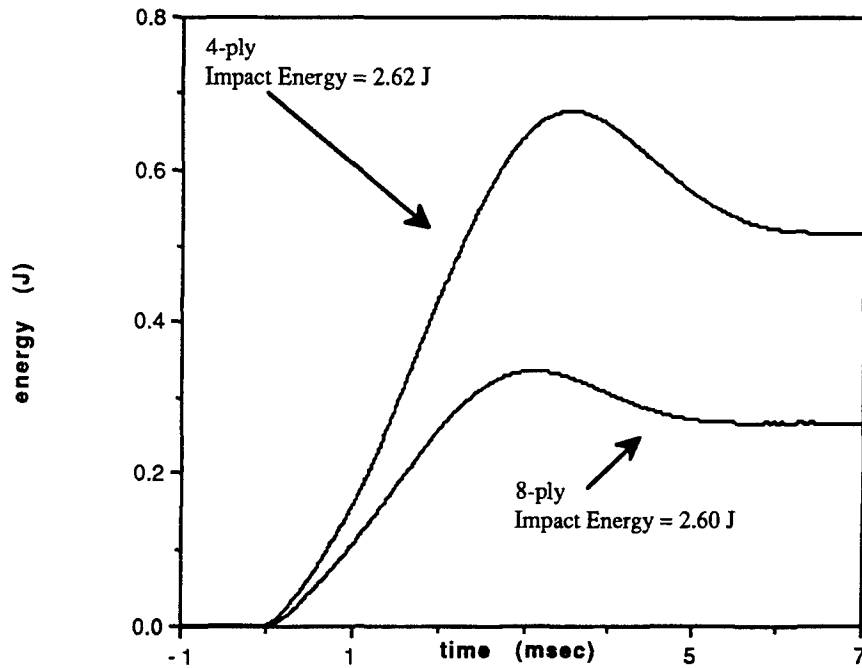


Figure 3.172. Comparison of Energy Curves (per ply) of Sandwich Panels with 4-ply and 8-ply Face Sheets at a Drop Height of 7.62 cm

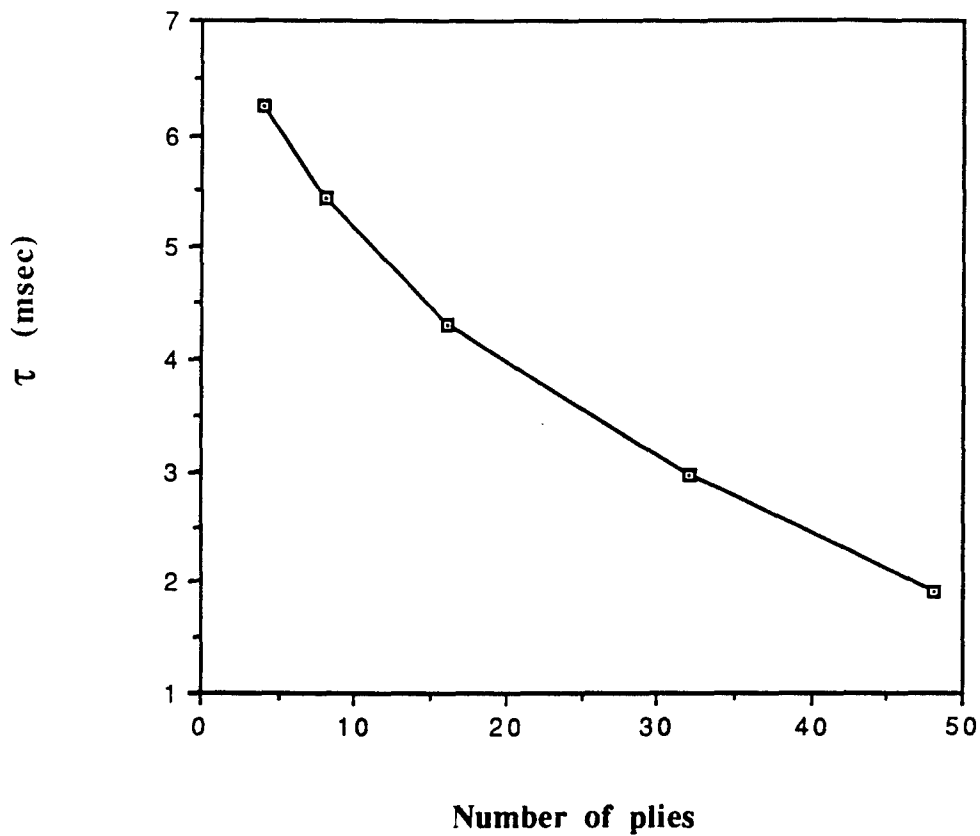


Figure 3.173. Time of Event vs Number of Plies of Face Sheet

3.174 show the time of event decreased as the face sheet thickness increased. This is indicative of quasi-static loading. According to Liu [36] and Finn [37], experiments have demonstrated that similar damage obtained from low-velocity impact could be produced by quasi-static transverse loads. Figure 3.174 also shows that the load-time curves for each ply lay-up changes dramatically in appearance. As the face sheet thickness increases, the dynamic characteristics, before major damage, becomes more obvious. This is apparent in the 48-ply thickness which has three load-time changes before maximum load.

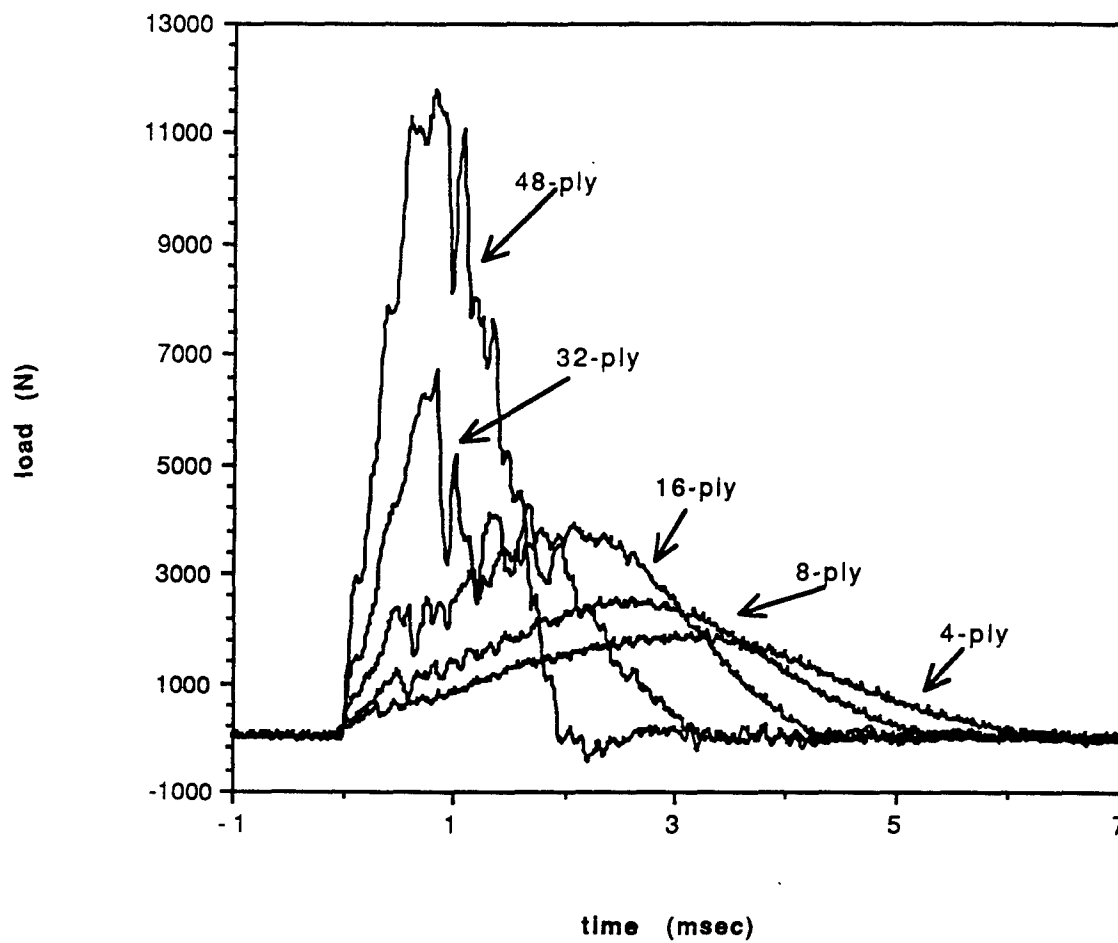


Figure 3.174. Comparison of Load Curves for all Face Sheet Thicknesses

Figures 3.175 - 3.190 compare the load and energy curves for the 16-ply and 32-ply at the same drop height of 12.70 cm (5.0 in), 13.97 cm (5.5 in), 15.24 cm (6.0 in) and 16.51 cm (6.5 in). The impact energies varied by no more than 4% at each drop height. Similar results as those for the comparison of the 4-ply and 8-ply sandwich panels can also be applied here.

Because the 16-ply and 32-ply sandwich panels were dropped at 4 different drop heights, the absorbed energies versus drop heights were plotted (Figure 3.191) as well as the damage areas versus the absorbed energies (Figure 3.192). As the drop height increased, the amount of absorbed energy also increased. For each test of the same drop height, the 32-ply sandwich panel absorbed more energy except for a drop height of 12.70 cm (5.0 in). This was the test of the 32-ply test series that was at an energy level near the threshold value. In Figure 3.192 shows the damage area versus the absorbed energy. Again, the test that was near the threshold value for the 32-ply had a damage area due to delamination below that of the 16-ply.

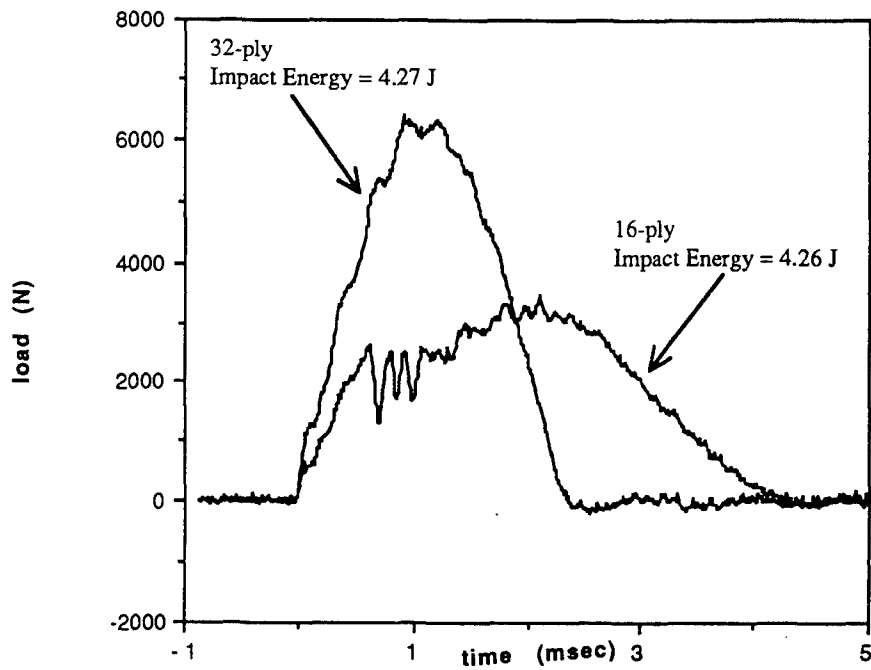


Figure 3.175. Comparison of Load Curves of Sandwich Panels with 16-ply and 32-ply Face Sheets at a drop height of 12.7 cm (5.0 in)

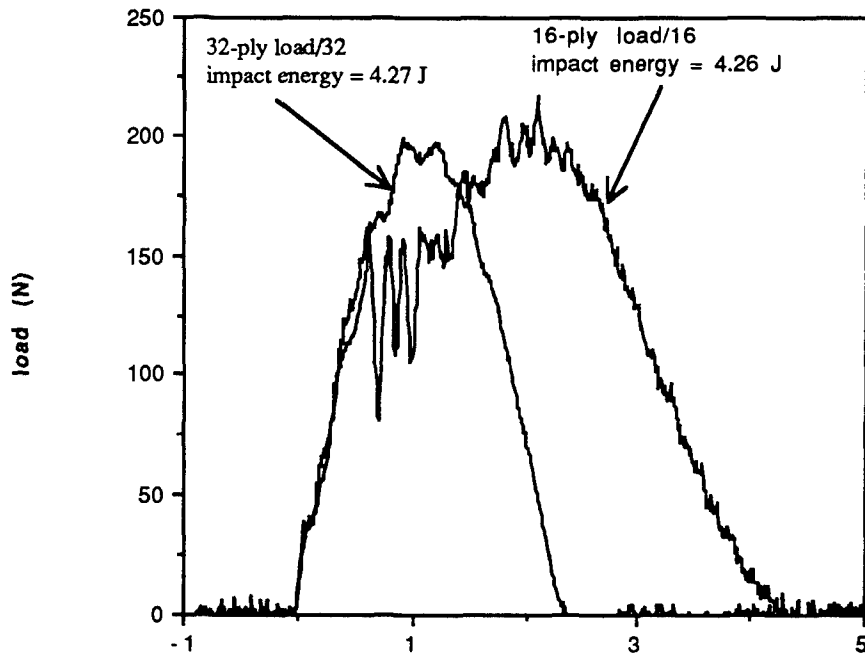


Figure 3.176. Comparison of Load Curves (per ply) of Sandwich Panels with 16-ply and 32-ply Face Sheets at a Drop Height of 12.7 cm (5.0 in)

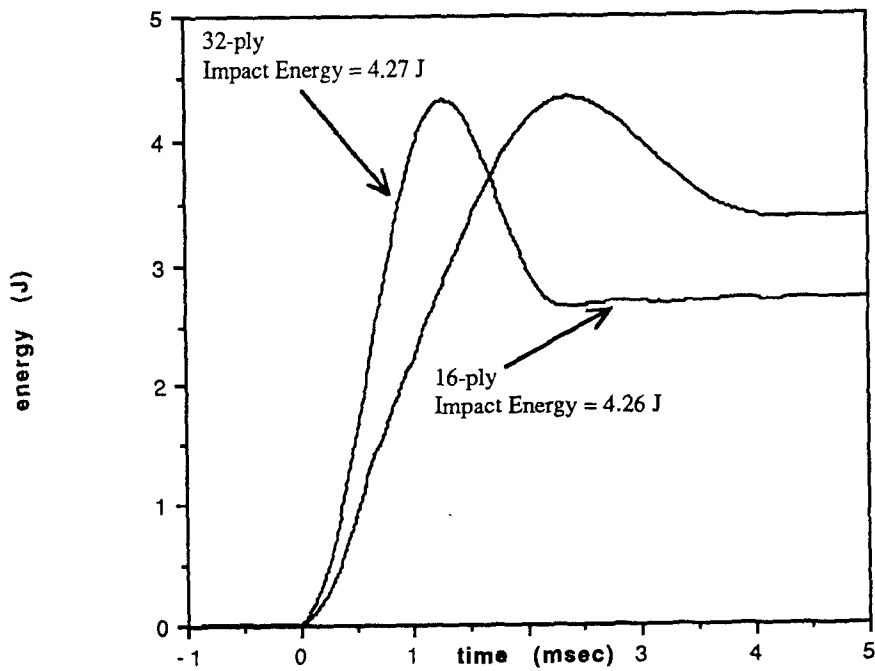


Figure 3.177. Comparison of Energy Curves of Sandwich Panels with 16-ply and 32-ply Face Sheets at a Drop Height of 12.7 cm (5.0 in)

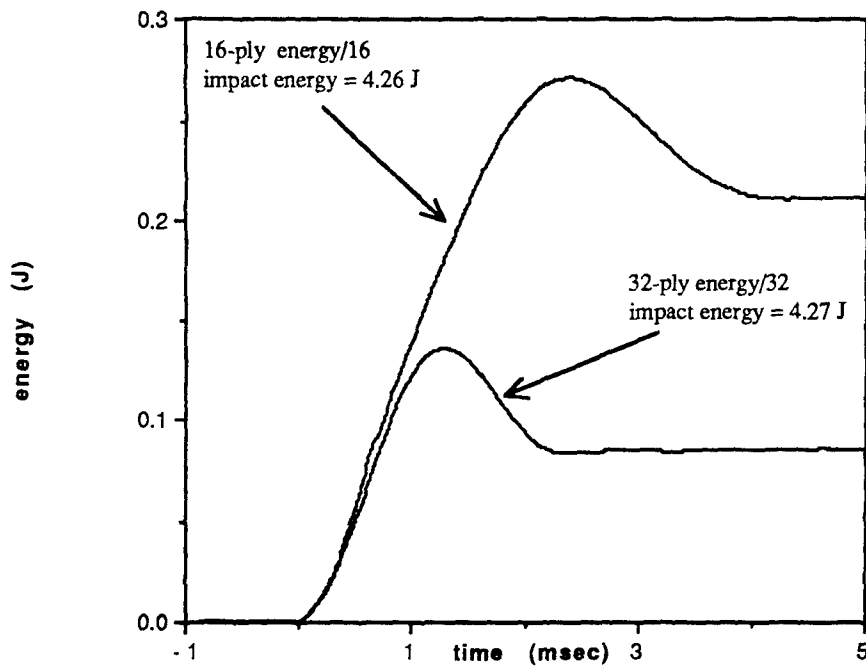


Figure 3.178. Comparison of Energy Curves (per ply) of Sandwich Panels with 16-ply and 32-ply Face Sheets at a Drop Height of 12.7 cm (5.0 in)

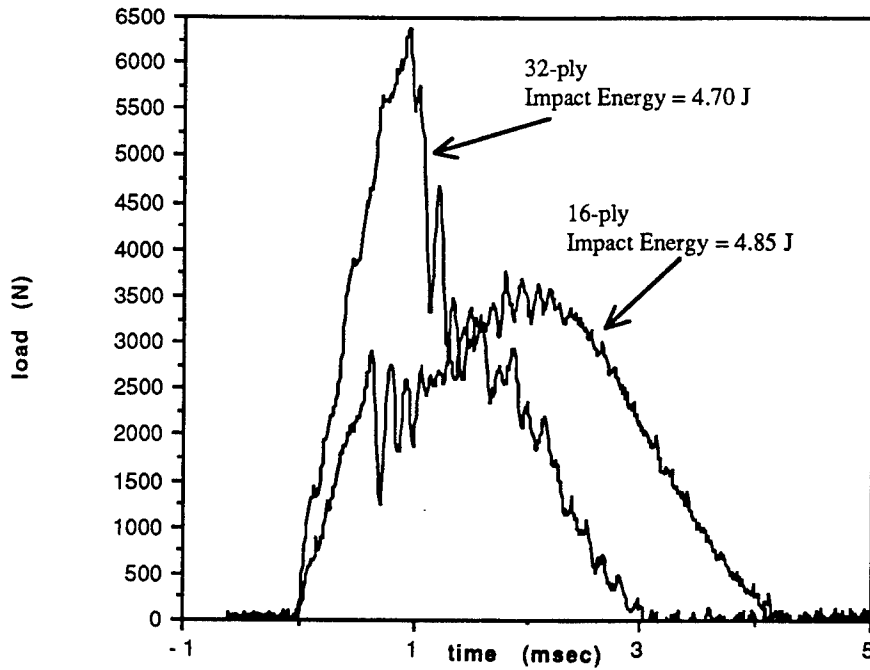


Figure 3.179. Comparison of Load Curves of Sandwich Panels with 16-ply and 32-ply Face Sheets at a drop height of 13.97 cm (5.5 in)

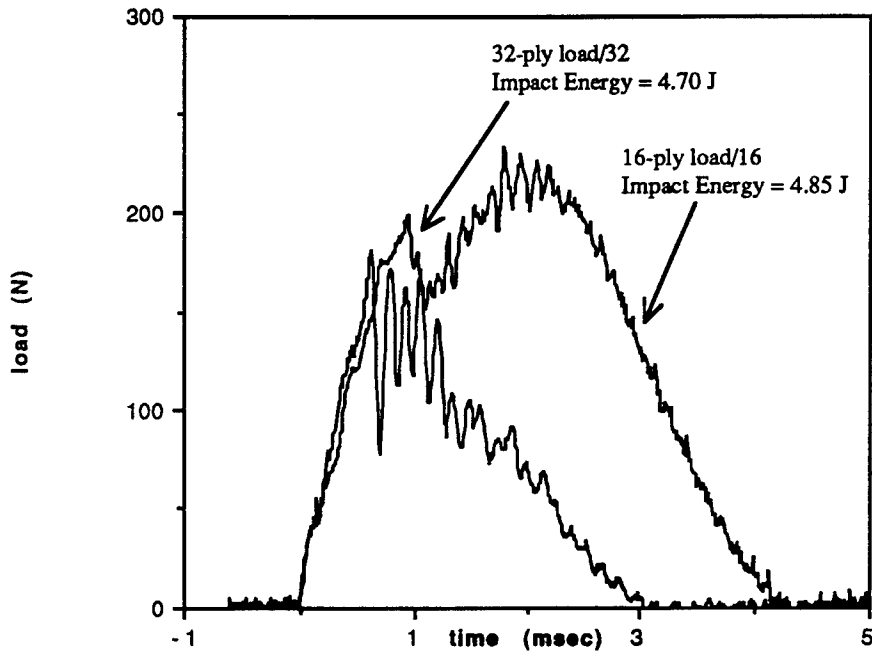


Figure 3.180. Comparison of Load Curves (per ply) of Sandwich Panels with 16-ply and 32-ply Face Sheets at a Drop Height of 13.97 cm (5.5 in)

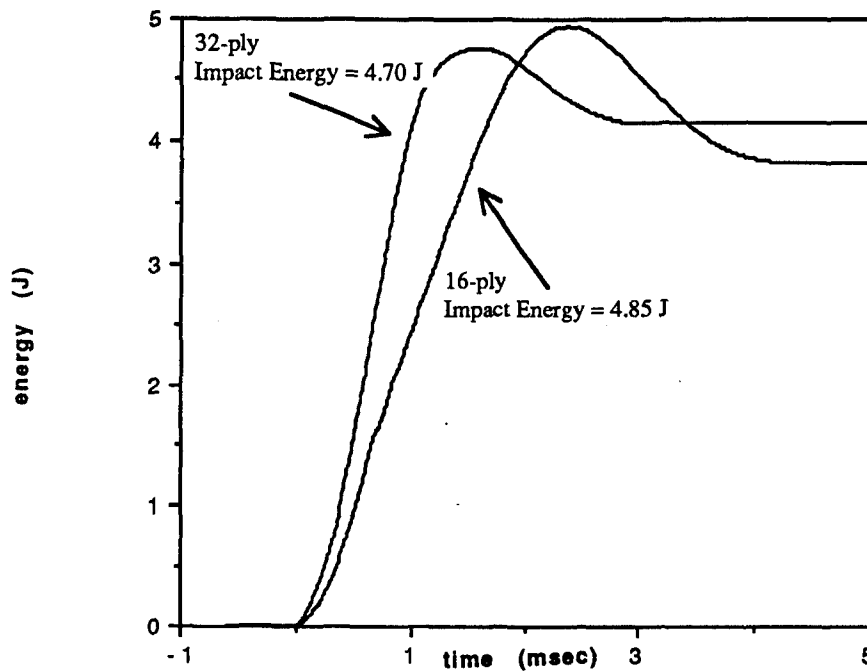


Figure 3.181. Comparison of Energy Curves of Sandwich Panels with 16-ply and 32-ply Face Sheets at a Drop Height of 13.97 cm (5.5 in)

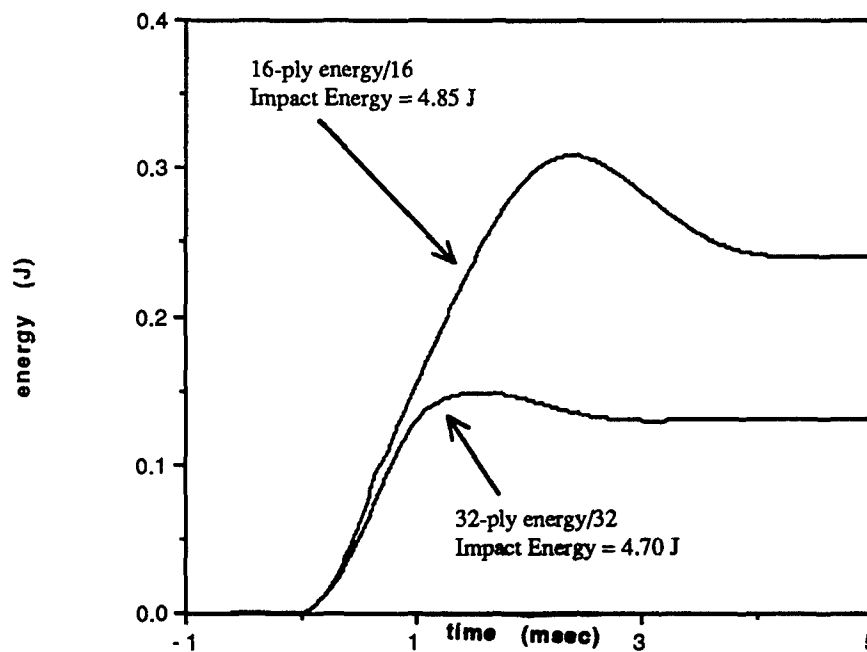


Figure 3.182. Comparison of Energy Curves (per ply) of Sandwich Panels with 16-ply and 32-ply Face Sheets at a Drop Height of 13.97 cm (5.5 in)

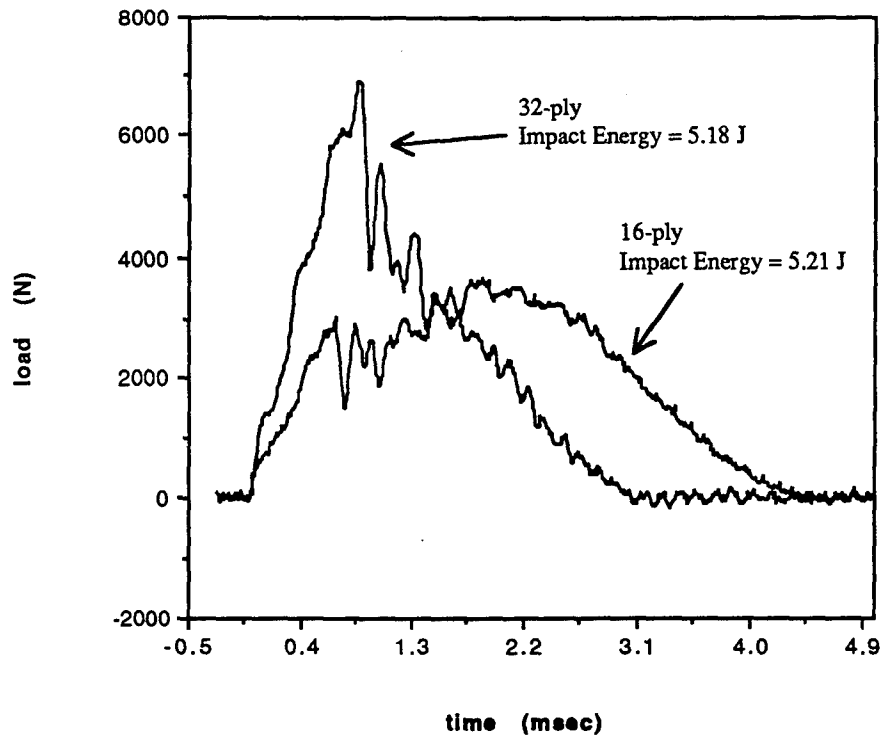


Figure 3.183. Comparison of Load Curves of Sandwich Panels with 16-ply and 32-ply Face Sheets at a drop height of 15.24 cm (6.0 in)

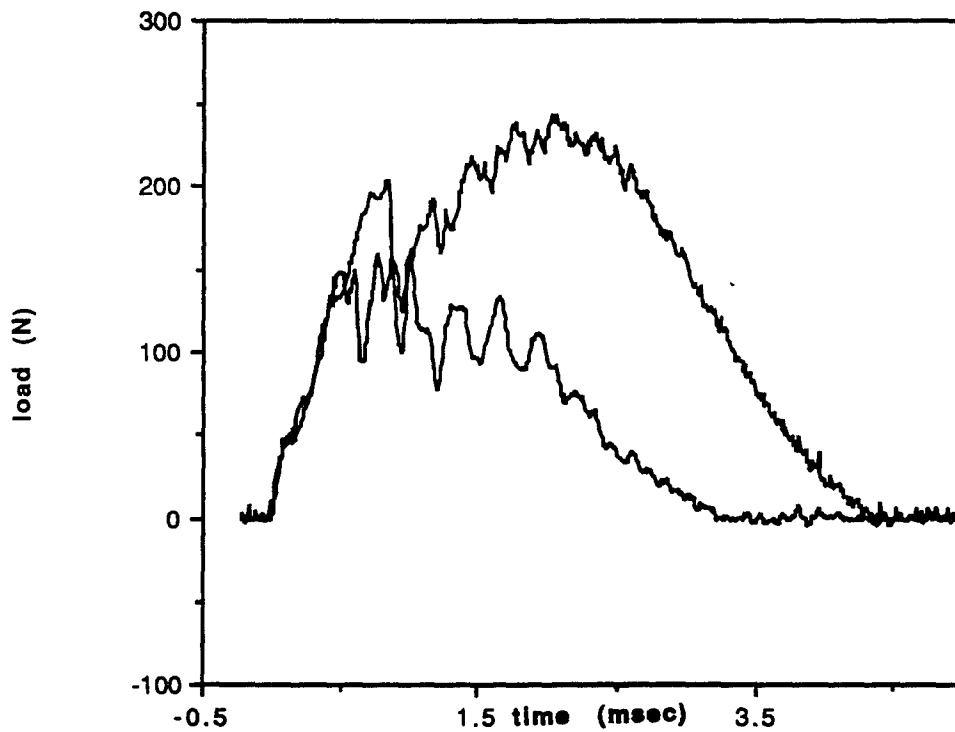


Figure 3.184. Comparison of Load Curves (per ply) of Sandwich Panels with 16-ply and 32-ply Face Sheets at a Drop Height of 15.24 cm (6.0 in)

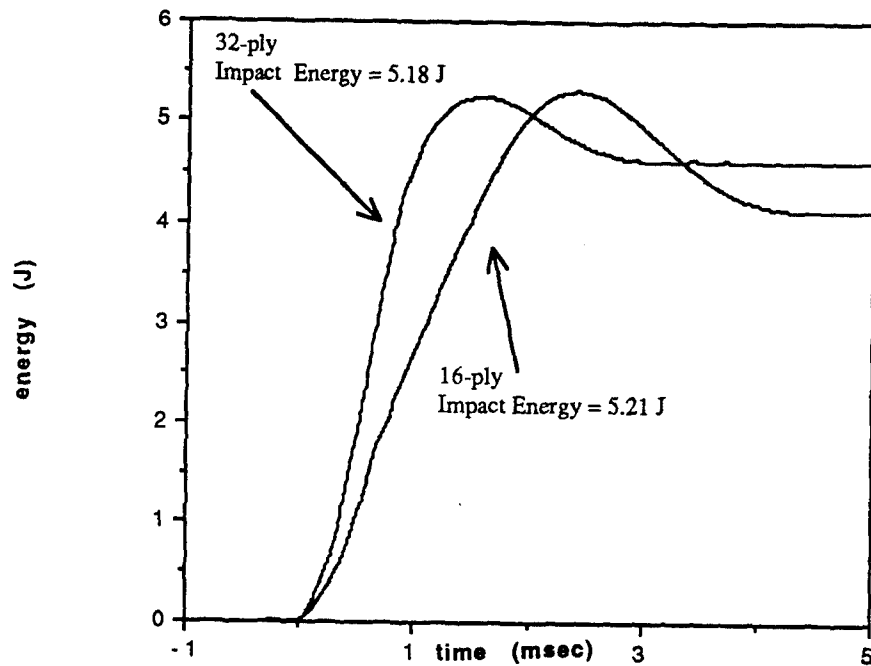


Figure 3.185. Comparison of Energy Curves of Sandwich Panels with 16-ply and 32-ply Face Sheets at a Drop Height of 15.24 cm (6.0 in)

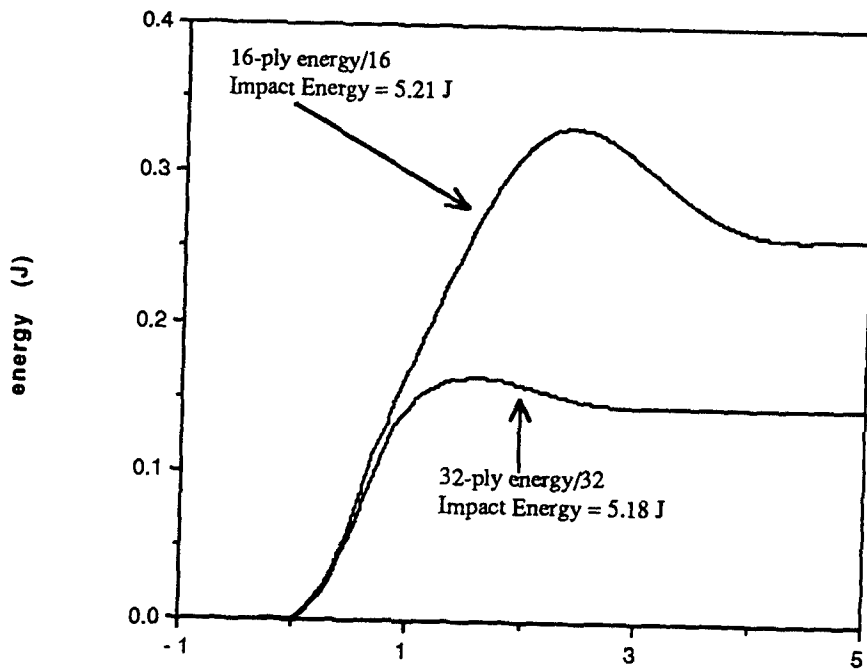


Figure 3.186. Comparison of Energy Curves (per ply) of Sandwich Panels with 16-ply and 32-ply Face Sheets at a Drop Height of 15.24 cm (6.0 in)

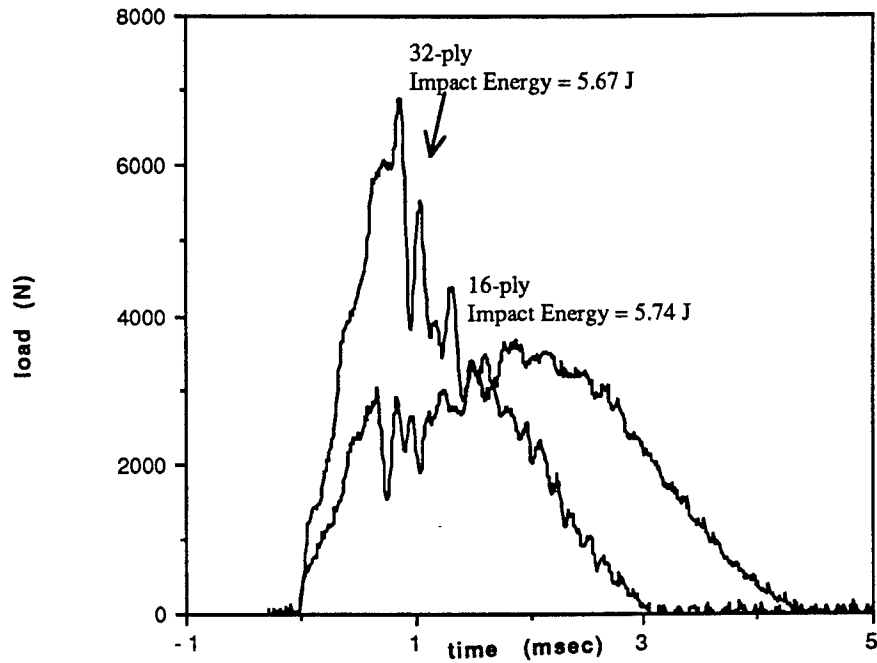


Figure 3.187. Comparison of Load Curves of Sandwich Panels with 16-ply and 32-ply Face Sheets at a drop height of 16.51 cm (6.5 in)

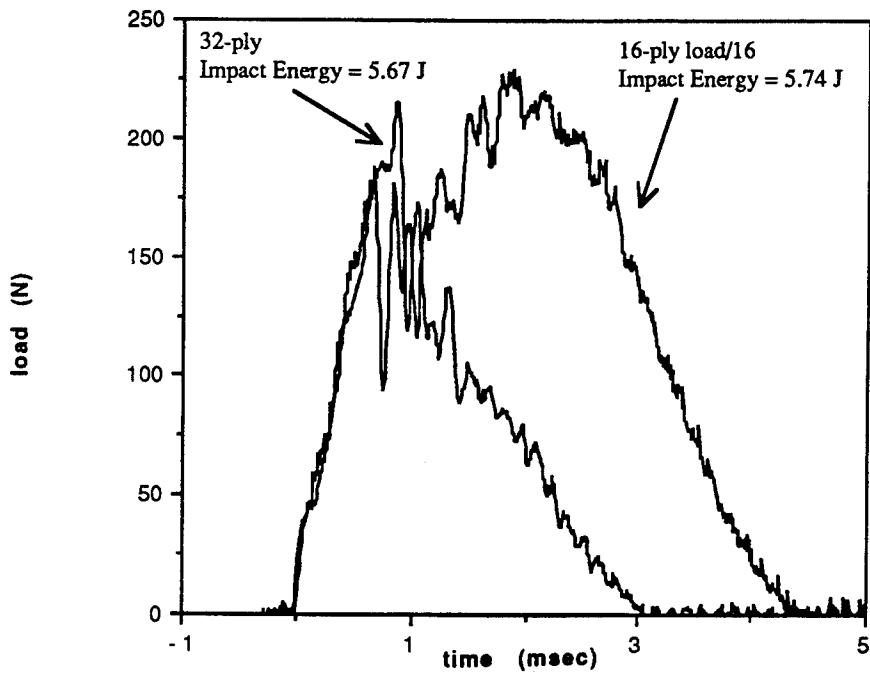


Figure 3.188. Comparison of Load Curves (per ply) of Sandwich Panels with 16-ply and 32-ply Face Sheets at a Drop Height of 16.51 cm (6.5 in)

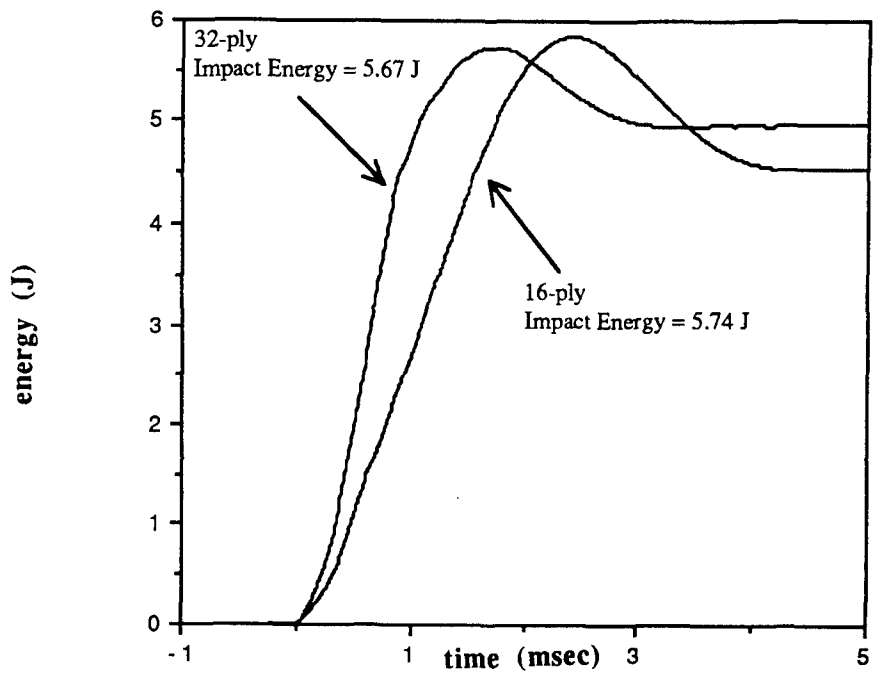


Figure 3.189. Comparison of Energy Curves of Sandwich Panels with 16-ply and 32-ply Face Sheets at a Drop Height of 16.51 cm (6.5 in)

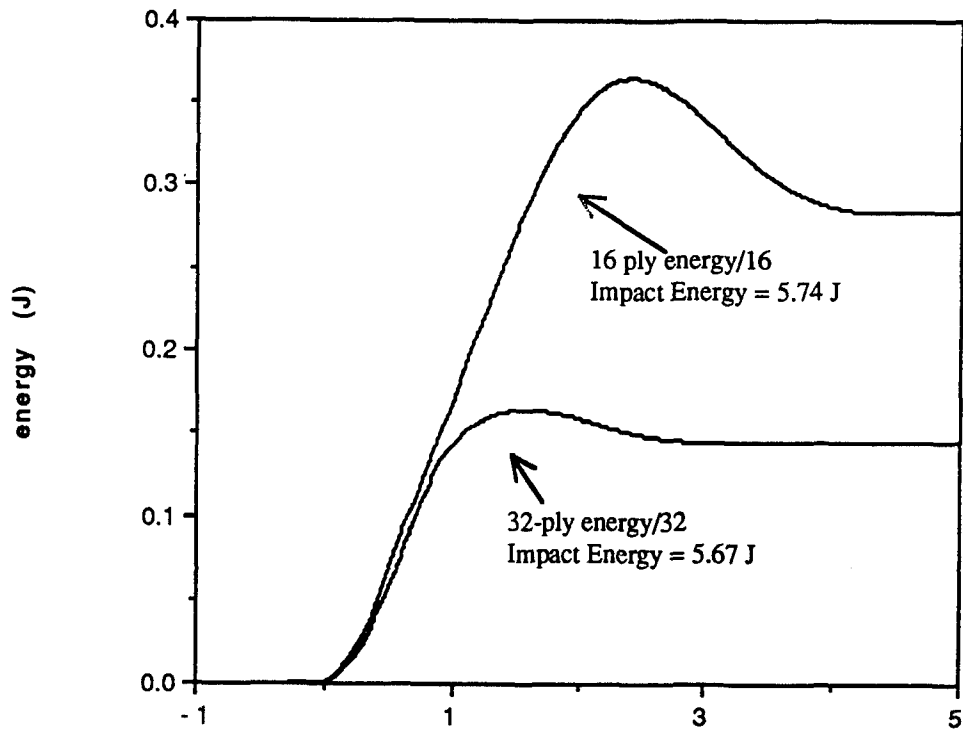


Figure 3.190. Comparison of Energy Curves (per ply) of Sandwich Panels with 16-ply and 32-ply Face Sheets at a Drop Height of 16.51 cm (6.5 in)

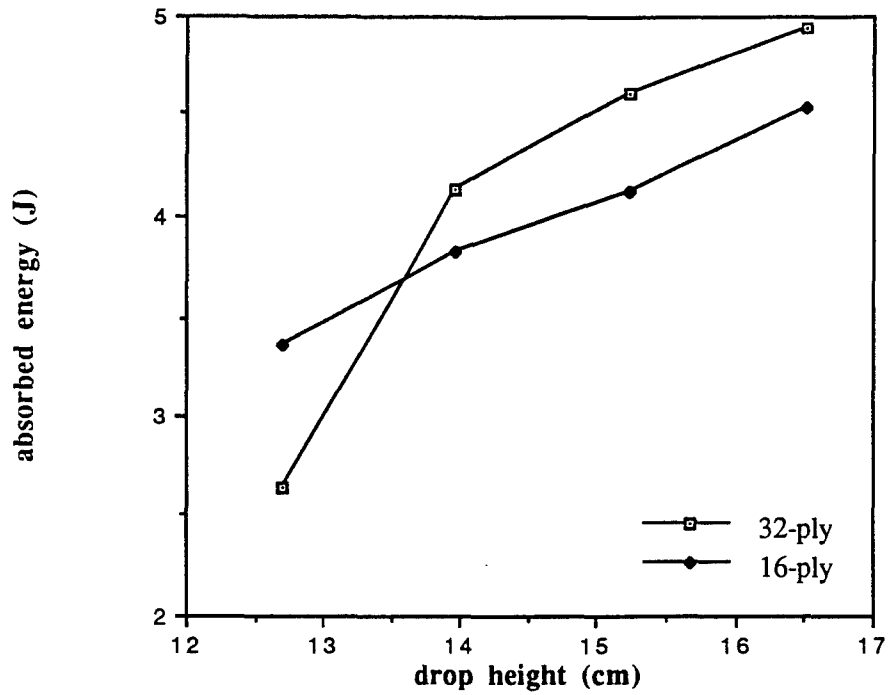


Figure 3.191. Comparison of Absorbed Energy vs Drop Height of Sandwich Panels with 16-ply and 32-ply Face Sheets

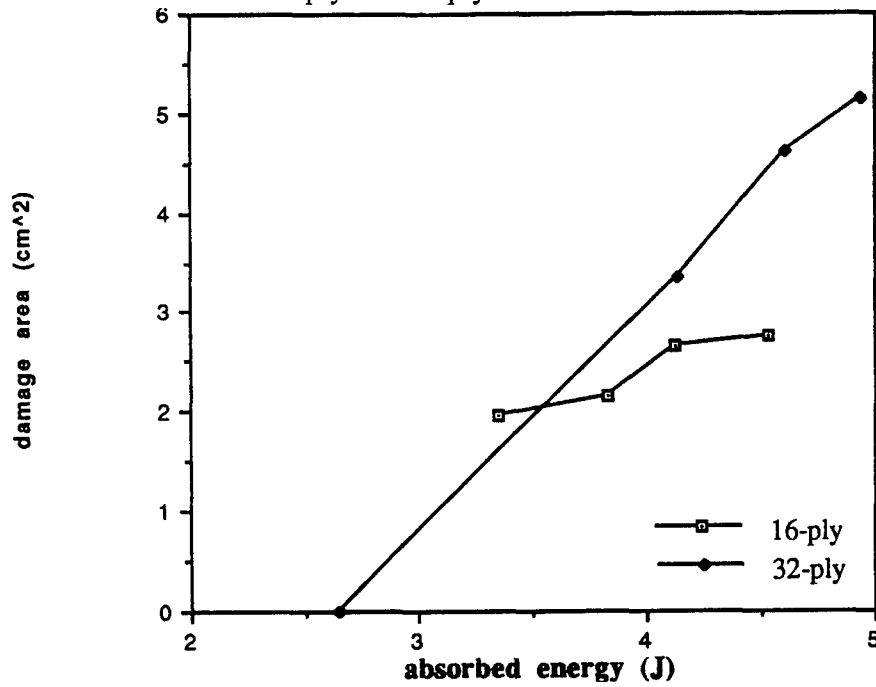


Figure 3.192 Comparison of Damage Area vs Absorbed Energy for Sandwich Panels with 16-ply and 32-ply Face Sheets

3.10 Summary

A total of 23 flat sandwich specimens with various face sheet thicknesses were subjected to low velocity impact with impact velocities and impact energies ranging from 0.84 m/s (2.76 ft/s) to 2.31 m/s (7.58 ft/s) and 1.27 J (0.94 ft-lb) to 9.67 J (7.13 ft-lb), respectively. A test summary is shown in Table 3.3.

TABLE 3-3. Summary of Test Data

Number of Plies	Time of Event (msec)	Maximum Impact Velocity (m/s)	Maximum Impact Energy (J)	Absorbed Energy at Max Impact Energy	Delamination Area at Max Impact Energy (cm ²)
4	6.26	1.20	2.62	2.076	2.2259
8	5.43	1.36	3.35	2.530	2.1403
16	4.31	1.78	5.74	4.530	2.7396
32	2.96	1.77	5.67	4.942	5.1368
48	1.93	2.31	9.67	7.311	6.6778

Conclusions

Based on the results from the low velocity impact test performed in this thesis for sandwich panels with AS4/3501-6 graphite/epoxy face sheet arranged in the following stacking sequences: $[0/90]_s$, $[0/90]_{2s}$, $[0/90]_{4s}$, $[0/90]_{8s}$ and $[0/90]_{12s}$, and 1.27 cm (0.5 in) thick, 145 kg/m^3 (9 lb/ft³), 3.175 mm (1/8") cell size Nomex honeycomb core, and FM 300-2 film adhesive the following conclusions are drawn:

1. Damage size due to delamination and failure mechanisms are dependent upon the location of the impact site with respect to core walls.
2. The core failure is dependent upon the face sheet thickness. The sandwich panels with thick face sheets received little or no damage to the core where as the thinner panels received significant amounts of core damage.
3. Delamination in the face sheets were only between plies of different orientations.
4. The higher interface delamination grew towards the impact site whereas the lower interface delamination grew away from the impact site.
5. Damage size increased as the impact energy increased.
6. The adhesive helped support the core walls.
7. The more flexible (thinner) the specimen, the greater the time of event.
8. Matrix cracking is a by-product of core failure.
9. The propagation of delamination is dependent upon face sheet thickness.
10. As the impact energy increases so does the amount of absorbed damage.
11. Characteristics of growth delamination are predicated upon fracture.

Appendix A - Test Plan

This appendix contains a copy of the Test Plan submitted to the Wright Laboratory. Such a plan is required by the lab for any specimen construction and testing. The plan details the specifications to construct the sandwich panels and the specimens required for basic property testing, as well as the placement of strain gages. Information on impacting the panels and post-impact analysis is also included.

TEST PLAN

An Investigation of Sandwich Flat Panels Under Low Velocity Impact

1. PROGRAM INFORMATION:

a. Organization	WL/FIBEA
b. Project Number	2401TI00
c. Security Classification	Unclassified
d. Project Engineer	Capt Timberlyn Harrington
e. Project Advisor	Dr. Anthony Palazotto
f. Project Sponsor	Dr. Gregory Schoeppner
g. Test Engineer	Larry Bates
h. Fabrication Engineer	Charles Ramsey
i. Test Location	WL/Structures Test Facility Bldg. 65, Area B

2. PROGRAM OBJECTIVES:

The objective of this effort is to evaluate the changing failure modes and mechanisms associated with increasing face sheet thickness of flat honeycomb sandwich plates under

low velocity impact.

3. TECHNICAL DESCRIPTION:

3.1 MATERIAL:

The specimens required for this program will be fabricated using the following material systems:

- a. Nomex HRH-10-1/8-9.0 honeycomb core, 1.27 cm (0.5 in) thick
145 kg/m (9 lbs/ft³) density, 3.175 mm (1/8") cell size.
- b. AS4/3501-6 Graphite/Epoxy
- c. Face sheet core adhesive FM 300-2 film adhesive,
0.254 mm (0.010 in) thick

3.2 STACKING SEQUENCE:

The following face sheet stacking sequences will be used for this program. These stacking sequences are as follows:

- [0/90]_S 4 plies
- [0/90]_{2S} 8 plies
- [0/90]_{4S} 16 plies
- [0/90]_{8S} 32 plies

[0/90]12S 48 plies

3.3 C-SCAN:

All face sheets will be subjected to thorough ultrasonic C-scan to detect flaws before fabrication. The final acceptance or rejection of panels will be made by the project engineer based upon the recommendations of the NDI engineer.

3.4 SPECIMENS:

One sandwich panel will be fabricated from the material systems shown in para 3.1 for EACH stacking sequence, see Fig. A.1. The panels will be cut into six 17.8 cm x 17.8 cm (7 in x7 in) sandwich specimens, see Fig. A.2, for a total of 30 impact specimens.

3.5 THICKNESS TOLERANCES:

The thickness of the face sheets will be measured at the locations shown in Fig. A.3. The face sheets will be uniform in thickness and the variations will not be in excess of 0.01524 mm (0.0006 in) per ply. Any specimen which does not comply with a thickness tolerance of 0.254 mm (0.01 in) will be rejected.

3.6 DATA AND REPORT:

Data acquired from this study will be compared and contrasted to an analytical study. The final results and discussion will be incorporated into a graduate thesis submitted by the project engineer to the Air Force Institute of Technology as a partial fulfillment of her Master of Aeronautical Degree requirements.

4.0 APPROACH:

4.1 BASIC PROPERTIES:

To determine the basic property data for the AS4/3501-6 material, 0° tension (0T), 0° compression (0C), 90° tension (90T), 90° compression (90C), and \pm 45° shear (SH) specimens will be fabricated, instrumented with CEA-03-062UR-350 strain gages, tested under static loading at a rate of 1.27 mm (0.05) inches per minute. The strain gages will be centered in the gage area. Two panels, A & B, will be fabricated for the testing of basic properties and will used as follows:

NAME	PANEL	DESCRIPTION
0T	A	1.27 cm (0.5 inch) wide tension specimens with standard tapered tabs (Fig. A.4, A.6 &A.8)
90T	A	2.54 cm (1.0 inch) wide tension specimens with standard tapered tabs (Fig. A.4, A.6 & A.8)
0C	A	1.91 cm (0.75) inch wide compression specimen with square ended tabs (Fig. A.4, A.6 &A.9)
90C	A	1.91 cm (0.75 inch) wide compression specimens with square ended tabs (Fig. A.4, A.6 &A.9)
SH	B	2.54 (1.0 inch) wide tension specimens with standard tapered tabs (Fig. A.5, A.7 & A.8)

The basic properties of the Nomex honeycomb will be obtained from the manufacturers specifications.

4.2 FABRICATION:

One sandwich panel will be fabricated for EACH stacking sequence. The sandwich panels will consist of 1.27 cm (0.5 in) thick 145 kg/m (9 lbs/ft³) density, 3.175 mm (0.125 in) cell size Nomex honeycomb core and AS4/3501-6 graphite/epoxy upper and lower face sheets.

The face sheets will be cured using the manufacturer's recommended cure cycle.

After cure, the core will be bonded to the face sheets with FM 300-2 film adhesive (0.254 mm, 0.010 in thick). The panels will then be cut using a water jet into 17.8 cm x 17.8 cm (7.0 in x 7.0 in) specimens.

4.3 IMPACT ENERGIES:

In Table A-1, the impact energy for each face sheet thickness is shown.

TABLE A-1

LOW VELOCITY IMPACT DAMAGE TEST MATRIX

<u>Number of Plies</u>	<u>Impact Energies (J)</u>
4	1.355
4	1.807
4	2.260
4	2.711
8	2.711
8	3.163
8	3.615
16	4.067
16	4.519
16	4.972
16	5.423
16	5.875
32	4.519
32	4.972
32	5.423
48	7.231
48	8.135
48	9.038
48	9.943

4.4 IMPACT PARAMETERS:

The specimens for each face sheet thickness shall be impacted with a 2.54 cm (1.0 in) diameter hemispherical tup. The height and weight of the impactor varies according to the desired impact energy. The impactor weighs 3.62 kg (8.00 lbs). These variables are displayed in Table A-2.

Table A-2

IMPACT PARAMETERS (NOMINAL)

<u>Impact Energy (Joules)</u>	<u>Height (cm)</u>	<u>Velocity (m/sec)</u>
1.356	3.8	0.865
1.808	5.1	0.999
2.260	6.4	1.116
2.712	7.6	1.223
3.163	8.9	1.321
3.616	10.2	1.412
4.067	11.4	1.498
4.519	12.7	1.579
4.971	14.0	1.656
5.423	15.2	1.730
5.875	16.5	1.800
7.231	20.3	1.997
8.134	22.9	2.118
9.039	25.4	2.233
9.943	27.9	2.342

4.5 POST-IMPACT:

- a. Following impact, the depth of the dent in the specimen will be measured by using a dial gage and recorded.
- b. The impact specimens will be subjected to pulse echo C-scan to determine the extent of damage. The results will be recorded.
- c. Selected impacted specimens at each face sheet thickness will be cut in half across the impact site. Micrographs of the subsequent cross sections will then be taken with the optical microscope.

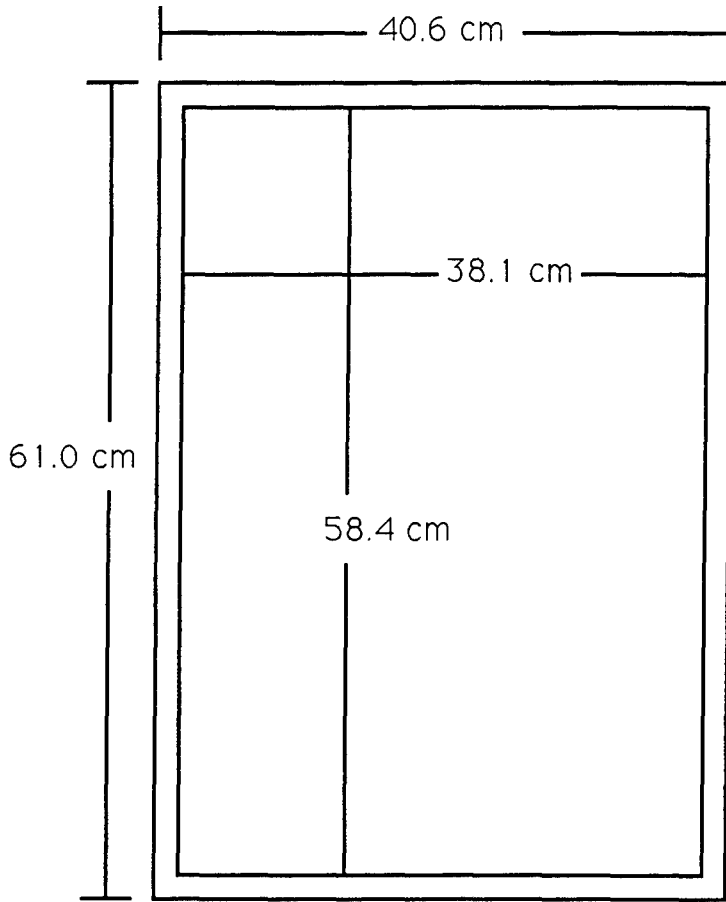


Figure A.1. Trim plan for sandwich panels

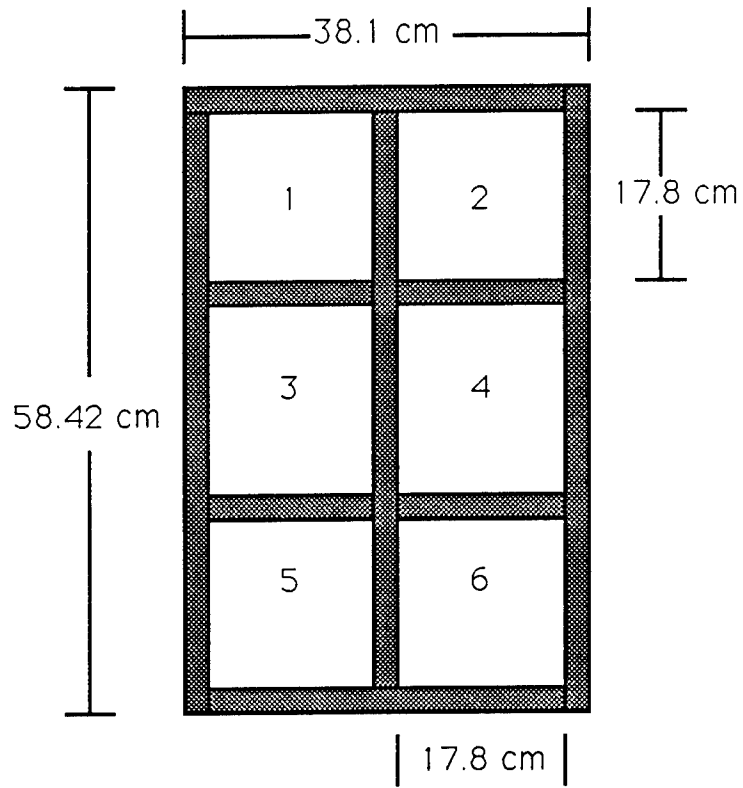


Figure A.2. Sandwich panel cut plan

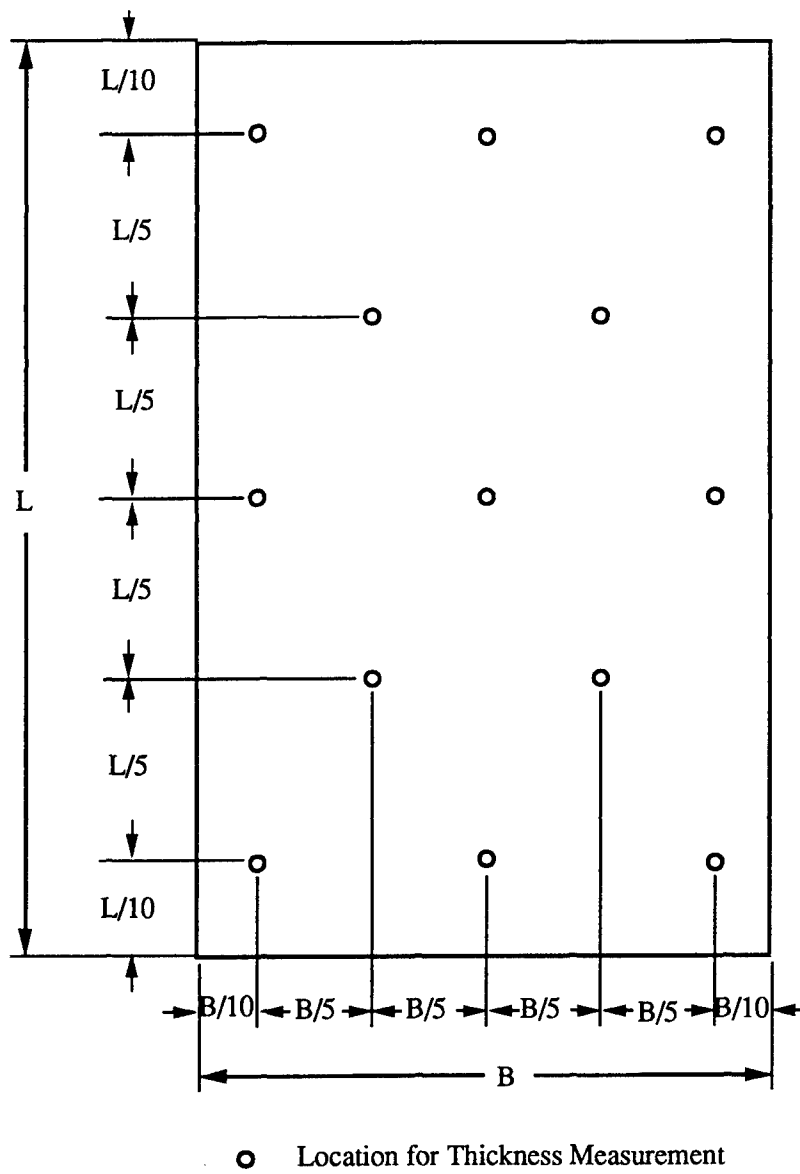


Figure A.3. Thickness Measurement Locations For Qualifications

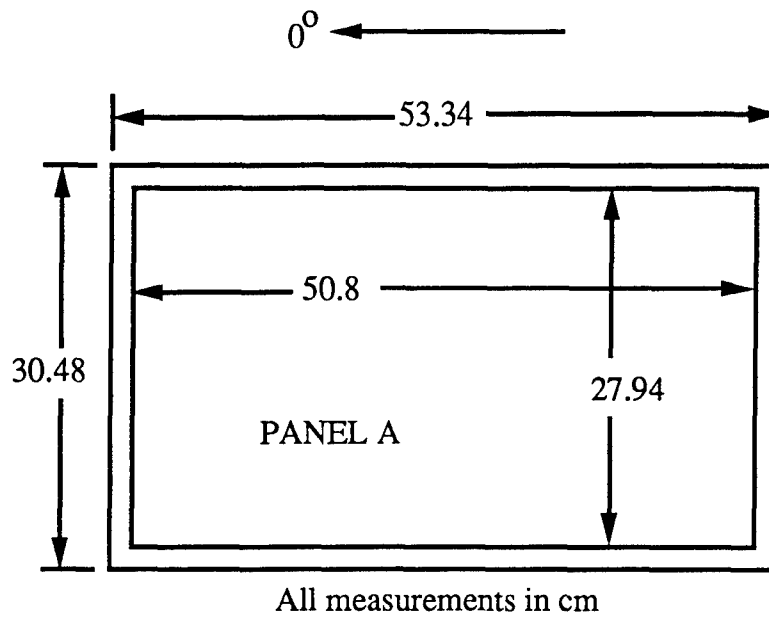


Figure A.4. Trim plan for unidirectional specimens panel A

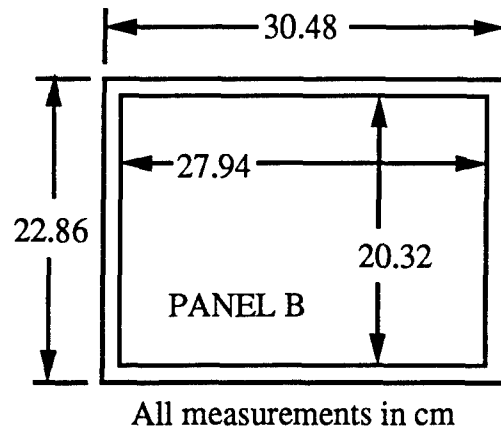
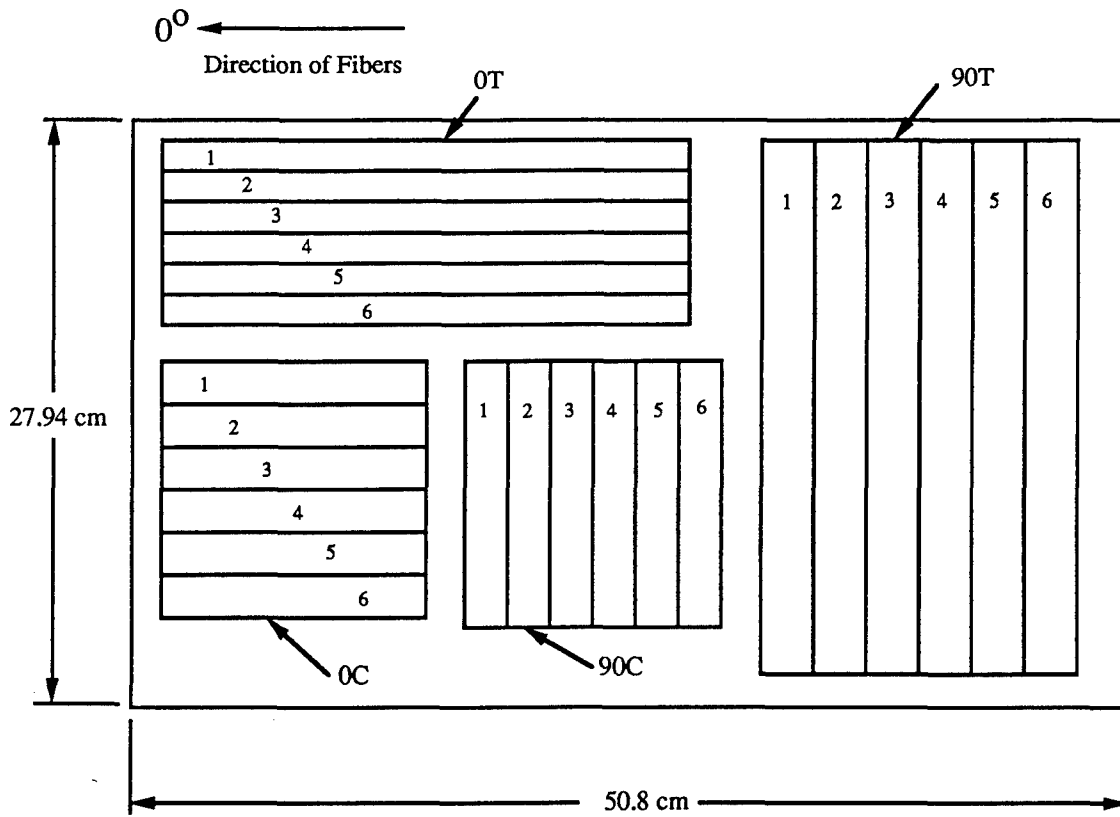
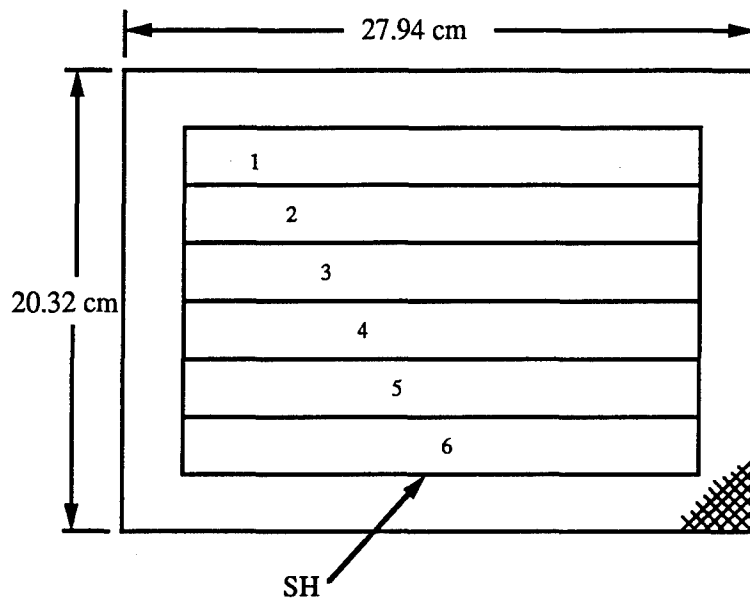


Figure A.5. Trim plan for shear specimens panel B



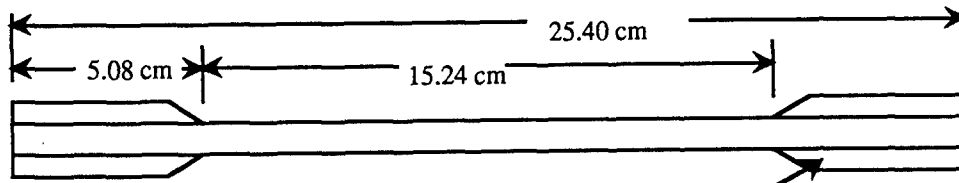
- Notes: 0T: Tension specimens 0 degree of size 25.4 cm by 1.27 cm.
 90T: Tension specimens 90 degree of size 25.4 cm by 2.54 cm.
 0C: Compression specimens 0 degree of size 12.7 cm by 1.91 cm.
 90C: Compression specimens 90 degree of size 12.7 cm by 1.91 cm.

Figure A.6. Panel 'A' cut plan



Notes: SH: Tension specimen ± 45 degree of size 22.86 cm by 2.54 cm.

Figure A.7. Panel 'B' cut plan



Fiberglass tabs (0.159 cm THK)
Standard 20 degree taper



B=1.91 cm for 0T specimens
B=2.54 cm for 90T and shear specimens

Figure A.8. 0T, 90T and Shear Tension Test Specimens

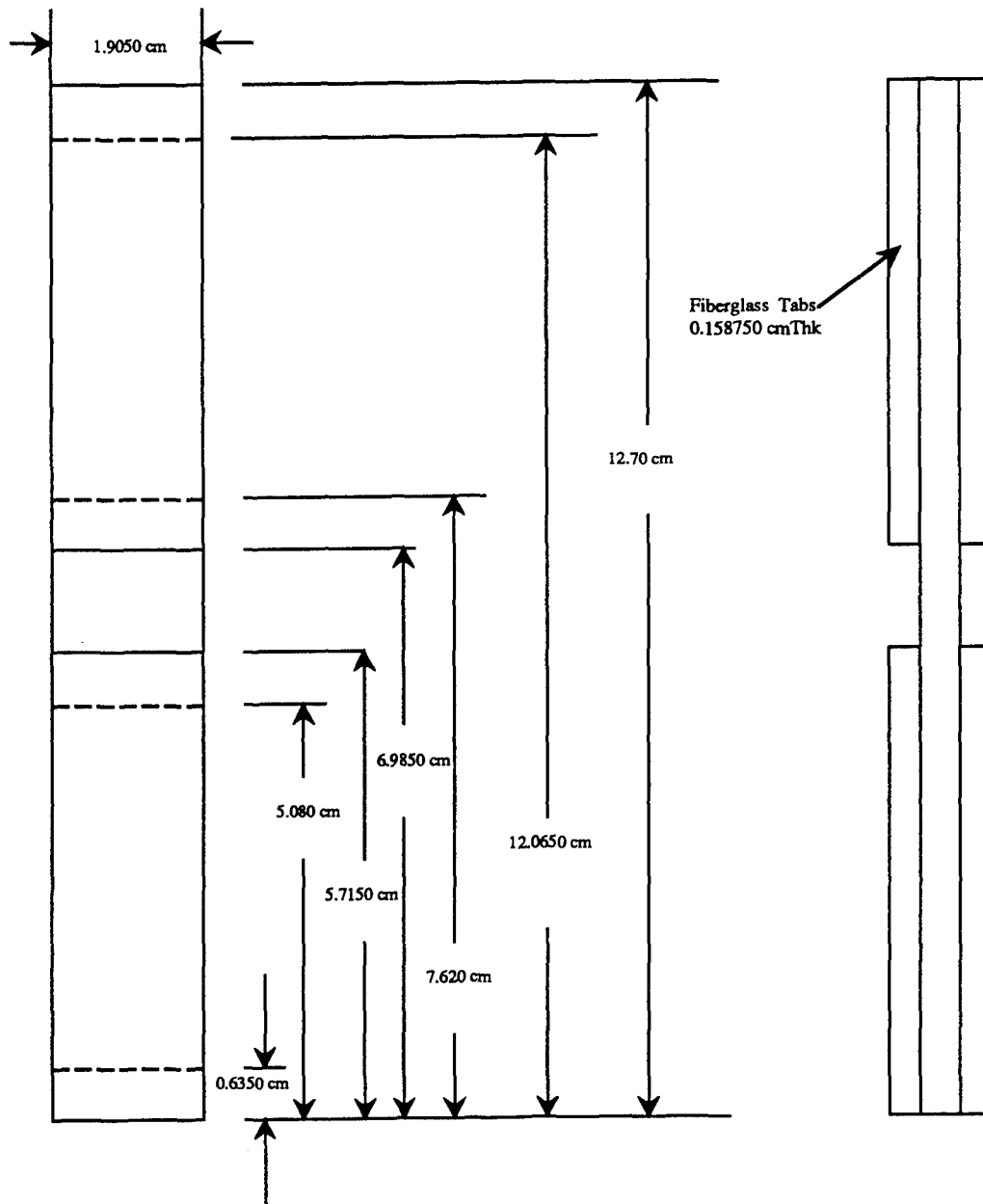


Figure A.9. 0C and 90C Test Specimens

Appendix B - Face Sheet Material Property Curves

To determine the basic property data for the AS4/3501-6 material, 0° tension, 0° compression, 90° compression, and $\pm 45^\circ$ shear specimens were fabricated, instrumented with CEA-03-062UR-350 strain gages, and tested under static load at a rate of 0.05 inches per minute. The strain gages were centered in the gage area. To ensure the accuracy of the data, six test were performed for each loading direction. The data is shown graphically in this appendix. Since the test compared well with each other, only one curve for each basic property is presented.

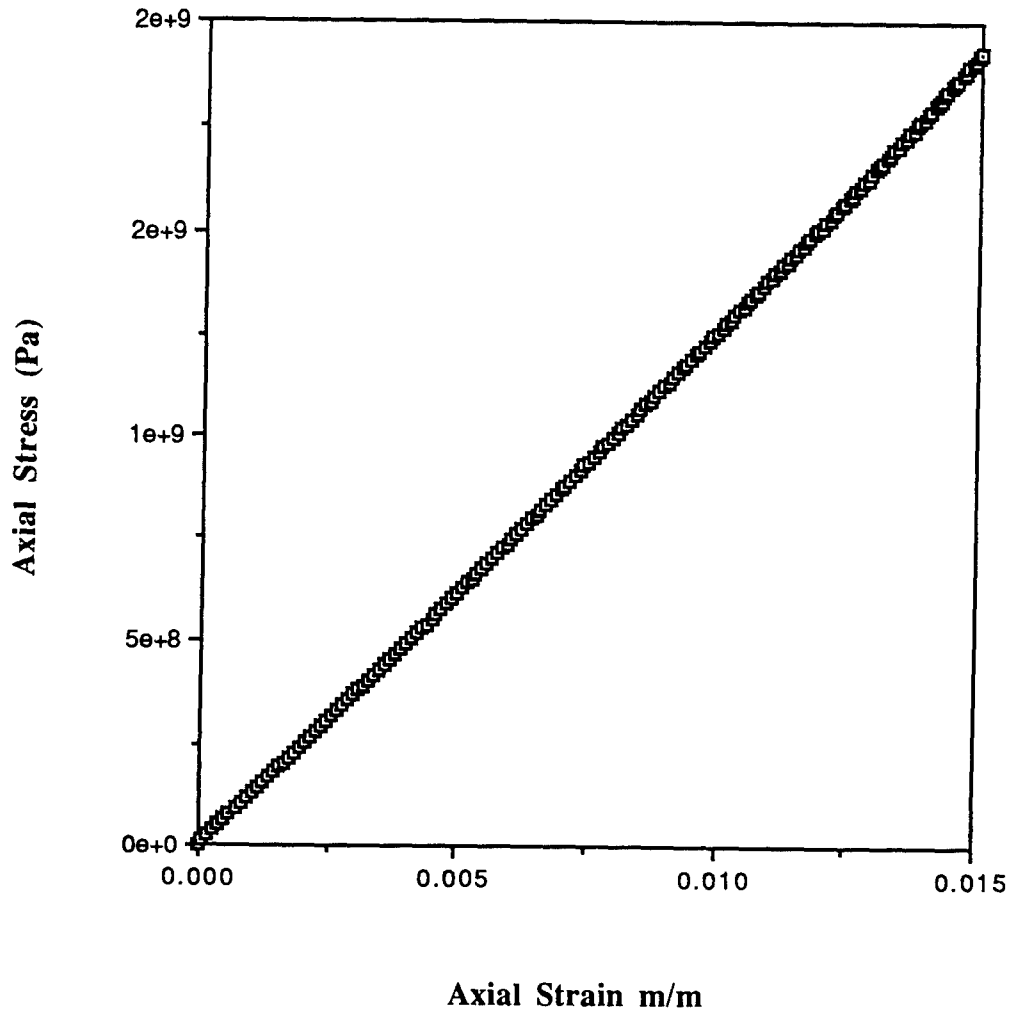


Figure B.1. Axial Stress (Sigma 1) vs Axial Strain (Epsilon 1) -
0 Degree Tension

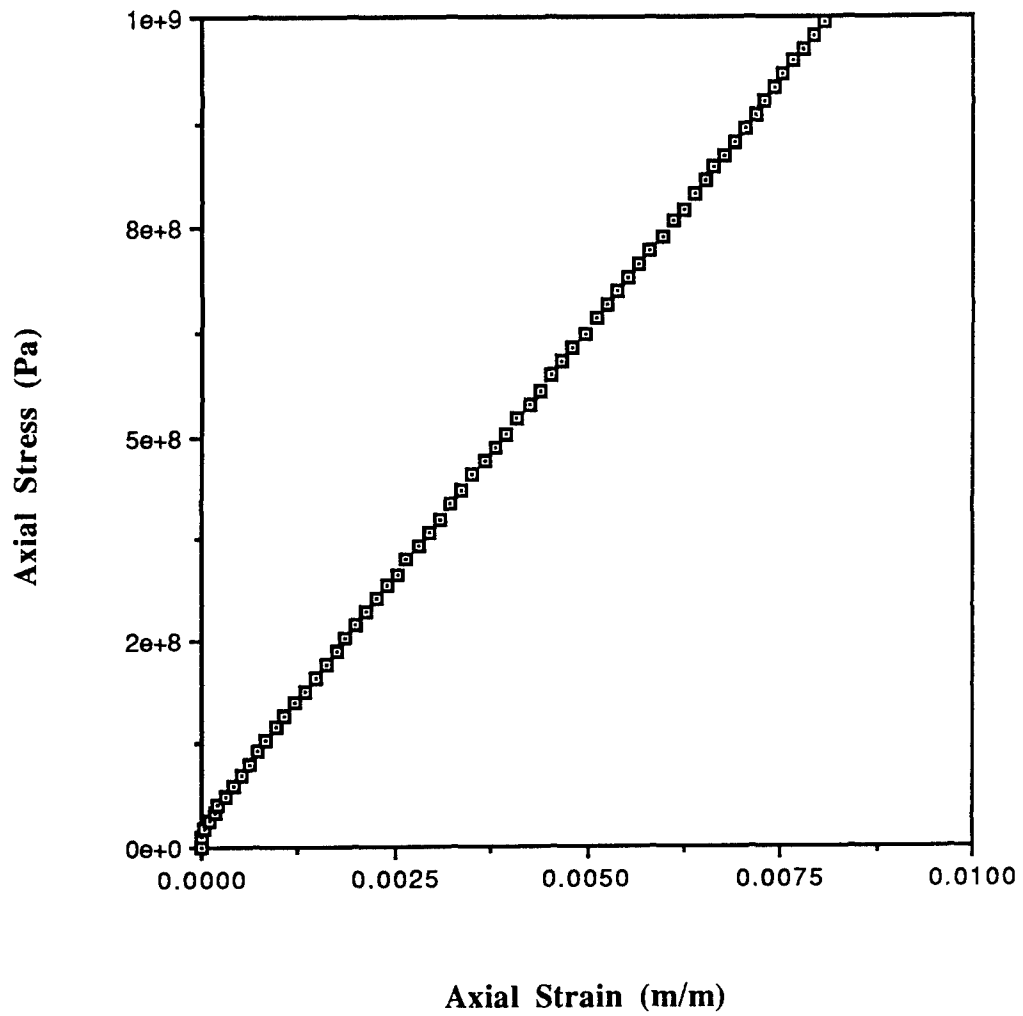


Figure B.2. Axial Stress (Σ_1) vs Axial Strain (ϵ_1) - 0 Degree Compression

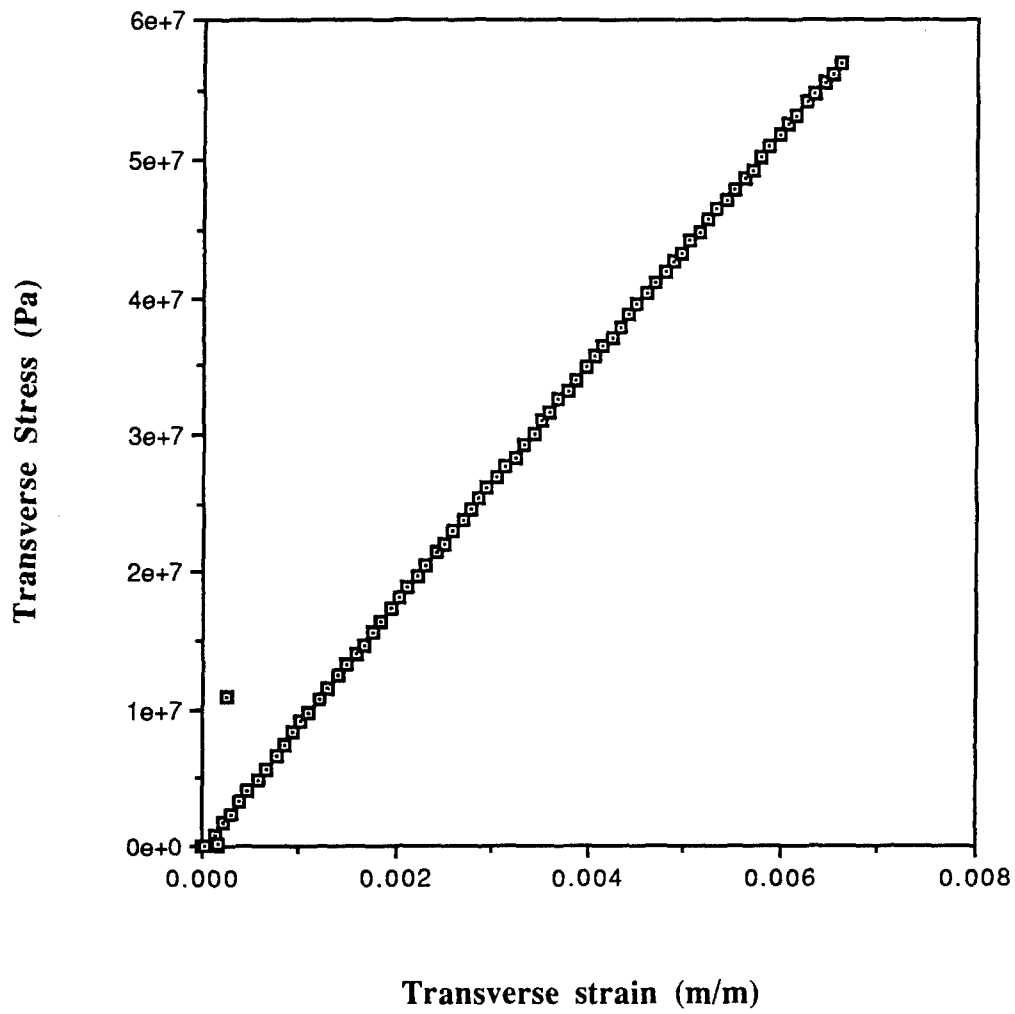


Figure B.3. Transverse Stress (Sigma 2) vs Transverse Strain (Epsilon 2) - 90 Degree Tension

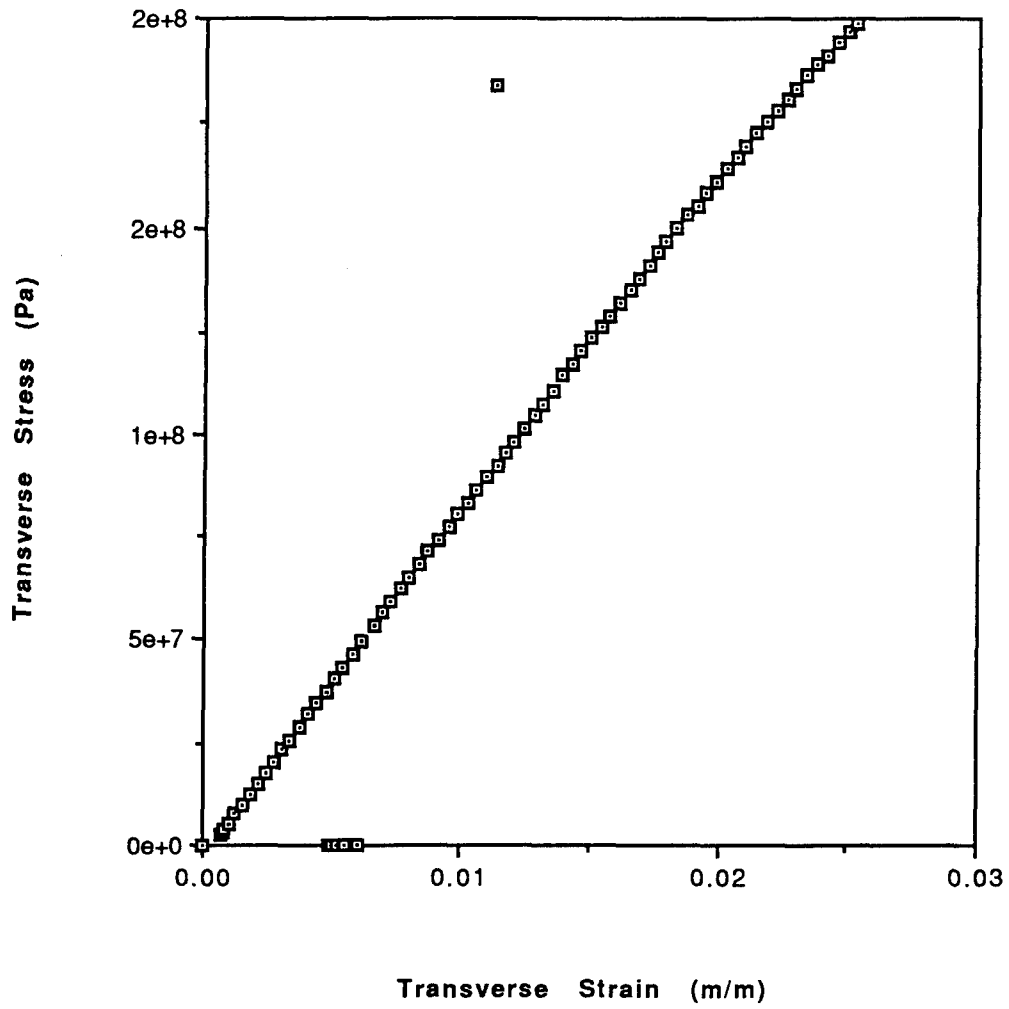


Figure B.4. Transverse Stress (σ_2) vs Transverse Strain (ϵ_2) - 90 Degree Compression

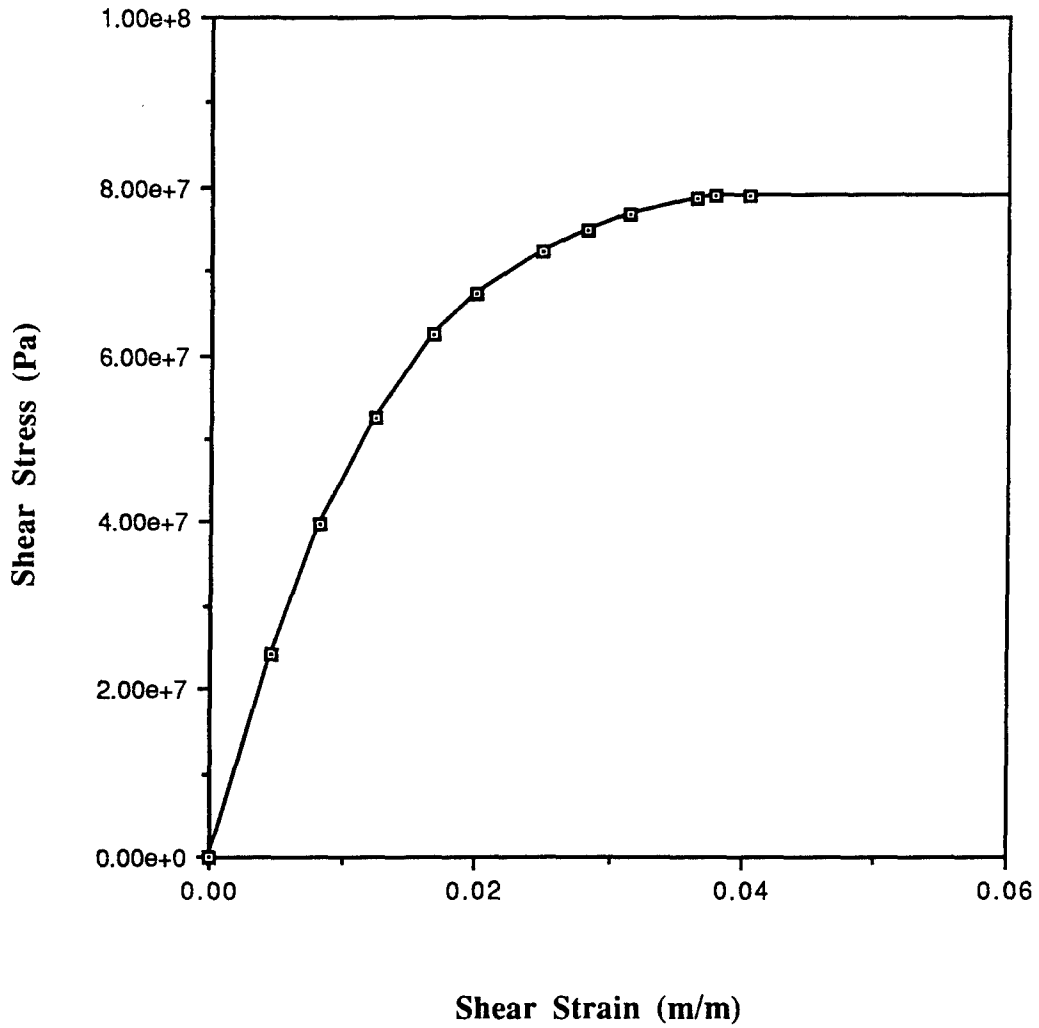


Figure B.5. Shear Stress (τ_{12}) vs Shear Strain (γ_{12}) - ± 45 Degree Tension

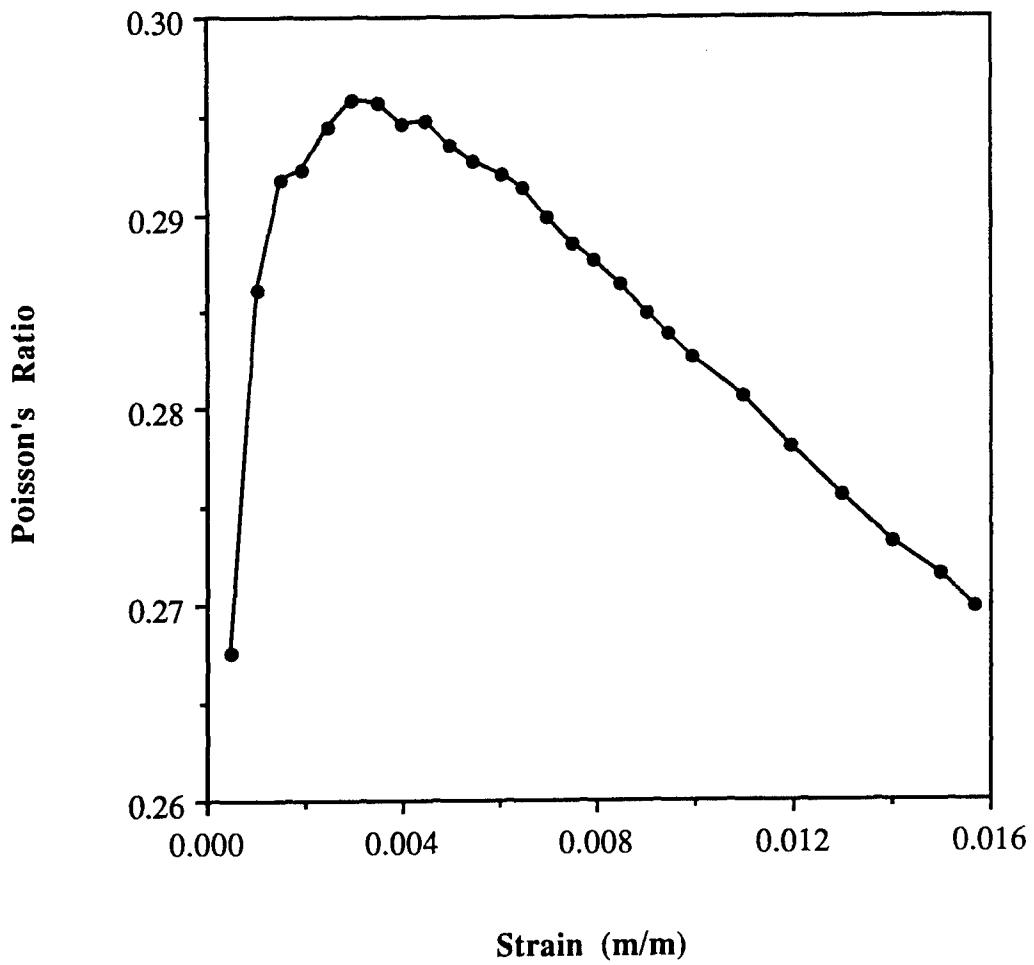


Figure B.6. Poisson's Ratio (Nu 12) vs Axial Strain (Epsilon 1) - 0 Degree Tension

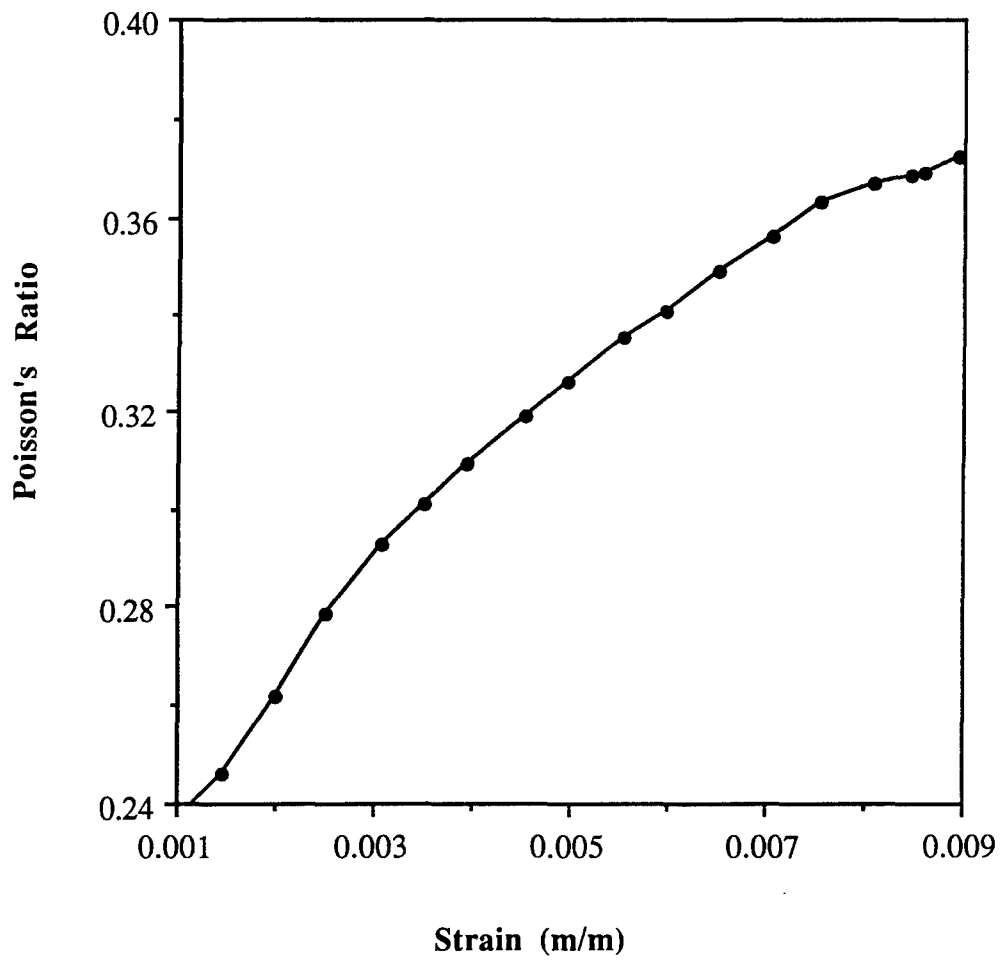


Figure B.7. Poisson's Ratio (Nu 12) vs Axial Strain (Epsilon 1) - 0 Degree Compression

Appendix C - Impact Testing Procedure

The step by step procedure followed when running the impact test on the General Research Corporation GRC 8250 Dynatup drop impact machine is presented in this appendix.

Impact Testing Procedure

1. Turn on the IBM PC-XT computer, and set all the system parameters (impactor weight, load cell sensitivity, date, time, and graph title).
2. Open air pressure valve and turn on pressure monitor. Make sure that the air pressure is between 28 - 29 psi (193053 - 199948 Pa).
3. Turn on the control box.
4. Check brakes by sliding a piece of paper between photo detector beam.
Reset brakes.
5. Open doors to the drop tower.
6. Raise impactor drop weight assembly to predetermined height.
7. Center between support block and hold-down plate. Bolt the plates together to hold sandwich plate firmly in place.
8. Place the secured specimen on the base plate centered below the tup.
9. Adjust the velocity detector and stop breaks to their proper position.
10. Close the doors to the drop tower. System will not work unless all doors are properly shut.
11. Initialize the data collection system.
12. Arm the system by lifting the cover on the ARM switch and pulling up the switch. An audible alarm will sound and the Arm indicator on the control box will glow red.

13. Release the impactor drop weight assembly by pushing the DROP button.
14. Lift the impactor drop weight assembly back up latch. The hook will automatically latch onto the impactor drop weight assembly. If the impactor drop weight assembly is too heavy to lift, push down the HOIST switch to lower the latch assembly. Stop when the impactor drop weight assembly is sensed. Releasing the HOIST switch allows the hook to automatically latch onto the impactor drop weight. Lift the impactor assembly weight up by pushing up on the HOIST button.
15. Open the drop tower doors to retrieve the secured specimen.
16. Remove the impacted specimen.
17. Repeat procedure with another specimen if necessary.

Appendix D - Dynatup Data Processing Technique

The computations used by the General Research Corporation GRC 8250 Dynatup drop impact machine to determine the impact velocity, absorbed energy, and displacements are provided in this appendix. These parameters can be displayed on screen immediately after completion using the General Research Corporation GRC 730-I Instrumented Impact Test Data System. This is an IBM PC-XT computer with a high speed data acquisition ability. The signals from both the load cell and velocity detector are collected, converted to engineering units and stored on a disk. The graphs generated from the impact test are in Chapter 3.

As explained by the manufacturer [13], if the time t_2-t_1 is the time from the first occlusion of the beam of light to the first reappearance of the beam, and the width of the velocity flag is x_2-x_1 , then

$$V_1 = \frac{(x_2-x_1)}{(t_2-t_1)} - 0.5g(t_2-t_1) \quad (D.1)$$

and

$$V_2 = \frac{(x_2-x_1)}{(t_2-t_1)} + 0.5g(t_2-t_1) \quad (D.2)$$

where V_1 is the velocity when the top of the flag crosses the detector, V_2 is the velocity when the bottom of the flag crosses the detector and g is the gravitational constant ($g=980 \text{ cm/ft}^2$; 32.2 ft/s^2). From (D.1) and (D.2) the impact velocity is

$$V_{\text{impact}} = V_2 + g(t_3-t_2) \quad (D.3)$$

where t_3-t_2 is the time when the bottom of the flag crosses the beam to the time when the impactor hits the panel. V_{impact} is the impact velocity used to calculate the impact energy and other parameters. The impact energy, E_{impact} , can then be found from

$$E_{\text{impact}} = \frac{m(V_{\text{impact}})^2}{2} \quad (D.4)$$

The impact energy can also be calculated based on the drop height as

$$E_{\text{impact}} = mgh \quad (\text{D.5})$$

where h is the drop height and m is the mass. It follows that the impact velocity is

$$V_{\text{impact}} = \sqrt{2gh} \quad (\text{D.6})$$

The impact velocity obtained from Equation (D.6) and Equation (D.3) differ by less than 0.1 ft/s under almost all conditions. The difference is caused by imprecision in the measurement of the drop height, which predictably becomes worse for very small drop heights. The impact velocities reported for each test are obtained from Equation (D.3) and the reported impact energies are obtained from Equation (D.4).

If the load cell is denoted by $P(t)$ and the impactor assembly weight by mg , then the total force acting on the load cell is

$$F(t) = mg - P(t) \quad (\text{D.7})$$

The impactor acceleration after release but before impact is g , so the acceleration during the impact occurrence is

$$a(t) = g - \frac{P(t)}{m} \quad (\text{D.8}).$$

It follows that the velocity function, $v(t)$, is

$$v(t) = \int a(t)dt = gt - \frac{1}{m} \int P(t)dt \quad (\text{D.9})$$

Signals from the load cell are sampled every 0.025 ms. If the impact takes place at sample zero with impact velocity $v_0 = V_{\text{impact}}$ and each time increment is $\Delta t = 0.025$ ms, then the velocity at the n th step is

$$v_n = v_0 + ng\Delta t - \frac{1}{m} \sum_{i=1}^n \left[\left(\frac{P_{i-1} + P_i}{2} \right) \Delta t \right] \quad (\text{D.10})$$

using the trapezoid rule to approximate the integrated impulse. This is the method in which the software numerically reduces the data.

The position is

$$x(t) = \int \left[\int a(t) dt \right] dt = \int v(t) dt \quad (D.11)$$

$$= \int g dt - \frac{1}{m} \int \left[\int P(t) dt \right] \quad (D.12)$$

In numerical form,

$$x_n = x_0 + \sum_{i=1}^n \left[\left(\frac{v_{i-1} + v_i}{2} \right) \Delta t \right] \quad (D.13)$$

Letting $x_0 = 0$ be the initial displacement,

$$x_n = \sum_{i=1}^n \left[\left(\frac{v_{i-1} + v_i}{2} \right) \Delta t \right] \quad (D.14)$$

The absorbed energy, $E_a(t)$, is the difference between the impact energy and the kinetic and the potential energies at time t . Setting time t equal to the time the impactor force drops to zero (i.e., it is no longer in contact with the panel) gives the energy absorbed during the test. The absorbed energy is

$$E_a(t_f) = T(0) - T(t_f) - V(t_f) \quad (D.15)$$

where $T(0)$ is the kinetic energy at the time of impact (the impact energy) and $T(t_f)$ and $V(t_f)$ are the kinetic and potential energies, respectively, of the impactor at the time the load drops to zero again. The kinetic and potential energies of the panel have been neglected in this calculation.

Bibliography

1. Becker, Walter E. U. S. Sandwich Panel Manufacturing/Marketing Guide. Stamford CT: Technomic Publishing Company, 1968.
2. Corden, John. "Honeycomb Structure," Composites. Vol. 1 of Engineering Materials Handbook. Metal Park, OH: ASM International, 1987.
3. The Basics on Bonded Sandwich Construction. Product Catalog TSB124. Dublin CA: Hexcel Corporation, 1984.
4. Structure Division, Wright Laboratory. "Damage Tolerance of Primary Sandwich Structure." Test Plan. 5 May 94.
5. Weeks, C. A. and C. T. Sun. Multi-core Composite Laminates. Unpublished draft report. Purdue University, West Lafayette, IN , no date [1994].
6. Agarwal, Bhagwan D., and Lawrence J. Broutman., Analysis and Performance of Fiber Composites, Second Edition, New York: John Wiley and Sons, 1990.
7. Madan, R. C., "Influence of Low-Velocity Impact on Composite Structures," Composite Structures, 3. ASTM STP 1110 Ed. T. K. O'Brien. 457-475. Philadelphia, 1991.
8. Kakarala, S. N. and J. L. Roche., "Experimental Comparison of Several Impact Test Methods," Instrumented Impact Testing of Plastics and Composite Material ASTM STP 936 ed Kessler, S. L. et al. 144-162. Philadelphia, 1986.
9. Foos, Brian C. Damage Progression in Composite Plates due to Low Velocity Impact. MS Thesis. Ohio State University, Columbus OH, 1990.
10. Perry, Ronald B. Impact Damage in Curved Graphite/Epoxy Panels with Clamped Edges, MS Thesis, AFIT/GAE/ENY/90D-19. School of Engineering, Air Force Institute of Technology (AU), Wright-Patterson AFB, OH. December 1990.
11. Demuts, E., R.S. Whitehead and R. B. Deo, "Assessment of Damage Tolerance in Composites," Composite Structures, 4: 45-58 (1989).
12. Schoeppner, G. A. "Low Velocity Impact Response of Tension Preload Composite Laminates," Proceedings of the 10th DOD/NASA/FAA Conference on Fibrous Composites in Structural Design. VIII-47 - VIII-61. April 1994.
13. Cruz, Juan R. Optimization of Composite Sandwich Cover Panels Subjected to Compressive Loadings., Report No. NASA TP-3173. NASA Langley Research Center, Hampton VA, December 1991.
14. Rix, Craig and Todd Saczalski. "Damage Tolerance of Composite Sandwich Panels," Proceedings of the 8th International Conference on Composite Materials. 3-I-1 to 3-I-10. Honolulu: 1991.

15. Jegley, D. "Impact-Damaged Graphite-Thermoplastic Trapezoidal-Corrugation Sandwich and Semi-Sandwich Panels," Journal of Composite Materials, 27: 526-537 (1993).
16. Chen, Chun-Hung, ming-Yan Chen and Jong-Pyng Chen., "The Residual Shear Strength and Compressive Strength of Carbon/Epoxy Composite Sandwich Structure after Low Velocity Impact," Proceedings of the 36th International SAMPE Symposium. 932-943. San Diego CA: 15-18 April 1991.
17. Kim, Chun-Gon, and Eui-Jin Jun. "Impact Characteristics of Composite Laminated Sandwich Structures." Report to Composite Materials Laboratory, Korea Institute of Machinery and Metals, Changwon Korea. 1991.
18. Caldwell, M. S., P. W. Borris, and R. Falabella. "Impact Damage Tolerance Tesing of Bonded Sandwich Panels," Proceedings of the 22nd International SAMPE Technical Conference. 509-520. 6-8 November 1990.
19. Lee, L. J., K. Y. Huang, and Y. J. Fann. "Dynamic responses of Composite Sandwich Plate Subjected to Low Velocity Impact," Proceedings of the 8th International Conference on Composite Materials. Paper 32-D. 1991.
20. Palm, Tod E. "Impact Resistance and Residual Compression Strength of Composite Sandwich Panels," Proceedings of the 8th International Conference on Composite Materials. Paper 3-G. 1991.
21. Tsang, P.H. Wilson and Paul A. Lagace., "Failure Mechanisms of Impact-Damaged Sandwich Panels under Uniaxila Compression," AIAA-94-1396-CP. American Institute for Aeronautics and Astronautics, Inc, 745-754, 1994.
22. Lagace P. A., and J. Williamson., "Contributions of the Core and Facesheet to the Impact Damage Resistance of Composite Sandwich Panels," Proceedings of the 10th DOD/NASA/FAA Conference. II-53 to II-73. Hilton Head Island, SC: 1-4 November 1993.
23. Lagace P. A., and J. Williamson., "Contributions of the Core and Facesheet to the Impact Damage Resistance of Composite Sandwich Panels," Proceedings of the 10th DOD/NASA/FAA Conference. II-53 to II-73. Hilton Head Island, SC: 1-4 November 1993.
24. Bitzer, T. N. Honeycomb Toughness and Proportional Limits. Report No. LSR 932277. Dublin CA: Hexcel Corporation, 5 August 1983.
25. Engineered Materials Department. FM 300-2 Film Adhesive - Modified Epoxy Resin Film. Product Description. Havre de Grace MD: American Cyanamid Company, 1990.
26. Daniels, John A. A Study of Failure Characteristics in Thermoplastic Composite Laminates Due to Eccentric Circular Discontinuity. MS Thesis, AFIT/GAE/ENY/89D-06. School of Engineering, Air Force Institute of Technology (AU), Wright-Patterson AFB OH, December 1989.

27. Schoeppner, Greg, Aerospace Engineer, Wright Laboratory, OH. Personal Conversation. 11 August 1994.
28. GRC 730-I Instrumented Impact Test Data System Instruction Manual, General Research Corporation, Santa Barbara CA, 1987.
29. Pinnel, Brad., Destructive Evaluation Engineer. Notes, on Cross-Sectioning for optical microscopy. University of Dayton Research Institute UDRI, Material Directorate, Wright Patterson AFB, October 1994.
30. Schoeppner, Greg. Wright Laboratory, OH. Personal Correspondence. 11 January 1994.
31. "Glossary of Advanced Composite Terms," Advanced Composites 1992 Bluebook: 19-27 (December 1991).
32. Tsai, Stephen W. Composite Design. (Third Edition). Dayton, OH: Think Composites, 1987.
33. Lammerant, L. and I. Verpoest., "The interaction between Matrix Cracks and Delaminations during Quasi-Static Impact of Composites," Composite Science and Technology, 51. 505-516 (1994).
34. Broek, David. Elementary Engineering Fracture Mechanics. (Fourth Edition). Dordrecht, The Netherlands: Kluwer Academic Publishers, 1991.
35. Bucinell, R. B., R.J. Nuismer, and J. L. Koury., "Response of Composite Plates to Quasi-Static Impact Events." Composite Materials: Fatigue and Fracture, 3: ASTM STP 1110, T. K. O'Brien, Ed., American Society for Testing and Materials, Philadelphia, 528-549. 1991.
36. Liu, D., et al, "Structural Degradation of Impacted Graphite/Epoxy Laminates," 56th Shock and Vibration Bulletin, pp.51-60, 1986.
37. Finn, S. R. and G. S. Springer, "Delamination in Composite Plates Under Transverse Impact Loads -A Model", Composite Structures, 23. 51-69 (1992).

VITA

Timberlyn Michelle Harrington was born in DeLand, Florida on 26 October 1967. She graduated Summa Cum Laude from DeLand High School in 1985 and attended Tuskegee University on an Air Force ROTC Scholarship. Graduating with Highest Honors and as a Distinguished Graduate in December 1989, Captain Harrington was commissioned into active duty and served as an Aircraft Battle Damage Repair Research and Development Engineer until May 1993. She then began her studies towards a Master of Science in Aeronautical Engineering, with studies in structures, at the Air Force Institute of Technology.

Timberlyn is married to Michael Harrington of Chicago, Illinois. She is the daughter of Mrs. Marie M. Birch.

Permanent Address: 680 South Parsons Avenue
DeLand, Florida 32720

REPORT DOCUMENTATION PAGE

Form Approved
OMB No. 0704-0188

Public reporting burden for this collection of information is estimated to average 1 hour per response, including the time for reviewing instructions, searching existing data sources, gathering and maintaining the data needed, and completing and reviewing the collection of information. Send comments regarding this burden estimate or any other aspect of this collection of information, including suggestions for reducing this burden, to Washington Headquarters Services, Directorate for Information Operations and Reports, 1215 Jefferson Davis Highway, Suite 1204, Arlington, VA 22202-4302, and to the Office of Management and Budget, Paperwork Reduction Project (0704-0188), Washington, DC 20503.

1. AGENCY USE ONLY (Leave blank)		2. REPORT DATE December 1994	3. REPORT TYPE AND DATES COVERED Master's Thesis
4. TITLE AND SUBTITLE AN EXPERIMENTAL INVESTIGATION OF SANDWICH FLAT PANELS UNDER LOW VELOCITY IMPACT		5. FUNDING NUMBERS	
6. AUTHOR(S) Timberlyn M. Harrington, Captain, USAF		8. PERFORMING ORGANIZATION REPORT NUMBER AFIT/GAE/ENY/94D-22	
7. PERFORMING ORGANIZATION NAME(S) AND ADDRESS(ES) Air Force Institute of Technology 2950 P Street Wright-Patterson AFB, OH 45433-7765		10. SPONSORING/MONITORING AGENCY REPORT NUMBER	
9. SPONSORING/MONITORING AGENCY NAME(S) AND ADDRESS(ES) Mr. William Baron WL/FIBA, Bldg 45 2130 Eighth St, Ste 1 Wright-Patterson AFB, OH 45433-7524		11. SUPPLEMENTARY NOTES	
12a. DISTRIBUTION/AVAILABILITY STATEMENT Approved for public release; distribution unlimited		12b. DISTRIBUTION CODE	
13. ABSTRACT (Maximum 200 words) This study evaluated the failure modes and mechanisms associated with increasing face sheet thickness of flat sandwich panels under low velocity impact. The sandwich panels were fabricated using 1.27 cm thick, 145 kg/m³ (9 lb/ft³), 3.175 mm (1/8") cell size Nomex honeycomb core, FM 300-2 film adhesive and AS4/3501-6 graphite/epoxy face sheets. The thickness of the core remained 1.27 cm, and the thickness of the adhesive remained 0.25 mm. The thickness of the face sheets varied using the following stacking sequences: [0/90]_s, [0/90]_{2s}, [0/90]_{4s}, [0/90]_{8s}, and [0/90]_{12s}. The sandwich panels were subjected to various low velocity impacts using the Dynatup Impact Test Machine. Pulse-Echo C-scans and optical microscopy of panel cross-sections were performed to characterize the damage. The cross-sections indicated that delamination and transverse cracking contribute to internal damage of the face sheets, while crushing, buckling, and crippling contribute to damage of the core. Cracks in the adhesive also contribute to damage in some cases.			
14. SUBJECT TERMS Composite panels, Composite plates, Graphite/Epoxy, Low Velocity Impact		15. NUMBER OF PAGES 274	
16. PRICE CODE		20. LIMITATION OF ABSTRACT UL	
17. SECURITY CLASSIFICATION OF REPORT Unclassified	18. SECURITY CLASSIFICATION OF THIS PAGE Unclassified	19. SECURITY CLASSIFICATION OF ABSTRACT Unclassified	20. LIMITATION OF ABSTRACT UL